Progesterone Receptor Membrane Component 1: Cellular Mechanisms and Involvement in Breast Cancer Pathology and Endometrial Decidualization

Inaugural-Dissertation

zur Erlangung des Doktorgrades
der Mathematisch-Naturwissenschaftlichen Fakultät
der Heinrich-Heine-Universität Düsseldorf

vorgelegt von

Nadia Stamm
aus Bolschevo in Russland

Düsseldorf, März 2025

Aus der Klinik für Frauenheilkunde und Geburtshilfe

Universitätsklinikum Düsseldorf

Direktorin: Frau Prof. Dr. med. Tanja Fehm

Gedruckt mit der Genehmigung der

Mathematisch-Naturwissenschaftlichen Fakultät der

Heinrich-Heine-Universität Düsseldorf

Berichterstatter:

1. Prof. Dr. Hans Neubauer

Klinik für Frauenheilkunde und Geburtshilfe

2. Prof. Dr. Thomas Heinzel

Institut für Physik der kondensierten Materie

Tag der mündlichen Prüfung: 20.05.2025

Table of Contents

1. List of Abbreviations

Co-IP	Co-Immunoprecipitation
CRISPR	Clustered Regularly Interspaced Palindromic Repeats
CYP450	Cytochrome P450 Monooxygenase
CYP19A	Aromatase
CYP27A1	Sterol 27-Hydroxylase
CYP51A1	Lanosterol Demethylase
CytB5	Cytochrome b5
DAPI	4’,6-Diamidin-2-phenylindol
DMSO	Dimethyl Sulfoxide
E2	Estradiol
EDTA	Ethylenediaminetetraacetic Acid
EGF	Epidermal Growth Factor
EGFR	Epidermal Growth Factor Receptor
ERα	Estrogen Receptor
EVC	Empty Vector Control
FCS	Fetal Calf Serum
FDFT1	Farnesyl-diphosphate Farnesyltransferase 1
FECH	Ferrochelatase
GFP	Green Fluorescent Protein
HA	Hemagglutinine
HEPES	4-(2-hydroxyethyl)-1-Piperazineethanesulfonic Acid
HER2	Human Epidermal Growth Factor Receptor 2
HR	Hormone Receptor

INSIG	Insulin-induced Gene 1 Protein
KO	Knockout
MAPR	Membrane Associated Progesterone Receptor
mPR	Membrane Progesterone Receptor
PARQ	Progestin and AdipoQ Receptors
PCR	Polymerase Chain Reaction
PGRMC1	Progesterone Receptor Membrane Component 1
PHB1/2	Prohibitin1/2
PI3K	Phosphoinositide 3-Kinase
PLA	Proximity Ligation Assay
PR	Progesterone Receptor
PVDF	Polyvinylidene Fluoride
RNase	Ribonuclease
RT	Room Temperature
SCAP	SREBP Cleavage-Activating Protein
SCD1	Stearoyl-CoA Desaturase 1
SDS	Sodium Dodecyl Sulfate
SDS-PAGE	SDS-Polyacrylamide Gel Electrophoresis
SH2/3	Src-Homology Domain 2/3
SQLE	Squalene Epoxidase
SREBP	Sterol Regulatory Element Binding Protein
TBST	TRIS-buffered Saline with Tween
Tff1	Trefoil Factor 1
TRIS	Tris-(hydroxymethyl)-Aminomethane

2. Abstract

Progesterone receptor membrane component 1 (PGRMC1) is a highly conserved multifunctional protein which is involved in key cellular pathways and associated with pathology. In breast cancer, PGRMC1 overexpression aligns with worse prognosis and overall survival, while in infertility-related diseases, PGRMC1-downregulation is often observed. Previous studies conducted in PGRMC1-overexpressing breast cancer cells revealed that PGRMC1 interacts with enzymes of the mevalonate pathway and the estrogen receptor α (ERα)-regulating proteins prohibitin 1 and prohibitin 2 (PHB1 and PHB2).

The aim of this study was to gain deeper insights into the association of PGRMC1 with cholesterol biosynthesis and into its crosstalk with ERα and thereby to elucidate potential implications in breast cancer and infertility.

In the first part, PGRMC1 interaction partners within the cholesterol synthesis pathway were confirmed at endogenous expression levels, and the abundance of cholesterol and neutral lipids was determined in PGRMC1-overexpressing cells. PGRMC1-overexpression was found to be associated with increased cholesterol and estradiol production, potentially intrinsically stimulating ERα signaling. Consequently, treatment with cholesterol-lowering statins reverted the proliferative benefit conveyed by PGRMC1.

In the second part of this work, CRISPR/Cas9-based PGRMC1-deficient breast cancer cell models were generated and characterized on genetic and functional levels. Importantly, deficiency of PGRMC1-protein was confirmed for at least two cell clones for each CRISPR/Cas9-treated cell line and the introduced mutations were assessed. Functionally, the PGRMC1-null cells did not display phenotypes observed in transient PGRMC1-knockdown cell models, indicating a possible compensation of PGRMC1-deficiency.

In the third part of this dissertation, PGRMC1 interactions with negative ERα-regulators, PHB1 and PHB2, were addressed. The interactions were found to be dependent on PGRMC1-S181 phosphorylation. Importantly, PGRMC1-PHB-interactions prevented PHB-binding to and negative regulation of ERα, potentially increasing oncogenic signaling.

In the fourth part, the PGRMC1-PHB-interactions were analyzed in another cellular system: decidualized endometrial stromal cells, following the hypothesis that this interaction axis will also affect this hormone-dependent process. PGRMC1-expression was found to follow a rise-

to-decline expression pattern during decidualization, accompanied by PGRMC1-PHB-interactions in the process. PGRMC1-downregulation before decidualization induction resulted in abrogation of the process, potentially mirroring PGRMC1-deficiency in infertility-related diseases.

Taken together, this work provides new insights into PGRMC1-implications in breast cancer pathology and impaired decidualization as a common feature of several infertility-related diseases. The collected evidence points towards a functional connection between PGRMC1 expression and ERα activation in breast cancer, through both deregulated sterol metabolism and through PHB-inhibition. The generated PGRMC1-knockout models may serve as a useful tool to understand compensation for PGRMC1-deficiency and thereby gain further insights into key PGRMC1 functions. This study emphasizes the implication of PGRMC1 in cancer hallmark-related mechanisms and might represent a new avenue to target hormone-dependent breast cancer in the future.

3. Kurzfassung

Progesterone receptor membrane component 1 (PGRMC1) ist ein multifunktionales hochkonserviertes Protein, das an grundlegenden zellulären Funktionen beteiligt ist. Die Deregulation von PGRMC1 trägt zur Tumorprogression des Mammakarzinoms und anderer Karzinome sowie zur weiblichen Infertilität bei. Während bei Ersterem eine erhöhte Expression mit einer schlechteren Prognose einhergeht, ist bei Letzterem PGRMC1 häufig vermindert exprimiert. Um den funktionalen Zusammenhang zwischen PGRMC1-Expression und den oben genannten Störungsbildern zu adressieren, wurden in vorangegangenen Untersuchungen PGRMC1-Interaktionspartner analysiert und Enzyme der Cholesterol-Biosynthese sowie negative Estrogenrezeptor α (ERα) -Regulatoren Prohibitin 1 und 2 (PHB1, PHB2) als Interaktionspartner identifiziert.

Ziel dieser Arbeit war die weitere Untersuchung der Beteiligung von PGRMC1 an der Cholesterol-Biosynthese und des möglichen Zusammenspiels von PGRMC1 mit ERα, um neue Erkenntnisse über die Rolle von PGRMC1 in der Brustkrebsprogression und in der Infertilität zu gewinnen.

Im ersten Teil der Arbeit wurden potenzielle PGRMC1-Interaktionspartner in der Cholesterol- und Lipid-Biosynthese bestätigt und die Menge an Cholesterol und Estradiol in PGRMC1-überexprimierenden Zellen gemessen. PGRMC1-Überexpression ging mit erhöhter Produktion beider Verbindungen einher, was möglicherweise die Proliferation ERα-positiver Brustkrebszellen intrinsisch stimuliert.

Im zweiten Teil des Projektes wurden CRISPR/Cas9-basierte PGRMC1-Knockout (KO) Zellen für drei verschiedene Brustkrebszelllinien erzeugt und charakterisiert. Die Abwesenheit des PGRMC1-Proteins wurde bestätigt, sowie die genetischen Veränderungen über Sanger-Sequenzierung adressiert. Interessanterweise deckte sich der PGRMC1-KO Phänotyp nicht mit dem des transienten PGRMC1-*Silencing*, was auf eine mögliche Kompensation des PGRMC1-Verlustes hindeutet.

Im dritten Teil wurden Interaktionen zwischen PGRMC1 und PHB1/2 analysiert, die von der PGRMC1-S181-Phosphorylierung nach Behandlung mit spezifischen Progestinen (z.B. Norethisteron, NET) abhängig sind. Bei Vorliegen der PGRMC1-PHB-Interaktionen nach Behandlung mit NET wurde die Assoziation zwischen ERα und PHBs schwächer, was möglicherweise eine indirekte Aktivierung von ERα zur Folge haben könnte. In PGRMC1-KO

Zellen blieben die ERα-PHB-Interaktionen nach Behandlung mit NET unverändert, was eine PGRMC1-Abhängigkeit dieses Effekts nahelegt.

Im letzten Teil dieser Arbeit wurden die PGRMC1-PHB-Interaktionen in dem zusätzlichen Modell der dezidualisierten Stromazellen des Endometriums untersucht, um den Zusammenhang zwischen PGRMC1-Expression und Infertilität zu beleuchten. PGRMC1-Expression folgte während der Dezidualisierung einem zunächst ansteigenden und später abfallenden Expressionsmuster. PGRMC1-*Silencing* vor Dezidualisierung verhinderte den Prozess, was eine wichtige Beobachtung im Hinblick auf die tendenziell geringere Expression von PGRMC1 bei Infertilität darstellt.

Die Ergebnisse dieser Studie deuten auf eine Beteiligung von PGRMC1 an der Tumorprogression ERα-positiver Mammakarzinome, was mutmaßlich durch die Aktivierung von ERα vermittelt wird. Somit stellt PGRMC1 einen wichtigen Faktor in der Progression ERα-positiver Mammakarzinome dar und sollte im Hinblick auf Therapieresistenzen weiter untersucht werden.

4. Introduction

4.1. PGRMC1 – A Conserved and Versatile Protein

The protein progesterone receptor membrane component 1 (PGRMC1) is one out of four members of the membrane associated progesterone receptor (MAPR)-family in humans (along with PGRMC2, neuferricin and neudesin) and is distinct from the nuclear progesterone receptor (PR) or membrane progesterone receptors (mPR) [1]. The common characteristic of MAPR proteins is their cytochrome b5 (cytb5)-like heme chelation domain and one N-terminal transmembrane helix [2]. *PGRMC1* was first cloned in 1996 by two research groups as the gene coding for a membrane-associated progesterone-binding protein in porcine liver [3] and a dioxin-induced protein in rat liver [4], and termed *mPR* and *25-Dx*, respectively. The human homolog was cloned in 1998 and given the designation *Hpr6.6* [5]. In the course of the following years, PGRMC1 was found to be identical with the previously described adrenocortical inner zone antigen in rat, pig and rabbit adrenal glands [6], and misidentified as the sigma2-receptor [7], [8], which was among other things based on the fact that both proteins exhibit physical and functional interaction [9]. It is important to note that, although termed *mPR* in pigs by Meyer *et al.*, PGRMC1 is structurally entirely different from the group of membrane progesterone binding receptors with seven transmembrane helices referred to as mPR, which belong to the class of progestin and adipoQ receptors (PAQR) [10].

PGRMC1 has been associated with a variety of different seemingly disparate biological functions and described in various cellular and animal systems. Investigation of PGRMC1 homologs revealed conserved structural motifs in various eukaryotic organisms down to yeast, indicating an ancestral role of the protein [11]. In fact, all vertebrates possess both PGRMC1 and PGRMC2 homologs, presumably developed by gene duplication; while in invertebrates and fungi, there is at least one homolog present (for nematode model organism *C. elegans*: Ventral Midline-1; for *D. melanogaster*: steroid binding protein; for *S. cerevisiae*: damage response protein 1 (Dap1)). Among these species, PGRMC1 homologs exert conserved functions that underpin their universal ancestral role, including binding of heme and regulation of sterol metabolism [12]. During animal evolution, PGRMC proteins acquired additional functions and merged into a more complex system of steroid receptors, making their contribution to cellular physiology putatively more versatile. PGRMC1 has been reported to be involved in drug metabolism, cholesterol and steroid biosynthesis [13], [14], autophagy [8], female murine reproductive function [15], amyloid beta binding in Alzheimer's disease

[16], insulin homeostasis [17], membrane trafficking [18], regulation of cell cycle [19] as well as cancer pathology [20], [21].

The following chapters will focus on molecular characteristics of PGRMC1 and its impact on biosynthesis and signaling pathways with a special focus on oncogenic pathways, central for this work.

4.2. PGRMC1 – Structure

PGRMC1 is a 195 amino acid protein with a predicted N-terminal transmembrane domain (amino acids 28 - 43), a cytochrome b5 (cytb5) -like domain (amino acids 70 - 172) and a molecular weight of approx. 25 kDa [11]. To solve PGRMC1 structure and address its heme binding properties, Kabe *et al.* used X-ray crystallography, NMR spectroscopy and UV-visible absorption spectrometry on bacterially expressed recombinant cytosolic PGRMC1-domain (amino acids 72-195 for crystal structure and 44-195 for NMR) in 2016. The resulting solely existing structure of cytosolic PGRMC1 (protein data base, 4X8Y) represents the cytb5 domain together with the C-terminus and visualizes heme-chelation [22]. This structure identified tyrosine Y113, a conserved residue across PGRMC1-homologs, to be the axial ligand for heme binding, which is a major deviation from cytochrome b5 proteins, where iron is chelated by two axial histidine residues [22]. Since in PGRMC1, heme is bound only by one axial ligand, the opposite axial surface of heme remains accessible, potentially allowing dimerization. Indeed, heme-bound PGRMC1 molecules were observed to dimerize *in vitro* by heme-stacking, and mutation of Y113 to phenyl alanine (Y113F) prevented both heme-binding and dimer-formation [22]. In 2021, McGuire *et al.* demonstrated on full-length PGRMC1 that the mutation Y113F alone was not sufficient to disrupt the binding of heme, but only in combination with K163A and Y164F [23] which stabilize heme in the PGRMC1 binding pocket by hydrogen bonding [22] (Figure 1).

Unfortunately, the crystal structure published in 2016 did not provide conformational information about the full-length protein or the trans-membrane domain. To address that, *in silico* modeling algorithms may provide a feasible tool, predicting an alpha-helix conformation of the trans-membrane domain and a structurally flexible linker-region between trans-membrane and cytb5 domains as well as flexible N- and C-termini [24]. In the linker region, PGRMC1 possesses an src-homology domain 3 (SH3) target sequence and in the cytb5 domain and the C-terminal unstructured region, another two src-homology domain 2 (SH2) target

sequences. These sequences are presumably important for protein-protein interactions and can be regulated by proximal casein kinase 2 (CK2) phosphorylation [25].

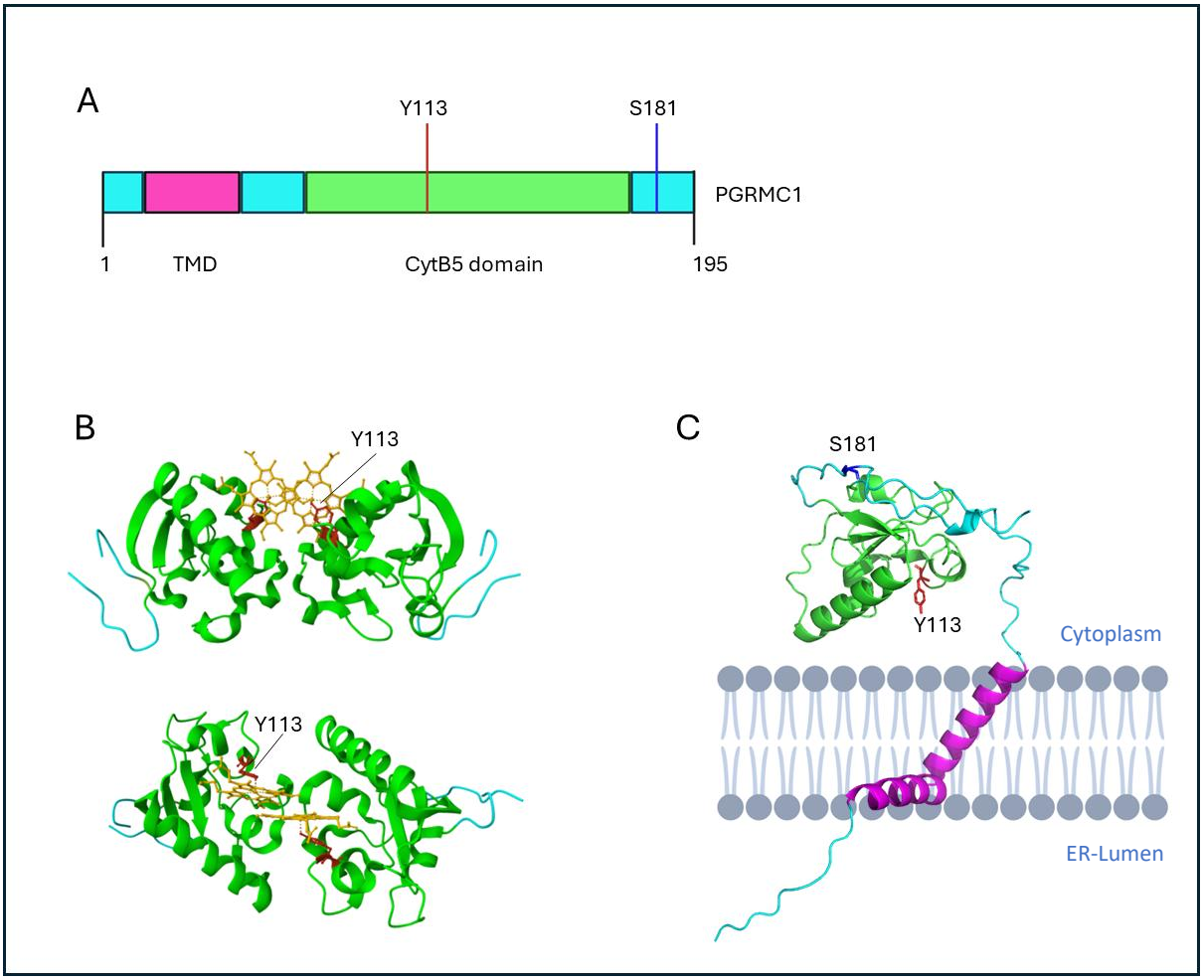

Figure 1: Schematic representation of PGRMC1 with its domains and structural motifs based on (Cahill, Jazayeri, Kovacevic, et al., 2016b) [2]. Important phosphorylation sites are highlighted in red. PGRMC1 has a transmembrane helix (TMH), a cytb5 domain as well as one src-homology 3 domain target sequence (SH3) and two src-homology 2 domain target sequences (SH2) important for interactions with other proteins. B: Structure of dimeric PGRMC1 as solved by Kabe *et al*. [22], Protein Data Base-ID: 4X8Y), visualized with the PyMOL software [26] with the axial tyrosine Y113 highlighted in red, and two heme molecules (one per PGRMC1-monomer) in yellow. The lower panel offers the view on heme stacking between two monomers. C: Structure of PGRMC1 whole protein predicted with alphafold [27] and visualized with PyMOL, image created with BioRender. All structures have the same color coding as the primary structure in A.

Importantly, PGRMC1 exhibits several phosphorylation sites which are differentially phosphorylated *in vivo*. Moreover, PGRMC1 exhibits two casein kinase (CK) phosphorylation sites (S57 and S181) in close proximity to the SH-domains which putatively influence the ability of PGRMC1 to interact with other proteins and may thereby regulate its function [25].

It is mainly expressed in mammalian liver and kidney, but can also be found in the brain, breast, reproductive tissue, heart, pancreas and other organs [5]. PGRMC1 has been mostly described in the endoplasmic reticulum, and this localization is the one with the highest consent among researchers [12]. Additionally, PGRMC1 has been found in the nucleolus [28],

in the cytoplasm [18] and in the mitochondrial membrane [29], emphasizing its potentially distinct functions. In the endoplasmic reticulum membrane, PGRMC1 mostly demonstrated a type 1 topology, presenting the C-terminus to the cytoplasm (Figure 1C) [12].

4.3. PGRMC1 – Associated Pathways

4.3.1. Impact on Heme Metabolism

Given the conserved structural motifs of PGRMC1 and ubiquitous presence of its homologs in (primitive) eukaryotic organisms, its primary function in cellular biology was hypothesized to concern basic cellular features like membrane trafficking and/or heme metabolism [12]. Indeed, PGRMC1's cytb5-like domain allows heme chelation, which has been demonstrated for murine PGRMC1 [30], rat PGRMC1 [31], human PGRMC1 [22] and for the yeast homolog Dap1 *in vitro* [32]. The occupation of PGRMC1 molecules with heme was reported to be around 0.6, indicating the existence of both the apo-PGRMC1 (without heme) and the holo-PGRMC1 (coordinating heme) [31]. Since heme is coordinated by only one axial ligand (Y113), the opposite axial site remains free to interact with other partners and potentially for dimerization, as demonstrated by Kabe *et al.* in 2016 and others.

Heme is an iron containing prosthetic group synthesized in the mitochondrial matrix and in the cytosol in a series of eight reactions and loaded with iron in the last step by the enzyme ferrochelatase (FECH). This last step is exerted in the mitochondria, where heme can be directly incorporated into mitochondrial respiratory complexes to serve in the electron transport chain [33]. However, heme is a nearly ubiquitous prosthetic group of hemoproteins with catalytic functions outside the mitochondria, e.g. in cytoplasm, in the nucleus, and in peroxisomes [34]. Heme is transported to respective localizations most likely not by diffusion, since unbound heme is reactive and may damage the cell by production of reactive oxygen species (ROS) or by unspecific reactions with cellular lipids. Instead, heme is bound to transport proteins that deliver it to specific destinations [33]. Intriguingly, the PGRMC1 homolog PGRMC2 has been recently demonstrated to act as a heme chaperone which shuttles heme from mitochondria to the nucleus [35]. For PGRMC1, a role as a heme chaperone has been hypothesized multiple times. As reviewed by McGuire *et al.*, the affinity of PGRMC1 for heme is similar to that of heme carriers, supporting this hypothesis [24]. Furthermore, the dissociation constant K_d of PGRMC1 is similar to free heme concentration in the cell, indicating sensitivity of PGRMC1 to cellular heme levels and compatible with description of both apo-

and holo-PGRMC1 species under physiological conditions [36]. Moreover, the possible heme-dependent dimerization of PGRMC1 could stabilize heme during transport.

In support of this hypothesis, PGRMC1 has been shown to interact with the iron transfer enzyme FECH in HEK293 cells [29] and in mouse liver [23]. Using mutant FECH proteins that mimic different conformations of FECH during the catalytic cycle, PGRMC1 was demonstrated to bind the enzyme in one specific conformation where heme has been newly synthesized [29]. In that situation, PGRMC1 could receive heme from FECH and safely transport it to hemoproteins at distant locations. One class of hemoproteins that interact with PGRMC1 are cytochrome p450 (CYP450) monooxygenases [22] and the nature of this interaction may be heme delivery to CYP450 enzymes by PGRMC1.

4.3.2. Interaction with CYP450-Enzymes

CYP450 monooxygenases are heme-binding enzymes responsible for oxidation of hydrophobic substances and therefore involved in metabolization of endogenous and exogenous water insoluble molecules. Further, CYP450 enzymes catalyze several reactions in the synthesis pathway of sterols (e.g. CYP51A1) and retinoids [37].

PGRMC1 was reported to interact with different CYP450 enzymes. For lanosterol demethylase, CYP51A1, this interaction was demonstrated in different studies, with one indicating a heme-dependent interaction [22] while conflicting findings indicated a heme-independent interaction with CYP51A1 and other CYP450-enzymes [23]. Intriguingly, interaction of PGRMC1 with CYP450 enzymes was not only demonstrated in human cells, but also for the *Schizosaccharomyces pombe* PGRMC1-homolog Dap1 with two CYP450 enzymes in the yeast sterol synthesis pathway - Erg11 and Erg5 - by Hughes *et al*. in 2007 [14]. Meanwhile, 19 CYP450 monooxygenases have been identified as potential PGRMC1 interaction partners by co-immunoprecipitation (and mass-spectrometry for one study) in mouse, human and yeast systems, as reviewed by McGuire *et al*. [24]. This list is likely not to be exclusive, since CYP450 expression is tissue-dependent and trigger-dependent for certain enzymes [38], [39]. Therefore, potential interaction of PGRMC1 with further CYP450 enzymes in different tissues or under different conditions may be possible. However, the biochemical nature of these interactions is not elucidated yet; and neither are the binding sites for CYP450 enzymes on PGRMC1 nor the dimerization status of PGRMC1 during those interactions known [24].

4.3.3. Impact on Sterol Homeostasis

Since the role of PGRMC1 in cholesterol and steroid synthesis is of special interest for this study, it shall be elucidated specifically.

Cholesterol homeostasis, involving uptake and export, metabolization, *de novo* synthesis, esterification and internalization into membranes, is strictly regulated. *De novo* synthesis of cholesterol is initiated by a protein complex including insulin induced gene 1 protein (INSIG), sterol regulatory element binding proteins (SREBPs), and SREBPs cleavage activation protein (SCAP) [13]. Under conditions of normal cholesterol levels, the complex consisting of INSIG/SREBPs/SCAP resides bound to the endoplasmic reticulum in an inactive state. As soon as sterol concentration drops under a certain level, the complex dissociates, SREBPs are cleaved by SCAP and escorted through the Golgi apparatus into the nucleus [40]. There, SREBPs co-activate transcription of sterol regulatory element responsive genes, leading to an up-regulation of the mevalonate pathway, increased cholesterol synthesis (mediated by SREBP-2) and fatty acid synthesis (mediated by SREBP-1). In fact, overexpression of SREBP-2 induces 12 genes responsible for cholesterol biosynthesis, including 3-hydroxy-3-methylglutaryl (HMG)-CoA synthase and HMG-CoA reductase, squalene synthase (FDFT1) and squalene epoxidase (SQLE) [41].

Interestingly, PGRMC1 has been discovered to directly interact with INSIG and SCAP, being mutually part of the complex and thereby contributing to cholesterol homeostasis [13]. Moreover, as discussed above, PGRMC1 interacts and activates CYP51A1 [14], an enzyme induced by SREBP-2 as part of the cholesterol synthesis pathway [41]. Once cholesterol is synthesized, PGRMC1 also influences its ATP-independent incorporation into the membrane and its step-wise conversion into estrogens via CYP19A1/aromatase [7]. The latter could contribute to the pathophysiology of breast cancer and will be discussed in the next section. In addition, farnesyl-pyrophosphate (FPP), an intermediate in cholesterol biosynthesis, is required for prenylation of proteins and synthesis of the co-enzymes ubiquinone and heme [42], closing the circle of heme metabolism.

4.4. PGRMC1 in (Breast) Cancer

4.4.1. Breast Cancer Physiology

In the year 2022, breast cancer had the highest incidence among women with an estimated number of 2.3 million new cases globally. Among women, breast cancer was also the leading

cause of cancer death [43]. In order to fight the disease, a deeper understanding of the molecular mechanisms of cancer formation and metastasis is needed.

Malignant transformation of healthy cells is a multistep process, characterized by acquisition of unnormal capabilities leading to autonomous cellular behavior. Over the course of lifetime and under pressure of environmental and intrinsic factors, cells acquire genetic alterations and epigenetic changes that govern tumorigenesis [44]. Although cancer is a highly heterogeneous disease, the acquired abnormal capabilities in the transformation process are shared by most cancers and were postulated as the “hallmarks of cancer” by Hanahan and Weinberg in 2000. Initially, six features were presented: self-sufficiency in growth-signals, insensitivity to antigrowth signals, evasion of apoptosis, limitless replicative potential, sustained angiogenesis and tissue invasion [45]. Meanwhile, these acquired features have been updated twice by the same authors, and now include 14 hallmarks of cancer [46]. Different cancers fulfil these hallmarks to a different extent and not every tumor subtype shows specific characteristics like genomic instability or inflammation. Some tumors are driven by deregulation or mutation of specific oncogenes (e.g. growth factor receptors) [47], while for other tumors no molecular driver can be identified [48]. Furthermore, loss or deactivation of characteristic tumor suppressor genes (surveillance genes, regulating e.g. DNA repair, cellular division and apoptosis) contributes to the tumorigenic cascade [49]. Knowledge about molecular characteristics of a tumor may provide treatment opportunities.

For breast cancer, classically four different molecular subtypes with characteristic features were defined, dependent on biomarkers expressed in malignant cells: estrogen receptor (ER), progesterone receptor (PR), human epidermal growth factor receptor 2 (HER2) and the proliferation marker Ki67 as immunohistochemical markers [50] (Table 1). Meanwhile, emerging data indicated existence of additional subgroups within the classical four, and cellular plasticity allows a continuous fluidity towards one or another subtype during disease progression, underlining the heterogeneity of breast cancer [51], [52], [53].

Table 1: Breast cancer subtypes based on immunohistochemical staining for estrogen receptor (ER), progesterone receptor (PR), human epidermal growth factor receptor 2 (HER2) and Ki67 as proliferation marker [50].

Subtype	ER/PR	HER2	Ki67
Luminal A	+	Not enriched	low
Luminal B	+	Not enriched	high
HER2-enriched	-	enriched	high
Triple negative	-	Not enriched	high

The molecular subtype is significantly associated with the course of disease as well as overall and relapse-free survival [54]. This is due to differences in malignancy between the subtypes on the one hand, and due to limited therapeutic options for triple negative breast cancer on the other hand, which are dependent on the expressed and targetable markers. Patients with hormone dependent luminal subtypes (around 70 % of all breast cancers) with expressed ER can be treated with endocrine therapy. While the first anti-estrogenic compound used for breast cancer treatment from the 1970ies – tamoxifen – is a competitive ER inhibitor [55], modern options additionally include aromatase inhibitors and selective ER degraders [56]. Patients with HER2-expressing cancers are regularly treated with anti-HER2 active agents (anti-HER2 antibodies, antibody-drug-conjugates and tyrosine kinase inhibitors). The therapy option of choice for patients with triple negative breast cancer (TNBC) is still mainly chemotherapy, with some additional options for specific cases [57].

4.5. Role of PGRMC1 in Breast Cancer Associated Pathways

PGRMC1 has been demonstrated to contribute to the development and progression of various cancers in multiple ways. *PGRMC1* mRNA is up-regulated in tumors of lung, head and neck, renal clear cells and esophagus [58]. On protein level, PGRMC1 was overexpressed in breast cancer tissues in multiple studies [20], [59], [60], in advanced cervical cancer [61], in lung cancer, ovarian cancer and head and neck cancer [62] and renal cell carcinoma [63]. Moreover, the increased expression of PGRMC1 in cancer tissue correlated with a worse prognosis and outcome for several cancer types, including lung- [62], renal cell- [63] and breast cancer [20].

4.5.1. Breast Cancer and Sterol Homeostasis

Dietary cholesterol has been associated with a risk for several types of cancer, among them prostate and breast cancer [64], [65], [66], [67]. However, older and recent studies failed to

provide a clear picture on the relationship between breast cancer risk, tumor initiation and plasma cholesterol level, providing controversial results [68].

Although the role of cholesterol in the initial formation of breast cancer is not elucidated yet, clear evidence exists that elevated cholesterol levels contribute to cancer proliferation and progression, once a tumor is formed. In cell lines as well as in animal models, low density lipoprotein (LDL) cholesterol promoted cell proliferation and tumor growth [69]. In mice models, high-fat/high-cholesterol diet resulted in enhanced tumor progression in transgenic mice spontaneously developing mammary cancer [70], and in immunodeficient mice orthotopically implanted with the TNBC cell line MDA-MB-231 [71]. Further, several groups reported that not only plasma cholesterol affects cancer cell proliferation [72], but also endogenous cholesterol levels can be elevated by cancer cells during cancer progression [73], [74].

The mode of action of cholesterol on tumor cells is diverse (Figure 2). Since rapidly proliferating cancer cells have an increased requirement for cholesterol as membrane component, its abundance may be a limiting factor for tumor growth [75]. Cholesterol is thought to be stored in intracellular lipid droplets [76]. Incorporated into the plasma membrane, cholesterol is a major component of lipid rafts - small rigid structures in the membrane high in saturated fatty acids, which contain a large number of signaling molecules [77]. Intracellular cholesterol concentration may influence the size and number of lipid rafts in cell membranes and thereby impact signaling cascades which are initiated at the membrane [78]. Indeed, cholesterol seems to affect lateral motion of the well characterized oncogenes epithelial growth factor receptor (EGFR) and HER2 through the membrane [79]. Moreover, elevated concentrations of cholesterol were reported to enhance activation of phosphoinositide 3-kinase (PI3K) and the serine/threonine kinase AKT, both downstream targets of EGFR [75], [80].

Furthermore, cholesterol is a precursor for steroid hormones such as estradiol (E2), which represents a major growth factor in hormone receptor positive breast cancers [81]. Besides, a number of biologically active cholesterol metabolites exist, which might partly act as selective estrogen receptor modulators (SERMs), thereby enhancing cell proliferation and tumor growth [82] (Figure 2).

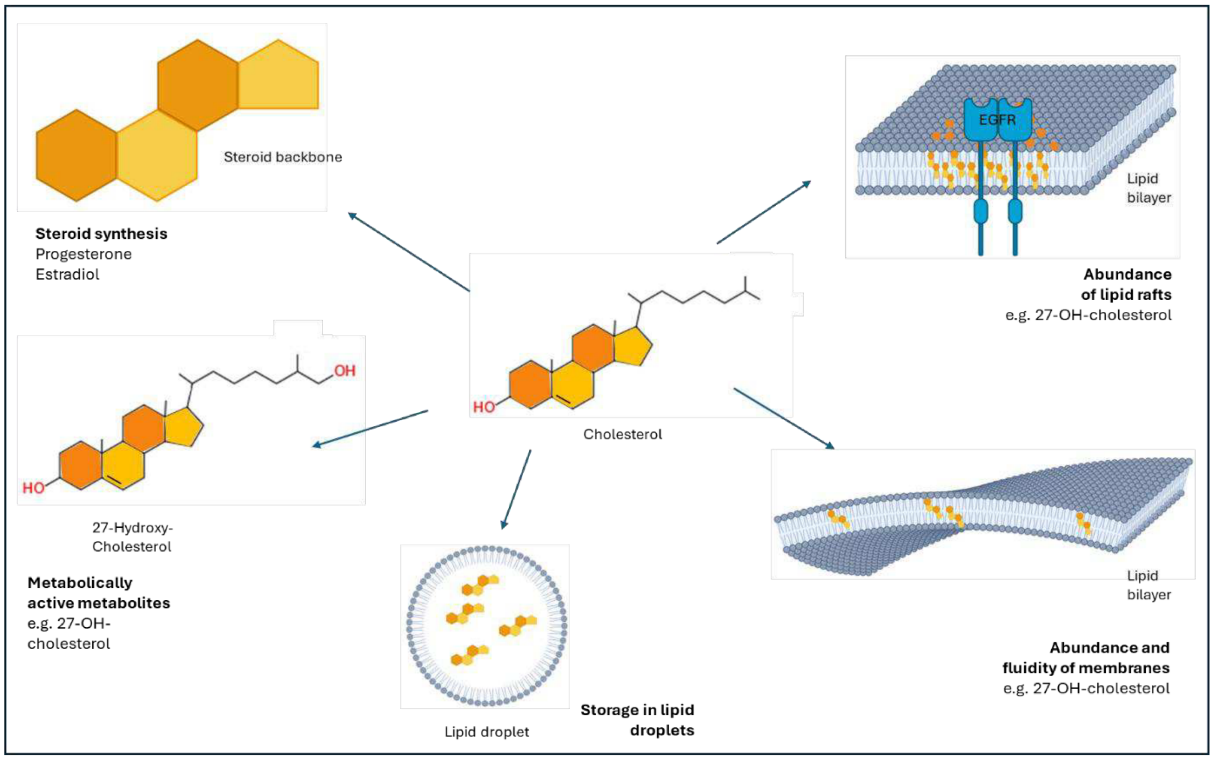

Figure 2: Potential mechanisms by which cholesterol influences breast cancer physiology, based on Nelson et al, 2014 [75]. As membrane component, cholesterol has an impact on membrane abundance and fluidity, and on lipid rafts, thereby influencing signaling and proliferation. It is furthermore a precursor for steroids and a number of biologically active signaling molecules. Created with BioRender.

With respect to cholesterol homeostasis, PGRMC1 may co-regulate cholesterol and steroid synthesis and thereby contribute to cancer pathophysiology. As reviewed above, PGRMC1 associates with the cholesterol-sensing complex Insig/SCAP/SREBP that regulates the mevalonate pathway [13] and moreover interacts with Cyp51A1, the CYP450 enzyme that synthesizes the first sterol, lanosterol [22]. Through enhancement of cholesterol production, PGRMC1 overexpression in breast cancer could lead to increased cancer progression. Further, PGRMC1 has been shown to associate with the Sigma-2 receptor, a protein that PGRMC1 was first mistaken for, and the complex increases cellular uptake of LDL [9]. This way, not only endogenous production but also uptake could potentially be co-regulated by PGRMC1.

4.5.2. PGRMC1 in Oncogenic Signaling

In breast cancer, the most frequently mutated or deregulated oncogenes are reportedly the receptor tyrosine kinase HER2, amplified in around 20%-30% of breast cancers [83], the estrogen receptor alpha (ERα), expressed in hormone receptor positive breast cancers and mutated in 30% of patients with relapse [84], and the kinases phosphatidylinositol 3-kinase (PI3K) and protein B kinase (AKT), mutated in approximately 45% of breast cancers [85]. ERα was recently associated with the promotion of translocations and focal amplifications of other

oncogenes, suggesting estrogen signaling as the mechanistic origin of breast cancer [86]. The receptor tyrosine kinase EGFR, a frequently activated oncogene in cancers, is expressed in 53% of breast cancers, mainly in hormone receptor negative subtypes, and associated with a worse prognosis [87]. For the gene encoding cell-cycle controlling protein cyclin D1, overexpression and amplification has been demonstrated in around 50% of breast cancers, although the relation between cyclin D1 expression and malignancy is controversial [88], [89]. These oncogenes confer proliferative signals to breast cancer cells and promote malignant transformation and cancer progression.

At the same time, deregulation or mutation of tumor suppressor genes guarding cell cycle, DNA replication and entrance into apoptosis occur for the tumor suppressors TP53 (around 30% of breast tumors [90]), phosphatase and tensin homolog PTEN (20% of breast tumors [91] and retinoblastoma (Rb; up to 30% of breast cancers [92]). Additionally, inherited germline mutations in the tumor suppressor genes breast cancer gene 1 and 2 (*BRCA1, BRCA2*), encoding for proteins involved in DNA repair, are associated with a cumulative breast cancer risk to age of 80 of around 70 % [93]. This list is not exclusive but shall underline the multifactorial and heterogeneous implications of cellular pathways in breast cancer progression.

PGRMC1 has been shown to influence some of the above-mentioned pathways in multiple ways. In two studies, PGRMC1 exhibited a proliferative effect in ERα positive breast cancer cell line MCF-7 in mouse xenograft models as well as in cell culture, when simultaneously treated with progestogens [94], [21]. The phosphorylation status of PGRMC1 differs between ERα positive and negative breast cancers, suggesting a hormone-dependent diversity of PGRMC1-related pathways [95]. Furthermore, PGRMC1 has been shown to bind EGFR and promote signaling, potentially leading to enhanced proliferation in cancer cells [22]. Downstream of EGFR, PGRMC1 is tightly connected to PI3K/Akt pathway, and signaling via PI3K/Akt is influenced by PGRMC1 phosphorylation [96]. A study in human pluripotent stem cells (hPSC) revealed that PGRMC1 suppresses both p53 and Wnt/β-catenin dependent pathways and promotes self-renewal and stemness of hPSC. In addition to p53, *Wnt* is a well characterized tumor suppressor gene, which is central in regulation of differentiation [97]. The implication of PGRMC1 in these mechanisms emphasizes its potential role in cancer development.

Taken together, PGRMC1 is involved in conserved cellular functions and key signaling pathways, suggesting its potential role during deregulation of essential mechanisms in disease. Although the major function of PGRMC1 in cellular biology is still subject of research, it has been associated with Alzheimer's disease, diabetes and cancer [12]. With respect to breast cancer, PGRMC1 expression correlates with worse outcomes and increased aggressiveness, potentially making PGRMC1 a marker of malignancy. A possible link of PGRMC1 and tumorigenesis could be cross-talk with oncogenic pathways, such as ERα- and EGFR-signaling. However, the superior role of PGRMC1 in cellular metabolism remains unclear.

4.6. Aim of the Study

To gain insights into basic PGRMC1 functions and thereby elucidate the mechanism of PGRMC1-involvement in breast cancer progression, this study focused on:

1. Analysis of PGRMC1 interaction partners and related pathways, originating from previous interactome studies performed by Ludescher (née Willibald) [98], with a special focus on mevalonate and lipid homeostasis;
2. Generation of new PGRMC1-null cellular breast cancer models using CRISPR/Cas9 technology to study potential effects of PGRMC1-deficiency;
3. Employment of all available models to analyze PGRMC1-interaction partners in the context of ERα-signaling upon stimulation with synthetic progestogens and confirm PGRMC1-dependent indirect ERα-regulation in hormone receptor positive breast cancer cells;
4. Expansion of the established findings on PGRMC1 interaction partners to an additional model, decidualization of endometrial stromal cells, emphasizing the broad context of PGRMC1's conserved ancient impact on cellular biology.

5. PGRMC1 Interacts with Enzymes in the Mevalonate Pathway (Aim 1)

5.1. Manuscript I

"Progesterone receptor membrane component 1 regulates lipid homeostasis and drives oncogenic signaling resulting in breast cancer progression"

Hannah Asperger, **Nadia Stamm**, Berthold Gierke, Michael Pawlak, Ute Hofmann, Ulrich M. Zanger, Annamaria Marton, Robert L- Katona, Andrea Buhala, Csaba Vizler, Jan-Philipp Cieslik, Eugen Ruckhäberle, Dieter Niederacher, Tanja Fehm, Hans Neubauer und Marina Ludescher

Original research article in *Breast Cancer Research*

Impact factor: 6.5 (2020)

Authorship: second author

Status: published in July 2020

DOI: 10.1186/s13058-020-01312-8

Full citation: Asperger, H., Stamm, N., Gierke, B. *et al.* Progesterone receptor membrane component 1 regulates lipid homeostasis and drives oncogenic signaling resulting in breast cancer progression. *Breast Cancer Res* **22**, 75 (2020). https://doi.org/10.1186/s13058-020-01312-8

Author contribution:

I planned and performed following experiments: validation of mass-spectrometry data by co-immunoprecipitation of PGRMC1 and western blot analysis of co-precipitated proteins (SCD1, Cyp51A1, FDFT1), proximity ligation assay (Figure 1, B-D), expression analysis of candidate proteins (Figure 2, C, F). I analyzed data, performed statistical tests and visualized the results for the respective experiments and revised the written manuscript.

5.2. Summary

This study investigates the role of PGRMC1 in breast cancer progression, focusing on its regulation of lipid homeostasis and involvement in oncogenic signaling pathways. To unravel PGRMC1's role in breast cancer progression, identification of PGRMC1 interaction partners was performed by co-immunoprecipitation and mass spectrometry, followed by functional analysis of these interactions.

PGRMC1 was detected to associate with enzymes in the cholesterol synthesis pathway, including CYP51, FDFT1, and SCD1, both in co-immunoprecipitation and proximity ligation assay. PGRMC1-overexpressing cells further exhibited higher cholesterol and neutral lipid levels, potentially promoted by the interactions detected before. Of note, levels of estradiol secreted to the culture medium were increased in PGRMC1-overexpressing cells. Moreover, overexpression of PGRMC1 enhanced cell proliferation both *in vitro* and in xenograft mouse models. Additionally, PGRMC1 influenced the formation of lipid rafts, potentially altering membrane receptor composition. In line with this finding, PGRMC1-overexpression led to enhanced EGFR and ERα signaling—key pathways in breast cancer progression. Importantly, depleting cholesterol through statin treatment reverted the growth advantage conferred by PGRMC1 overexpression, indicating that lipid metabolism was central to PGRMC1's oncogenic effects.

In conclusion, PGRMC1 promoted cancer cells proliferation by modulating cholesterol metabolism, lipid raft formation, and activating ERα and EGFR signaling. These findings suggest that targeting PGRMC1 or cholesterol synthesis pathways could provide novel therapeutic strategies for hormone receptor-positive breast cancer.

Asperger et al. Breast Cancer Research (2020) 22:75
https://doi.org/10.1186/s13058-020-01312-8

Breast Cancer Research

RESEARCH ARTICLE Open Access

Progesterone receptor membrane component 1 regulates lipid homeostasis and drives oncogenic signaling resulting in breast cancer progression

Hannah Asperger[1], Nadia Stamm[1], Berthold Gierke[2], Michael Pawlak[2], Ute Hofmann[3], Ulrich M. Zanger[3], Annamaria Marton[4], Robert L. Katona[5], Andrea Buhala[4], Csaba Vizler[4], Jan-Philipp Cieslik[1], Eugen Ruckhäberle[1], Dieter Niederacher[1], Tanja Fehm[1], Hans Neubauer[1*†] and Marina Ludescher[1†]

Abstract

Background: PGRMC1 (progesterone receptor membrane component 1) is a highly conserved heme binding protein, which is overexpressed especially in hormone receptor-positive breast cancer and plays an important role in breast carcinogenesis. Nevertheless, little is known about the mechanisms by which PGRMC1 drives tumor progression. The aim of our study was to investigate the involvement of PGRMC1 in cholesterol metabolism to detect new mechanisms by which PGRMC1 can increase lipid metabolism and alter cancer-related signaling pathways leading to breast cancer progression.

Methods: The effect of PGRMC1 overexpression and silencing on cellular proliferation was examined in vitro and in a xenograft mouse model.
Next, we investigated the interaction of PGRMC1 with enzymes involved in the cholesterol synthesis pathway such as CYP51, FDFT1, and SCD1. Further, the impact of PGRMC1 expression on lipid levels and expression of enzymes involved in lipid homeostasis was examined. Additionally, we assessed the role of PGRMC1 in key cancer-related signaling pathways including EGFR/HER2 and ERα signaling.

Results: Overexpression of PGRMC1 resulted in significantly enhanced proliferation. PGRMC1 interacted with key enzymes of the cholesterol synthesis pathway, alters the expression of proteins, and results in increased lipid levels. PGRMC1 also influenced lipid raft formation leading to altered expression of growth receptors in membranes of breast cancer cells. Analysis of activation of proteins revealed facilitated ERα and EGFR activation and downstream signaling dependent on PGRMC1 overexpression in hormone receptor-positive breast cancer cells. Depletion of cholesterol and fatty acids induced by statins reversed this growth benefit.

(Continued on next page)

* Correspondence: Hans.Neubauer@med.uni-duesseldorf.de
†Hans Neubauer and Marina Ludescher contributed equally to this work.
[1]Department of Obstetrics and Gynecology, University Hospital and Medical Faculty of the Heinrich-Heine University Duesseldorf, Life Science Center, Merowingerplatz 1A, 40225 Düsseldorf, Germany
Full list of author information is available at the end of the article

(Continued from previous page)
Conclusion: PGRMC1 may mediate proliferation and progression of breast cancer cells potentially by altering lipid metabolism and by activating key oncogenic signaling pathways, such as ERα expression and activation, as well as EGFR signaling. Our present study underlines the potential of PGRMC1 as a target for anti-cancer therapy.

Keywords: PGRMC1, Breast cancer, Tumor progression, Cholesterol, Lipids, Estrogen receptor α, HER2, EGFR, Breast cancer signaling pathway

Background

With approximately 25% of all new cancer cases, breast cancer is the most common cancer in women [1] and responsible for the highest fraction of cancer death [2]. Therefore, the investigation of underlying mechanisms on molecular levels and the discovery of new therapy approaches are research goals of utmost significance.

Progesterone receptor membrane component 1 (PGRMC1) is a highly conserved protein, which is primarily found in the liver and kidney but also expressed in various tissues such as brain, breast, lung, pancreas, and reproductive tissues [3–5].

PGRMC1 has been confirmed to play a role in carcinogenesis especially in breast cancer and may therefore represent a target for cancer therapy [6]. In many studies, upregulation of PGRMC1 protein and mRNA was detected in malignancies including colon, lung, ovary, cervix, and breast [7–11]. Besides, PGRMC1 expression correlates with metastasis to lymph nodes, larger tumor size, and poorer overall- and tumor-free survival [9, 12]. Further, interactions of PGRMC1 or its homologous proteins with cytochrome P450 enzymes (CYPs) have been reported, for example by stably binding heme in its cytb5 related domain [3, 5, 13–15]. PGRMC1 leads to resistance against chemotherapeutic agents like doxorubicin, cisplatin, and paclitaxel [13, 16, 17]. Moreover, different authors discuss an involvement of PGRMC1 in cholesterol synthesis via interaction with CYPs [3, 5, 18]. The role of cholesterol in cancer is still not fully evaluated. Many studies describe an association of high plasma and endogenous cholesterol levels with (breast) cancer development and progression [19–21], pointing towards a major role in cancer. Elevated cholesterol and steroid levels may affect carcinogenesis in different ways, e.g., in saturating the increased requirement for membrane components due to abundant cell growth [22]. Furthermore, high cholesterol levels result in an increase in the size and number of lipid rafts. Since lipid rafts contain several signaling molecules, differences in lipid rafts are modulating signaling cascades [23, 24], such as EGFR and HER2 signaling and expression [25]. In addition, cholesterol is the precursor of steroid hormones like estradiol (E2), the important growth factor for hormone receptor-positive breast cancer [26].

The aim of the present study was to investigate the impact of PGRMC1 on lipid metabolism, lipid raft formation, and its contribution to breast cancer progression and cancer-associated signaling pathways in hormone receptor-positive (MCF7) and hormone receptor-negative (MDA-MB-231) cells. For this purpose, interaction of PGRMC1 with enzymes of the mevalonate pathway was evaluated. Subsequently, effects of PGRMC1 expression on cholesterol and lipid levels were investigated. A special focus was placed on PGRMC1-dependent expression and signaling of ERα and EGFR/HER2. To explore the impact of modified lipid and steroid metabolism (due to PGRMC1 expression), breast cancer cell growth was further explored by PGRMC1 overexpression and -silencing.

Methods

Cells and cell culture

MCF7, T47D, and MDA-MB-231 cells were purchased from the ATCC (Manassas, Virginia). Cells were maintained in RPMI 1640 medium (Thermo Fisher Scientific, Waltham, Massachusetts), supplemented with 10% (v/v) fetal bovine serum (Thermo Fisher Scientific, Waltham, Massachusetts), 100 units/mL penicillin/streptomycin (Thermo Fisher Scientific, Waltham, Massachusetts), and 0.025 mol/L HEPES (Thermo Fisher Scientific, Waltham, Massachusetts) in a humidified incubator at 37 °C with 5% CO_2. Cells (passage number ≤ 25) were authenticated regularly by Microsynth AG (Balgach, Switzerland) using STRS analysis. The last authentication was performed on May 22, 2018.

Transfection of cell lines

Cells were transfected with the expression vector pcDNA3.1/Hygro(+) (Thermo Fisher Scientific, Waltham, Massachusetts), containing 3x HA-tagged (3x human influenza hemagglutinin-tagged) PGRMC1, using Lipofectamine™ 2000 transfection reagent (Thermo Fisher Scientific, Waltham, Massachusetts) (MCF7/PGRMC1, T47D/PGRMC1 and MDA-MB-231/PGRMC1). As a control, we used cells transfected with the "empty" vector (MCF7/EVC, T47D/EVC, and MDA-MB-231/EVC). Stable transfection was verified by PCR, western blot, and immunofluorescence staining, to isolate PGRMC1-over-expressing clones.

siRNA silencing of endogenous PGRMC1

For silencing of endogenous PGRMC1 in MCF7 cells, FlexiTube GeneSolution for PGRMC1 (Qiagen, Hilden, Germany) was used, containing four siRNAs that specifically target human PGRMC1 mRNA. Cells were harvested after cultivation for 24 h, 48 h, and 72 h at 37 °C to verify silencing by western blot analysis.

For MTT assays, cells were pre-incubated with siRNA against PGRMC1 for 24 h at 37 °C in cell culture flasks to silence the endogenous protein. Subsequently, the cells were seeded in 96-well plates and again treated with siRNA. Cell viability was measured after 24 h, 48 h, and 72 h at 37 °C of incubation.

MTT assay

Cells (5×10^4 cells per well) were seeded in triplicates in 96-well plates in complete medium. Cells were either grown (for different timespans) in full medium without or with treatment. Afterwards cells were incubated with 0.25 mg/ml MTT solution for 3 h. After 1 h of incubation with DMSO, absorption at 540 nm was determined with TECAN Spark®.

Quantification of lathosterol and cholesterol

Cholesterol and lathosterol were quantified by gas chromatography-mass spectrometry analysis as described previously (Maier et al., 2009), with minor modifications.

Western blot analysis

Samples for western blot analysis and the respective molecular weight marker were loaded onto Mini-PROTEAN® Precast Gel and separated via SDS-Page at 150 V. We activated the PVDF membrane with methanol. Transmission of proteins was performed for 16 h at 4 °C and 10 mA in blotting buffer. Afterwards, unspecific binding was blocked by incubation of the PVDF membrane with the transferred proteins with blocking solution for 1 h at room temperature. Primary antibody in respective concentration was added in blocking solution and incubated for 16 h at 4 °C. Subsequently, a secondary antibody was applied in 20% blocking solution at room temperature. Proteins were detected using Amersham™ ECL™ Western Blotting Detection Reagent.

Co-immunoprecipitation

Immunoprecipitation of HA-tagged PGRMC1 and HA-tagged PGRMC1-variants was performed using the Pierce™ HA-Tag IP/Co-IP Kit according to the manufacturer's instructions. Cells overexpressing GFP-tagged PGRMC1 were used as a negative control. Cell pellets were resuspended in Co-IP lysis buffer. An amount of 500-µg protein was incubated with anti-HA agarose slurry at 4 °C overnight. For elution, proteins were denatured in sample buffer at 95 °C for 5 min and the eluent was supplemented with 1 M DTT. The elution of PGRMC1 and mutual interaction partners was analyzed directly via mass spectrometry (explained in the supplements), SDS-PAGE, and western blot.

Proximity ligation assay (PLA)

The PLA procedure was performed using the Duolink® PLA Kit. Cells were grown in chamber slides. Incubation with the primary antibody cocktail containing anti-PGRMC1 antibody and antibody against one of the possible interaction partners (or rabbit isotype IgG as negative control) was performed overnight at 4 °C.

Additionally, staining with anti-cytokeratin antibody for 1 h was performed after amplification. Afterwards, cells were stained with DAPI for 10 min and analyzed by fluorescence microscopy within 1 week.

Reverse phase protein array (RPPA)

RPPA using Zeptosens technology was used for analysis of signaling protein expression and activity profiling.

RPPA assay images were analyzed using ZeptoVIEW Pro 3.1 array analysis software. Sample signals were quantified as protein-normalized, blank-corrected mean fluorescence intensities (NFI) of the single spots applying linear fits and interpolation to the mean of the four printed sample dilutions (eight spots per sample).

qRT-PCR

RNA was isolated from a cell pellet of 0.5×10^6 cells using the RNeasy Mini Kit (Qiagen, Hilden, Germany) according to the manufacturer's specifications.

Reverse transcription of RNA into cDNA was performed with the Omniscript RT kit (Qiagen, Hilden, Germany) according to the manufacturer's instructions. For qPCR, QuantiFast SYBR Green PCR kit (Qiagen, Hilden, Germany) and RT [2] qPCR Primer assays for ESR1, HER2, TFF1, Myc, CCND1, PGR, SCD, FASN, HMGS1, SREBF1, SREBF2, LDLR, ACAT1, and PDH (Qiagen, Hilden, Germany) were used according to the manufacturer's specifications. qPCR was performed using the LightCycler® 480 System (Roche, Penzberg, Germany).

Estradiol ELISA

Supernatants of MCF7/EVC and MCF7/PGRMC1 cells were analyzed for 17β-Estradiol (E2) concentrations using a commercially available kit (ab108667, Abcam plc, Cambridge, UK) according to the manufacturer's specifications.

Staining for lipid rafts and HER2

Co-staining of HER2 with lipid rafts was performed in PGRMC1 overexpressing MCF7 and MDA-MB-231 cells

and their respective empty vector controls. Cells were seeded in a chamber slide for 24 h. Afterwards, the medium was removed, and the cells were incubated for another 24 h with medium containing stripped FCS and were then incubated for 24 h with medium containing normal FCS. Staining of lipid rafts was performed using Vybrant™ Alexa Fluor™ 488 Lipid Raft Labeling Kit. Afterwards, cells were fixed with 4% formaldehyde for 10 min. DAKO® protein block was used to block unspecific binding sites for 1 h. Following this, cells were stained with antibodies specific for HER2 (ab16901) over night at 4 °C followed by an anti-mouse secondary-antibody (Alexa Fluor 549 labeled) for 1 h. As negative control mouse isotype IgG was used. After this, staining with DAPI was performed. Subsequently cells were examined by fluorescence microscopy using Axioplan 2 Imaging (Carl Zeiss Microscopy GmbH, Jena, Germany). For analyzing the amounts of lipid rafts and HER2 via flow cytometry, cells were seeded in culture flasks and synchronized as described above. Staining and fixation was performed as described above. The emission (488 nm wavelength) was detected via high throughput flow cytometry (CyAn, Beckman Coulter, Brea, USA).

Staining of lipid droplets

For visualizing of lipid droplets in PGRMC1 overexpressing MCF7, T47D, and MDA-MB-231 cells and their respective empty vector controls via fluorescence microscopy, the cells were grown in chamber slides for 24 h. Afterwards cells were stained with BODIPY™ 493/503 (Sigma-Aldrich, St. Louis, Missouri) solubilized in FCS-free medium and 2% BSA for 30 min. Cells were fixed with 4% formaldehyde for 10 min, stained with DAPI, and examined by fluorescence microscopy. For analyzing amounts of lipid droplets via flow cytometry, cells were grown for 24 h and harvested with trypsin. Staining was performed as described above. The emission (488-nm wavelength) was detected via high throughput flow cytometry (CyAn, Beckman Coulter, Brea, USA).

Scatter plots of breast cancer microarray data

We obtained normalized microarray data (Affymetrix Human Genome U133A Array) from the Gene Expression Omnibus (GEO, NCBI) [27]. The samples were normalized using global scaling by the data set authors. We confirmed the value distribution using mean values and boxplots. Technical replicates were averaged. The values of a selected panel of reporters were correlated against a PGRMC1 reporter utilizing Spearman's correlation.

Xenograft models

NOD.CB17-Prkdc^{scid} (SCID) mice (female, 6-weeks old) were obtained from the Jackson Laboratory (Bar Harbor, Maine) and were bred in the SPF animal facility of the Institute of Genetics at the Biological Research Centre, Szeged, Hungary. Young adult SCID female mice were transplanted subcutaneously in the flank with 17β-estradiol pellet (containing biodegradable carrier-binder, 1.7 mg/pellet, 60-day release; SE-121, Innovative Research of America, Sarasota, Florida) under pentobarbital anesthesia. The next day, the mice were injected subcutaneously with 3×10^6 tumor cells in the opposite flank. The mice were checked daily, and the tumor size was measured twice weekly. At the end of the experiment, the animals were euthanized, by pentobarbital overdose, and the tumors dissected.

Treatment with simvastatin

For treatment with simvastatin, cells (10^5 cells per well) were seeded in 96-well plates in complete medium for 24 h/37 °C. Afterwards, the medium was removed and the cells were incubated with 100, 50, 25, 12.5, 6.25, and 3.125 μg/mL simvastatin for MCF7 cells and 20, 10, 5, 2.5, 1.25, and 0.625 μg/mL simvastatin for MDA-MB-231. MTT assays were performed after 24 h, 48 h, and 72 h.

Statistical analysis

All experiments were performed with several independent biological replicates and repeated a minimum of three iterations. Results are reported as means with standard deviation. The data were tested for normal distribution using Shapiro-Wilk and Kolmogorov-Smirnov test. Differences between groups were determined by unpaired Student's t test. Statistical analysis was performed using R (RStudio) and IBM SPSS. Spearman's ρ was calculated in R using normalized microarray data and was plotted as a scatterplot using the ggpubr R library. $p < 0.05$ was considered as statistically significant.

Results

PGRMC1 promotes viability of breast cancer cells and growth of xenograft tumors while PGRMC1 inhibition and downregulation reduce viability of breast cancer cells

As already shown in previous studies by us and others, PGRMC1 overexpression results in increased proliferation of tumor cells [28–30]. In accordance with these results, in our study, MCF7/PGRMC1 and T47D/PGRMC1 cells also profit from a significantly higher viability compared to the respective empty vector control cells (Fig. 1b, supplemental Figure 1A). For MDA-MB-231 cells overexpressing PGRMC1, no such effects can be observed (Fig. 1b). To further strengthen our theory, we examined the impact of PGRMC1 silencing on tumor proliferation by knocking down endogenous PGRMC1 expression. As hypothesized, the knockdown of PGRMC1 led to significantly decreased viability of MCF7 and T47D

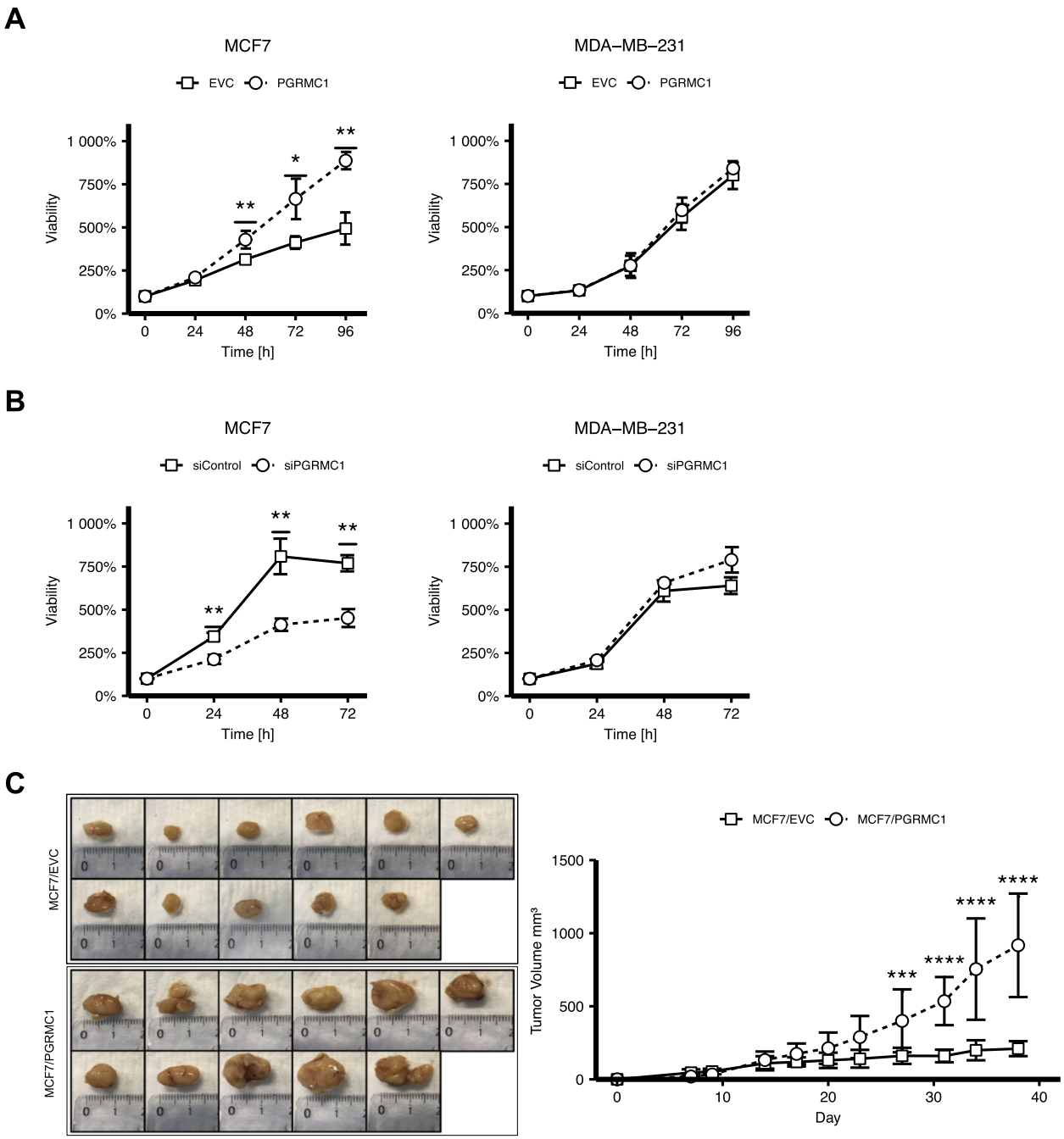

Fig. 1 **a** Cell viability of MCF7/EVC and MCF7/PGRMC1 cells as well as MDA-MB-231/EVC and MDA-MB-231/PGRMC1 cells ($n = 3$). Viability was analyzed by MTT assay at $t = 0$ h, 24 h, 48 h, 72 h, and 96 h/37 °C. Values were normalized to $t = 0$ (100%). *$p \leq 0.05$, **$p \leq 0.01$ (Student's t test, $n = 3$). **b** Cell viability of MCF7 and MDA-MB-231 cells, treated with siRNA against *PGRMC1* (siPGRMC1) and scrambled siRNA (siControl) (Student's t test, $n = 3$). Viability was analyzed at $t = 0$ h, 24 h, 48 h, and 72 h/37 °C. Values were normalized to $t = 0$ (100%). *$p \leq 0.05$, **$p \leq 0.01$ (Student's t test, $n = 3$). **c** Tumor volumes of immunodeficient mice bearing human breast cancer MCF7/EVC and MCF7/PGRMC1 xenografts. ***$p \leq 0.001$, ****$p \leq 0.0001$ (Student's t test, $n = 11$ mice each group). Images of tumor tissue dissected from each mouse

cells but not of MDA-MB-231 cells (Fig. 1a, supplemental Figure 1B).

To validate and strengthen the in vivo findings of Ruan et al. [30], to verify "our" cell models but also to extend the data to other ER-positive BC cells, we investigated effects of PGRMC1 overexpression on MCF7 and T47D breast cancer cell growth in a xenograft model. On that account, MCF7/PGRMC1 and T47D/PGRMC1 cells were injected into the flanks of immunodeficient mice. As control, we used EVC cells.

Subsequently, the size of the developed tumor mass was measured. As assumed, mice injected with PGRMC1 overexpressing breast cancer cells matured significantly larger tumor masses, than mice injected with the respective EVC cells (Fig. 1c, supplemental Figure 1C).

PGRMC1 interacts with proteins of the mevalonate pathway

As already shown in previous studies from different research groups, PGRMC1 might regulate cholesterol synthesis in different ways, e.g., by activating enzymes of the mevalonate pathway like CYP51/lanosterol demethylase or by binding to the proteins Insig and Scap, which span the endoplasmic reticulum and sense cholesterol levels [31, 32]. In our present study, we focused on this regulating influence and its possible involvement in PGRMC1-induced breast cancer promotion.

In order to get a broader view about the role of PGRMC1 in this context, we screened for potential PGRMC1 interaction partners by mass spectrometry analysis of proteins co-immunoprecipitated from whole cell lysates of MCF7 cells that had been transfected with PGRMC1-HA, utilizing an antibody directed against the HA-tag (Fig. 2a). Among proteins with higher significance, we found various potential interaction partners involved in the mevalonate pathway (e.g., SCD1, FDFT1, and CYP51A1) and cellular transport processes such as vesicle trafficking (e.g., Coatomer subunit beta and Coatomer subunit gamma-1) and nuclear export or import (e.g., Exportin-1, Exportin-2, Exportin-5, Exportin-7 or Importin-4 and Importin-5) processes. Since SCD1, FDFT1, and CYP51A1 indicate a high evidence for protein interaction with PGRMC1 and since they play an important role in cholesterol metabolism, we scrutinized these interactions. Interaction of PGRMC1 with SCD1, FDFT1, and CYP51A1 was confirmed by immunoprecipitating PGRMC1-HA in MCF7/PGRMC1 cells and by subsequently visualizing the respective interaction partners via western blot (Fig. 2b). To verify the observed interactions in different cell lines independently of PGRMC1 overexpression and immunoprecipitation, we performed proximity ligation assay of candidate proteins with endogenous PGRMC1 in MCF7 (Fig. 2c) and MDA-MB-231 cells (supplemental Figure 1B). Interactions between PGRMC1 and the respective enzymes are represented by single spots in fluorescence microscopy. While in MCF7 cells, a high number of spots per cell were visible for the interaction with CYP51, FDFT1, and SCD1, the low number of spots in MDA-MB-231 cells indicated no or little interaction (Fig. 2d). Interactions of PGRMC1 with FDFT1 and SCD1 were also observed in T47D cells (supplemental Figure 2B,C). Western blot analysis of protein expression of SCD1, FDFT1, and CYP51 revealed higher CYP51 and SCD1 protein levels in MCF7/PGRMC1 cells compared to MCF7/EVC, while no difference in MDA-MB-231/PGRMC1 cells could be observed compared to MDA-MB-231/EVC cells (Fig. 2e). These results implicate not only a direct interaction of PGRMC1 with SCD1, FDFT1, and CYP51, but also an increased PGRMC1-driven upregulation of these enzymes in estrogen receptor-positive cells, that appeared absent in hormone receptor-negative cells.

Overexpression of PGRMC1 leads to higher levels of cholesterol in hormone receptor-positive breast cancer cells

We hypothesized that the interaction of PGRMC1 with enzymes of the mevalonate pathway might alter their function and thus affects cholesterol synthesis, resulting in elevated cholesterol levels, which may provide energy and components supporting cancer metabolism. Therefore, we measured intracellular cholesterol levels in synchronized PGRMC1 overexpressing and empty vector control MCF7 and MDA-MB-231 cells via mass spectrometry (Fig. 2f). Overexpression of PGRMC1 in MCF7 cells caused a significant increase ($p < 0.05$) of intracellular cholesterol levels compared to the empty vector control, while no difference in MDA-MB-231/PGRMC1 cells was observed (Fig. 2f). Additionally, levels of lathosterol, a precursor of cholesterol, were measured (Fig. 2f). For MCF7/PGRMC1 cells, we detected a significantly decreased ratio compared to MCF7/EVC cells. Interestingly, a significantly decreased ratio of lathosterol/cholesterol in MDA-MB-231/PGRMC1 cells was observed compared to MDA-MB-231/EVC cells, pointing towards a small influence of PGRMC1 on cholesterol de novo synthesis in these cells. The data reveal an impact of PGRMC1 on de novo synthesis of cholesterol regarding cholesterol levels and enzymatic turnover.

Upregulation of ERα, ERα downstream targets, and E2 levels mediated by PGRMC1

Since cholesterol is the precursor for steroid hormones, we assumed that enhanced cholesterol synthesis may affect E2 levels. E2 plays an essential role in hormone receptor-positive breast cancer, e.g., by activating ERα which is leading to tumor proliferation. E2 levels were determined in the supernatant of MCF7/PGRMC1 cells by ELISA (Fig. 3a). Consistent with the higher amounts of cholesterol in MCF7/PGRMC1 cells, we found significantly increased levels of E2 in the supernatant of MCF7/PGRMC1 cells in comparison to MCF7/EVC cells. To analyze the effect of higher E2 levels in MCF7/PGRMC1 cells on breast cancer signaling, we determined the expression of different proteins known to play a role in key signaling cascades in breast cancer via reverse phase protein array technology (RPPA) (Fig. 3b). RPPA analysis revealed significantly ($p < 0.05$) elevated

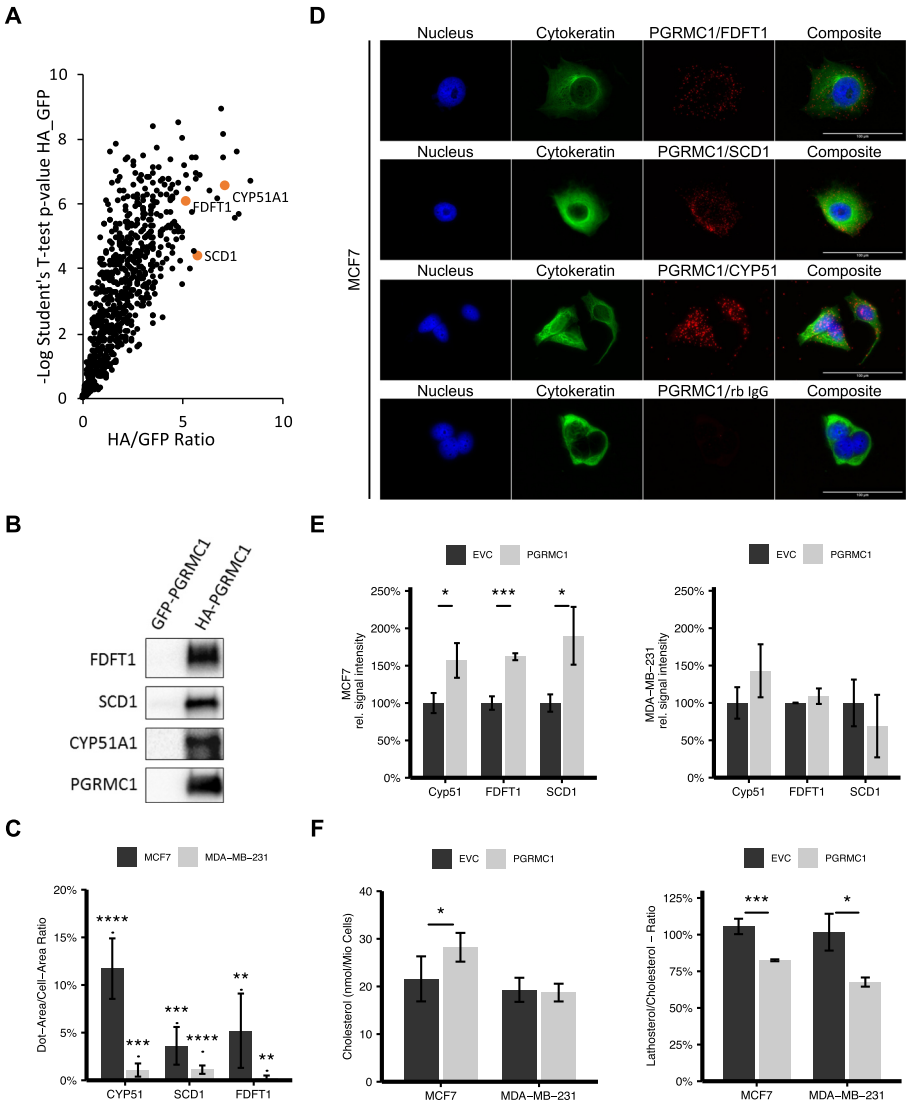

Fig. 2 **a** Scatter plot of proteins with significantly higher intensities in PGRMC1-HA samples compared to PGRMC1-GFP samples identified by mass spectrometry. The most significant proteins exhibit very high value for Student's *t* test difference HA_GFP and –log Student's *t* test *p* value HA_GFP and are found in the upper right corner. Highlighted are proteins with important functions in steroid synthesis. **b** Detection of co-immunoprecipitated proteins CYP51A1, Stearoyl-CoA desaturase (SCD1), and FDFT1 by western blot. **c** Verification of the interactions via proximity ligation assay. Quantification of dots per cell. **d** Visualization via immunofluorescence microscopy. **e** Quantification of protein expression of CYP51, SCD1, and FDFT1 in MCF7/PGRMC1 cells and MDA-MB-231/PGRMC1 cells compared to their respective empty vector control by western blot. $*p \leq 0.05$, $***p \leq 0.001$. **f** Detection of cholesterol and its precursor lathosterol in PGRMC1 overexpressing cells compared to the empty vector control cells with mass spectrometry $*p \leq 0.05$, $***p \leq 0.001$ (Student's *t* test, $n = 3$)

expression of ERα in MCF7/PGRMC1 cells compared to MCF7/EVC cells (Fig. 3b). Subsequently higher levels of HER2 and c-Myc proteins, whose expression depend on the transcriptional activity of ERα, were observed while c-Fos and PR levels were not altered (Fig. 3b). To verify the results from RPPA, western blots were performed to detect protein expression of ERα, HER2, and c-Myc (Fig. 3c). In MCF7/PGRMC1 cells, expression of ERα, HER2, and c-Myc is increased. Because E2 activates ERα and our previous studies have demonstrated higher E2 levels in MCF7/PGRMC1 cells compared to MCF7/EVC (Fig. 3a), we analyzed ERα phosphorylation at S118 (ERα-P-S118), which was also significantly increased ($p < 0.01$) in MCF7/PGRMC1 cells compared to MCF7/EVC (Fig. 3c). Additionally, we performed qPCR analysis of mRNA expression for ESR1, Tff1, HER2, CCND1, Myc, and PGR in the PGRMC1 overexpressing cell lines in comparison to the empty vector control (Fig. 3d, supplemental Figure 3B). In MCF7/PGRMC1 and T47D/PGRMC1 we detected higher mRNA levels for ESR1 and

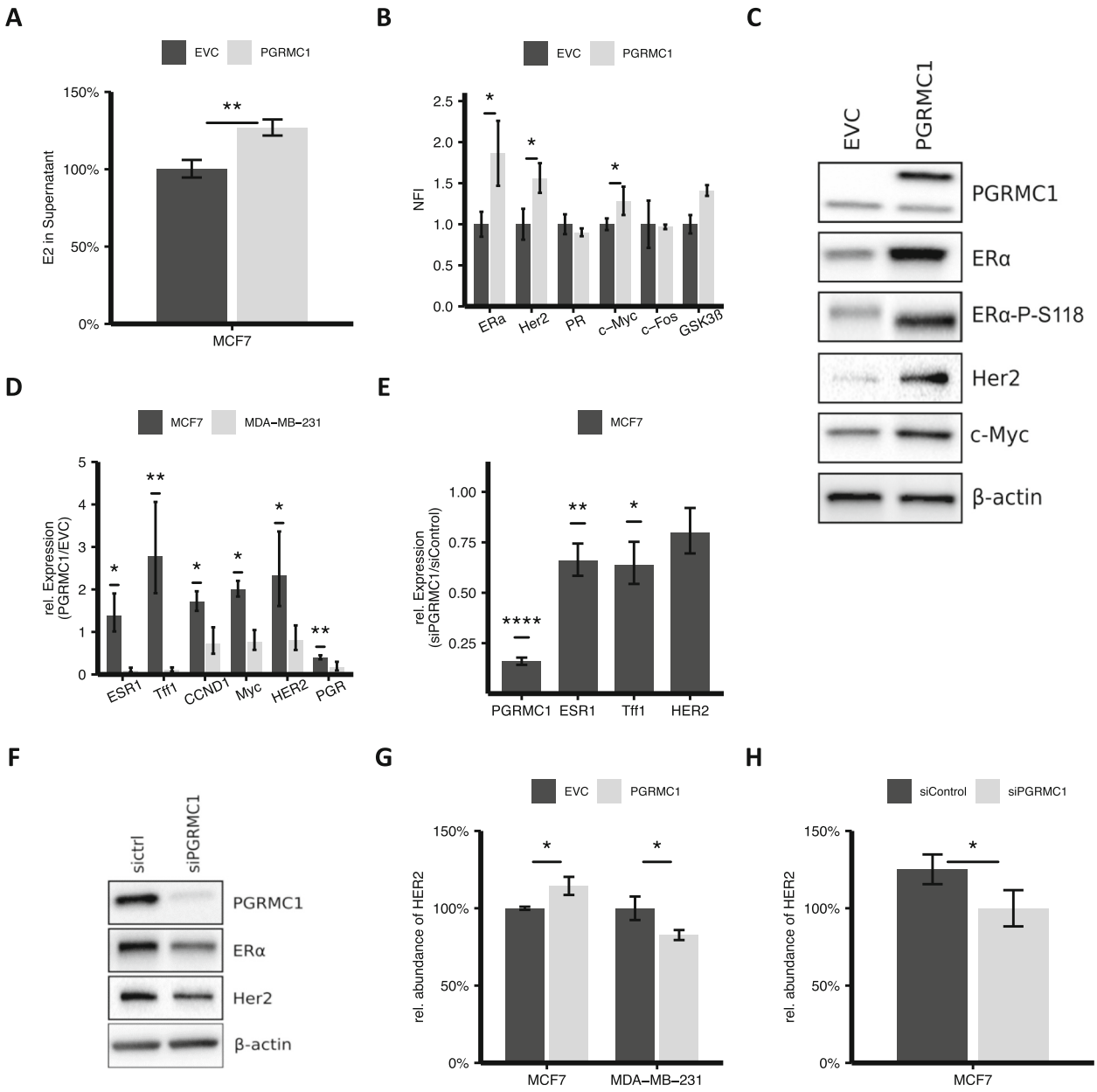

Fig. 3 **a** Amount of E2 in the supernatant of MCF7/PGRMC1 cells compared to the empty vector control after 48 h, detected with ELISA. $^{**}p \leq 0.01$. **b** NFI (blank-corrected mean fluorescence intensity) ratio of protein expression of ERα, Her2, PR, c-Myc, and c-Fos analyzed by RPPA. Protein expression was normalized to MCF7/EVC and protein expression measured in MCF7/EVC cells was set to 1. Up-/downregulation of protein expression in MCF7/PGRMC1 cells were calculated. $^{*}p \leq 0.05$ (Student's *t* test, $n = 3$). **c** Western blot analysis of ERα, Her2, and c-Myc protein levels in MCF7/EVC and MCF7/PGRMC1 cells. Representative picture of 3 independent analyses. **d** qRT-PCR analysis of *ESR1*, *TFF1*, *HER2*, *CCND1*, *Myc*, and *PGR* mRNA expression in MCF7/EVC and MCF7/PGRMC1 cells, MDA-MB-231/EVC and MDA-MB-231/PGRMC1 cells. $^{*}p \leq 0.05$, $^{***}p \leq 0.001$ (Student's *t* test, $n = 3$). **e** qRT-PCR analysis of *PGRMC1*, *ESR1*, *HER2*, and *TFF1* mRNA expression in MCF7 siCtrl and MCF7 siPGRMC1 cells. $^{*}p \leq 0.05$, $^{**}p < 0.01$, $^{****}p \leq 0.0001$ (Student's *t* test, $n = 3$). **f** Western blot analysis of ERα and Her2 protein levels in MCF7 siCtrl and MCF7 siPGRMC1 cells. Representative blot from 3 independent analyses. **g** Quantification of HER2 protein in membranes of unpermeabilized MCF7/EVC and MCF7/PGRMC1 cells, MDA-MB-231/EVC and MDA-MB-231/PGRMC1 cells, and MCF7 siCtrl and MCF7 siPGRMC1 cells **(h)** via flow cytometry. $^{*}p \leq 0.05$ (Student's *t* test, $n = 3$)

the ERα-dependent gene trefoil factor 1 (Tff1), CCND1 and Myc as reporter genes for ERα activation compared to MCF7/EVC and T47D/EVC. Interestingly, mRNA levels of PGR were significantly lower in the PGRMC1 overexpressing cells compared to their empty vector control. To further consolidate our hypothesis, we significantly silenced ($p < 0.01$) PGRMC1 expression by siPGRMC1 (Fig. 3e). As expected, the expression of ERα,

ESR1, and Tff1 were significantly downregulated (Fig. 3e), albeit no significant upregulation was detected for mRNA levels of HER2 pointing towards a post-transcriptional regulation of HER2 levels by PGRMC1 (Fig. 3e). In accordance, western blot analysis revealed decreased expression of ERα and HER2 in MCF7/siPGRMC1 (Fig. 3f). Previous studies revealed that HER2 overexpression causes deformation of the cell membrane and a subsequent disruption of epithelial features independent of receptor signaling [25, 33]. We demonstrated higher HER2 expression on the surface of non-permeabilized MCF7/PGRMC1 cells compared to MCF7/EVC cells using flow cytometry (Fig. 3g). Similarly, HER2 levels were reduced on the surface of MCF7/siPGRMC1 cells (Fig. 3h). MDA-MB-231/PGRMC1 cells even showed lower expression of HER2 compared to MDA-MB-231/EVC cells (Fig. 3g).

PGRMC1 overexpressing breast cancer cells show higher amounts of neutral lipids and lipid droplets

Lipid droplets recently emerged as new organelles not only due to their role in energy storage, but also as modulators of cell signaling and lipid homeostasis in several diseases including breast cancer [34–36].

By altering cholesterol levels in breast cancer cells, PGRMC1 could have a major influence on tumor growth via an enhanced lipid droplet formation in hormone receptor-positive breast cancer. To quantify the amount of neutral lipids, PGRMC1 overexpressing cell lines and their respective empty vector control were examined by BODIPY® staining of neutral lipids respectively lipid droplets. Subsequent flow cytometry analysis showed that PGRMC1 overexpressing hormone receptor-positive cells have a significantly higher amount of neutral lipids in comparison to the empty vector control (Fig. 4a, supplemental Figure 4A). Interestingly, we found significantly lower levels of lipids in MDA-MB-231/PGRMC1 cells compared to MDA-MB-231/EVC (Fig. 4a). Our results point towards an upregulation of lipid synthesis due to PGRMC1 overexpression in hormone receptor-positive breast cancer, which might lead to enhanced tumor growth.

PGRMC1 fuels endogenous lipid synthesis and lipid uptake and upregulates enzymes of the cholesterol metabolism

Besides the direct interaction of PGRMC1 with enzymes of the mevalonate pathway, the influence of PGRMC1 on lipid metabolism might be explained by increased mRNA expression of enzymes involved in endogenous and exogenous lipid metabolism.

Quantitative PCR analysis revealed increased levels of mRNA for SREBF1, SREBF2, LDLR, HMGS1, SCD, FASN, and ACAT1 in MCF7/PGRMC1 cells compared to MCF7/EVC cells (Fig. 4b, supplemental Figure 4B). These enzymes are not only key players in cholesterol and fatty acid synthesis, but also upregulated in breast cancer and they are associated with a worse outcome. In MDA-MB-231 cells, PGRMC1 overexpression did not result in higher expression of the abovementioned proteins (Fig. 4b). To show the increasing effect of PGRMC1 on expression of enzymes of the lipid metabolism, we obtained normalized microarray data of 63 hormone receptor-positive breast cancers tissue samples [37]. Spearman's correlation between the PGMRC1 expression level and various expression levels of proteins (FASN, FDFT1, HMGCS1, HMGCR, LDLR, SCD) indicated positive correlations between PGRMC1 and the respective enzymes in luminal A breast cancer tissue samples (Fig. 4c). Our findings advert to a complex and diverse impact of PGRMC1 on lipid homeostasis in breast cancer.

PGRMC1 enhances expression of lipid rafts in cell membranes of breast cancer cells

Lipid rafts are cholesterol-rich microdomains in cell membranes, which have functions in cell proliferation and growth, membrane trafficking, metastasis, and apoptosis [23, 24, 38]. Furthermore, lipid raft formation in cell membranes is influenced by FDFT1 activity [39]. Since lipid rafts play a role in breast cancer progression and due to the fact that (a) PGRMC1 overexpressing hormone receptor-positive breast cancer cells have higher amounts of cholesterol and that (b) PGRMC1 interacts with FDFT1, we determined the abundance of lipid rafts in MCF7 and MDA-MB-231 cells with PGRMC1 overexpression and respective empty vector control as well as in MCF7 cells treated with siRNAs directed against PGRMC1, to knockdown PGRMC1 (Fig. 4d). Cells were stained with Vybrant™ Alexa Fluor™ 488 Lipid Raft Labeling Kit and detected by flow cytometry. MCF7/PGRMC1 cells showed significantly higher levels of lipid rafts compared to the respective empty vector control (Fig. 4d, upper). In addition, we found significantly lower expression of lipid rafts when endogenous PGRMC1 was knocked down in MCF7 cells (Fig. 4d, lower). Interestingly, lipid rafts were decreased in PGRMC1 overexpressing MDA-MB-231 cells (Fig. 4d).

Elevated proliferation mediated by lipid rafts is, among others, attributed to modulation of signaling functions of growth factor receptors like the ErbB (HER) receptor family.

Since we found higher expression of HER2 in the membrane of PGRMC1 overexpressing MCF7 cells (Fig. 3g), we analyzed the HER2 expression in lipid rafts in more detail.

PGRMC1 overexpressing MCF7 and MDA-MB-231 cells and respective empty vector control cells were co-

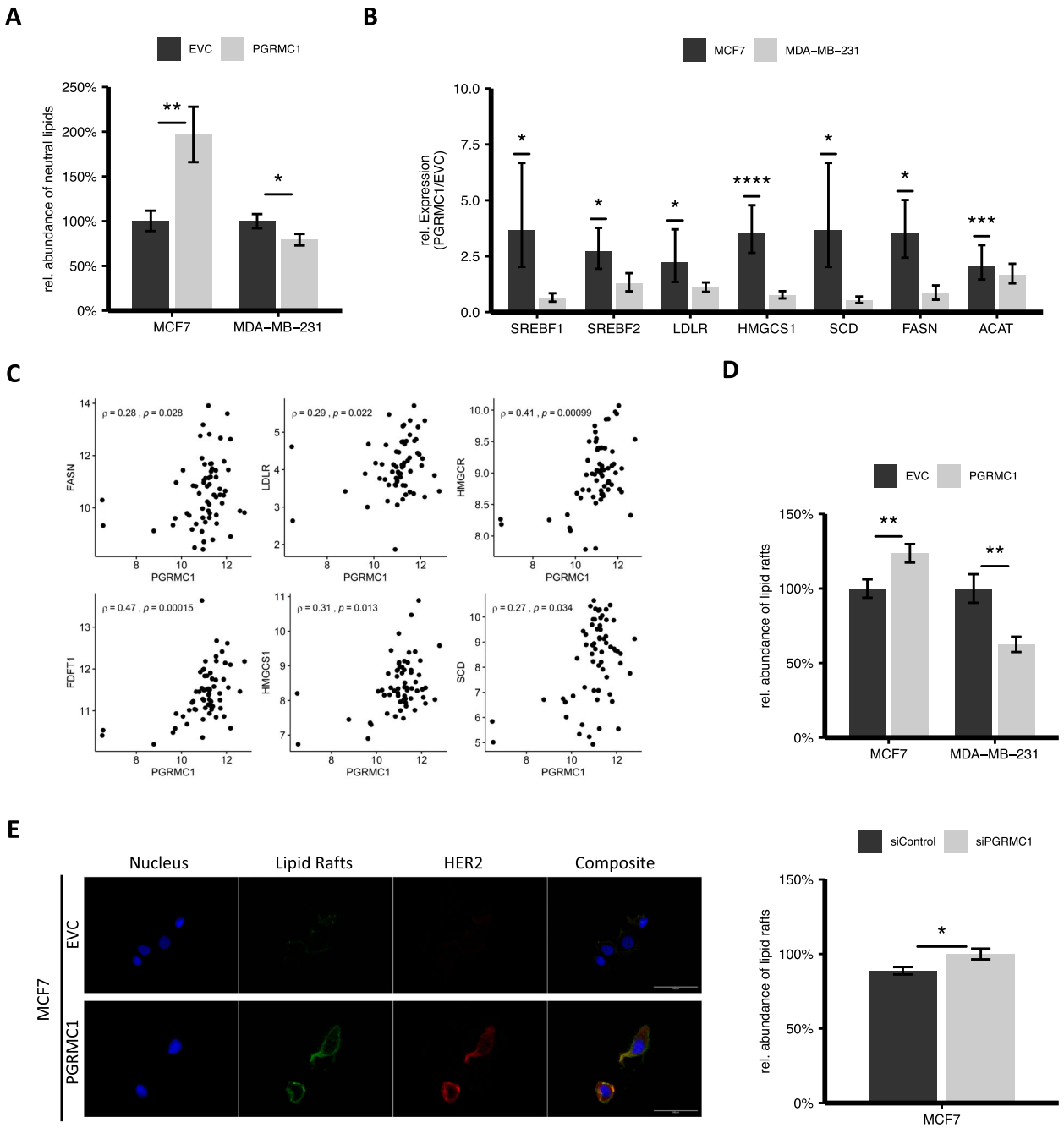

Fig. 4 a Detection of neutral lipids and lipid droplets in MCF7/EVC and MCF7/PGRMC1, MDA-MB-231/EVC and MDA-MB-231/PGRMC1 cells by BODIPY® staining and quantification via flow cytometry. *$p \leq 0.05$, **$p \leq 0.01$. (Student's *t* test, $n = 3$). **b** qRT-PCR analysis of SREBF1, SREBF2, LDLR, HMGS1, SCD, FASN, ACAT mRNA expression in MCF7/PGRMC1 and MDA-MB-231/PGRMC1 cells compared to the respective EVC cells. *$p \leq 0.05$, **$p \leq 0.01$, ***$p \leq 0.001$ (Student's *t* test, $n = 3$). **c** Spearman's correlation between the PGMRC1 expression level and various expression levels of proteins (FASN, FDFT1, HMGCS1, HMGCR, LDLR, SCD) involved in lipid metabolism. Data obtained from normalized microarray data (Affymetrix Human Genome U133A Array) of 63 hormone receptor-positive breast cancer tissue samples. **d** Detection of lipid rafts in cell membranes of MCF7/EVC and MCF7/PGRMC1 cells, MDA-MB-231/EVC and MDA-MB-231/PGRMC1 cells, and MCF7 siCtrl and MCF7 siPGRMC1 cells by Vybrant™ Alexa Fluor™ 488 and subsequent quantification via flow cytometry. *$p \leq 0.05$, **$p \leq 0.01$ (Student's *t* test, $n = 3$). **e** Immunofluorescence staining with Vybrant™ Alexa Fluor™ 488, fluorescence immunocytochemistry for HER2, and nuclear staining with DAPI. 63-fold magnification. Cells were grown on chamber slides for 24 h

stained for HER2 and lipid rafts (Fig. 4e, supplemental Figure 3C). Especially in MCF7/PGRMC1 cells, we found a strong co-localization of HER2 in lipid rafts (Fig. 4e).

PGRMC1 influences activation of EGFR signaling

Another important member of the ErbB receptor family, which plays a major role in breast cancer signaling, is the EGFR. Several studies suggest that PGRMC1 may promote EGFR phosphorylation and activation [8, 9, 13, 40]. The hypothesis of PGRMC1 enhancing EGFR signaling was investigated by reverse phase protein array (RPPA) with a focus on phosphorylation of EGFR and its downstream targets in MCF7/PGRMC1 and MCF7/EVC cells (Fig. 5a). Our results point towards an increased phosphorylation of EGFR (p-Tyr1068), Akt (p-Ser473 and p-Thr308), MEK1/2 (p-Ser217/Ser221), ERK1/2 (p-Thr202/Tyr204), and S6 (p-Ser240/Ser244) in PGRMC1/MCF7 cells compared to EVC cells (Fig. 5a). In combination with our results from immunofluorescence staining, this suggests that there might exist a powerful link between PGRMC1 expression and activation of oncogenic signaling pathways in MCF7 cells (Fig. 5c).

To verify the RPPA results, we performed western blot analysis of EGFR signaling induced with EGF (Fig. 5b). Phosphorylation of EGFR, Akt, MEK1/2, and ERK1/2 was observed (Fig. 5b). Compatible, significantly elevated levels of EGFR (p-Tyr1068), Akt (p-Ser473), MEK1/2 (p-Ser217/Ser221), and ERK1/2 (p-Thr202/Tyr204) were monitored in MCF7/PGRMC1 cells. In contrast, expression levels of total protein did not vary significantly (Fig. 5c). MDA-MB-231 showed no difference in expression levels of EGFR (p-Tyr1068), Akt (p-Ser473), MEK1/2 (p-Ser217/Ser221), and ERK1/2 (p-Thr202/Tyr204), suggesting a subordinated role of PGRMC1 in EGFR signaling in triple-negative breast cancer (supplemental Figure 4A, 4B).

Cholesterol and fatty acid depletion induced by statins reverses the growth benefit interceded by PGRMC1

Our findings suggest a complex and broad role of PGRMC1 in cholesterol and lipid metabolism (Fig. 5d). Based on our research concerning the influence of PGRMC1 on lipid homeostasis and increased viability of PGRMC1 overexpressing cells, we hypothesized that a higher lipid synthesis might lead to a survival benefit of PGRMC1 overexpressing cells.

To verify this hypothesis, we treated PGRMC1 overexpressing MCF7 and MDA-MB-231 cells and the respective controls with different concentrations of simvastatin, a competitive inhibitor of HMG-CoA reductase, and performed subsequent viability assays (Fig. 5d).

Interestingly, contrary to expectations, inhibition of HMG-CoA reductase and following depletion of cholesterol not only assimilated viability in MCF7/PGRMC1 cells compared to MCF7/EVC cells, but even led to inferior viability. This suggests a higher dependence of PGRMC1 overexpressing cells on cholesterol. Intriguingly, MDA-MB-231 cells with PGRMC1 overexpression reacted similar to MCF7 cells (Fig. 5d).

Discussion

Although previous studies report on the proliferative effect of PGRMC1 in breast cancer, little is known about the mechanisms by which PGRMC1 effects carcinogenesis. Therefore, our present study focuses on the modifying function of PGRMC1 on lipid metabolism and oncogenic signaling. Evidence is pointing towards a meaningful impact of modified lipid metabolism in breast cancer progression and metastasis [41–44]. Although one of the most relevant mechanisms of energy usage of cancer cells is their increase in glucose uptake and their use of non-oxidative glycolysis, also known as Warburg effect, breast cancer cells upregulate lipid de novo synthesis and the uptake of free fatty acids and low-density lipoproteins [44, 45]. Our findings suggest the function of PGRMC1 as an important enhancer especially of lipid synthesis resulting in oncogenic signaling and tumor progression. For the first time, we detected enhanced mRNA expression of proteins regulating lipid synthesis and uptake in PGRMC1 overexpressing hormone receptor-positive MCF7 and T47D cells resulting in significantly higher lipid levels in MCF7/PGRMC1 and T47D/PGRMC1 cells compared to the empty vector control cells. Further, we could demonstrate that PGRMC1 interacts with CYP51, FDFT1, and SCD1, which are major players in lipogenesis. Interestingly, these interactions are less pronounced in MDA-MB-231 cells. An explanation for the lower interaction might be that triple-negative breast cancer cells have been reported to cover their needs for lipids via the uptake of exogenous fatty acids in contrast to performing lipid de novo synthesis [44, 46].

A possible result of the detected interactions between PGRMC1 and CYP51, FDFT1, and SCD1 could be the increase of cholesterol and neutral lipid levels in MCF7/PGRMC1 and T47D/PGRMC1 cells. Since cholesterol is the precursor of steroid hormones like estradiol, elevated levels of cholesterol may subsequently lead to higher levels of estradiol as indicated by our measurements in the supernatant of MCF7/PGRMC1 cells of this scenario. One consequence could be that PGRMC1 promotes tumor progression by upregulation of ERα protein and ESR1 mRNA directly via a transcriptional mechanism or indirectly via elevated steroid synthesis. Since various studies showed an upregulation of steady-

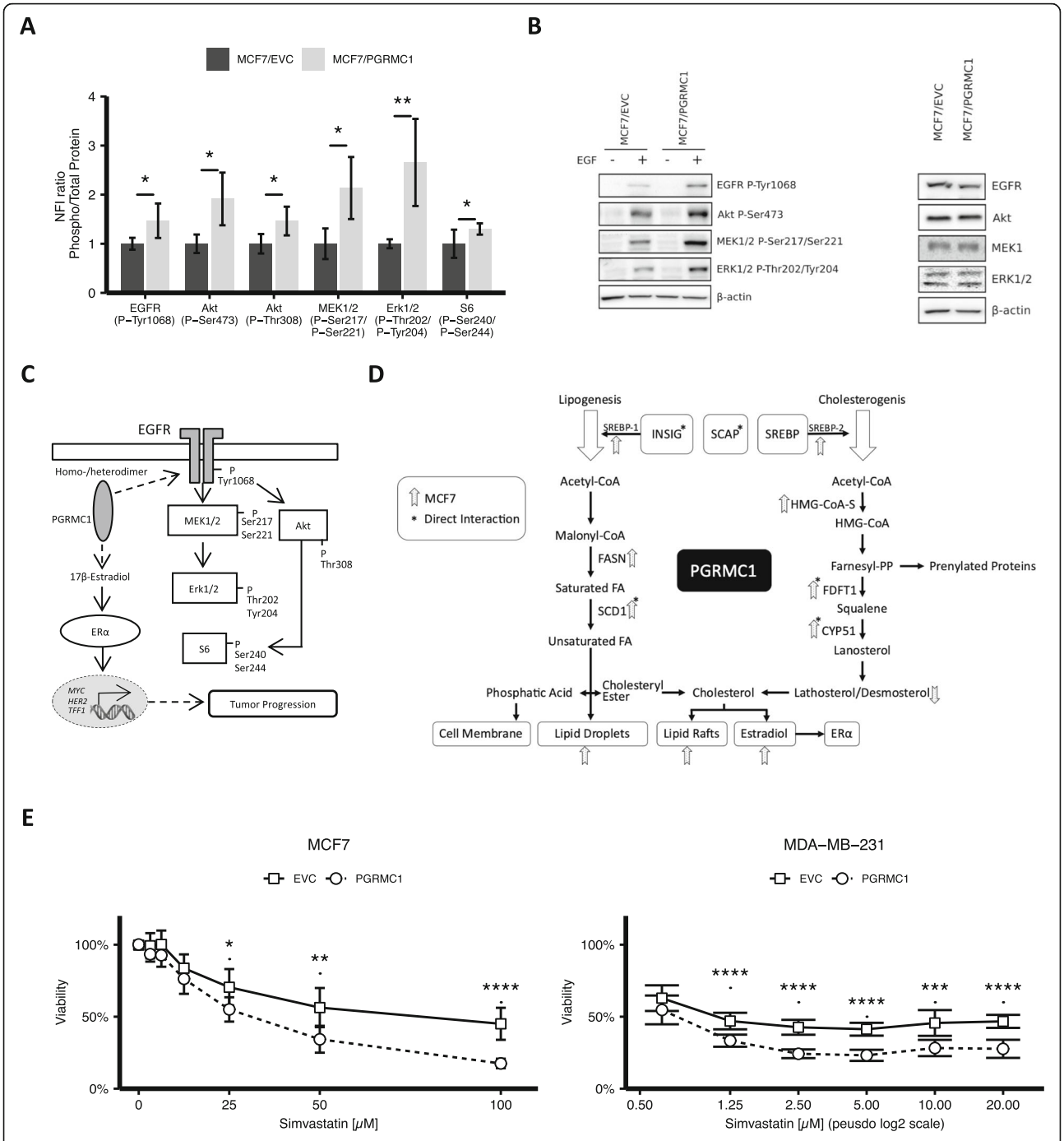

Fig. 5 (See legend on next page.)

(See figure on previous page.)
Fig. 5 a Protein phosphorylation of EGFR P-Tyr1068, Akt P-Ser473, Akt P-Thr308, MEK1/2 P-Ser217/Ser221, Erk1/2 P-Thr202/Tyr204, and S6 P-Ser240/Ser244 analyzed by RPPA. NFI (blank-corrected mean fluorescence intensity) ratio of phospho-protein/total protein was calculated, normalized to MCF7/EVC, and ratio in MCF7/EVC cells was set to 1. Up-/downregulation of protein phosphorylation in MCF7/PGRMC1 cells was calculated. *$p \leq 0.05$, **$p \leq 0.01$ (Student's t test, $n = 3$). **b** Protein phosphorylation of EGFR P-Tyr1068, Akt P-Ser473, MEK1/2 P-Ser217/Ser221, and Erk1/2 P-Thr202/Tyr204 verified by western blot analysis. Cells were treated with EGF (10 ng/mL) for 10 min/37 °C. Representative blot of 3 independent analyses**.** Total protein expression of EGFR, Akt, MEK1/2, and Erk1/2 verified by western blot analysis. Representative blot of 3 independent analyses shown. **c** PGRMC1 mediates phosphorylation of EGFR and its downstream targets and upregulates E2 levels, ERα expression, and ERα-target genes. EGFR phosphorylation activates the MAPK signaling cascade (including MEK1/2-, ERK1/2-, and S6-phosphorylation) and PI3K signaling cascade (including Akt- and S6-phosphorylation). Phosphorylation of S6 induces transcription of genes, involved in the regulation of cell cycle progression, cell proliferation, and glucose homeostasis. ERα translocates into the nucleus upon ligand-dependent or ligand-independent activation and acts as a transcription factor to transcribe genes involved in tumor progression. **d** Overview of the influence of PGRMC1 in cholesterol and lipid metabolism. **e** MCF7/EVC and MCF7/PGRMC1 cells were treated with 100 μM, 50 μM, 25 μM, 12.5 μM, 6.25 μM, and 3.175 μM simvastatin and respective DMSO control. MDA-MB-231/EVC and MDA-MB-231/PGRMC1 cells were treated with 20 μM, 10 μM, 5 μM, 2.5 μM, 1.25 μm, and 0.625 μM simvastatin and respective DMSO control. Viability was analyzed by MTT assay at $t = 24$ h, $t = 48$ h, $t = 72$ h and 37 °C. Depicted are results after 48 h of treatment. Viability is normalized on the DMSO control. p values were adjusted using the Bonferroni correction ($n_{doses} = 6$; $n_{replicates} = 9$)

state ERα levels by long-term exposure to E2 [47], increased levels of ERα plus a simultaneous autocrine/paracrine activation by E2 may trigger a proliferative cycle support in tumor growth. For the first time, we also observed that PGRMC1 impacts on lipid rafts, another regulator of cancer progression. Lipid rafts are important, e.g., in modulation of membrane geometry, lateral movement of molecules, and signal transduction [23, 48]. We observed increased lipid raft formation in PGRMC1 overexpressing hormone receptor-positive breast cancer cells. The co-localization of HER2 in lipid rafts, also reported by other research groups [49, 50], may influence EGFR signaling. Zhuang et al. reported an EGF-induced and constitutive signaling via the Akt serine-threonine kinase and subsequent survival in cancer cells [51]. Furthermore, EGFR and HER2 localization in lipid rafts is discussed to play a role in cancer cell drug resistance, e.g., regarding treatment with trastuzumab or tyrosine kinase inhibitors [49, 50]. On the other hand, Orr et al. showed that altered cholesterol levels modify the mobility of EGFR in the cell membrane leading to its decreased activation due to reduced dimerization of EGFR monomeres [25]. The relevant role of PGRMC1 in promoting phosphorylation and activation of receptors for example by heme-dependent PGRMC1 dimerization has already been reported [8, 9, 13, 40]. Here, elevated phosphorylation levels of EGFR and its downstream targets in MCF7/PGRMC1 cells were discovered. The crosstalk between EGFR/Her2 and ERα signaling cascades has often been reported, whereby ERα can induce the E2-dependent activation of the EGFR signaling pathway by promoting phosphorylation of Akt (P-Ser473) via the non-genomic pathway. Alternatively, ERα activation can be accomplished independently of estrogens by EGFR-activated MAPK-signaling or PI3K pathway [52, 53]. In the current study, we demonstrate that both MAPK and PI3K pathway components (i.e., MEK1/2, ERK1/2, and AKT) are activated in PGRMC1 overexpressing MCF7 cells. This may lead to increased ERα activation and finally to increased cancer proliferation. Additionally, ERα and HER2 correlate positively in HER2 non-overexpressing breast cancer [54, 55]. Hence, higher levels of ER in MCF7/PGRMC1 cells could lead to higher expression of HER2. However, the influence of PGRMC1 on EGFR/HER2 signaling in lipid rafts and its impact on tumor progression requires further studies.

Due to the role of the mevalonate pathway and its dual role in cholesterol synthesis and prenylation of signaling proteins, statins have been tested as anti-cancer drugs. Statins block the HMG-CoA reductase, the gatekeeper of the mevalonate pathway. We speculated due to increased activation of the mevalonate pathway and due to higher cholesterol and neutral lipids production that PGRMC1 overexpressing cells may be more dependent on the mevalonate pathway. Hence, they might be more susceptible to statin treatment [56–60]. For the first time, we detected that MCF7/PGRMC1 and MDA-MB-231/PGRMC1 cells are more sensitive to treatment with simvastatin compared to the respective controls. We assume that PGRM C1 overexpression leads to higher dependence on cholesterol and fatty acids of cancer cells due to an alteration of fatty acid metabolism, by enhanced driving of the mevalonate pathway and related synthesis of the isoprenoids geranylgeranyl pyrophosphate (GGPP) and farnesyl pyrophosphate (FPP) [61, 62], e.g., leading to inhibition of small Rho GTPase prenylation [63].

Indeed, PGRMC1 might also reduce viability of breast cancer cells under treatment with statins, because PGRMC1 is known to interact with CYP enzymes [3, 5, 13–15]. Specifically, inhibition of cytochromes P450 could increase the concentration of simvastatin, since statins are metabolized by CYP3A4.

Hence, PGRMC1 overexpressing tumors may be an interesting target for additional cholesterol lowering therapy.

Conclusion

We demonstrate that PGRMC1 mediates progression of breast cancer cells potentially by altering cholesterol and lipid metabolism and activating key drivers of tumor progression in breast cancer, namely ERα expression and activation, as well as EGFR signaling. Our data underline the contribution of PGRMC1 to especially hormone receptor-positive breast cancer pathogenesis in vitro and in vivo and suggest its potential as a target for anti-cancer therapy.

Supplementary information

Supplementary information accompanies this paper at https://doi.org/10.1186/s13058-020-01312-8.

Additional file 1.

Abbreviations

ACAT1: Acetyl-Coenzyme A acetyltransferase 1; Akt: Protein kinase B; BODIPY: Difluoro {2-[1-(3,5-dimethyl-2H-pyrrol-2-ylidene-N)ethyl]-3,5-dimethyl-1H-pyrrolatoN} boron; BSA: Bovine serum albumin; CK-2: Casein kinase-2; CYP: Cytochromes P450; DAPI: 4,6-Diamidin-2-phenylindol; E2: 17β-Estradiol; EGF: Epidermal growth factor; EGFR: Epidermal growth factor receptor; ELISA: Enzyme-linked immunosorbent assay; Erk1/2 (MAPK p44/42): extracellular signal-regulated kinases; ERα: Estrogen receptor α; FASN: Fatty acid synthase; FCS: Fetal calf serum; GFP: Green fluorescent protein; HA: Hemagglutinin; Her2: Human epidermal growth factor receptor-2; HMGS: 3-Hydroxy-3-methylglutaryl coenzyme A synthase; INSIG: Insulin-induced gene protein; LDLR: Low-density lipoprotein receptor; MEK1 (MAP2K1): Mitogen-activated protein kinase kinase 1; MEK2 (MAP2K2): Mitogen-activated protein kinase kinase 2; NFI: Blank-corrected mean fluorescence intensity; PGRMC1: Progesterone receptor membrane component-1; PR: Progesterone receptor; RPPA: Reverse phase protein array; SCAP: SREBP cleavage-activating protein; SCD1: Stearoyl-CoA desaturase1; FDFT1: Farnesyl-diphosphate farnesyltransferase 1 (Squalene Synthase); SREBP1/2: Sterol regulatory element-1/2; TFF1: Trefoil factor 1

Acknowledgements

This study contains results of the dissertation "Role of PGRMC1 in breast cancer progression and increased breast cancer risk upon progestin-based hormone therapy" submitted to the Faculty of Mathematics and Natural Sciences at the Heinrich-Heine-University Duesseldorf on 30 September 2017 by Marina Ludescher (née Willibald).

Authors' contributions

HA, NS, ML, and HN were responsible for conceptual design of the study. HA, NS, ML, MP, and CV designed the experiments. HA, ML, NS, BG, AM, AB, and UH performed the experiments. HA, ML, MP, CV, JC, and UH analyzed the data. HA, NS, ML, HN, MP, and CV interpreted the findings. HA wrote the original draft. HA, ML, MP, CV, RLK, UH, UMZ, and HN critically revised the manuscript. RLK, ER, DN, TF, UZ, and HN contributed to the project administration. All authors read and approved the final manuscript.

Funding

This work was supported by the German Research Foundation (Deutsche Forschungsgemeinschaft, DFG, NE 805/6-1), by the German Academic Exchange Service (ID-57215625), and by GINOP grants (GINOP-2.3.2-15-2016-00001 and GINOP-2.3.2-15-2016-00039). Parts of this project were also supported by the Wilhelm Sander Foundation (2013.126.1), by the Robert Bosch Foundation (Stuttgart, Germany), and by the Brigitte and Dr. Konstanze Wegener Foundation (Duesseldorf, Germany).

Availability of data and materials

The microarray data analyzed during the current study are available in the Gene Expression Omnibus under the ID GSE129560. [https://www.ncbi.nlm.nih.gov/geo/query/acc.cgi?acc=GSE129560]. The remaining datasets used and analyzed during the current study are available from the corresponding author on reasonable request.

Ethics approval and consent to participate

All animal experiments were performed in accordance with animal experimentation and ethics guidelines of the EU (2010/63/EU). Experimental protocols were approved by the Review Committee of Biological Research Centre of the Hungarian Academy of Sciences and the responsible governmental agency (clearance number: CSI/01/1489-5/2014).

Consent for publication

Not applicable.

Competing interests

The authors declare that they have no competing interests.

Author details

[1]Department of Obstetrics and Gynecology, University Hospital and Medical Faculty of the Heinrich-Heine University Duesseldorf, Life Science Center, Merowingerplatz 1A, 40225 Düsseldorf, Germany. [2]NMI TT Pharmaservices, Protein Profiling, Reutlingen, Germany. [3]Dr. Margarete Fischer-Bosch Institute of Clinical Pharmacology and University of Tübingen, Stuttgart, Germany. [4]Institute of Biochemistry, Biological Research Centre, Szeged, Hungary. [5]Institute of Genetics, Biological Research Centre, Szeged, Hungary.

Received: 11 March 2020 Accepted: 30 June 2020
Published online: 13 July 2020

References

1. Bray F, Ferlay J, Soerjomataram I, Siegel RL, Torre LA, Jemal A. Global cancer statistics 2018: GLOBOCAN estimates of incidence and mortality worldwide for 36 cancers in 185 countries. CA Cancer J Clin. 2018;68(6):394–424. https://doi.org/10.3322/caac.21492.
2. Ferlay J, Soerjomataram I, Dikshit R, et al. Cancer incidence and mortality worldwide: sources, methods and major patterns in GLOBOCAN 2012. Int J Cancer. 2015;136(5):E359–86. https://doi.org/10.1002/ijc.29210.
3. Kimura I, Nakayama Y, Konishi M, et al. Functions of MAPR (membrane-associated progesterone receptor) family members as heme/steroid-binding proteins. Curr Protein Pept Sci. 2012;13(7):687–96. https://doi.org/10.2174/138920312804142110.
4. Gerdes D, Wehling M, Leube B, Falkenstein E. Cloning and tissue expression of two putative steroid membrane receptors. Vol 379; 1998.
5. Ryu CS, Klein K, Zanger UM. Membrane associated progesterone receptors: promiscuous proteins with pleiotropic functions - focus on interactions with cytochromes P450. Front Pharmacol. 2017;8. https://doi.org/10.3389/fphar.2017.00159.
6. Cahill MA, Jazayeri JA, Catalano SM, Toyokuni S, Kovacevic Z, Richardson DR. The emerging role of progesterone receptor membrane component 1 (PGRMC1) in cancer biology. Biochim Biophys Acta - Rev Cancer. 2016;1866(2):339–49. https://doi.org/10.1016/j.bbcan.2016.07.004.
7. Zhang Y, Ruan X, Willibald M, et al. May progesterone receptor membrane component 1 (PGRMC1) predict the risk of breast cancer? Gynecol Endocrinol. 2016;32(1):58–60. https://doi.org/10.3109/09513590.2015.1078303.
8. Ahmed IS, Rohe HJ, Twist KE, Craven RJ. Pgrmc1 (progesterone receptor membrane component 1) associates with epidermal growth factor receptor and regulates erlotinib sensitivity. J Biol Chem. 2010;285(32):24775–82. https://doi.org/10.1074/jbc.M110.134585.
9. Hampton KK, Stewart R, Napier D, Claudio PP, Craven RJ. PGRMC1 elevation in multiple cancers and essential role in stem cell survival. Adv Lung Cancer. 2015;04(03):37–51. https://doi.org/10.4236/alc.2015.43006.
10. Mir SUR, Ahmed ISA, Arnold S, Craven RJ. Elevated progesterone receptor membrane component 1/sigma-2 receptor levels in lung tumors and plasma from lung cancer patients. Int J Cancer. 2012;131(2). https://doi.org/10.1002/ijc.26432.
11. Willibald M, Wurster I, Meisner C, et al. High level of progesteron receptor membrane component 1 (PGRMC 1) in tissue of breast cancer patients is associated with worse response to anthracycline-based neoadjuvant therapy. Horm Metab Res. 2017;49(8):595–603. https://doi.org/10.1055/s-0043-113635.

12. Ruan X, Zhang Y, Mueck AO, et al. Increased expression of progesterone receptor membrane component 1 is associated with aggressive phenotype and poor prognosis in ER-positive and negative breast cancer. Menopause. 2017;24(2):203–9. https://doi.org/10.1097/GME.0000000000000739.
13. Kabe Y, Nakane T, Koike I, et al. ARTICLE Haem-dependent dimerization of PGRMC1/Sigma-2 receptor facilitates cancer proliferation and chemoresistance. Nat Commun. 2016;6. https://doi.org/10.1038/ncomms11030.
14. Ahmed IS, Rohe HJ, Twist KE, Mattingly MN, Craven RJ. Progesterone receptor membrane component 1 (Pgrmc1): a heme-1 domain protein that promotes tumorigenesis and is inhibited by a small molecule. J Pharmacol Exp Ther. 2010;333(2):564–73. https://doi.org/10.1124/jpet.109.164210.
15. Mansouri MR, Schuster J, Badhai J, et al. Alterations in the expression, structure and function of progesterone receptor membrane component-1 (PGRMC1) in premature ovarian failure. Hum Mol Genet. 2008;17(23):3776–83. https://doi.org/10.1093/hmg/ddn274.
16. Lin ST, May EWS, Chang JF, Hu RY, Wang LHC, Chan HL. PGRMC1 contributes to doxorubicin-induced chemoresistance in MES-SA uterine sarcoma. Cell Mol Life Sci. 2015;72(12):2395–409. https://doi.org/10.1007/s00018-014-1831-9.
17. Friel AM, Zhang L, Pru CA, et al. Progesterone receptor membrane component 1 deficiency attenuates growth while promoting chemosensitivity of human endometrial xenograft tumors. Cancer Lett. 2015;356(2):434–42. https://doi.org/10.1016/j.canlet.2014.09.036.
18. Cahill MA, Medlock AE. Thoughts on interactions between PGRMC1 and diverse attested and potential hydrophobic ligands. J Steroid Biochem Mol Biol. 2017;171:11–33. https://doi.org/10.1016/j.jsbmb.2016.12.020.
19. Antalis CJ, Uchida A, Buhman KK, Siddiqui RA. Migration of MDA-MB-231 breast cancer cells depends on the availability of exogenous lipids and cholesterol esterification. Clin Exp Metastasis. 2011;28(8):733–41. https://doi.org/10.1007/s10585-011-9405-9.
20. Marwarha G, Raza S, Hammer K, Ghribi O. 27-hydroxycholesterol: a novel player in molecular carcinogenesis of breast and prostate cancer. Chem Phys Lipids. 2017;207:108–26. https://doi.org/10.1016/j.chemphyslip.2017.05.012.
21. Menendez JA, Lupu R. Fatty acid synthase and the lipogenic phenotype in cancer pathogenesis. Nat Rev Cancer. 2007;7(10):763–77. https://doi.org/10.1038/nrc2222.
22. Nelson ER, Chang C Yi, McDonnell DP. Cholesterol and breast cancer pathophysiology. Trends Endocrinol Metab 2014;25(12):649–655. doi:https://doi.org/10.1016/j.tem.2014.10.001.
23. Mollinedo F, Gajate C. Lipid rafts as major platforms for signaling regulation in cancer. Adv Biol Regul. 2015;57:130–46. https://doi.org/10.1016/j.jbior.2014.10.003.
24. Li YC, Park MJ, Ye SK, Kim CW, Kim YN. Elevated levels of cholesterol-rich lipid rafts in cancer cells are correlated with apoptosis sensitivity induced by cholesterol-depleting agents. Am J Pathol. 2006;168(4):1107–18. https://doi.org/10.2353/ajpath.2006.050959.
25. Orr G, Hu D, Özçelik S, Opresko LK, Wiley HS, Colson SD. Cholesterol dictates the freedom of EGF receptors and HER2 in the plane of the membrane. Biophys J. 2005;89(2):1362–73. https://doi.org/10.1529/biophysj.104.056192.
26. Fox EM, Andrade J, Shupnik MA. Novel actions of estrogen to promote proliferation: integration of cytoplasmic and nuclear pathways. Steroids. 2009;74(7):622–7. https://doi.org/10.1016/j.steroids.2008.10.014.
27. Barrett T, Wilhite SE, Ledoux P, et al. NCBI GEO: Archive for functional genomics data sets - Update. Nucleic Acids Res. 2013;41(D1). doi:https://doi.org/10.1093/nar/gks1193.
28. Zhao Y, Ruan X, Wang H, et al. The presence of a membrane-bound progesterone receptor induces growth of breast cancer with norethisterone but not with progesterone: a xenograft model. Maturitas. 2017;102:26–33. https://doi.org/10.1016/j.maturitas.2017.05.007.
29. Schneck H, Ruan X, Seeger H, et al. Membrane-receptor initiated proliferative effects of dienogest in human breast cancer cells. Gynecol Endocrinol. 2013;29(2):160–3. https://doi.org/10.3109/09513590.2012.730572.
30. Ruan X, Gu M, Cai G, et al. Progestogens and PGRMC1-dependent breast cancer tumor growth: an in-vitro and xenograft study. Maturitas. 2019;123:1–8. https://doi.org/10.1016/j.maturitas.2019.01.015.
31. Rohe HJ, Ahmed IS, Twist KE, Craven RJ. PGRMC1 (progesterone receptor membrane component 1): a targetable protein with multiple functions in steroid signaling, P450 activation and drug binding. Pharmacol Ther. 2009;121(1):14–9. https://doi.org/10.1016/j.pharmthera.2008.09.006.
32. Xu J, Zeng C, Chu W, et al. Identification of the PGRMC1 protein complex as the putative sigma-2 receptor binding site. Nat Commun. 2011;2(1). https://doi.org/10.1038/ncomms1386.
33. Chung I, Reichelt M, Shao L, et al. High cell-surface density of HER2 deforms cell membranes. Nat Commun. 2016;7. https://doi.org/10.1038/ncomms12742.
34. Koizume S, Miyagi Y. Lipid droplets: a key cellular organelle associated with cancer cell survival under normoxia and hypoxia. Int J Mol Sci. 2016;17(9):1–23. https://doi.org/10.3390/ijms17091430.
35. Baenke F, Peck B, Miess H, Schulze A. Hooked on fat: the role of lipid synthesis in cancer metabolism and tumour development. Dis Model Mech. 2013;6(6):1353–63. https://doi.org/10.1242/dmm.011338.
36. Blücher C, Zilberfain C, Venus T, et al. Single cell study of adipose tissue mediated lipid droplet formation and biochemical alterations in breast cancer cells. Analyst. 2019;144(18):5558–70. https://doi.org/10.1039/c9an00816k.
37. Sinn BV, Fu C, Lau R, et al. SET ER/PR: a robust 18-gene predictor for sensitivity to endocrine therapy for metastatic breast cancer. npj Breast Cancer. 2019;5(1). https://doi.org/10.1038/s41523-019-0111-0.
38. de Laurentiis A, Donovan L, Arcaro A. Lipid rafts and caveolae in signaling by growth factor receptors. Open Biochem J. 2007;1:12–32. https://doi.org/10.2174/1874091X00701010012.
39. Brusselmans K, Timmermans L, Van De Sande T, et al. Squalene synthase, a determinant of raft-associated cholesterol and modulator of cancer cell proliferation. J Biol Chem. 2007;282(26):18777–85. https://doi.org/10.1074/jbc.M611763200.
40. Aizen J, Thomas P. Role of Pgrmc1 in estrogen maintenance of meiotic arrest in zebrafish oocytes through Gper/Egfr. J Endocrinol. 2015;225(1). https://doi.org/10.1530/JOE-14-0576.
41. OF K, Noory MA, Robertson GP. The role of cholesterol in cancer. Cancer Res. 2016;76(8):2063–70. https://doi.org/10.1158/0008-5472.CAN-15-2613.
42. Gorin A, Gabitova L, Astsaturov I. Regulation of cholesterol biosynthesis and cancer signaling. Vol 12. Elsevier Ltd; 2012:710–716. doi:https://doi.org/10.1016/j.coph.2012.06.011.
43. McDonnell DP, Park S, Goulet MT, et al. Obesity, cholesterol metabolism, and breast cancer pathogenesis. Cancer Res. 2014;74(18):4976–82. https://doi.org/10.1158/0008-5472.CAN-14-1756.
44. Monaco ME. Fatty acid metabolism in breast cancer subtypes. Oncotarget. 2017;8(17). https://doi.org/10.18632/oncotarget.15494.
45. Medes G, Thomas A, Weinhouse S. Metabolism of neoplastic tissue. IV. A study of lipid synthesis in neoplastic tissue slices in vitro. Cancer Res. 1953;13(1):27–9.
46. Antalis CJ, Arnold T, Rasool T, Lee B, Buhman KK, Siddiqui RA. High ACAT1 expression in estrogen receptor negative basal-like breast cancer cells is associated with LDL-induced proliferation. Breast Cancer Res Treat. 2010;122(3):661–70. https://doi.org/10.1007/s10549-009-0594-8.
47. Pinzone JJ, Stevenson H, Strobl JS, Berg PE. Molecular and cellular determinants of estrogen receptor alpha expression. Mol Cell Biol. 2004;24(11):4605–12. https://doi.org/10.1128/MCB.24.11.4605-4612.2004.
48. Lingwood D, Simons K. Lipid rafts as a membrane-organizing principle. Science. 2010;327(5961):46–50. https://doi.org/10.1126/science.1174621.
49. Menendez JA, Vellon L, Lupu R. Targeting fatty acid synthase-driven lipid rafts: a novel strategy to overcome trastuzumab resistance in breast cancer cells. Med Hypotheses. 2005;64(5):997–1001. https://doi.org/10.1016/J.MEHY.2004.09.027.
50. Irwin ME, Mueller KL, Bohin N, Ge Y, Boerner JL. Lipid raft localization of EGFR alters the response of cancer cells to the EGFR tyrosine kinase inhibitor gefitinib. J Cell Physiol. 2011;226(9):2316–28. https://doi.org/10.1002/jcp.22570.
51. Zhuang L, Lin J, Lu ML, Solomon KR, Freeman MR. Cholesterol-rich lipid rafts mediate Akt-regulated survival in prostate cancer cells. Cancer Res. 2002;62(8):2227–31.
52. Egloff AM, Rothstein ME, Seethala R, Siegfried JM, Grandis JR, Stabile LP. Cross-talk between estrogen receptor and epidermal growth factor receptor in head and neck squamous cell carcinoma. Clin Cancer Res. 2009;15(21):6529–40. https://doi.org/10.1158/1078-0432.CCR-09-0862.
53. Stoica GE, Franke TF, Moroni M, et al. Effect of estradiol on estrogen receptor-α gene expression and activity can be modulated by the ErbB2/PI 3-K/Akt pathway. Oncogene. 2003;22(39):7998–8011. https://doi.org/10.1038/sj.onc.1206769.
54. Alqaisi A, Chen L, Romond E, et al. Impact of estrogen receptor (ER) and human epidermal growth factor receptor-2 (HER2) co-expression on breast

cancer disease characteristics: implications for tumor biology and research. Breast Cancer Res Treat. 2014;148(2):437–44. https://doi.org/10.1007/s10549-014-3145-x.
55. Pinhel I, Hills M, Drury S, et al. ER and HER2 expression are positively correlated in HER2 non-overexpressing breast cancer. Breast Cancer Res. 2012;14(2). https://doi.org/10.1186/bcr3145.
56. Swanson K, Hohl R. Anti-cancer therapy: targeting the mevalonate pathway. Curr Cancer Drug Targets. 2006;6(1):15–37. https://doi.org/10.2174/156800906775471743.
57. Ahern TP, Pedersen L, Tarp M, et al. Statin prescriptions and breast cancer recurrence risk: a Danish nationwide prospective cohort study. J Natl Cancer Inst. 2011;103(19):1461–8. https://doi.org/10.1093/jnci/djr291.
58. Murtola TJ, Visvanathan K, Artama M, Vainio H, Pukkala E. Statin use and breast cancer survival: a nationwide cohort study from Finland. PLoS One. 2014;9(10). https://doi.org/10.1371/journal.pone.0110231.
59. Borgquist S, Bjarnadottir O, Kimbung S, Ahern TP. Statins: a role in breast cancer therapy? J Intern Med. 2018;284(4):346–57. https://doi.org/10.1111/joim.12806.
60. Beckwitt CH, Brufsky A, Oltvai ZN, Wells A. Statin drugs to reduce breast cancer recurrence and mortality. Breast Cancer Res. 2018;20(1):144. https://doi.org/10.1186/s13058-018-1066-z.
61. Liao JK. Isoprenoids as mediators of the biological effects of statins. J Clin Invest. 2002;110(3):285–8. https://doi.org/10.1172/jci200216421.
62. Ahern TP, Lash TL, Damkier P, Christiansen PM, Cronin-Fenton DP. Statins and breast cancer prognosis: Evidence and opportunities. Lancet Oncol. 2014;15(10). https://doi.org/10.1016/S1470-2045(14)70119-6.
63. Alizadeh J, Zeki AA, Mirzaei N, et al. Mevalonatecascade inhibition by simvastatin induces the intrinsic apoptosis pathway via depletion of isoprenoids in tumor cells. Sci Rep. 2017;7. https://doi.org/10.1038/srep44841.

Publisher's Note

6. Generation and Analysis of PGRMC1-Deficient Breast Cancer Cells (Aim 2)

6.1. Background and Aim

PGRMC1 expression in breast cancer is associated with worse prognosis and lower response to anthracycline therapy [20]. Since it is overexpressed in a fraction of breast cancers, these observations suggest that PGRMC1 could be addressed as a therapeutic target. In *Asperger et al.*, we have demonstrated that treatment with a cholesterol-lowering statin is particularly efficient on PGRMC1-overexpressing hormone receptor positive MCF7 cells [99]. PGRMC1 expression could therefore be used as a marker to identify patients qualifying for combined therapy with statins. Furthermore, PGRMC1-targeting agents could be established as a therapeutic approach in future, although the existing inhibitor AG-205 exhibits PGRMC1-unrelated effects and research is needed to design a PGRMC1-specific inhibitor [100].

To extend the available cellular models for PGRMC1 *in vitro* studies and to gain broader knowledge on effects of long-term PGRMC1-deficiency, stable PGRMC1-knockout cells lines of different breast cancer subtypes were established using the CRISPR/Cas9 technology. The obtained clonal cell lines were further characterized with respect to genetic, phenotypic and functional consequences of PGRMC1 deficiency and the results were brought into the context of former observations on PGRMC1 overexpression and transient downregulation in the respective cell lines.

The CRISPR/Cas9 system was published in 2007 as an adaptive immune system in bacteria [101], and first exploited by Emmanuelle Charpentier and Jennifer Doudna in a seminal study in 2012 as a programmable and versatile gene editing tool [102]. Basically, procaryotic clustered regularly interspaced palindromic repeats (CRISPR), first observed in *E. coli* in 1987 [103], describe a region in the procaryotic genome which integrates pieces of degraded viral DNA following an infection, creating a bacterial immune memory. In case of a subsequent infection with the same virus, transcription of the CRISPR locus with the respective “spacers” (integrated viral DNA sequences) allows CRISPR associated (Cas) endonucleases to specifically target and rapidly degrade the viral genome. In the CRISPR locus, the repetitive stable sequence encodes for an RNA molecule capable of building a complex with the Cas enzyme, while the spacers provide unique sequences specific for viral target sites. After transcription, the long primary transcript is processed into CRISPR-derived RNAs (crRNAs), each containing a Cas enzyme binding site and a sequence complementary to the viral genome. Bound to Cas

endonucleases, these complexes patrol the cytoplasm and hydrolyze complementary DNA sequences [104].

After the primary publication, multiple applications for usage of CRISPR/Cas system to engineer cellular genomes were developed. In the simplest approach, by transfection of cells (either on a plasmid or by electroporation) with a Cas endonuclease and a modified crRNA containing a sequence complementary to the desired gene (called guide RNA, gRNA), the DNA sequence of interest can be hydrolyzed. The resulting double strand break is usually repaired by the cellular DNA repair systems [105]. The error-prone non-homologous end joining (NHEJ) pathway ligates breaks of the double strand, resulting in a certain percentage of mutations, mostly insertions or deletions at the break site, leading to nonsense or frameshift mutations. Depending on the location in the gene, these small mutations may lead to amino acid exchanges, truncated proteins, failed transcription or unstable mRNA, potentially leading to a loss-of-function of the protein or entirely absent protein. The double strand break may also be repaired by homology directed repair (HDR), which is more active in the synthesis phase of the cell cycle. This repair system relies on the homologous chromosome as a template for *de-novo* synthesis of the damaged DNA, involves proof-reading and is considered to be precise [106]. HDR can be hijacked by introducing an alternative homologous template (e.g. a plasmid) carrying the desired modification to the cell, which will then be precisely integrated into the genome at the site of the double strand break.

In this project, CRISPR/Cas9 technology was used to generate PGRMC1 knockout cell lines of different breast cancer subtypes. The aim was to receive a PGRMC1-null background by completely deleting the protein without any other genetic modifications including stable Cas9 overexpression or expression of any marker proteins. The benefits and disadvantages of this approach will be discussed later.

6.2. Material and Methods

6.2.1. Materials

6.2.1.1. Chemicals

Table 2: List of utilized chemicals.

Chemical	**Source**
Acetic acid	Merck KGaA, Darmstadt, Germany
Agar	Merck KGaA
Agarose	Sigma-Aldrich Corporation, St. Louis, Missouri, USA
Bovine serum albumin (BSA)	Sigma-Aldrich Corporation
Calcium chloride	Merck KGaA
Dimethyl sulfoxide (DMSO)	Sigma-Aldrich Corporation
3-(4,5-Dimethylthiazol-2-yl)-2,5-Diphenyltetrazoliumbromid (MTT)	Sigma-Aldrich Corporation
Epithelial growth factor (EGF)	Miltenyi, Bergisch Gladbach, Germany
Ethanol absolute	Merck KGaA
Ethylenediaminetetraacetic acid (EDTA)	Merck KGaA
Glycerol	Sigma-Aldrich Corporation
Glycine	Merck KGaA
Manganese (II) chloride	Sigma-Aldrich Corporation
2-Mercaptoethanol	Sigma-Aldrich Corporation
Methanol	Sigma-Aldrich Corporation
4-Morpholinepropanesulfonic acid (MOPS)	Carl Roth GmbH & Co. KG, Karlsruhe, Germany
Nonidet P-40 (NP-40)	Sigma-Aldrich Corporation
Norethisterone (NET)	Merck KGaA
Potassium acetate	Riedel-de Haën, Seelze, Germany
Potassium hydroxide solution	Merck KGaA
Sodium chloride (NaCl)	Merck KGaA
Sodium dodecyl sulfate (SDS)	Merck KGaA

Sodium deoxycholate	Sigma-Aldrich Corporation
Tris(hydroxymethyl)aminomethane (TRIS)	Merck KGaA
Tween 20	Sigma-Aldrich Corporation
Hydrochloric acid (HCl)	Merck KGaA

6.2.1.2. Cell Lines

Table 3: List of utilized and newly generated breast cancer cell lines. Stably transfected cell lines were produced previously as described in Neubauer *et al.* [95]. DSMZ: German collection of microorganisms and cell cultures GmbH.

Cell line	**Properties**	**Source/ reference**
MCF-7	Breast cancer cell line, Luminal A subtype	DSMZ [107]
MCF7/PGRMC1	Hemagglutinin (HA)-tagged PGRMC1 wildtype overexpressing MCF-7 cells, stably transfected with pcDNA3.1 vector	[95]
MCF-7/EVC	MCF-7 cells stably transfected with empty vector pcDNA3.1	
MCF7/PGRMC1-KO	PGRMC1-deficient MCF7 cells; generated by CRISPR/Cas9 approach as part of this work	[108]
MCF7/PGRMC1-Control	MCF7 control cells, generated as part of this work	
T-47D	Breast cancer cell line, luminal A subtype	DSMZ [107]
T-47D/PGRMC1-KO	PGRMC1-deficient T47D cells; generated by CRISPR/Cas9 approach as part of this work	
T47D/PGRMC1-Control	T47D control cells, generated as part of this work	
MDA-MB-231	Breast cancer cell line, Basal-like subtype	DSMZ [109]
MDA-MB-231/ PGRMC1-KO	PGRMC1-deficient MDA-MB-231 cells; generated by CRISPR/Cas9 approach as part of this work	
MDA-MB-231/ PGRMC1-Control	MDA-MB-231 control cells, generated as part of this work	

6.2.1.3. Antibodies

Table 4: List of antibodies utilized in western blotting.

Antibody	Species	Used concentration/ dilution	Order number	Source
Antibodies for Western blotting				
anti-PGRMC1	goat	0.5 µg/ml	Ab48012	Abcam, Cambridge, United Kingdom
Anti-PGRMC1	mouse	0.4 µg/ml	sc-393015	Santa Cruz Biotechnology, Dallas, USA
Anti-β-Actin	mouse	0.2 µg/ml	sc-47778	
Anti-PGRMC1	rabbit	1:1000	D6M5M	Cell Signaling, Danvers, Massachusetts, USA
Anti-ERα	Rabbit	1:1000	D8H8	
Anti-EGFR	rabbit	1:1000	D38B1	
Anti-EGFR pY1068	mouse	1:1000	1H12	
Anti-MEK	mouse	1:1000	4694S	
Anti-MEK pS217/S221	rabbit	1:1000	9121S	
Anti-ERK	rabbit	1:1000	4695S	
Anti-ERK pT202/Y204	rabbit	1:1000	4370S	
AKT	rabbit	1:1000	4685S	
Anti-AKT pS473	rabbit	1:1000	4060S	

6.2.1.4. Oligonucleotides

Table 5: List of utilized primers. Primers für the PGRMC1 gene were design using the Primer3.org online tool and ordered from Metabion international.

PCR Primer	Sequence, 5'→3'	Source
Exon1_fw	TTCGACGGCGTCCAGGAC	Metabion international, Planegg, Germany
Exon1_rev	TTCTTTTGTCTCCAAGCCCC	

Exon2_fw	GGGGCTATGTTGATGAATAGGG	
Exon2_rev	GCAGCAGTGAGGTCAGAAAG	
Exon3_fw	GGCAAGGACGGTGGTATAAAC	
Exon3_rev	CGGGCACTCTCATCTTTTGG	
M13fw	GTAAAACGACGGCCAG	Biomedical Research Center, Heinrich-Heine-University (BMFZ)

6.2.1.5. Kits and Commercial Reagents

Table 6: List of utilized kits and commercial reagents sorted by application.

Kit/ reagent	Source
CRISPR/Cas9-based PGRMC1-KO generation	
PGRMC1 CRISPR/Cas9 KO Plasmid (h)	Santa Cruz Biotechnologies
CRISPR/Cas9 KO Control Plasmid	Santa Cruz Biotechnologies
Lipofectamine™ 3000 Transfection Reagent	Thermo Fisher Scientific, Waltham, USA
Polymerase chain reaction agarose gel electrophoresis	
DreamTaq PCR Master Mix (2x)	Thermo Fisher Scientific
6x TriTrack DNA Loading Dye	Thermo Fisher Scientific
GelRed nucleic acid gel stain	Biotium, Fremont, USA
Gene Ruler Ultra Low Range DNA Ladder	Thermo Fisher Scientific
MassRuler Low Range DNA Ladder	Thermo Fisher Scientific
Sequencing	
TA Cloning Kit	Thermo Fisher Scientific
QIAEX II Gel Extraction Kit	Qiagen, Venlo, The Netherlands
S.O.C. Medium	Thermo Fisher Scientific
QIAGEN Plasmid Mini Kit	Qiagen
QIAmp DNA Micro Kit	Qiagen
S.O.C. Medium	Thermo Fisher Scientific
Western Blot	
PhosStop (Phosphatase Inhibitor)	Roche Diagnostics, Basel, Switzerland

cOmplete ULTRA tablets (protease inhibitor)	Roche Diagnostics
Pierce BCA Protein Assay Kit	Thermo Fisher Scientific
Laemmli buffer 4 x	Bio-Rad Laboratories, Hercules, USA
Precision Plus Protein All Blue Prestained Standard	Bio-Rad Laboratories
Amersham ECL Western Blotting Detection Reagents	GE Healthcare Life Sciences, Chicago, USA
Cell proliferation assessment	
CellTrace CFSE Cell proliferation Kit	Thermo Fisher Scientific
Measurement of neutral lipids	
BODIPY 493/503	Thermo Fisher Scientific

6.2.1.6. Consumption Items

Table 7: List of utilized general consumption items.

Consumption item	**Source**
Multi-well cell culture plates (96-/48-/6-well)	Greiner Bio-One, Kremsmünster, Austria
Cell culture flasks (T-25/T-75/T-175)	Greiner Bio-One
8-well 0.2 ml PCR tube strips	BrandTech Scientific, Essex, USA
DNA LoBind tubes, (1.5 ml)	Eppendorf AG, Hamburg, Germany
Protein LoBind tubes (1.5 ml)	Eppendorf AG
Safe-lock tubes (1.5 ml, 2.0 ml)	Eppendorf AG
Polypropylene tubes (15 ml/50 ml)	Greiner Bio-One
Immun-Blot PVDF membrane and filter papers	Bio-Rad Laboratories
Mini-PROTEAN Precast Gels (12-well/15-well)	Bio-Rad Laboratories
Pipette tips (10 µl/100 µl/200 µl/1000 µl)	Starlab Group, Hamburg, Germany
Stripettes (5 ml/10 ml/25 ml)	Greiner-Bio-One

6.2.1.7. Media and Solutions for Cell Culture

Table 8: List of media and solutions for cell culture.

Medium/solution	Source
(1x) Dulbecco's phosphate-buffered saline (DPBS)	Gibco, Thermo Fisher Scientific
Fetal bovine serum (FBS)	
Fetal bovine serum, charcoal stripped	
HEPES 1 M buffer solution	
Penicillin/Streptomycin 10000 U/ml	
RPMI 1640 Medium, L-Glutamine	
RPMI 1640 Medium, L-Glutamine, no phenol red	
0.5% Trypsin-EDTA (10x)	
OptiMEM serum reduce medium	

6.2.1.8. Buffers and Solutions

Table 9: List of utilized buffers and the corresponding recipes.

Buffer/solution	Components
TBST	20 mM TRIS 150 mM NaCl 0.1 % Tween-20 pH 7.6
RIPA buffer	50 mM TRIS 150 mM NaCl 1 % NP-40 0.5 % sodium deoxycholate 0.1 % SDS pH 7.6 Supplemented with phosphatase inhibitor and protease inhibitor before use

SDS buffer	25 mM TRIS 192 mM Glycin 0.1 SDS pH 8.3
Sample buffer	4 × Laemmli buffer 10 % 2-mercaptoethanol
Western blotting buffer	25 mM TRIS 200 mM Glycin 20 % Methanol
Blocking solution	5 % (w/v) BSA in TBST
LB medium for *E. coli*	20 g LB-Bouillon (Sigma Aldrich, L3022) 1 L H_2O autoclaved
LB Agar for *E. coli*	1.5 % agar in LB medium autoclaved
TFB-1	30 mM Potassium acetate 100 mM $RbCl_2$ 10 mM $CaCl_2$ 50 mM $MnCl_2$ 15 % Glycerol pH 5.8
TFB-2	10 mM MOPS 75 mM $CaCl_2$ 10 mM $RbCl_2$ 15 % Glycerol pH 6.6 (KOH)
TAE buffer	40 mM TRIS 20 mM acetic acid 1 mM EDTA pH 8.5

6.2.2. Methods

6.2.2.1. Cell Biological Methods

6.2.2.1.1. Cultivation of Human Breast Cancer Cell Lines

Human breast cancer cell lines MCF7, T47D, MDA-MB-231 and all transfected cell lines were subjected to short tandem repeat (STR)-analysis prior to experiment start. The analysis was performed by the cell line authentication service of the company Microsynth AG.

All cells were cultured in RPMI medium supplemented with 10 % FCS, 25 mM HEPES and 1 % penicillin/streptomycin. This medium is later referred to as culture medium. Cells were incubated in cell culture flasks at 37 °C with 5 % CO_2 in humidified atmosphere and passaged at 80 – 90 % confluency. For passaging, cells were washed with pre-warmed PBS buffer, detached with 0.05 % trypsin-EDTA at 37 °C for 5 min and resuspended in culture medium. After centrifugation at 1100 rpm for 5 min the cell pellet was resuspended in fresh culture medium and an appropriate cell number was transferred into a new flask.

6.2.2.1.2. Cryoconservation

For long time storage, cells were harvested at 80 – 90 % confluency as described in 6.2.2.1.4, the cell pellet was resuspended in 1 ml freezing medium (composed of 45 % culture medium, 45 % FCS and 10 % DMSO as cryoprotectant) and frozen in cryo-tubes at -80 °C in a freezing container. After 24 h, the cryotubes were maintained in liquid nitrogen atmosphere.

When taken into culture, cryo-stocks were thawed quickly at 37 °C, diluted with 10 ml culture medium and centrifuged at 1100 rpm for 5 min. The cell pellet was carefully resuspended in fresh medium and transferred into a new flask.

6.2.2.1.3. Synchronization of Cells in Minimal Medium

To exclude the influence of cell cycle dependent protein expression on the experimental outcome, cells were synchronized for certain experiments. For this purpose, cells were seeded in an appropriate density in culture medium. After 24 h, the medium was replaced by RPMI medium (no phenol red) containing 10 % charcoal stripped FCS, 25 mM HEPES and 1 % penicillin/streptomycin (referred to as stripped medium) and incubated for another 24 h. Finally, the medium was changed again to culture medium for 24 h and the following experiment was started directly afterwards.

6.2.2.1.4. Harvesting of Cells for Further Analysis

Harvesting of cells for gene expression analysis via western blot was performed by mechanical detachment. Culture flasks or 6-well plates were placed on ice and washed twice with ice-cold PBS. An appropriate amount of ice-cold PBS was applied, and cells were detached with a cell scraper, resuspended and centrifuged 5 min at 1100 rpm. Supernatant was removed and the cell pellet was stored at -80 °C.

6.2.2.1.5. Harvesting of Cells for Direct Polymerase Chain Reaction

For PCR screening of CRISPR/Cas9 generated PGRMC1-knockout clones, pellets of each clone were harvested from a 48-well plate. Therefore, the cells were washed with PBS and detached with 0.05 % trypsin-EDTA at 37 °C for 5 min. Cells were resuspended in an appropriate volume of culture medium, half of the suspension was transferred into a reaction tube and centrifuged at 500 x g for 5 min. The pellet was washed twice with ice-cold PBS and stored at -80 °C for further analysis.

6.2.2.1.6. Generation of Breast Cancer Cell-Conditioned Culture Medium

For generation of conditioned medium, cells of an early passage (<10) were seeded in T175 flasks and incubated for 48 h. At a confluency of maximal 80 %, medium was aspirated, filtered through a 0.2 µm sterile filter and stored as conditioned medium at -20 °C until usage.

6.2.2.1.7. Treatment

Hormones

To monitor response of breast cancer cell lines to progestin treatment in dependence of PGRMC1 expression level, cells were seeded in technical triplicates in 96-well plates in culture medium. After 24 h of incubation medium was aspirated, cells were washed 1× with sterile PBS to remove any hormone residues and incubated with stripped medium for 48 h. Subsequently, medium was replaced by stripped medium containing either NET in 10^{-6} M, E2 in 10^{-8} M, or EGF in 10 ng/ml. For control, 0.01 % DMSO in stripped medium was used. For assessment of cell proliferation, plates were incubated for 72 h followed by MTT assay.

EGF

Short-term treatment of breast cancer cell lines with EGF was conducted to assess phosphorylation of EGFR and its downstream targets. Cells were seeded in 6-well plates in culture medium and synchronized as described in 6.2.2.1.3. Following 24 h of incubation in

culture medium, cells were stimulated with 10 ng/ml EGF for 10 min, placed on ice and harvested according to 6.2.2.1.4.

6.2.2.1.8. MTT-Assay

To assess cell proliferation, MTT assay was used as a metabolic surrogate for cell number. After growth on 96-well plates in technical triplicates for a defined time period (specified for each experiment), medium was replaced by MTT-medium, containing 0.25 mg/ml MTT in assay medium (culture medium or stripped medium, depending on the assay), diluted from a 5 mg/ml MTT-stock in PBS. MTT-medium was incubated on the cells for 3 h, followed by extraction of the produced formazan with DMSO for 30 min at 37 °C and 300 rpm on a plate shaker. Extinction was measured on TECAN SPARK plate reader at 540 nm.

6.2.2.1.9. CFSE-Assay

To measure proliferation of breast cancer cell lines independently of metabolism, the CellTrace CFSE Cell Proliferation Kit was used according to manufacturer's specifications. First, cells were detached as described in 6.2.2.1.4 and washed in PBS. One aliquot of CellTrace dye was dissolved in 18 µl DMSO and diluted 1:1000 in PBS. Cell pellets were resuspended in dye solution and incubated for 20 min at 37 °C protected from light. Subsequently, five times the staining volume of culture medium was added to cells followed by 5 min incubation at 37 °C. Cells were centrifuged at 1100 rpm for 5 min and the pellet was resuspended in fresh pre-warmed culture medium. Each cell line was seeded into 4 wells of a 6-well plate (1 well per day of analysis) and incubated at 37°C and 5 % CO_2. The remaining stained cells were centrifuged and resuspended in PBS to be analyzed via flow cytometry. Proliferation was measured over 5 days by detaching the cells of one 6-well as described in 4.2.1., resuspending in PBS and detecting green fluorescence of the CellTrace dye every 24 h by flow cytometry (excitation 492 nm, emission 517 nm). Fold decreased mean fluorescence over day 0 was calculated for each measurement after setting the gates for living single cells using the FlowJo v10.8 Software (BD Life Science).

6.2.2.1.10. Transfection with CRISPR-Cas9 Plasmids

For generation of PGRMC1-knockout breast cancer cell lines, cells were transiently transfected with commercially available CRISPR/Cas9-plasmids designed for PGRMC1-knockout. The transfection plasmid mix that was employed in this project comprises of three plasmids, each containing the expression system for the *Streptococcus pyogenes* Cas9 enzyme transcribed

from the 2A promotor, the sequence for green fluorescent protein (GFP) under control of an internal ribosomal entry site (IRES) to identify transfected cells, and a unique sequence for a PGRMC1-specific guide RNA (gRNA) under control of U6 promotor. Both promotors are constitutively active in mammal cells. Using this plasmid mix for transfection, all three plasmids were administered simultaneously to the cells. For control, a plasmid containing Cas9-enzyme sequence, GFP sequence and an unspecific gRNA sequence was used. The transfection was carried out using lipofectamine 3000 reagent according to manufacturer's instructions. For transfection, cells of an early passage (<5) were seeded in culture medium and incubated for 24 h. On the day of transfection, plasmid-DNA was diluted in OptiMEM und supplemented with P3000 agent, and mixed with Lipofectamine 3000, diluted in OptiMEM. After 10 min of incubation at room temperature, fresh culture medium was applied on the cells and the transfection complexes were pipetted dropwise onto the cells. For expression of the CRISPR/Cas9 compounds and the accomplishment of the CRISPR-reaction, cells were incubated for 48 h. Subsequently, single cells were distributed into 96-wells either by FACS for GFP-positive (transfected) cells or by limiting dilution for generation of single cell clones.

6.2.2.1.11. FACS Sorting for GFP-Positive Single Cells

For generation of single cell clones and selection of PGRMC1-knockout cells from the transfected bulk population, FACS sorting for cells expressing GFP from the IRES on the transfection plasmid was performed. Cells were therefore detached 48 h post-transfection according to 6.2.2.1.4, centrifuged at 1000 rpm for 5 min, resuspended in fresh culture medium and filtered through a 100 µm filter. FACS was performed by the Core Facility Flow Cytometry at the Medical Faculty of the University Clinic Duesseldorf. GFP-positive single cells were sorted into 96-well plates containing 50 µl of conditioned medium for the respective cell line (6.2.2.1.6). Cells were further incubated with monitoring by microscopy and regular medium change using conditioned medium until formation of colonies.

6.2.2.1.12. Subcloning by Limiting Dilution

An alternative method of subcloning was simultaneously used to receive single cell colonies. Cells were detached 48 h post-transfection, resuspended in culture medium and counted. Using dilution series, a cell concentration of 5-10 cells/ml was adjusted in conditioned medium for the respective cell line, and 100 µl of the suspension were seeded into each inner well of a 96-well plate (wells B2-G11). The outer wells were filled with 100 µl PBS to avoid evaporation

during long-term culture. Cells were further incubated with monitoring by microscopy and regular medium change using conditioned medium until formation of colonies.

6.2.2.1.13. Clonal Expansion of Transfected Cells

When single cell colonies reached a size of approximately ¼ of a 96-well, cells were detached, transferred into a well of a 48-well-plate in culture medium and further incubated until reaching a confluency of appr. 80 %. Subsequently, cells were detached and subjected to a direct screening PCR for confirmation of genetic modification of the PGRMC1 locus.

6.2.2.2. Molecular Biological Methods

6.2.2.2.1. DNA Isolation

DNA-isolation was performed using the QIAmp DNA Mini Kit. For DNA isolation, a number of a minimum of 0.5 million cells was harvested and washed twice with PBS. The pellet was resuspended in 200 µl PBS, supplemented with 20 µl Proteinase K and 200 µl Buffer AL and incubated for 10 min at 56 °C. The further procedure was carried out according to manufacturer's instructions.

6.2.2.2.2. Polymerase Chain Reaction

Screening for single cell clones with genetically modified PGRMC1-loci was performed by direct polymerase chain reaction (PCR) from harvested cells. The establishment of the PGRMC1-knockout screening PCR is described in detail in chapter 6.3.1.1. Briefly, cell pellets from a 48-well were resuspended in TRIS lysis-buffer and incubated at 99 °C for 15 min. Cell debris was pelleted for 20 min at 14000 rpm and the lysate was transferred into a fresh tube and stored at 20°C until direct PCR. The primers were designed to bind shortly upstream or downstream each of the gRNAs binding sites to detect deletions in the respective sequence using the Primer3 online tool [110], pre-tested with respect to hybridization temperature and concentration on purified genomic breast cancer cell DNA and on copy DNA (cDNA). For PCR, a master mix with DreamTaq Polymerase was prepared according to manufacturer's instructions, using a combination of appropriate primers in concentration of 5 nM, selected depending on the application (screening or sequencing) and specified in each respective experiment. PCR conditions are indicated in Table 10. For subsequent analysis of PCR products, 5 µl of each PCR reaction was mixed with 1 µl of TriTrack loading dye and separated on a 3 % agarose gel containing 0.01 % GelRed and GeneRuler Ultra Low Range DNA Ladder or GeneRuler Low Range DNA Ladder as size reference.

Table 10: PCR cycler program for screening and sequencing PCR.

Cycles		Temperature	Duration
1	Polymerase activation	95 °C	3 min
30	Denaturation	95 °C	30 sec
	Primer annealing	58 °C	30 sec
	Extension	72 °C	1 min
1	Final extension	72 °C	5 min

6.2.2.2.3. Sequencing of PCR-Fragments

To assess genomic changes introduced by the CRISPR/Cas9 reaction to the PGRMC1-locus, PCR products were sequenced by Sanger sequencing method. For sequencing of PCR samples containing only one product, sequencing was performed after extraction of the band from the gel. Therefore, a volume of minimum 40 µl PCR reaction was loaded on a 1 % agarose gel after performing the PCR according to 6.2.2.2.2. Separation of PCR bands was evaluated under UV light; bands were excised from the gel with a sharp scalpel and placed in a 1.5 ml reaction tube with transferring as little agarose as possible. Extraction of PCR products from the gel was then performed using the QIAEX II Gel Extraction Kit according to manufacturer's specifications. Products were eluted in 12 µl pure water, quantified at the NanoDrop spectrophotometer and subjected to Sanger sequencing.

For PCR samples containing multiple products, the latter were integrated into a TA-cloning vector and amplified in *E. coli* beforehand. Therefore, the Thermo Fisher TA Cloning Kit was employed according to manufacturer's recommendations. Briefly, 1 µl of fresh PCR product generated by DreamTaq as described in 6.2.2.2.2 was ligated into the pCR 2.1 vector using the standard kit protocol. Transformation of *E. coli* with the pCR 2.1 vector, plating of bacterial suspension on agar plates and expansion of single bacterial colonies in overnight cultures was performed as described 6.2.2.3.2. Plasmids were isolated from each of the overnight cultures using the Qiagen Plasmid Mini Kit according to the instructions. DNA was eluted from the column in 50 µl nuclease-free water and concentration was determined at the NanoDrop spectrophotometer. To confirm successful isolation of vector containing insert, isolated plasmid DNA was subjected to a control PCR using the same primer combination as for the initial gene fragment amplification.

Hereafter, Sanger sequencing of the isolated plasmid DNA/ purified PCR band was conducted in cooperation with Prof. Dr. Karl Köhrer at the Heinrich-Heine University biomedical research center (BMFZ) using the M13 forward primer for plasmids and the respective PCR primers for excised bands. For analysis, the obtained sequences were aligned to genomic or transcript sequence of PGRMC1 (Ensembl ID: PGRMC1-gene: ENSG00000101856; PGRMC1-transcript: ENST00000217971.8) using the online alignment tool MultAlin [111]. Furthermore, nucleotide sequences were translated into amino acid sequences with ExPASy online tool [112] to decipher potential consequences of the detected alterations on protein level.

6.2.2.3. Microbiological Methods

6.2.2.3.1. Generation of Competent *E. coli*

For generation of competent *E. coli* TOP10, bacteria were grown in 5 ml LB medium without antibiotics overnight at 37 °C. The overnight culture was transferred into 200 ml LB medium in a baffled flask and incubated at 37 °C under decent shaking to an optical density (OD_{550}) of 0.6. The suspension was centrifuged at 4°C and 4000 rpm for 10 min in 50 ml portions, the pellets were resuspended in 20 ml ice-cold TFB-1 buffer each and incubated on ice for 10 min. Subsequently, bacteria were centrifuged at 4°C and 4000 rpm for 10 min, resuspended in 2 ml ice-cold TFB-2 buffer and incubated on ice for 15 min. Competent *E. coli* were divided into 100 µl aliquots, shock-frozen in liquid nitrogen and stored at -80 °C.

6.2.2.3.2. Transformation of *E. coli*

The ampicillin sensitive *E. coli* TOP10 strain was used to amplify plasmid DNA following TA-cloning. For transformation, one aliquot of competent *E. coli* was thawed on ice, a volume of 2 µl of the ligation reaction was mixed with 8 µl nuclease-free water and added to the bacterial suspension. After incubation on ice for 30 min, a heat shock was performed for 1 min at 42 °C. A volume of 250 µl S.O.C medium was added and bacteria were incubated at 37 °C and 600 rpm on a reaction tube shaker for 1 h. Finally, the suspension was plated on agar plates containing LB medium with 1.5 % (w/v) agar and 100 µg/ml ampicillin and incubated overnight upside-down at 37 °C. After 24 h, 5 ml LB medium containing 100 µg/ml ampicillin were inoculated with a single bacterial colony picked from the agar plate with a sterile pipet tip and incubated at 37 °C overnight to amplify plasmid DNA.

6.2.2.4. Protein Chemical Methods

6.2.2.4.1. Western Blot

For analysis of protein expression, pellets harvested as described in 4.2.4 were thawed on ice, resuspended in RIPA buffer and pulse-vortexed for 10 sec. Cell suspension was incubated for 20 min at 4 °C and 750 rpm on an orbital shaker and centrifuged for 20 min at 14000 rpm at 4°C. The supernatant was transferred into a fresh reaction tube and protein concentration was determined using the Pierce™ BCA Protein Assay Kit according to the manufacturer's specifications. An amount of 25 µg protein containing 1 × Laemmli sample buffer with 2-mercaptoethanol was analyzed via western blotting.

Samples for protein expression analysis and molecular weight marker were loaded onto Mini-PROTEAN Precast Gel and separated by sodium dodecyl sulfate polyacrylamide gel electrophoresis (SDS-PAGE) at 150 V in SDS-PAGE buffer. For blotting, the PVDF membrane was activated in methanol and all components for blotting were equilibrated in blotting buffer for 5 min. Proteins were transferred from the gel onto the membrane for 16 h at 4 °C and 10 mA in western blotting buffer. The membrane containing the proteins was equilibrated shortly in TBST buffer. Unspecific binding was blocked with blocking solution for 1 h at RT and gentile shaking. Primary antibody was applied in the respective concentration (Table 4) in blocking solution overnight at 4 °C. The membrane was washed 3 × 10 min in TBST and incubated with the secondary antibody (conjugated with horseradish peroxidase) in 1 % BSA in TBST for 1 h at RT and gentile shaking. After washing 3 × 10 min in TBST, proteins were detected using the Amersham ECL Western Blotting Detection Reagent.

6.2.2.4.2. Statistical Analysis

All statistically evaluated results were confirmed in at least three independently performed experiments. Statistical analysis was performed using GraphPad PRISM 9.5.0 software. Datasets were tested for normal distribution by Kolmogorov-Smirnov and Shapiro-Wilk test. Statistical significances were determined using two-way ANOVA for groups with two tested parameters or one-way ANOVA for one tested parameter. The specific test and the calculated significance are indicated for each experiment. A statistically significant difference was assumed at a value of $p < 0.05$.

6.3. Results

6.3.1. Generation of PGRMC1-Deficient Breast Cancer Cell Lines

6.3.1.1. Establishment of Direct Multiplex Screening PCR for Clones with *PGRMC1*-Modified Locus

For the CRISPR/Cas9 reaction, a commercially available system of 3 expression plasmids was used, each containing the gene for canonical Cas9 with green fluorescent protein (GFP) under control of an IRES and a unique gRNA specific for PGRMC1 (see 6.2.2.1.10). For clarity, the PGRMC1 locus, the applied gRNAs, the mRNA and the resulting protein are schematically depicted in Figure 3.

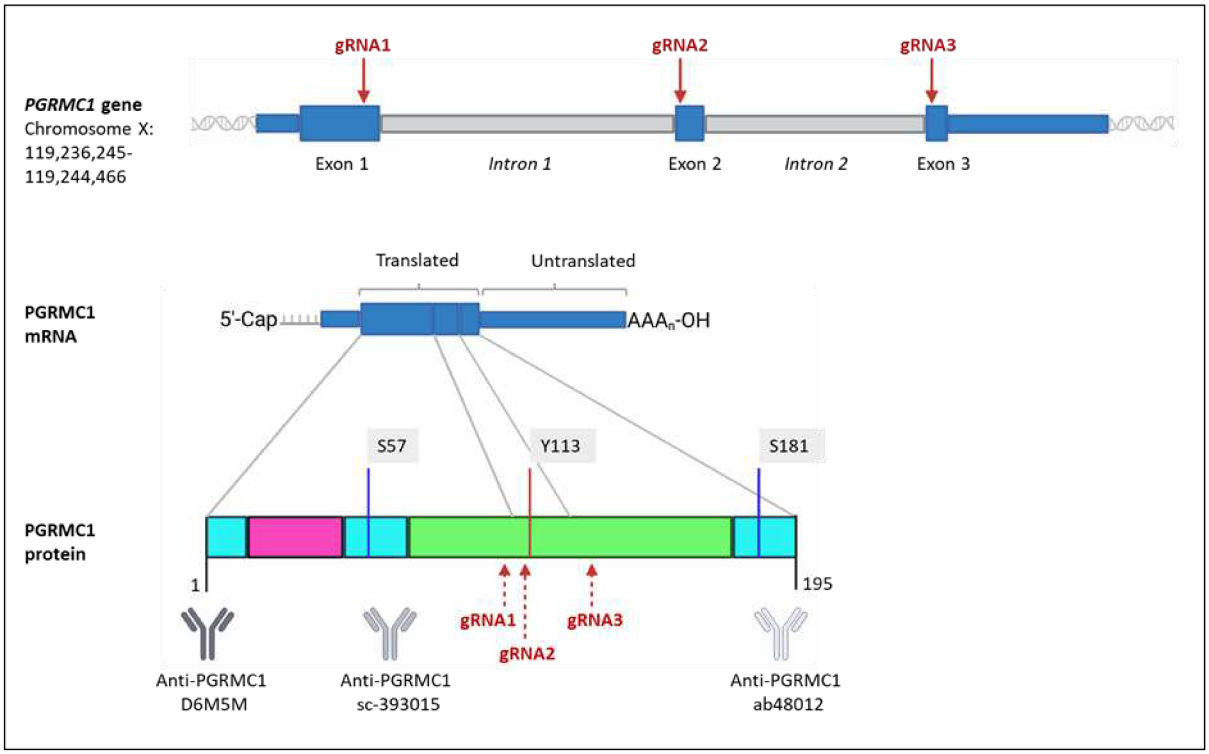

Figure 3: Schematic representation of the PGRMC1 locus, the PGRMC1 mRNA and protein, adapted from Ensembl, ID ENSG00000101856. The PGRMC1 locus is located on the X-chromosome, with 3 exons (blue) and 2 introns (grey), with the translated regions in thick blue bars. The position of gRNAs is represented by red arrows. Spliced PGRMC1 mRNA contains a translated region in thick blue bars, a 5'-Cap structure and a 3'-poly-adenine-tail (AAA_n). The PGRMC1 protein is presented in the same color code as in Figure 1 (Introduction). Magenta: trans-membrane helix, cyan: unstructured regions, green: cytb5-domain. The binding sites for different PGRMC1-antibodies are indicated by the antibody-symbols, the protein structures that correspond to the gRNA-binding sites on DNA are marked with dotted red arrows. Important phosphorylation sites are marked with flags. Created with BioRender.

The gRNA sequences were obtained from the manufacturer upon request and further verified and checked for off-target sites using the online gRNA design tools chopchop by the University of Bergen [113] and RGenome by Seoul National University [114]. Results of this analysis are summarized in Table 11. Of note, especially gRNA2 was predicted to have 16 off-target sites considering 3 mismatches.

Table 11: Sequences of purchased gRNAs, their binding sites and predicted off-target sites. For prediction, online tools chopchop by University of Bergen [113] and RGenome by Seoul National University [114] were used. [1]: predicted by RGenome; [2]: predicted by chopchop.

	gRNA sequence	Binding site	Off-target sites with 0 mismatches	Off-target sites with 3 mismatches
gRNA1	GGCCGCAAATTCTACGGGCC	chrX:119236669; Exon 1	0[1,2]	2[1,2]
gRNA2	CTTCCAGCAAAGACCCCATA	chrX: 119240313; Exon 2	0[1,2]	16[1,2]
gRNA3	TCCAGTCAAGTATCATCACG	chrX: 119243145; Exon 3	0[1]	0[1]

To establish a direct screening PCR for subsequent detection of successfully modified cells, PCR primers were designed to flank each gRNA binding site and produce PCR products with a length between 200 and 250 bp (Figure 4). The rationale was to combine all primers into one multiplex screening PCR, allowing detection of all large modifications in one PCR reaction per sample. On genomic DNA of the parental cells, primer combinations of exon1_fw and exon2-rev or exon3rev would not result in any products if using the standard amplification time for short fragments of 1 min. Theoretically, in case of transfection of one cell with two or three of the plasmids simultaneously and subsequent CRISPR/Cas9-introduced multiple double strand breaks, one or both introns could be deleted after error-prone NHEJ repair, along with a significant part of an exon. In case of large deletions, primers for different gRNA binding sites which are several kilobases apart from each other on the original genomic locus would land in close proximity and produce bands of predicted sizes of 187 bp, 188 bp or 162 bp, respectively. Any random rearrangements or small mutations created by NHEJ repair could not be predicted but could lead to a phenotypical PGRMC1 deficiency. Therefore, any unexpected changes in the PCR profile during screening were to be further analyzed. Primers were selected to have similar melting temperatures to be combined in one multiplex PCR and to produce PCR products of distinguishable sizes in agarose gel electrophoresis.

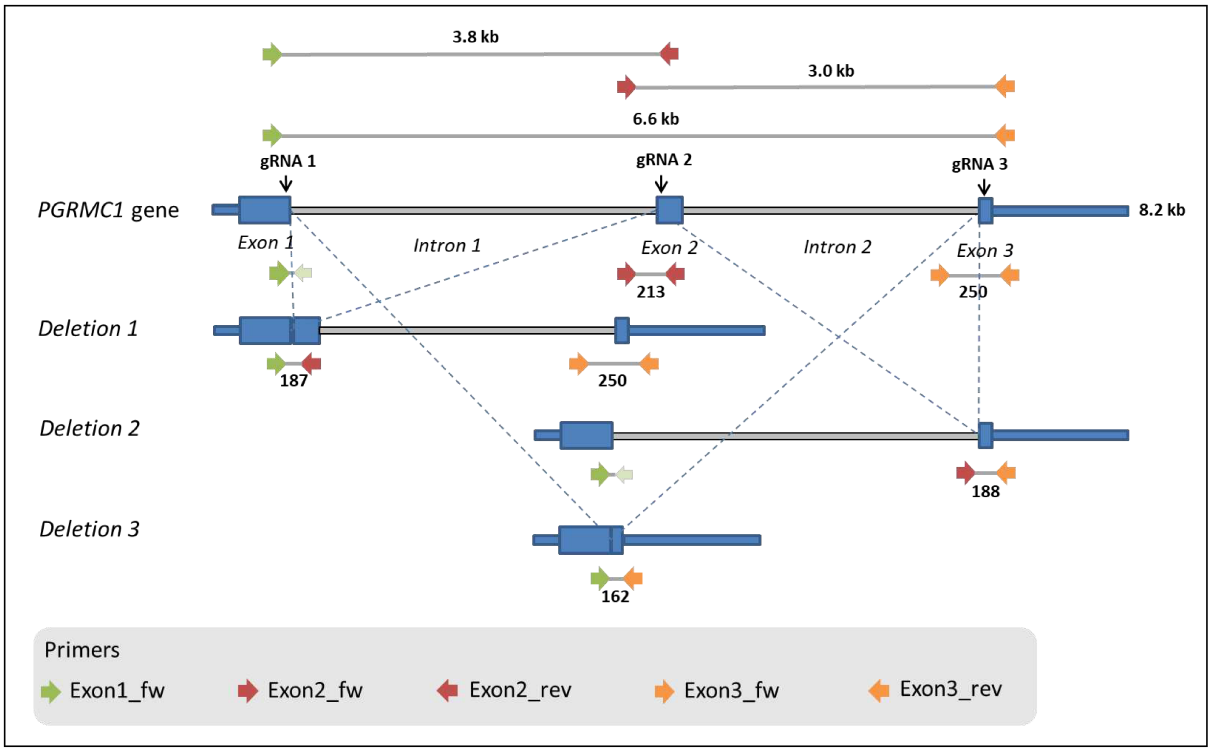

Figure 4: Schematic representation of the *PGRMC1* locus, the position of selected primers and the applied gRNAs. Modifications of the locus in case of intron deletions (along with parts of the exons) are indicated in dotted blue lines. Resulting PCR product sizes are indicated under each primer combination. Created with BioRender.

Subsequently, selected primers were tested with respect to hybridization temperature, specificity and amplification efficiency in direct PCR. DNA isolation was intended to be omitted on PGRMC1 knockout clones to reduce costs and accelerate the screening process. Therefore, pellets of parental MCF7 cells were lysed at 95°C for 10 min in different solvents and conditions ((1) ultrapure water, (2) TRIS lysis buffer, (3) TRIS lysis buffer followed by proteinase K digestion for 15 min at 56 °C with subsequent inactivation at 96 °C for 5 min), centrifuged at 14000 rpm for 20 min and the lysate directly subjected to a PCR reaction. Purified MCF7 DNA served as reference to control efficiency of adjacent primers in direct PCR, while reverse transcribed copy DNA (cDNA) of purified MCF7 mRNA was used to test the combination of primers exon1_fw and exon2_rev or exon3_rev, respectively. Primer pairs were tested individually and combined into a multiplex reaction; PCR products were separated on a 3 % agarose gel by electrophoresis (6.2.2.2.2). After testing the annealing temperature, a hybridization at 58 °C was selected for future PCR reactions. With regard to lysis buffer, different solvents did not have any influence on PCR efficiency or specificity. Since the TRIS buffer without proteinase K does not require the digestion step and therefore minimizes time for sample preparation, it was selected as lysis buffer for future screening. Concerning the specificity and efficiency of the designed primers, two of the combinations (exon2_fw +

exon2_rev; exon3_fw + exon3_rev) produced a single defined PCR product of the predicted size, while the pair exon_1_fw + exon1_rev resulted in a weak band. However, primer exon1_fw combined with either exon2_rev or exon3_rev produced the predicted products on cDNA, demonstrating its efficiency. Therefore, an alternative reverse-primer for the binding site of gRNA1 was designed and tested (Exon2_rev2) which did not produce any PCR product (data not shown). The combination of all six primers in a multiplex PCR provided two PCR products of 213 and 250 bp with no product for the binding site of gRNA1. Since the establishment of a reverse primer in the first GC-rich intron was unsuccessful, screening PCR was set up using a combination of five primers (exon1_fw, exon2_fw, exon2_rev, exon3_fw, exon3_rev), allowing detection of all theoretically predicted CRISPR/Cas9 generated genetic variants.

6.3.1.2. PCR-Screening Successfully Identified PGRMC1-Deficient Single Cell Clones

After establishment of the screening PCR, breast cancer cells were transfected with CRISPR/Cas9 plasmids harboring an expression system for Cas9, GFP under control of an IRES and a PGRMC1-targeting gRNA or with a control plasmid encoding for an unspecific gRNA according to 6.2.2.1.10. To generate single cell clones, transfected cells were either sorted by FACS for GFP-positive cells directly into wells of 96-well plates, or subcloned by limiting dilution. To support survival and proliferation of single cells, sterile filtered conditioned medium of the respective cell line was used. Subsequently, 96-well plates were further incubated with regular medium change until formation of colonies. Cell colonies of appropriate size were transferred into wells of a 48-well plate and aliquots of the pellets were harvested for screening. After lysis and centrifugation, supernatants containing genomic DNA were subjected to direct multiplex screening PCR as established in 6.3.1.1. A representative agarose gel of transfected and subcloned MCF7 cells is depicted in Figure 5. As control, purified genomic DNA of parental MCF7 cells was used.

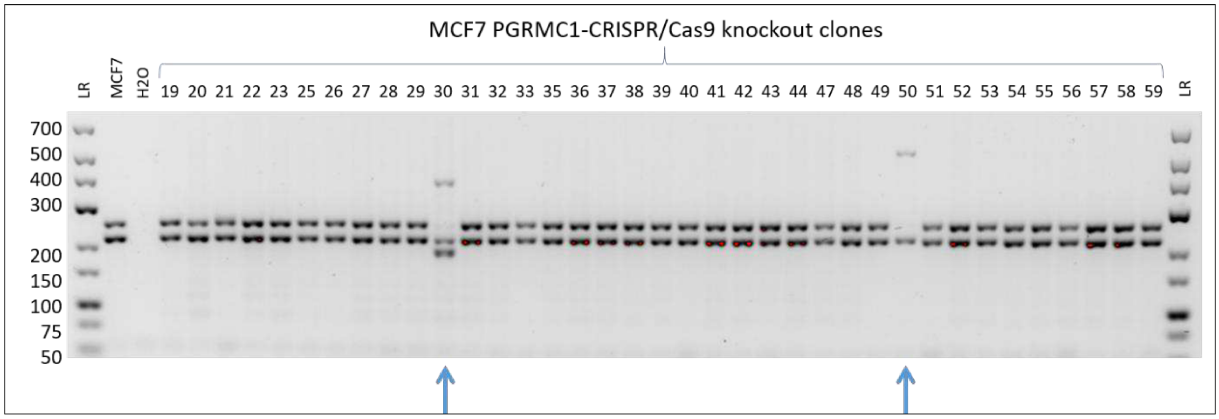

Figure 5: Representative 3% agarose gel of screening PCR for PGRMC1-knockout clones. Direct PCR was conducted with the previously established protocol using primers exon1_fw, exon 2_fw, exon2_rev, exon3_fw, exon3_rev on lysates of single cell clones from 48-well format. For control, purified DNA from parental MCF7 cells or ultrapure water (H2O) was used. Size reference: low range DNA ladder (LR) reaching from 25 bp to 700 bp; band sized are indicated in the left panel. Numbers from 19 – 59: lysates from expanded single cells clones, transfected with CRISPR/Cas9 plasmids targeting PGRMC1. MCF7 reference bands correspond to products of exon2_fw + exon2_rev (213 pb, lower band) and exon3_fw + exon3_rev (250 bp, upper band). Clones 30 and 50 demonstrate an aberrant band pattern with additional bands, potentially corresponding to deletions and rearrangements.

The multiplex screening PCR and subsequent agarose gel electrophoresis identified clones with aberrant bands, divergent from PCR products on the original PGRMC1 sequence. PCR on the reference MCF7 genome provided two products of predicted sizes (213 bp and 250 bp), corresponding to the target region of gRNA2 and gRNA3, while most of the clones presented the identical band pattern and were therefore not considered as knockout clones. Screening PCR detected bands lower in size, possibly corresponding to the predicted 187 bp or 188 bp bands, on a few clones (like clone MCF7/PGRMC1-KO30). Some clones demonstrated unpredicted PCR products, e.g. clone MCF7/PGRMC1-KO30, -KO50, with a band size over 400 bp. For CRISPR/Cas9 control clones, only the original MCF7 band pattern was detected, as expected. Since any of the aberrations in PCR band pattern, even unpredicted ones, could result in silenced *PGRMC1* locus, all clones with an aberrant band pattern and control clones were expanded, secured in cryo-conserved stocks and aliquots were harvested for expression analysis on mRNA and protein level. Importantly, not all subcloned single cells formed a colony that could be analyzed. The numbers of screened clones for each cell line and the knockout-rates for every cell line are summarized in Supplementary Table 1. The highest rate CRISPR/Cas9 modified cells was achieved by FACS-based subcloning.

6.3.1.3. PGRMC1-Deficient Breast Cancer Cells Were Successfully Generated by CRISPR/Cas9 Approach

Selected clones of each cell line presenting aberrant PCR band pattern and control clones were validated on protein level by western blotting according to 6.2.2.4.1, using an N-terminus-binding anti-PGRMC1 antibody (Figure 6).

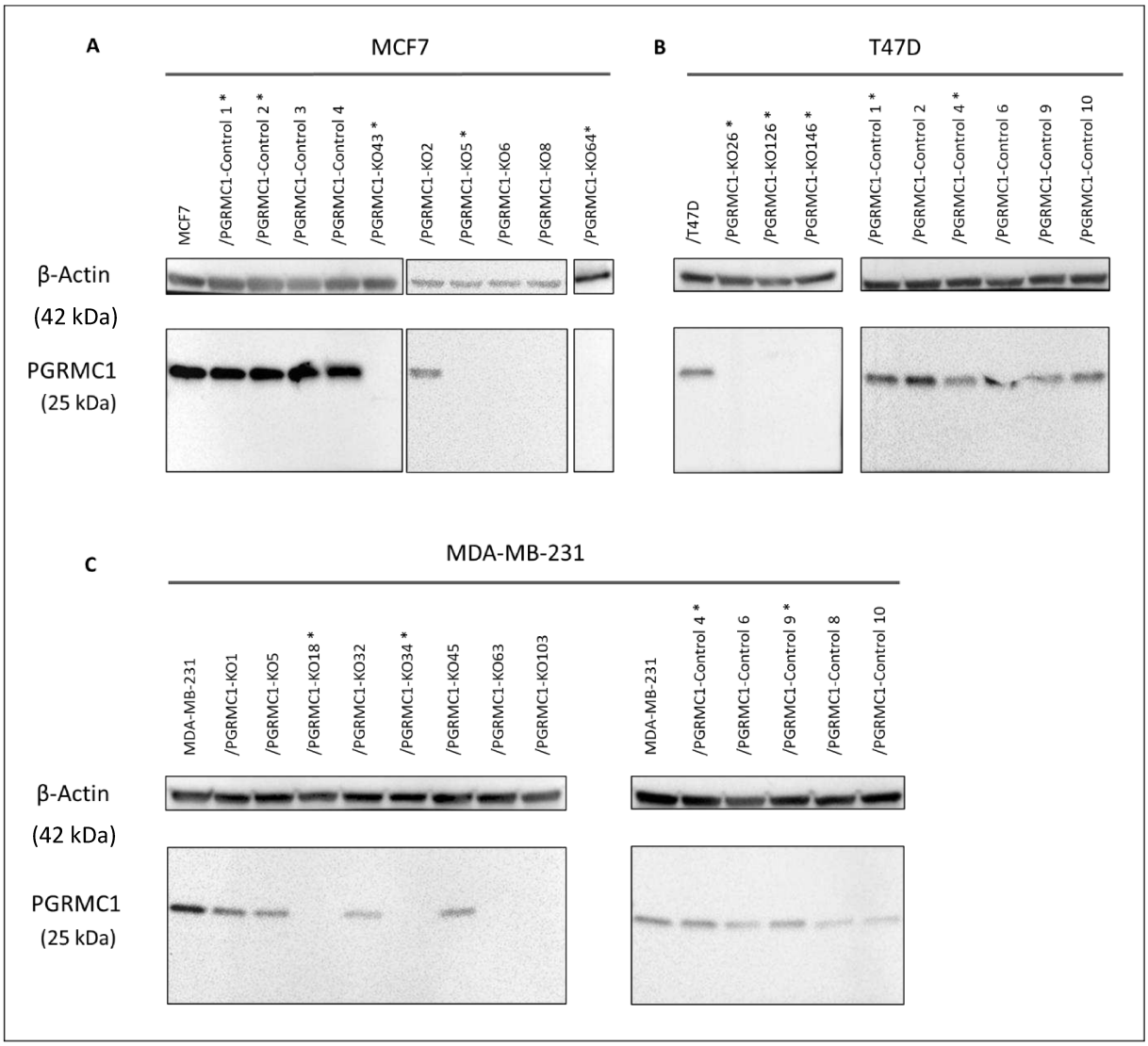

Figure 6: Western blot analysis of some PGRMC1-KO and -Control clones of MCF7, T47D and MDA-MB-231 cells. A: Parental MCF7, MCF7/PGRMC1-Control and MCF7/PGRMC1-KO cells. B: Parental T47D, T47D/PGRMC1-Control and T47D/PGRMC1-KO cells. C: Parental MDA-MB-231, MDA-MB-231/PGRMC1-Control and MDA-MB-231/PGRMC1-KO cells. PGRMC1 was detected by the N-Terminus binding antibody (Cell Signaling). For loading control, β-Actin was detected. Clones selected for further analysis are marked with an asterisk (*).

For further characterization, up to three clones for each cell line and two control clones were tested on protein level using up to three different PGRMC1-specific antibodies, to potentially identify truncated or aberrant protein. For this purpose, a C-terminus-binding antibody and an antibody directed against the cytochrome P450 domain of the protein were additionally detected in western blotting in a master thesis supervised as part of this dissertation [115].

For most of the selected and analyzed clones, PGRMC1 protein (25 kDa) could not be detected in western blotting with either of the antibodies, pointing towards a successful PGRMC1 knockout in those cells. Both the C-terminus-binding and the cytochrome P450-binding antibodies detect additional faint bands of higher sizes present in every sample independently of the CRISPR/Cas9 reaction, suggesting a cross-reactivity of these antibodies with other unidentified proteins. However, in MCF7/KO43, a weak band of lower size was detected with the N-terminus-binding antibody (Figure 7), while in T47D/KO126, a band of higher size and low intensity could be identified (Supplementary Figure 2). These bands could correspond to truncated or structurally different PGRMC1-proteins with low stability or low affinity to the applied antibodies.

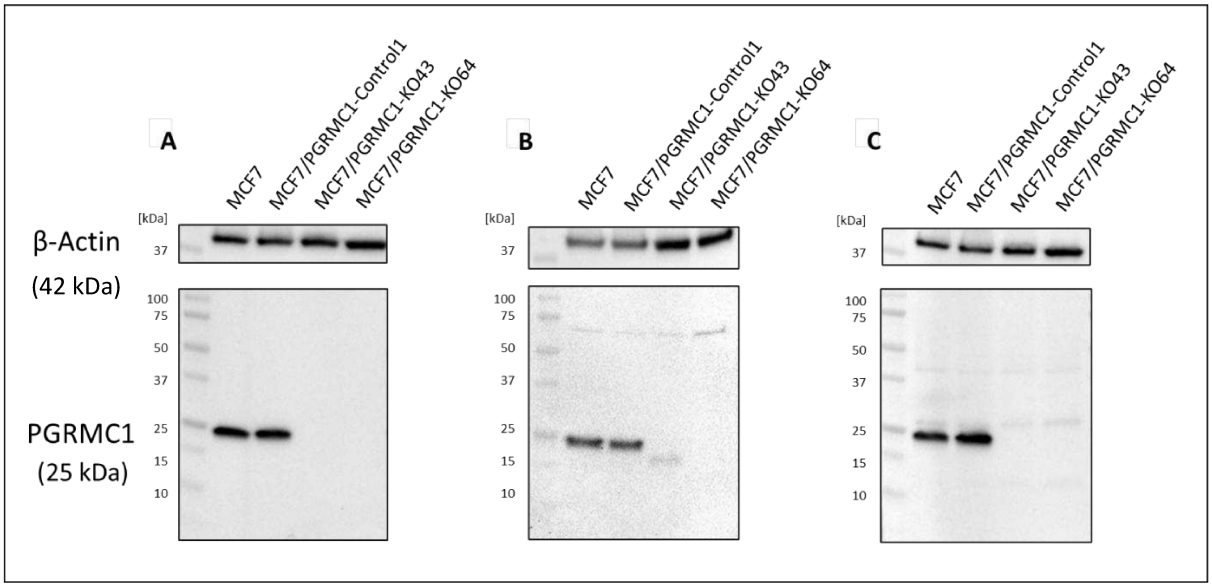

Figure 7: Western blot of CRISR/Cas9-modified MCF7-cells. Whole cell lysates of MCF7 parental cells, MCF7/PGRMC1-Control1 and MCF7/PGRMC1-KO43 and -KO6 were blotted and analyzed with three different α-PGRMC1 antibodies. A: N-terminus detecting antibody (Cell signaling); B: antibody binding part of the CytB5 domain (Santa Cruz); C: Antibody binding the C-terminus of PGRMC1 (Abcam). As loading control, β-Actin was detected. Adapted according to Oles, 2013.

Taken together, PGRMC1-deficient cells for the cell lines MCF7, T47D and MDA-MB-231 were successfully generated. However, the aberrations detected by PCR were heterogenous, and the modifications introduced to the cells by CRISPR/Cas9 were putatively unexpected.

To address and dissect genetic changes generated by CRISPR/Cas9 in PGRMC1-knockout clones, the cells were analyzed on genetic level by sequencing of the aberrant PGRMC1 bands and of the transcribed mRNA, if detected. Additionally, cells were characterized on functional level to detect a putative “PGRMC1-KO” phenotype.

6.3.2. Characterization of PGRMC1-Knockout Breast Cancer Cells

6.3.2.1. CRISPR/Cas9 Introduced Genetic Variations in Selected Single Cell Clones Are Manifold

The aim of this sub-project was to generate stable well-characterized PGRMC1-knockout cell clones without any permanent insertion of resistance cassettes into the cells' genomic DNA and with ideally solely *PGRMC1* locus (partially) deleted. Absence of the PGRMC1-protein in western blotting suggests a successful generation of various knockout cells. Nevertheless, truncations or small changes in the primary structure (amino acid exchanges) in the PGRMC1 protein may present as full knockout on protein level, if they affect epitopes of the antibodies. Therefore, an additional sequencing of detected transcripts and PCR bands was performed.

Purified DNA of the selected clones was therefore subjected to PCR using the CRISPR/Cas9 screening primer pairs and the PCR products were analyzed on a 3 % agarose gel. For PCR reactions with one band, the PCR product was purified by excision of the band from the gel and sequenced by Sanger sequencing using the PCR primers. In case of multiple PCR products, TA-cloning into vector pCR™2.1 and purification by transformation of *E. coli* with obtained vectors was performed according to 6.2.2.3.2. Amplified vectors with integrated PCR fragments were isolated from *E. coli* and subjected to Sanger sequencing using M13_fw primer, with respective sequence located on the vector site. TA-cloning was performed by Julia Oles within her master thesis supervised by me as part of this dissertation. PCR-bands used for sequencing are depicted in Supplementary Figure 3.

The mutations generated by the CRISPR-reaction and detected on DNA and on mRNA (if present) were aligned to the PGRMC1-transcript (Ensemble ID: ENST00000217971.8) using the MultAlin online tool [111]. An overview of detected mutations is provided in supplementary table 1. For instance, mutations in exon 2 or exon 3 were most frequent, leading to either an insertion or a deletion of nucleotides from DNA at that locus. In some clones, large deletions could be identified. For a better overview, graphical presentations of mutations in MCF7/CRISPR-KO cells are depicted in Figure 8. The respective deletions are marked with a red crossed rectangle.

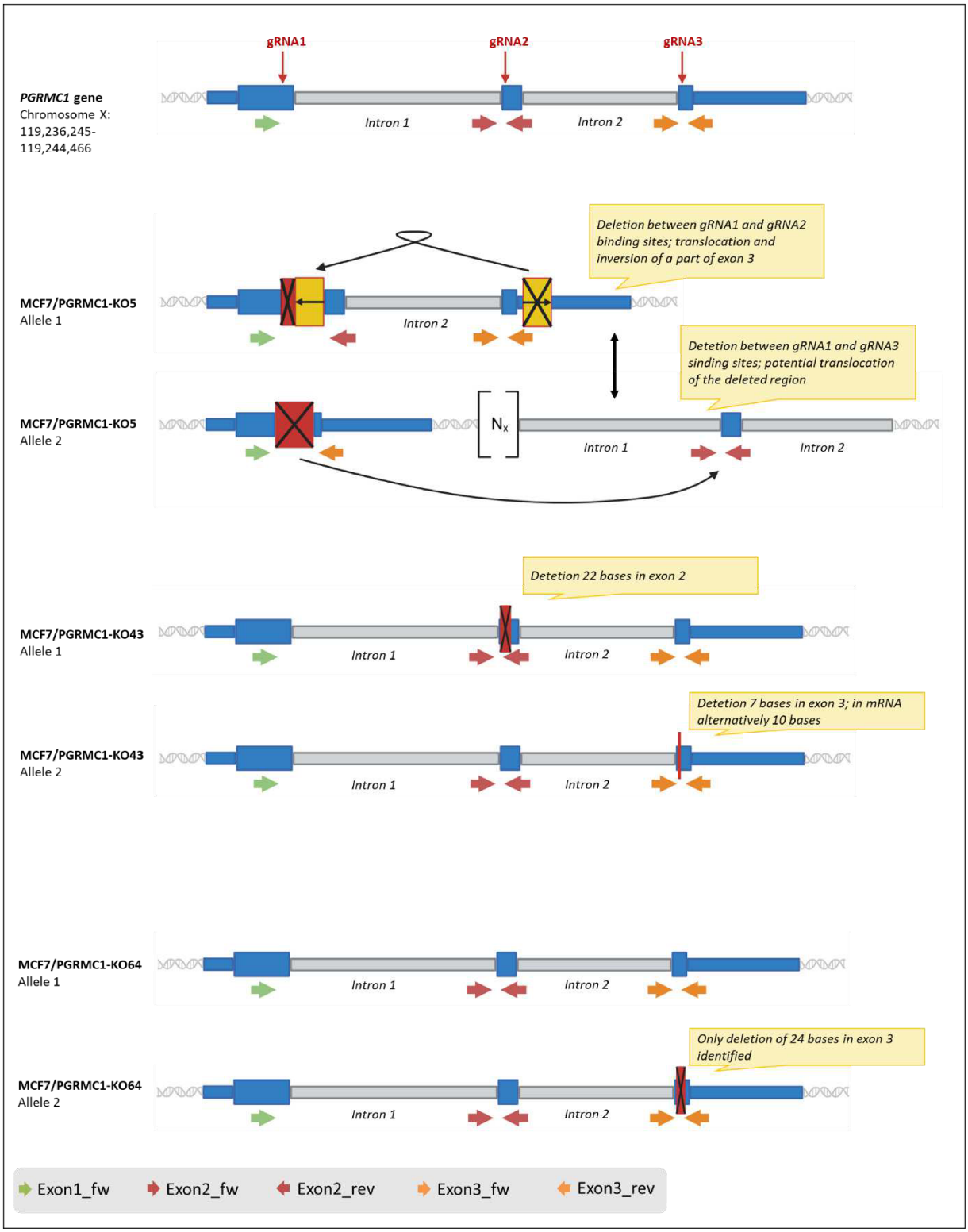

Figure 8: Graphical representation of mutations detected in MCF7/PGRMC1-KO cells. Upper panel depicts the original PGRMC1 locus with gRNA and primer binding sites. For MCF7/PGRMC1-KO5, the combination of PCR band sequences indicates large deletions and rearrangements on both alleles. For MCF7/PGRMC1-KO43 and -KO64, relatively small deletions in exon 2 and/or exon 3, respectively, have been generated by CRISPR/Cas9 approach. For clone MCF7/PGRMC1-KO43, two different isoforms were identified on mRNA level, presumably resulting from alternative splicing. Clones MCF7/PGRMC1-KO5 and -KO64 are completely absent of a PGRMC1 protein band in western blot. Created with BioRender.

In case of MCF7/PGRMC1-KO5, large deletions spanning one or both introns along with parts of the exons were detected. For instance, on allele 2, the region between gRNA1 and gRNA3 binding sites was deleted, bringing the primers exon1_fw and exon3_rev in proximity, resulting in a PCR band which is not produced from the original gene. However, simultaneous presence of the PCR product of the red primer pair indicates that this sequence was not degraded, but rather translocated into a distinct location in DNA that could not be evaluated with the applied methods and is therefore speculative. On allele 1, part of the deleted exon3 was inverted and inserted into the former intron 1. Whether this inserted region originates from the same allele is speculative, indicated by the double-sided black arrow in Figure 8. For clones MCF7/PGRMC1-KO43 and -KO64, cDNA could be detected at a low abundance and sequenced.

For these two clones, the detected mutated cDNA was translated into protein using the Expasy online tool (Supplementary Figure 4). Interestingly, the small 7 bp deletion in exon 3 in MCF7/PGRMC1-KO43 resulted in two cDNA forms (deletion of 7 bp or 10 bp, respectively). For the potentially resulting truncated proteins, if produced, folding, structure, stability and function may be impaired. This is strengthened by the observation that MCF7/PGRMC1-KO64 lacked any PGRMC1 protein in western blotting and MCF7/PGRMC1-KO43 demonstrated a light band of lower size (Figure 6). For clones MCF7/PGRMC1-KO5, T47D/PGRMC1-KO146, MDA-MB-231/PGRMC1-KO18 and MDA-MB-231/PGRMC1-KO34, no transcript could be detected in PCR.

In case of heterozygosity of the observed DNA modifications and the presence of one intact PGRMC1 allele, an important information is that PGRMC1 is located on a region of the X-chromosome which is permanently silenced due to X-chromosomal inactivation for gene doses effects. The implication of this fact will be discussed later to the full extent. However, to exclude the possibility of re-activation of the intact allele, if present and silenced, the representative generated MCF7-clones were cultured long-term (up to passage 52) and absence of PGRMC1-protein was verified by western blotting (see Supplementary Figure 5).

6.3.2.2. PGRMC1-Knockout Cells Do Not Exhibit Any Distinct Phenotype Postulated by Previous Experiments

After demonstrating PGRMC1-deficiency in the generated clones, the knockout cell lines were tested on previously established read-outs to analyze effects of permanent PGRMC1-loss on

basic cell functions. As demonstrated in the first manuscript, in PGRMC1-overexpressing MCF7 cells, cellular proliferation was significantly increased, assessed by measuring activity of mitochondrial reductases as surrogate for cell number by MTT assay. On the contrary, transient knock-down of PGRMC1 by siRNA resulted in significantly reduced proliferation [99]. To address proliferation of long-term PGRMC1-deficient MCF7 cells, CFSE assay was performed as an alternative method of proliferation analysis, independent of cellular metabolism (Figure 9).

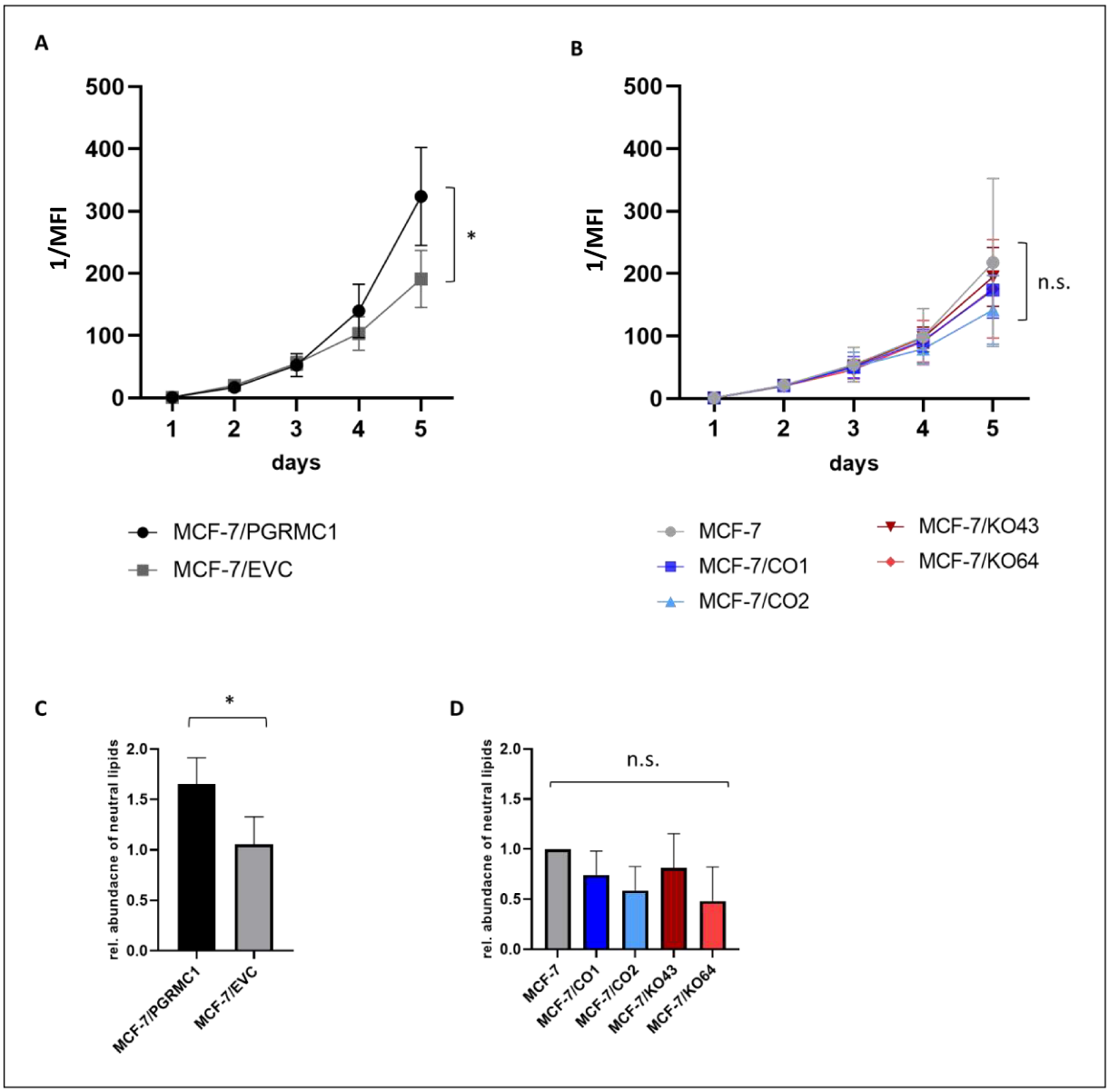

Figure 9: Characterization of MCF7/PGRMC1-KO cells' proliferation and abundance of neutral lipids. PGRMC1-overexpressing MCF7 cells MCF7/PGRMC1 and respective control cells MCF7/EVC were analyzed for reference. A: CFSE assay for MCF7/PGRMC1 and MCF7/EVC cells over a time period of 5 days. B: CFSE assay for parental MCF7 cells, MCF7/PGRMC1-Control and MCF7/PGRMC1-KO cells. Significance was tested by two-way ANOVA. C: Abundance of neutral lipids in MCF7/PGRMC1 and MCF7/EVC cells measured by BODIPY assay. Significance was tested by student's t-test. D: Abundance of neutral lipids in parental MCF7, MCF7/PGRMC1-Control and MCF7/PGRMC1-KO cells measured by BODIPY assay. Significance was tested by one-way ANOVA and multiple comparison analysis, Bonferroni-corrected. *: $p < 0.05$. Adapted from Oles, 2013.

The CFSE assay relies on incorporation of a fluorescent dye into the cells, which is subsequently divided between the daughter cells with each mitosis. The rate of fluorescence decrease over the course of time corresponds to the rate of cellular division. In addition to PGRMC1-KO cells, MCF7/PGRMC1 and MCF7/EVC cells were included for reference.

The CFSE assay demonstrated an increased proliferation rate of MCF7/PGRMC1 cells as published before. For MCF7/PGRMC1-KO cells lines, no significant result could be observed. All CRISPR/Cas9 manipulated cell lines proliferated with a rate similar to the parental MCF7 cells (Figure 9A-B).

Since in previously published results we demonstrated a significantly increased level of neutral lipids in hormone receptor positive MCF7/PGRMC1 cells, we tested selected PGRMC1-deficient clones for neutral lipid abundancy in BODIPY-assay. Therefore, cells were synchronized as described in 6.2.2.1.3, stained with BODIPY ™ 493/503 fluorescent dye and analyzed by flow cytometry. As previously, MCF7/PGRMC1 and respective control cells were used as a reference. While in MCF7/PGRMC1 cells, neutral lipids were significantly elevated, confirming previous results, no significant difference could be observed for PGRMC1-deficient cell lines compared to parental MCF7 (Figure 9C-D).

The results of the previous section (CFSE assay, BODIPY assay) were generated in course of the master project by Julia Oles, supervised as part of this dissertation [115]. Furthermore, the previously published analysis showed an increased phosphorylation of EGFR and of downstream kinases AKT, ERK and MEK in MCF7/PGRMC1. Moreover, PGRMC1 has been reported to interact with EGFR and stabilize the receptor, resulting in increased EGFR signaling [22]. To address this finding in PGRMC1-deficient MCF7 cells, MCF7/PGRMC1-KO were treated with 10 ng/ml EGF for 10 min as described in 6.2.2.1.7. Subsequently, western blot analysis was performed for detection of EGFRpY1068, MEKpS217/221, AKTpS473, and ERKpT202/Y204, the amount of respective total proteins for EGFR, MEK, AKT, and ERK, and additionally PGRMC1, and β-actin as loading control (Figure 10).

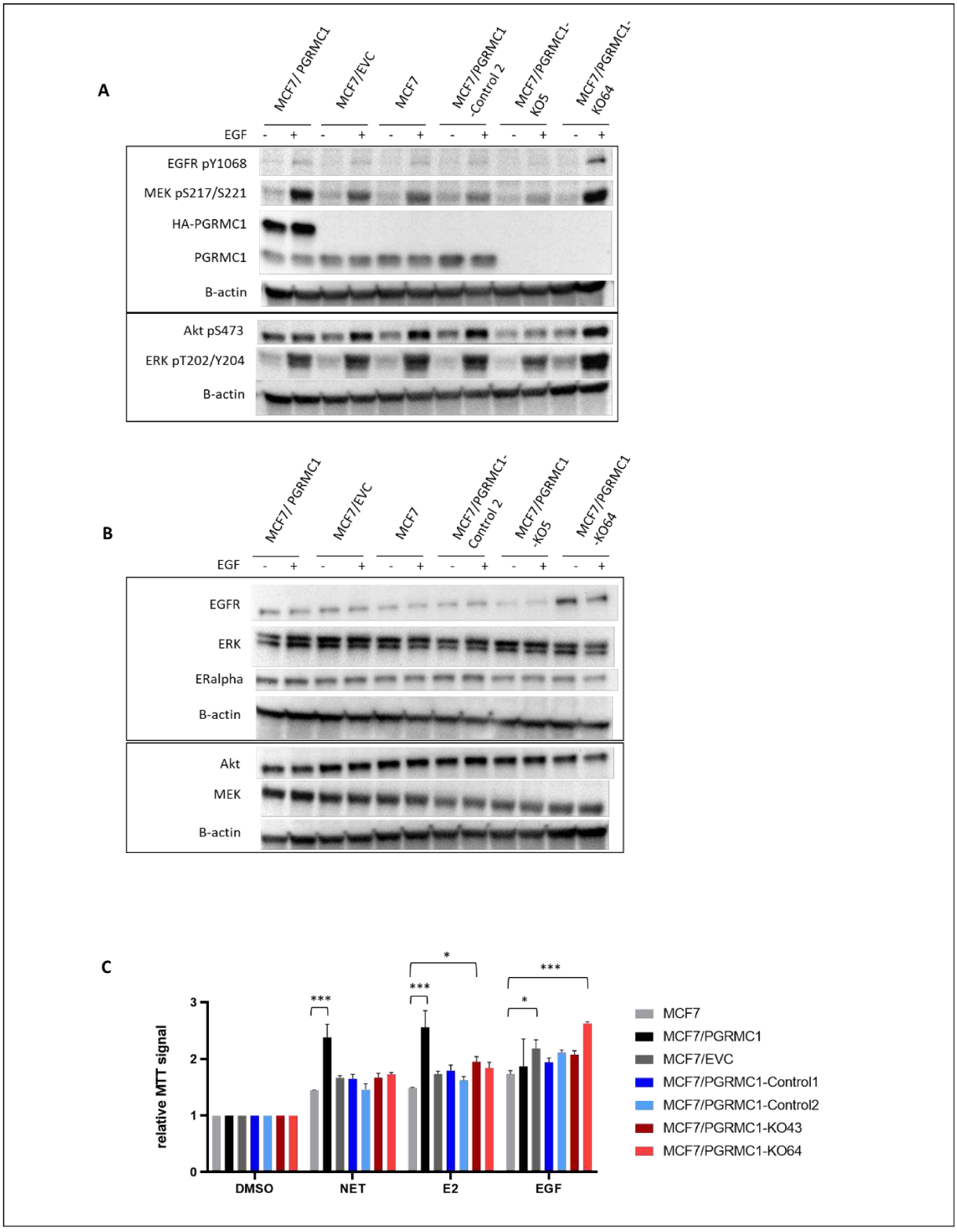

Figure 10: Activation of oncogenic signaling upon stimulation with hormones in MCF7 cells with different PGRMC1-expression levels. A+B: Westen blot analysis of whole cell lysates of MCF7/PGRMC1, MCF7/EVC, parental MCF7, MCF7/PGRMC1-Control2, MCF7/PGRMC1-KO5 and -KO64 upon stimulation with 10 ng/ml EGF or control medium for 10 min. A: Detection of pEGFR, pMEK, pERK, pAKT, PGRMC1 and β-Actin on two separate blots (upper panel and lower panel). For blot 1, sequence of detection was as follows: 1. MEKpS217/S221, 2. PGRMC1, 3. B-Actin. For blot 2, sequence of detection was as follows: 1. ERK pT202/Y204, 2. B-Actin. B: Detection of total protein levels of EGFR, MEK, ERK, ERα and β-Actin on two different blots (upper panel and lower panel). For blot 1, sequence of detection was as follows: 1. EGFR, 2. ERK, 3. ERα, 4. β-Actin. For blot 2, sequence of detection was as follows: 1. MEK, 2. Akt, 3. B-Actin. C: MTT assay as surrogate for proliferation on MCF7, MCF7/PGRMC1, MCF7/EVC, MCF7/PGRMC1-Control1, -Control2, MCF7/PGRMC1-KO43, -KO64 cells upon treatment with the

hormones NET, E2, EGF and DMSO as control. Significance was calculated by two-way ANOVA and multiple comparison analysis, Bonferroni-corrected. Significance is given in reference to parental MCF7. If not stated otherwise, not significant. *: p<0.05; ***: p<0.001.

Interestingly, the long-term PGRMC1-deficient cells did not present any overarching deficiency phenotype. While for MCF7/PGRMC1-KO5, a less prominent phosphorylation of MEK, AKT and ERK could indeed be observed, the second tested clone MCF7/PGRMC1-KO64 presented an opposite phenotype with phosphorylation as strong as in MCF7/PGRMC1 (Figure 10A). Of note, the same clone demonstrated an increased expression of total EGFR compared to parental MCF7 (Figure 10B), indicating an enhanced activity of the EGFR-pathway. However, no common phenotype was detected for PGRMC1-deficient MCF7-cells.

To address the consequence of EGFR activation on proliferation of breast cancer cells with different PGRMC1 expression levels, an MTT assay after treatment of cells with 10 ng/ml EGF for 72 h was performed (6.2.2.1.8, Figure 10C). Additionally, to address the effect of NET and E2 on PGRMC1-KO cells, these compounds were included in the assay. For NET and E2, only MCF7/PGRMC1 and MCF7/PGRMC1-Control 2 cells demonstrated significantly increased response compared to parental MCF7. The proliferative effect of NET and E2 on MCF7/PGRMC1 was most pronounced with proliferation increased more than 2-fold compared to DMSO. To EGF, the clone MCF7/PGRMC1-KO64 reacted with highest proliferation, consistent with the increased EGFR-expression and EGFR and AKT phosphorylation in these cells.

Taken together, PGRMC1-deficient breast cancer cells were successfully generated using the CRISPR/Cas9 technology. PGRMC1 protein could not be detected in most of these cells. Two clones (MCF7/PGRMC1-KO43; T47D/PGRMC1-KO126) demonstrated truncated or modified protein, weakly detected. The generated clones were characterized by sequencing of DNA fragments and cDNA, and further by performing functional assays in MCF7-cells to compare cells with different PGRMC1-expression levels. PGRMC1-KO cells did not establish the same phenotype as cells with transient PGRMC1-down-regulation (compare manuscript 1 [99]). Neither proliferation, nor neutral lipid content of long-term PGRMC1-null MCF7-cells were significantly different from parental MCF7. Concerning expression of kinases involved in oncogenic signaling, the two tested MCF7/PGRMC1-KOs presented different phenotypes, with -KO64 having a higher expression of EGFR and increased phosphorylation of EGFR, MEK, AKT and ERK compared to MCF7, while -KO5 had lower or equal expression of the same proteins compared to MCF7 cells.

7. Activated PGRMC1 Interacts with Prohibitins and Indirectly Regulates ERα-Signaling

7.1. PGRMC1 as Putative Progesterone Receptor

Despite its name, PGRMC1's ability to bind progesterone (P4) has not been proven yet and existing evidence is contradictory.

When Meyer *et al.* identified PGRMC1 from porcine liver membrane extracts, they reported it as part of a progesterone-binding fraction. The authors determined binding affinities for different membrane fractions, using radioactively labeled progesterone [3]. However, the study was performed on cell extracts and not on purified protein, therefore the binding activity may correspond to another protein in that fraction, possibly associated with PGRMC1, and not PGRMC1 itself. In 2008, a GFP-PGRMC1 fusion protein was purified and tested for P4-binding by Peluso *et al.* Importantly, the authors determined radioactively labeled-P4 binding ability of spontaneously immortalized granulosa cells, which was decreased after PGRMC1 knockdown. Furthermore, they performed PGRMC1-mutational studies and identified the transmembrane domain as the putative P4 binding site [116]. Later, Kaluka *et al.* performed UV-Vis spectrometry to measure progesterone binding to purified truncated PGRMC1, lacking the transmembrane domain (amino acids 72-195). In this study, progesterone addition resulted in changes in heme spectra, pointing towards conformational changes at the chelated heme. The authors concluded that PGRMC1 binds progesterone in proximity of heme or both ligands simultaneously [117]. However, binding of P4 could occur indirectly and be mediated by another protein that interacts with PGRMC1. For instance, PGRMC1 was reported to bind membrane progesterone receptor alpha (mPRα), and increased PGRMC1 expression resulted in elevated mPRα in the plasma membrane and increased P4 binding [118]. Up to date, both direct P4 binding and indirect binding via interaction with a P4-binding adapter protein remain possible.

7.2. PGRMC1 and Hormone Replacement Therapy

Several risk factors are associated with development of breast cancer, such as advancing age, early menarche, late menopause, low parity, advanced age at first pregnancy, as well as weight gain and a diet high in saturated fats, which is often associated with a high uptake of cholesterol [44]. An additional factor for increased breast cancer risk is uptake of exogenous progestins, synthetic progesterone derivatives, in form of oral contraception with progestin-

only medication and hormone replacement therapy (HRT) [119], [120]. HRT is administered to peri- and postmenopausal women to counteract deprivation of endogenous estrogens and ease climacteric symptoms. In addition to estrogen, HRT usually includes progesterone or progestins to prevent development of endometrial hyperplasia due to estrogen administration [121].

To study HRT-associated breast cancer risk, several studies were conducted, with the prospective "Million Women Study" in the United Kingdom having the largest cohort. This study revealed that the use of HRT, especially estrogen-progestin combination therapy, significantly increased the risk of breast cancer [122]. Interestingly, the risk is unequal for different progestins, with highest relative risk for medrogestone (2.74), cyproterone acetate (2.57) and norethisterone acetate (2.11), while the natural P4 did not increase the risk for breast cancer in combination with estrogen (relative risk: 1.08) [123]. On molecular level, progestins are thought to confer their function mainly through the nuclear PR but were further reported to bind other steroid receptors and mPR. Additionally, PGRMC1 was connected to progestin signaling by Neubauer *et al.*, who published several studies describing effects of certain progestins on PGRMC1-overexpressing breast cancer cells. The group observed that ERα-positive breast cancer cells with stable exogenous PGRMC1 overexpression established a higher sensitivity to treatment with norethisterone (NET), resulting in an increased proliferation. Interestingly, P4 did not exhibit any proliferative effect on the same cells. Later, Willibald *et al.* from our group performed immunoprecipitation of overexpressed 3×haemagglutinin (HA)-tagged PGRMC1 (HA-PGRMC1), followed by mass spectrometry for prominent PGRMC1 phosphorylation sites, to detect possible direct modifications of PGRMC1 after progestin treatment. Upon treatment with NET, PGRMC1 established increased phosphorylation of S181, while other detected phosphorylation sites (S57, Y113, T178) were not enriched. Importantly, S181 phosphorylation was detected after 24 hours of NET treatment, indicating a slow kinetic of PGRMC1 phosphorylation at this residue, which is possibly not a result of direct progestin binding [124]. However, the findings described in this section point towards a possible involvement of PGRMC1 in HRT-associated breast cancer risk, especially in case of high PGRMC1 tissue expression and uptake of breast cancer-risk increasing progestins.

To further dissect the mechanism of PGRMC1-associated progestin-induced breast cancer cell proliferation, Ludescher (née Willibald) performed a co-immunoprecipitation of HA-PGRMC1

after stimulation with NET and detected the putative interaction partners of PGRMC1. Among other proteins, the mitochondrial chaperons and transcription factor regulators prohibitin 1 and prohibitin 2 (PHB1; PHB2) were found to interact with PGRMC1 [98]. Interestingly, PHBs were reported to negatively regulate oncogenic ERα-signaling, which is the main stimulatory pathway in hormone receptor positive breast cancer cells. In the following manuscript, we aimed to uncover the mechanistic interplay between PGRMC1, PHBs and ERα and thereby to collect evidence on how PGRMC1 may contribute to increased breast cancer risk under HRT.

7.3. Manuscript II (Aim 3)

"PGRMC1 promotes progestin-dependent proliferation of breast cancer cells by binding prohibitins resulting in activation of ERα signaling"

Yingxue Bai, Marina Ludescher, Gereon Poschmann, Kai Stühler, Martine Wyrich, Julia Oles, André Franken, Mahdi Rivandi, Anna Abramova, Florian Reinhardt, Eugen Ruckhäberle, Dieter Niederacher, Tanja Fehm, Michael A Cahill, **Nadia Stamm**[*+] and Hans Neubauer[*+]

[*]: These authors contributed equally to this manuscript.

[+]: Corresponding authors.

Original research article in *Cancers*

Impact factor: 6.6 (2021)

Authorship: Shared senior author, corresponding author

Status: published in November 2021

DOI: 10.3390/cancers13225635

Full citation: Bai Y, Ludescher M, Poschmann G, Stühler K, Wyrich M, Oles J, Franken A, Rivandi M, Abramova A, Reinhardt F, Ruckhäberle E, Niederacher D, Fehm T, Cahill MA, Stamm N, Neubauer H. PGRMC1 Promotes Progestin-Dependent Proliferation of Breast Cancer Cells by Binding Prohibitins Resulting in Activation of ERα Signaling. Cancers (Basel). 2021 Nov 11;13(22):5635. doi: 10.3390/cancers13225635. PMID: 34830790; PMCID: PMC8615993.

Author contribution:

I planned experiments and discussed and analyzed data, I performed statistical analyses for all experiments, did literature research and conceptual design of the manuscript. I generated and validated the PGRMC1-knockout and respective control cells used in Figure 4C-D and others. I prepared the original draft and figures for publication together with Yingxue Bai and Marina Ludescher. I revised the written draft and adapted the reviewed manuscript, uploaded and managed publication.

7.4. Summary

Combined HRT with specific progestins like MPA or NET is associated with increased breast cancer risk. In breast cancer cell lines, PGRMC1 overexpression resulted in an increased response to NET, and NET stimulation led to PGRMC1 phosphorylation at S181. These findings suggested that PGRMC1 may functionally contribute to increased breast cancer progression upon HRT.

To address this hypothesis, PGRMC1-overexpressing breast cancer cells were stimulated with NET and PGRMC1 interaction partners were analyzed by co-immunoprecipitation and PLA. PGRMC1 was found to interact with the negative ERα-regulators PHB1 and PHB2. PHBs were previously reported to regulate transcriptional activity ERα and other transcription factors. The PGRMC1-PHB-interaction was dependent on PGRMC1-S181 phosphorylation after treatment with proliferation-promoting progestins NET, MPA, drospirenone and dydrogesterone, and was neither detected in PGRMC1-phosphorylation-deficient cells, nor after treatment with progestins that did not increase proliferation. Furthermore, when PGRMC1 interacted with PHBs, the latter exhibited less interaction with ERα, while ERα target gene transcription was significantly elevated. Importantly, ERα-prohibitin-interaction was not disrupted by NET in PGRMC1-KO cells, indicating a PGRMC1-specific effect.

These results suggested a PGRMC1-mediated displacement of PHBs from ERα, which in turn activated ERα signaling and enhanced the proliferation of breast cancer cells. Thereby, PGRMC1 could act as an indirect co-regulator of ERα activity and promote oncogenic signaling.

cancers

MDPI

Article

PGRMC1 Promotes Progestin-Dependent Proliferation of Breast Cancer Cells by Binding Prohibitins Resulting in Activation of ERα Signaling

Yingxue Bai [1], Marina Ludescher [1], Gereon Poschmann [2], Kai Stühler [2,3], Martine Wyrich [1], Julia Oles [1], André Franken [1], Mahdi Rivandi [1], Anna Abramova [1], Florian Reinhardt [1], Eugen Ruckhäberle [1], Dieter Niederacher [1], Tanja Fehm [1], Michael A. Cahill [4,5], Nadia Stamm [1,*,†] and Hans Neubauer [1,*,†]

1 Department of Obstetrics and Gynecology, University Hospital and Medical Faculty of the Heinrich-Heine University Duesseldorf, Merowingerplatz 1a, 40225 Duesseldorf, Germany; yingxue.bai@med.uni-duesseldorf.de (Y.B.); ludescher.marina@gmail.com (M.L.); Martine.Wyrich@hhu.de (M.W.); julia.oles@hhu.de (J.O.); andre.franken@med.uni-duesseldorf.de (A.F.); mahdi.rivandi@med.uni-duesseldorf.de (M.R.); anna.abramova@med.uni-duesseldorf.de (A.A.); florian.reinhardt@med.uni-duesseldorf.de (F.R.); eugen.ruckhaeberle@med.uni-duesseldorf.de (E.R.); niederac@med.uni-duesseldorf.de (D.N.); tanja.fehm@med.uni-duesseldorf.de (T.F.)

2 Institute for Molecular Medicine, University Hospital and Medical Faculty of the Heinrich-Heine University Duesseldorf, Universitaetsstr. 1, 40225 Duesseldorf, Germany; gereon.poschmann@hhu.de (G.P.); kai.stuehler@hhu.de (K.S.)

3 Molecular Proteomics Laboratory, BMFZ, Heinrich Heine University Duesseldorf, Universitaetsstr. 1, 40225 Duesseldorf, Germany

4 School of Dentistry and Medical Sciences, Charles Sturt University, Wagga Wagga, NSW 2678, Australia; mcahill@csu.edu.au

5 ACRF Department of Cancer Biology and Therapeutics, The John Curtin School of Medical Research, Canberra, ACT 2601, Australia

* Correspondence: nadia.stamm@med.uni-duesseldorf.de (N.S.); hans.neubauer@med.uni-duesseldorf.de (H.N.); Tel.: +49-211-81-06026 (H.N.)

† These authors contributed equally to this work.

Simple Summary: Combined menopausal hormone therapy is associated with increased breast cancer risk in postmenopausal women. In our previous studies, progesterone receptor membrane component 1 (PGRMC1) was shown to play a role in progestins' elicitation of enhanced proliferation of breast cancer cells. Here we describe a potential mechanism by which PGRMC1 contributes to breast cancer progression via interaction with prohibitins, inhibiting their function as transcriptional repressors. This facilitates estrogen receptor alpha (ERα) transcriptional activity and enhances oncogenic signaling upon treatment with certain progestins, including norethisterone and dydrogesterone. Our data underline the contribution of PGRMC1 to especially hormone receptor positive breast cancer pathogenesis and demonstrate the need for further studies to understand its role in cancer.

Abstract: In previous studies, we reported that progesterone receptor membrane component 1 (PGRMC1) is implicated in progestin signaling and possibly associated with increased breast cancer risk upon combined hormone replacement therapy. To gain mechanistic insight, we searched for potential PGRMC1 interaction partners upon progestin treatment by co-immunoprecipitation and mass spectrometry. The interactions with the identified partners were further characterized with respect to PGRMC1 phosphorylation status and with emphasis on the crosstalk between PGRMC1 and estrogen receptor α (ERα). We report that PGRMC1 overexpression resulted in increased proliferation of hormone receptor positive breast cancer cell lines upon treatment with a subgroup of progestins including norethisterone and dydrogesterone that promote PGRMC1-phosphorylation on S181. The ERα modulators prohibitin-1 (PHB1) and prohibitin-2 (PHB2) interact with PGRMC1 in dependency on S181-phosphorylation upon treatment with the same progestins. Moreover, increased interaction between PGRMC1 and PHBs correlated with decreased binding of PHBs to ERα and subsequent ERα activation. Inhibition of either PGRMC1 or ERα abolished this effect. In summary, we provide strong evidence that activated PGRMC1 associates with PHBs, competitively removing

Citation: Bai, Y.; Ludescher, M.; Poschmann, G.; Stühler, K.; Wyrich, M.; Oles, J.; Franken, A.; Rivandi, M.; Abramova, A.; Reinhardt, F.; et al. PGRMC1 Promotes Progestin-Dependent Proliferation of Breast Cancer Cells by Binding Prohibitins Resulting in Activation of ERα Signaling. *Cancers* **2021**, *13*, 5635. https://doi.org/10.3390/cancers13225635

Academic Editor: Jerome Solassol

Received: 12 October 2021
Accepted: 8 November 2021
Published: 11 November 2021

them from ERα, which then can develop its transcriptional activities on target genes. This study emphasizes the role of PGRMC1 in a key breast cancer signaling pathway which may provide a new avenue to target hormone-dependent breast cancer.

Keywords: PGRMC1; progesterone; progestins; breast cancer; estrogen receptor; hormone therapy; PHB1; PHB2

1. Introduction

Breast cancer accounts for almost one in four cancer cases among women, making it the most commonly diagnosed cancer and the leading cause of cancer death (15.5%) [1]. Approximately 70% of all breast cancers diagnosed in postmenopausal women are hormone receptor-positive [2].

Factors contributing to breast cancer risk besides lifestyle are reproductive and hormonal risk factors like overall exposure to sex hormones during early menarche and late menopause, but also uptake of exogenous hormones like oral contraceptives and hormone replacement therapy (HT) [3–5]. The latter is administered peri- and post-menopausal for treatment of climacteric symptoms to improve quality of life [6]. HT that only includes the use of estrogens is referred to as estrogen-only hormone therapy (EHT) [7]. However, in addition to estrogens, HT usually includes co-treatment with progestins, synthetic derivates of gestagens, added to prevent the development of endometrial hyperplasia and an associated risk of endometrial cancer due to estrogen administration. This HT is referred to as combined estrogen-progestin hormone therapy (CHT) [8].

Various prospective large cohort studies, such as the Million Women Study (1,084,110 women) and the Women's Health Initiative (27,547 women), overwhelmingly suggest that combined hormone therapy (CHT), relatively to EHT, increases the risk of breast cancer, indicating a potential role of progestins in breast carcinogenesis [7,9,10]. Fournier et al. demonstrated that the risk of breast cancer differs, depending on the type of progestin used. With a relative risk of 2.74 (95% confidence interval (CI): 1.42–5.29), 2.57 (95% CI: 1.81–3.65) and 2.11 (95% CI: 1.56–2.86) the progestins medrogestone, cyproterone acetate and norethisterone acetate were found to exhibit the highest breast cancer risk. In contrast to combined estrogen/progestin therapy, no increased breast cancer risk has been reported for the combined therapy of estrogens and progesterone (4-Pregnene-3,20-dione: hereafter P4) (relative risk: 1.08 (95% CI: 0.89–1.31) (relative risk: 1.08 (95% CI: 0.89–1.31) [6]. Although evidence points towards a significant contribution of certain progestins to breast cancer risk, the cellular mechanisms underlying this observation are unclear. Most effects observed upon progestin treatment refer to their action on the nuclear Progesterone Receptor (PR), but also other hormone receptors like the androgen receptor and the glucocorticoid receptor are reported to be targeted by progestins or their metabolites [11–14]. Recent studies further indicate potential effects of progestins on Progesterone Receptor Membrane Component-1 (PGRMC1) [15–17].

PGRMC1 is expressed in different cellular systems and contexts and has a wide range of cellular functions [17,18]. It was discovered by Meyer et al., when searching for alternative membranous high affinity P4 binding sites and was therefore suggested as a putative progesterone receptor [19,20]. Since then, PGRMC1 has been associated with P4 responses in various cell systems [21–23]. Furthermore, the multiple functions exerted by PGRMC1 include cholesterogenesis [24] and interactions with CYP450 enzymes that metabolize steroid hormones and chemotherapeutics [25,26].

In previous studies, we provided evidence that PGRMC1 is involved in the mode of action of progestins on breast cancer cells [27,28]. PGRMC1 was demonstrated to confer progestin responsiveness, which results in enhanced proliferation of MCF7 breast cancer cells in vitro and in vivo [27,29,30], indicating a potential role of PGRMC1 in increased breast cancer risk upon progestin-based HT [31]. We further examined the biological

activity of progestins associated with regulation of PGRMC1 activity and discovered that PGRMC1 is phosphorylated at the Casein Kinase 2 (CK2) phosphorylation consensus site S181, and thus potentially activated by the progestin norethisterone (NET) [27]. Considering that PGRMC1 is expressed in breast tissue and overexpressed in breast cancer [16], further investigation of progestin-dependent PGRMC1 signaling in breast cancer cells is essential for a better understanding of the effects of progestins on breast cancer risk.

Therefore, the aim of this study was to gain deeper insight into PGRMC1-mediated breast cancer progression upon progestin treatment and the signaling pathways involved. For this purpose, potential PGRMC1-interaction partners in breast cancer cells were evaluated with norethisterone (acetate) (NET) treatment. A special focus was placed on progestin-dependent implication of PGRMC1 in ERα signaling and regulation of prohibitins (PHBs), which are reported to function as transcription factor modulators [32], and can occupy protein complexes with PGRMC1, although direct physical contact has not been demonstrated [33]. Here, we provide evidence that crosstalk exists between PGRMC1 and ERα that could promote progression of breast cancer.

2. Materials and Methods

2.1. Cells and Cell Culture

MCF7, T47D and MDA-MB-231 cells were purchased from the ATCC (Manassas, VA, USA (HTB-22, HTB-133 and CRM-HTB-26)). Cells overexpressing 3× human influenza hemagglutinin (HA)-tagged PGRMC1 (termed MCF7/PGRMC1, T47D/PGRMC1 and MDA-MB-231/PGRMC1) and their respective negative empty vector control cells (MCF7/EVC, T47D/EVC and MDA-MB-231/EVC) were generated via stable transfection with the expression vector pcDNA3.1/Hygro (+) (Thermo Fisher Scientific, Waltham, MA, USA, V87020), containing 3×HA-tagged PGRMC1 as described elsewhere [24,29]. Prior to this study, MCF7 cells overexpressing GFP-tagged PGRMC1 (termed MCF7/PGRMC1-GFP) [24] and the phosphorylation-deficient PGRMC1-site mutants S57A (MCF7/PGRMC1-S57A), S181A (MCF7/PGRMC1-S181A) and a double site mutant S57A/S181A (MCF7/PGRMC1-S57A/S181A) [34] were established and described in previous publications. PGRMC1-deficient MCF7 cells (MCF7/PGRMC1-KO) were generated by transient transfection of MCF7 cells with 'PGRMC1 CRISPR/Cas9 KO Plasmid (h)' (Santa Cruz Biotechnology, CA, USA, sc-401945, containing a mixture of three expression plasmids each encoding for the Cas9 enzyme and a PGRMC1-specific gRNA) using Lipofectamine 3000 (Thermo Fisher Scientific, L3000001). For control (MCF7/PGRMC1-KO/Control), cells were transfected with respective amount of 'CRISPR/Cas9 KO Control Plasmid' (Santa Cruz Biotechnology, sc-418922, encodes for the Cas9 enzyme and an unspecific gRNA). Cells were trypsinized 48 h post-transfection and single clones were selected by limiting dilution in 96-well Plates. Single cell colonies were screened for a successful PGRMC1-knockout by PCR, expanded and validated by western blotting and immunofluorescence staining. All cells were maintained in RPMI 1640 medium (Thermo Fisher Scientific, 2340229), supplemented with 10% (*v*/*v*) fetal bovine serum (Thermo Fisher Scientific, 2333352), 100 units/mL penicillin/streptomycin (Thermo Fisher Scientific, 2321118) and 0.025 mol/L HEPES (Thermo Fisher Scientific, 2192897) (hereafter referred to as complete medium) in a humidified incubator at 37 °C in the presence of 5% CO_2. Cells (passage number $\leq$ 25) were regularly tested negative for mycoplasma and regularly authenticated by Microsynth AG (Balgach, Switzerland) using STR analysis.

2.2. Treatment

Hormones: For progestin treatment, cells were seeded in complete medium. After 24 h, the medium was changed to a phenol-red free RPMI 1640 medium (Thermo Fisher Scientific, 2300455) supplemented with 10% charcoal stripped fetal bovine serum (Thermo Fisher Scientific, 22361499), 100 units/mL penicillin/streptomycin (Thermo Fisher Scientific, 2321118) as well as 25 mM HEPES (hereafter referred to as stripped medium) and cells were incubated for another 48 h. Treatment was performed with NET

(Sigma-Aldrich, St. Louis, MO, USA, N1200000), dydrogesterone (DYD) (Sigma-Aldrich, Y0001004), drospirenon (DSP) (Sigma-Aldrich, Y0001105), medroxyprogesterone (acetate) (MPA) (Sigma-Aldrich, M0250000), cyproterone (acetate) (CPA) (Sigma-Aldrich, C3283000), nomegestrel (acetate) (NOM) (Sigma-Aldrich, N1080005) and P4 (Sigma-Aldrich, Y0001665) at concentrations of 10^{-6}, 10^{-7}, 10^{-8} and 10^{-9} M (from 10^{-2} M stock solutions in DMSO) or the respective amount of DMSO (Sigma-Aldrich, D8418) as a control for a defined time period (72 h for MTT assay, 24 h for mass spectrometry analysis, RPPA, Western blot, co-immunoprecipitation (Co-IP), PLA and qRT-PCR) in stripped medium.

AG-205: To investigate effects of PGRMC1 inhibition on cell proliferation, MCF7 cells were treated with the putative PGRMC1 inhibitor AG-205 (Sigma-Aldrich, A1487) (see discussion). Cells were seeded in complete medium. After 24 h, the medium was changed to stripped medium (see above) with 25 $\times$ 10^{-6} M AG-205 (from 10^{-2} M stock solution in DMSO) or DMSO (0.25%) as control and incubated for another 48 h. Treatment was performed with NET or DYD at concentration of 10^{-6} M or DMSO (0.01%) as a control for 24 h in stripped medium.

Fulvestrant: To investigate effects of ERα downregulation on cell proliferation, MCF7/PGRMC1 and MCF7/EVC cells were treated with the selective estrogen receptor degrader fulvestrant (Sigma-Aldrich, Y0001399) [35]. Cells were seeded in complete medium containing 10^{-7} M fulvestrant (from 10^{-3} M stock solution) or DMSO (0.01%) as control. After 24 h, the medium was changed to stripped medium containing 10^{-7} M fulvestrant and cells were incubated for another 48 h. Treatment was performed with NET or DYD at concentrations of 10^{-6} M or DMSO (0.01%) as a control, for indicated time periods (72 h for MTT assay, 24 h for qRT-PCR) in stripped medium. For MTT assay, cells were cultured in fulvestrant-containing complete medium for 24 h before seeding into 96-well plates.

2.3. MTT Assay

Cells (1 $\times$ 10^4 cells per well) were seeded in triplicates in 96-well plates in complete medium and grown for 24 h followed by starvation in stripped medium for 48 h and treatment with hormones as described above. On the day of the assay, cells were incubated with 0.25 mg/mL MTT solution (Sigma-Aldrich, 042K5313) for 3 h at 37 °C followed by 1 h of incubation with DMSO at 37 °C and 300 rpm in a microplate shaker. Absorption was measured at 540 nm using TECAN Spark® spectrophotometer.

2.4. Western Blot Analysis

Cells were washed twice with ice cold PBS (Thermo Fisher Scientific, 2176323) and detached from the culture flasks using cell scrapers (Greiner Bio-One, Solingen, Germany). Cell pellets were lysed in RIPA buffer (50 mM TRIS (Sigma-Aldrich, T1503), 150 mM NaCl (VWR corporation, 16C030032), 1% NP-40 (Sigma-Aldrich, 74385), 0.5% sodium deoxycholate (Sigma-Aldrich, D6750), 0.1% SDS (Sigma-Aldrich, S34121136), phosphatase inhibitor (Roche, 49121300) and protease inhibitor (Roche, 49422800)) and protein concentration was determined using BCA assay (Thermo Fisher Scientific, 23225). 30 µg of whole cell protein supplemented with 4 $\times$ Laemmli buffer (Bio-Rad, Feldkirchen, Germany, 1610747) containing 2-Mercaptoethanol (Sigma-Aldrich, M6250) and the respective molecular weight marker were loaded onto Mini-PROTEAN® Precast Gels (Bio-Rad, 4568123) and separated via SDS-Page at 100 V. Western blotting was performed as described elsewhere [27]. For signal detection the following antibodies were used: pSer181-PGRMC1 (EMBL, Monoclonal Antibody Core Facility, Monterotondo, Italy, #3G11A2, antibody not commercially available) [36], PGRMC1 (Cell signaling, Danvers, MA, USA, D6M5M), PHB1 (Cell signaling, 2426S), PHB2 (Cell signaling, 14085S) and β-actin (Santa Cruz Biotechnology, sc-47778). For validation of PGRMC1 knockout, we additionally used a second anti-PGRMC1 antibody (Abcam, Cambridge, UK, ab48012).

2.5. Co-Immunoprecipitation

Co-IP of HA-tagged PGRMC1 and HA-tagged PGRMC1-variants was performed as previously described [24].

2.6. Mass Spectrometry

PGRMC1 was immunoprecipitated from four individual replicates MCF7/PGRMC1 cells of following groups: HA-PGRMC1 DMSO, HA-PGRMC1 NET, GFP-PGRMC1 DMSO, GFP-PGRMC1 NET. Samples were processed by in-gel digestion and proteins were identified by mass spectrometry on an Orbitrap Elite instrument as described [27]. For data analysis, the MaxQuant environment (version 1.5.3.8, Max Planck Institute of Biochemistry, Planegg, Germany) was used with standard parameters if not otherwise stated. Spectra were searched against 20187 Swiss-Prot entries from the Homo sapiens proteome (UP000005640, downloaded on 18 November 2015 from UniProt KB). Label-free quantification was enabled as well as the 'match between runs' option. Tryptic cleavage specificity was chosen, as well as carbamidomethyl at cysteines as fixed and methionine oxidation, and acetylation at protein N-termini as variable modifications. Mass tolerances were 20 ppm (first search) and 4.5 ppm (second search after recalibration) for precursor masses and 0.5 Da for fragment masses. Peptides and proteins were accepted at a false discovery rate of 1%. Proteins were only considered for further analysis when showing at least two peptides and four valid values in at least one group. Missing values were imputed for global statistical calculation using random values from a downshifted normal distribution (1.8 SD downshift, width 0.3 SD). For statistical analysis, a two-way ANOVA was calculated within the R environment (The R foundation for statistical computing) and p-values were corrected for multiple testing by the method of Benjamini and Hochberg (corrected values are reported). Potential PGRMC1 interacting proteins were selected by a ratio HA/GFP > 2 and additionally a corrected p-value < 0.01 for the variable "TAG" in the ANOVA. For the 253 remaining proteins additionally Welch-tests were performed for the comparison of NET and DMSO treated HA-PGRMC1 samples. All captured proteins along with the statistical data are provided in Supplementary Table S1 (Appendix A). The mass spectrometry proteomics data have been deposited to the ProteomeXchange Consortium via the PRIDE [37] partner repository with the dataset identifier PXD028537.

2.7. qRT-PCR

RNA was isolated from a cell pellet of 1×10^6 cells using the RNeasy Mini Kit (Qiagen, Hilden, Germany, 74104) according to the manufacturer's specifications. Reverse transcription of RNA into cDNA was performed with the Omniscript RT kit (Qiagen, 205113) according to the manufacturer's instructions. For qPCR, QuantiFast SYBR Green PCR kit (Qiagen, 204054) and RT^2 qPCR Primer assays for *TFF1* (Qiagen, PPH00998C) and *PDH* (Qiagen, PPH13220A) were used according to the manufacturer's specifications. qPCR was performed using the LightCycler® 480 System (Roche, Penzberg, Germany).

2.8. Immunofluorescence Staining

Cells were spun on glass slides, fixed with 4% PFA (Sigma-Aldrich, 20649296018) for 10 min at room temperature and washed three times for 5 min with washing buffer (Dako, Glostrup, Denmark, S3006). Afterwards, cells were permeabilized with 0.1% Triton X-100 (Sigma-Aldrich, T8787) in PBS for 10 min at room temperature (RT) and washed three times for 5 min with washing buffer. DAKO Protein Blocking Solution (Dako, X0909) was added and incubated for 1 h at RT. Cells were subjected to immunofluorescence staining with primary antibodies specific for PGRMC1 (Abcam ab48012), ERα (Abcam ab259427), PHB1 (Abcam ab75766) and PHB2 (Cell signaling 14085S) overnight at 4 °C. Afterwards, the slides were washed three times for 5 min with washing buffer and a respective fluorophore labeled secondary antibody (anti-goat: Invitrogen, A11055; anti-mouse: Invitrogen, 745480; anti-rabbit: Invitrogen, A31573) was added to the samples and incubated for 1 h at RT in the dark. The slides were washed three times for 5 min with washing buffer and incubated

with DAPI (Thermo Fisher Scientific, 15733122) for 5 min at RT. Antibody incubation steps were performed in a humidified chamber. The slides were washed with distilled water, mounted with Fluorescent Mounting Medium (Dako, S3023) and dried overnight. The cells were examined by fluorescence microscopy using the Axioplan 2 Imaging fluorescence microscope.

2.9. Proximity Ligation Assay

The proximity ligation assay (PLA) procedure was performed using the Duolink® PLA Kit (Sigma-Aldrich, DUO92008) according to the manufacturer's instructions. Cells were spun on glass slides, fixed and permeabilized as described above. Incubation with the primary antibody cocktail containing anti-PGRMC1 antibody (Abcam, ab48012) or anti-ERα antibody (Abcam, ab259427) with PHB1 (Abcam, ab75766) or PHB2 (Cell signaling, 14085S) antibody was performed overnight at 4 °C. Negative control PLA was performed using respective isotype control antibodies (goat isotype, Abcam ab37373; mouse isotype, Abcam ab37355; rabbit isotype, Abcam ab37415). Nuclear DNA was labeled with DAPI for 10 min and slides examined by fluorescence microscopy within one week after storage at 4 °C in the dark. Each red dot represented a single interaction. Dots per cell were quantified using imageJ software [38].

2.10. Statistical Analysis

All experiments were performed as several independent biological replicates and repeated a minimum of three times. Results were reported as means with standard deviation. If not stated otherwise, data were tested for normal distribution using Shapiro-Wilk test and QQ normality plots and analyzed by one-way or two-way ANOVA (unmatched data) using GraphPad Prism (version 9.2.0, GraphPad Software, Inc., La Jolla, CA, USA). Differences between groups were calculated with the Bonferroni post-hoc test. $p < 0.05$ was considered as statistically significant. The exact test applied is described in the respective figure legend.

3. Results

3.1. PGRMC1 Promotes Proliferation of Breast Cancer Cells upon Progestin Treatment

As already shown in previous studies, PGRMC1 represents a potential integration point and transmitter of progestin signals responsible for the growth and proliferation of breast cancer cells [27,29]. To further study this effect, we used the HA-tagged PGRMC1-overexpressing breast cancer cell lines MCF7/PGRMC1, T47D/PGRMC1 and MDA-MB-231/PGRMC1 as well as the respective empty vector control cell lines MCF7/EVC, T47D/EVC and MDA-MB-231/EVC, and performed the MTT assay to measure activated metabolism as surrogate for cell proliferation upon treatment with various progestins used in CHT. For the ERα/PR positive cell lines MCF7/PGRMC1 and T47D/PGRMC1, treatment with the progestins NET, DYD and DSP (10^{-6} M) significantly increased cell proliferation compared to the respective EVC cells while no effects were observed after treatment with CPA, NOM and P4 (10^{-6} M) (Figure 1A,B). For MCF7/PGRMC1 cells, significantly higher proliferation was also observed after treatment with MPA (10^{-6} M). In contrast, treatment of PGRMC1-overexpressing MDA-MB-231 cells with any progestin (10^{-6} M) or P4 (10^{-6} M) did not increase their proliferation compared to MDA-MB-231/EVC cells (Figure 1C), suggesting that progestin-mediated PGRMC1 signaling is mediated by proteins which are expressed in the HR positive cell lines MCF7 and T47D, but not in the triple-negative cell line MDA-MB-231.

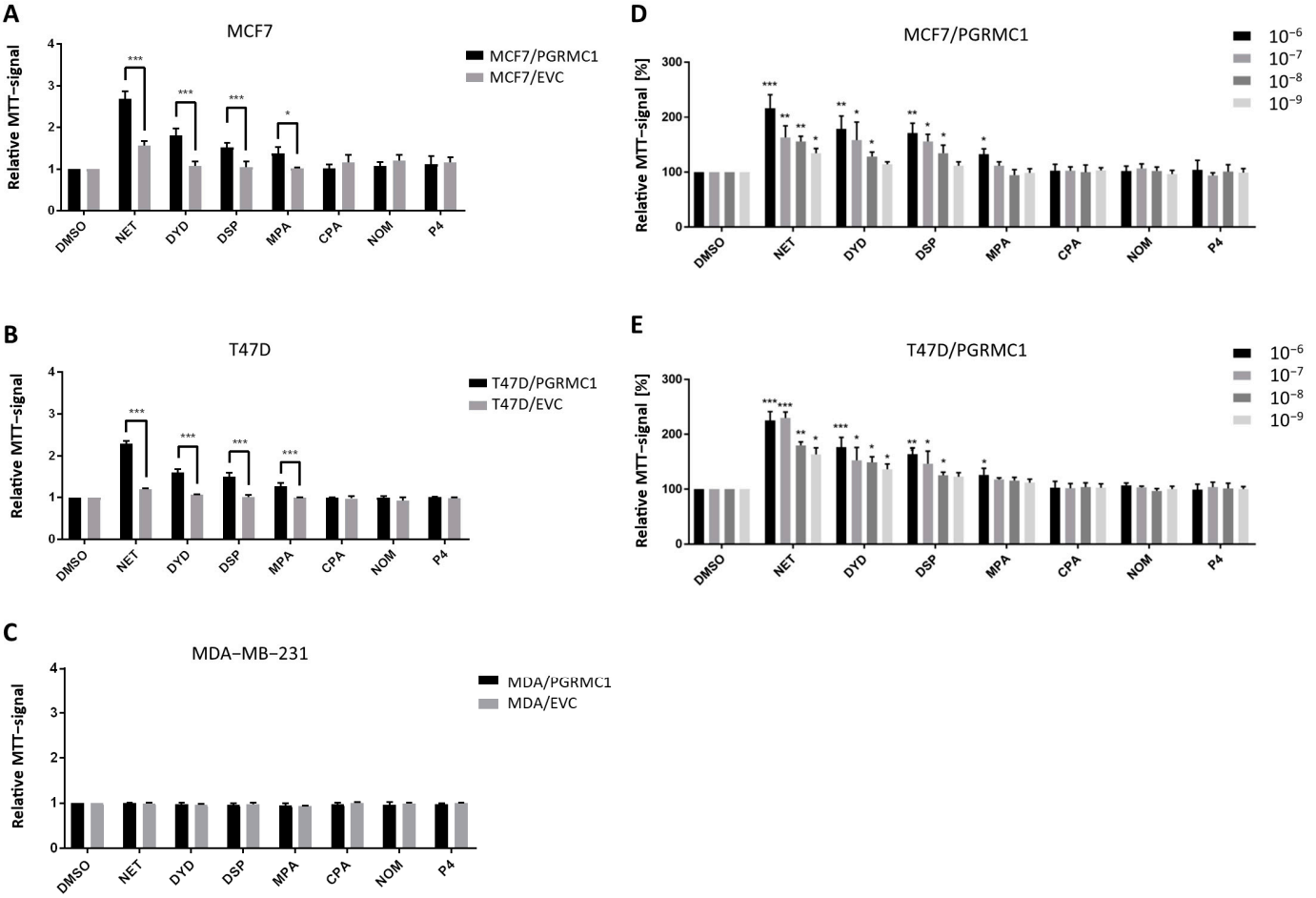

Figure 1. PGRMC1 promotes proliferation of breast cancer cells upon progestin treatment. Relative MTT-signal as surrogate for cell number of (**A**) MCF7/PGRMC1 and MCF7/EVC cells, (**B**) T47D/PGRMC1 and T47D/EVC cells, (**C**) MDA-MB-231/PGRMC1 and MDA-MB-231/EVC cells. Cells were treated with different progestins in the concentration of 10^{-6} M. Relative MTT-signal of (**D**) MCF7/PGRMC1 and (**E**) T47D/PGRMC1 cells treated with different concentrations of progestins (10^{-6}–10^{-9} M) for 72 h. Values were normalized to respective DMSO treated cells. Statistical analysis was performed with twoway ANOVA and Bonferroni post−hoc test. *: $p < 0.05$, **: $p < 0.01$, ***: $p< 0.001$.

To analyze if effects of progestins on MCF7/PGRMC1 and T47D/PGRMC1 cells can be observed at very low concentrations, cells were treated with progestins in concentrations ranging from 10^{-6} M to 10^{-9} M. For NET, we detected significantly higher proliferation for PGRMC1-overexpressing cells even at 10^{-9} M compared to DMSO treated cells (Figure 1D,E), whereas the respective EVC cells only responded at higher concentrations (Figure S1A,B). For DYD and DSP, significantly elevated proliferation compared to the DMSO control was observed at concentrations down to 10^{-8} M, while for MPA only the concentration of 10^{-8} M resulted in increased proliferation (Figure 1D,E). As in the previous experiment, CPA, NOM and P4 treatment did not influence proliferation of MCF7/PGRMC1 and T47D/PGRMC1 cells compared to DMSO control at any concentration (Figure 1D,E).

Taken together, these results demonstrate that PGRMC1-overexpression sensitizes ERα/PR positive luminal breast cancer cells to treatment with specific progestins (NET, DYD, DSP, and MPA; proliferation-promoting progestins, hereafter referred to as PPPs), while other progestins (CPA, NOM and P4; non-proliferation-promoting progestins, hereafter referred to as N-PPPs) did not enhance proliferation under any condition. The increase of proliferation in MCF7/EVC and T47D/EVC cells after treatment with NET, DYD and DSP or NET and DYD, respectively (Figure S1A,B), may be conducted via the endogenously expressed PGRMC1 which is still present in our system.

3.2. PGRMC1 Associates with the ERα-Modulators PHB1 and PHB2 upon Treatment with NET

To gain insight into the mechanism by which PGRMC1 impacts proliferation of breast cancer cells, we screened for potential PGRMC1 interaction partners upon treatment with the PPP NET by mass spectrometry analysis of proteins co-immunoprecipitated from whole-cell lysates of MCF7/PGRMC1 cells utilizing an antibody directed against the HA-tag (Table S1). The volcano plot (Figure 2A) stratifies proteins exhibiting significantly increased signals in Co-IP pellets from the NET treated MCF7/PGRMC1 samples compared to Co-IP pellets from the corresponding DMSO treated MCF7/PGRMC1 cells. These could represent progestin-dependent PGRMC1 interaction partners. In the NET and the DMSO-treated MCF7/PGRMC1 cells, similar amounts of PGRMC1 proteins were precipitated as indicated by similar signal intensities (Figure S2). Significantly less PGRMC1 protein was precipitated by anti-HA beads in the DMSO and NET treated MCF7/PGRMC1-GFP control cells where PGRMC1 lacked the HA-tag (Figure S2), indicating the specificity of the assay for the presence of the HA-antigen in the PGRMC1 target protein.

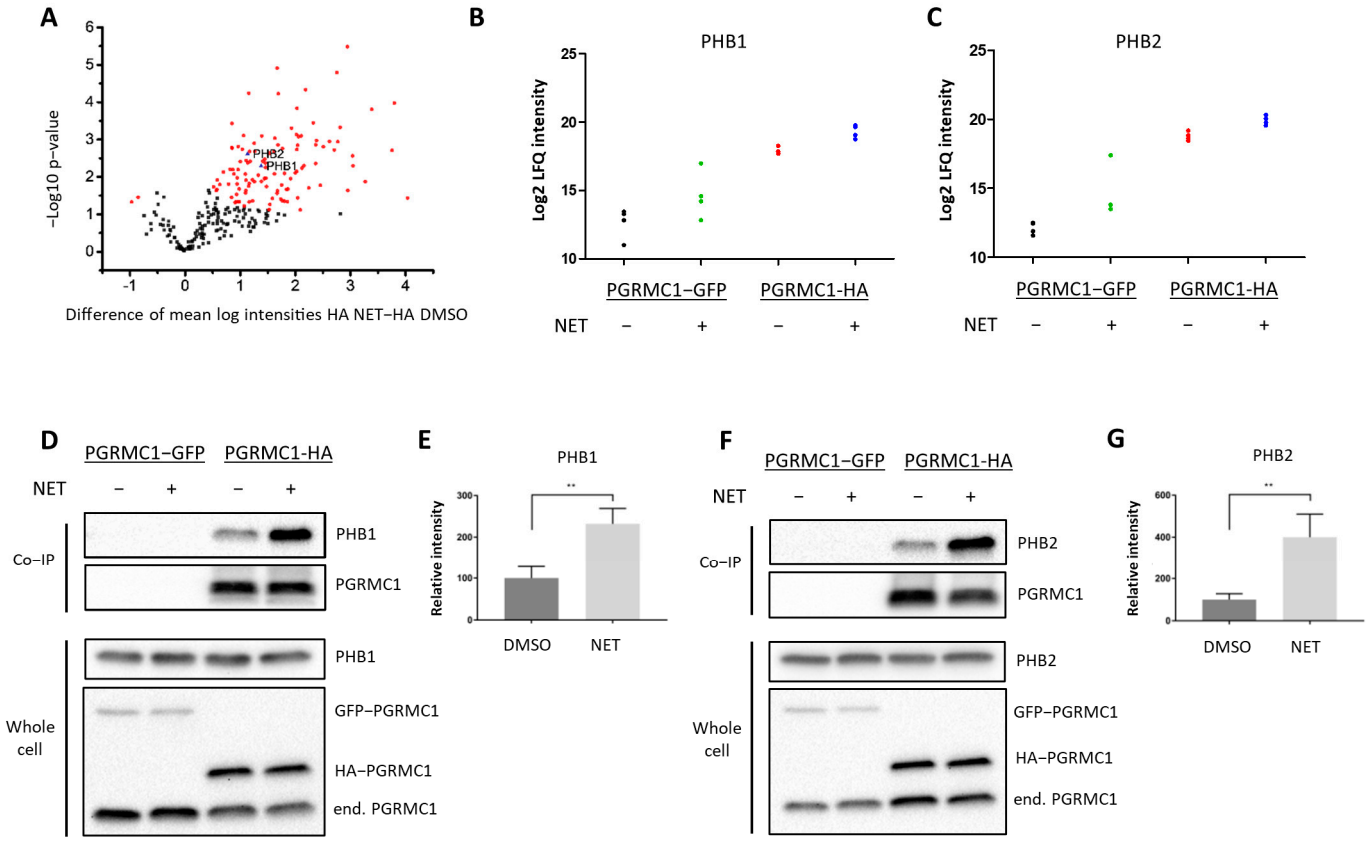

Figure 2. PGRMC1 interacts with the ERα-modulators PHB1 and PHB2 upon treatment with NET. Analysis of immunopurified (HAbased) samples of MCF7/PGRMC1-GFP cells (PGRMC1-GFP) and MCF7/PGRMC1 cells (PGRMC1-HA) treated with DMSO or NET (10^{-6} M) for co-precipitated proteins. (**A**) Volcano plot showing the result of a Welch's *t*-test including 253 proteins with an increased abundance as revealed by a two-way ANOVA after HA-based enrichment. Proteins represented by red dots and blue triangles show a significantly altered abundance (FDR 0.01%). Mass spectrometry results for co-precipitated (**B**) PHB1 or (**C**) PHB2, log2 normalized intensity +: significantly different (Welch's test). (**D**,**F**) Western blot analysis for co-precipitated (**D**) PHB1 or (**F**) PHB2 (upper panel) and the protein level of PHB1, PHB2 and PGRMC1 in whole cell lysates from the same cells (lower panel). (**E**,**G**) Densitometric analysis for precipitated (**E**) PHB1 or (**G**) PHB2. Signal intensity was normalized to PGRMC1-HA/DMSO. Difference between DMSO- and NET-treated samples was calculated with unpaired Student's *t*-test. **: $p < 0.01$.

Since the initial results point towards progestin-dependent increase of proliferation in ERα/PR-positive PGRMC1-overexpressing cell lines, we hypothesized that progestin-mediated PGRMC1 signaling is dependent on factors present in luminal cell types of breast cancer. Among proteins with higher signal intensities in NET treated MCF7/PGRMC1 cells compared to DMSO treated cells we found Prohibitin-1 (PHB1) (ANOVA *p*-value, corrected for multiple testing: tag 5.7×10^{-7}, treatment 0.005) (Figure 2B) and Prohibitin-2 (PHB2) (ANOVA *p*-value, corrected for multiple testing: tag 3.2×10^{-7}, treatment 0.01) (Figure 2C). We had previously identified that both proteins were present in AG-205-dependent Co-IP pellets with PGRMC1 [33]. Both PHBs are suggested to modulate transcriptional activity by directly or indirectly interacting with transcription factors, including transcriptional repression of ERα [39–41]. PHB2 is known as an ERα co-regulator that potentiates the inhibitory activities of antiestrogens and represses the activity of estrogens [42]. Due to their role as transcription factor modulators, we were interested in the association between PGRMC1 and PHB1 and PHB2 upon progestin treatment.

The results from mass spectrometry were verified by Co-IP followed by Western blot analysis. Both PHB1 (Figure 2D,E and Figure S13) and PHB2 (Figure 2F,G and Figure S14) exhibited significantly higher signals in MCF7/PGRMC1 cells after NET treatment. These results indicate augmented interaction of PHB1 and PHB2 with protein complexes containing PGRMC1 in the presence of NET compared to DMSO treatment.

3.3. PGRMC1-S181-Phosphorylation Correlates with Increased Cell Proliferation and PHB Binding upon Progestin Treatment

PGRMC1 is subject to differential phosphorylation, which has been reported to potentially regulate its functions [43,44]. As previously published, we have investigated PGRMC1 phosphorylation upon progestin treatment in MCF7/PGRMC1 cells by Co-IP and subsequent mass spectrometry and identified S181 as the PGRMC1 site whose phosphorylation was significantly increased upon treatment with NET [27]. To further investigate a potential relationship between PGRMC1-S181 phosphorylation and elevated cell proliferation, we used MCF7/PGRMC1, MCF7/EVC and MCF7/PGRMC1-S181A cells, the latter of which express a S181A-phosphorylation deficient PGRMC1-variant. We measured PGRMC1-S181 phosphorylation by Western blot of whole cell lysates upon treatment with both PPPs as well as N-PPPs. Both endogenously and exogenously expressed PGRMC1 showed increased S181 phosphorylation in PPP-treated MCF7/PGRMC1 cells compared to DMSO-treated cells, whereas PGRMC1 protein levels were comparable for all cells (Figure 3A–C and Figure S15). For the exogenously expressed PGRMC1, the most prominent effect was observed after stimulation with NET, DYD and DSP, with a clear trend for MPA. MCF7/EVC cells also exhibited increased S181-phosphorylation of endogenous PGRMC1 upon PPP treatment (Figures S3A,B and S18). In MCF7/PGRMC1-S181A cells, similar results were observed, except that the exogenous PGRMC1-S181A protein was not phosphorylated on S181 (Figures S3C,D and S19).

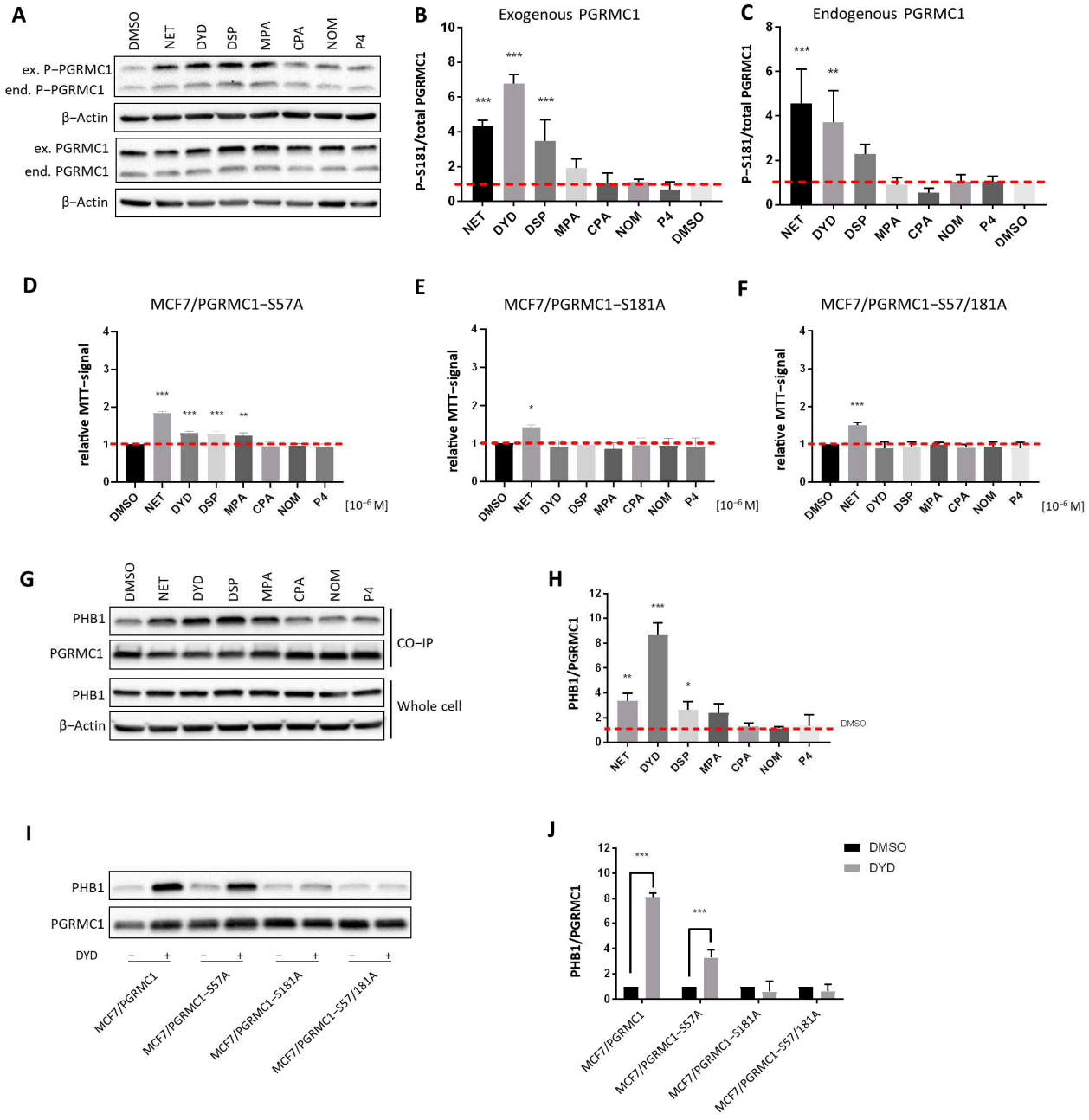

Figure 3. PGRMC1-S181-phosphorylation is essential for increased cell proliferation and PHB binding upon progestin treatment. (**A**) Western blot analysis of PGRMC1-S181-phosphorylation and PGRMC1 protein levels in whole cell lysates of MCF7/PGRMC1 cells after treatment with progestins (10^{-6} M) and DMSO. S181-phosphorylation occurs on both the endogenous PGRMC1 (lower band, ≈25 kDa) and exogenous HA-tagged PGRMC1 (upper band, ≈28 kDa). Densitometric analysis of Western blot results for S181-phosphorylation of (**B**) exogenous PGRMC1 and (**C**) endogenous PGRMC1 relatively to total PGRMC1 protein level. (**D**–**F**) Relative MTT signal as surrogate for cell number of (**D**) MCF7/PGRMC1-S57A, (**E**) MCF7/PGRMC1-S181A, (**F**) MCF7/PGRMC1-S57A/S181A cells treated with different progestins (all 10^{-6} M) or DMSO for 72 h. Values were normalized to DMSO treated cells. (**G**) Western blot analysis of immunopurified HA-tagged PGRMC1 and co-precipitated PHB1 from MCF7/PGRMC1 cells treated with different progestins (10^{-6} M) and DMSO (upper panel) and PHB1 protein level in whole cell lysates in the same cells (lower panel). (**H**) Densitometric analysis of co-precipitated PHB1 (**I**) Western blot analysis of immunopurified HA-tagged PGRMC1-variants and co-precipitated PHB1 after treatment with DYD (10^{-6} M) or DMSO. (**J**) Densitometric analysis of co-precipitated PHB1. (**B**,**C**,**H**,**J**) Signal intensity was normalized to corresponding DMSO-control and signal intensity of total PGRMC1 (**B**,**C**) or each precipitated PGRMC1-variant (**H**,**J**). Statistical analysis was performed by one-way ANOVA (**A**–**H**) or two-way ANOVA (**J**) and Bonferroni post-hoc tests. *: $p < 0.05$, **: $p < 0.01$, ***: $p < 0.001$.

To investigate the functional connection between PGRMC1-S181-phosphorylation and increased proliferation, the proliferation of the phosphorylation deficient MCF7/PGRMC1-S181A cells upon treatment with progestins was investigated. In addition, we used the cell line MCF7/PGRMC1-S57A, which overexpresses the phosphorylation deficient PGRMC1 variant S57A, and the double-variant cell line MCF7/PGRMC1-S57A/S181A [34]. The phosphorylation site S57 was previously not found to be differentially phosphorylated upon NET treatment in MCF7/PGRMC1 cells [27] and therefore served as a control. In accordance with our previous findings, the proliferation of the control cell line MCF7/PGRMC1-S57A significantly increased after stimulation with PPPs (Figure 3D), similarly to MCF7/PGRMC1 cells, whereas the proliferation of MCF7/PGRMC1-S181A (Figure 3E) cells and MCF7/PGRMC1-S57A/S181A (Figure 3F) cells increased only after NET treatment. This result suggested that PGRMC1-S181-phosphorylation was important for the proliferative effect observed upon PGRMC1 overexpression and PPP treatment.

After demonstrating that PGRMC1-S181 phosphorylation accompanied the increase in proliferation observed after treatment with PPPs, we investigated whether this phosphorylation was crucial for the recruitment of PHBs to PGRMC1. Since the Co-IPs followed by mass spectrometry and Western blot indicated that PHB1 and PHB2 interacted with PGRMC1 upon treatment with NET, we next performed the Co-IP after treatment with both PPPs and N-PPPs and analyzed the precipitated proteins by Western blotting. Both PHB1 and PHB2 showed significantly higher abundance in PGRMC1 Co-IP pellets upon treatment with the PPPs NET, DYD and DSP and a clear trend for MPA compared to treatment with DMSO in MCF7/PGRMC1 (Figure 3G,H, Figures S4A,B and S16) and T47D/PGRMC1 cell lines (Figures S4C–F, S21 and S22). PHB1 and PHB2 association was especially strong for DYD-treated cells whereas PHB1 and PHB2 protein levels were similar in all cell lysates (Figure 3G, Figures S4A and S20). PHB1 or PHB2 levels in Co-IP precipitates after N-PPP treatments were not significantly different than control levels. Co-IPs with lysates of cells overexpressing phosphorylation-deficient PGRMC1-variants demonstrated that PGRMC1-S181 is crucial for the recruitment of PHBs to Co-IP pellets after treatment with PPPs. PHB1 (Figure 3I,J and Figure S17) and PHB2 (Figures S4G,H and S23) could be precipitated by PGRMC1 from lysates of the control cell line MCF7/PGRMC1-S57A but not from Co-IP pellets from MCF7/PGRMC1-S181A and MCF7/PGRMC1-S57A/S181A cells. Taken together, these results suggest that treatment with PPPs leads to PGRMC1-S181 phosphorylation and increased interaction of PHB1 and PHB2 with protein complexes containing PGRMC1.

3.4. PGRMC1-PHB1/PHB2 Association Diminishes PHB1/PHB2 Binding to ERα

Since PHB1 and PHB2 were reported to regulate ERα signaling, which is a central oncogenic pathway in luminal breast cancer, we focused on the implication of PGRMC1 in the ERα signaling network and its possible involvement in breast cancer promotion. According to literature, PHB2 directly interacts with ERα and represses its transcriptional activity [39]. Therefore, we investigated the associations between endogenously expressed PGRMC1 and PHBs or ERα and PHBs, respectively, by PLA in parental MCF7 and T47D cells-independent of overexpression and immunoprecipitation. For this experiment, NET and DYD were used representatively for the PPP group while P4 and DMSO served as controls. Upon treatment with NET and DYD, a significantly higher number of PLA interactions between PGRMC1 and PHB1 (Figure 4A,B) or PHB2 (Figure S5A,B) could be observed in both cell lines compared to treatment with P4 and DMSO (T47D in Figure S7A–D).

Regarding the interaction between ERα and PHB1 or PHB2, we obtained the inverse picture: treatment with NET or DYD led to significantly less interactions than the treatment with P4 or DMSO (Figure 4A,B and Figure S5A,B, T47D in Figure S7A–D), while the protein expression levels of all tested proteins remained unchanged (Figure S10).

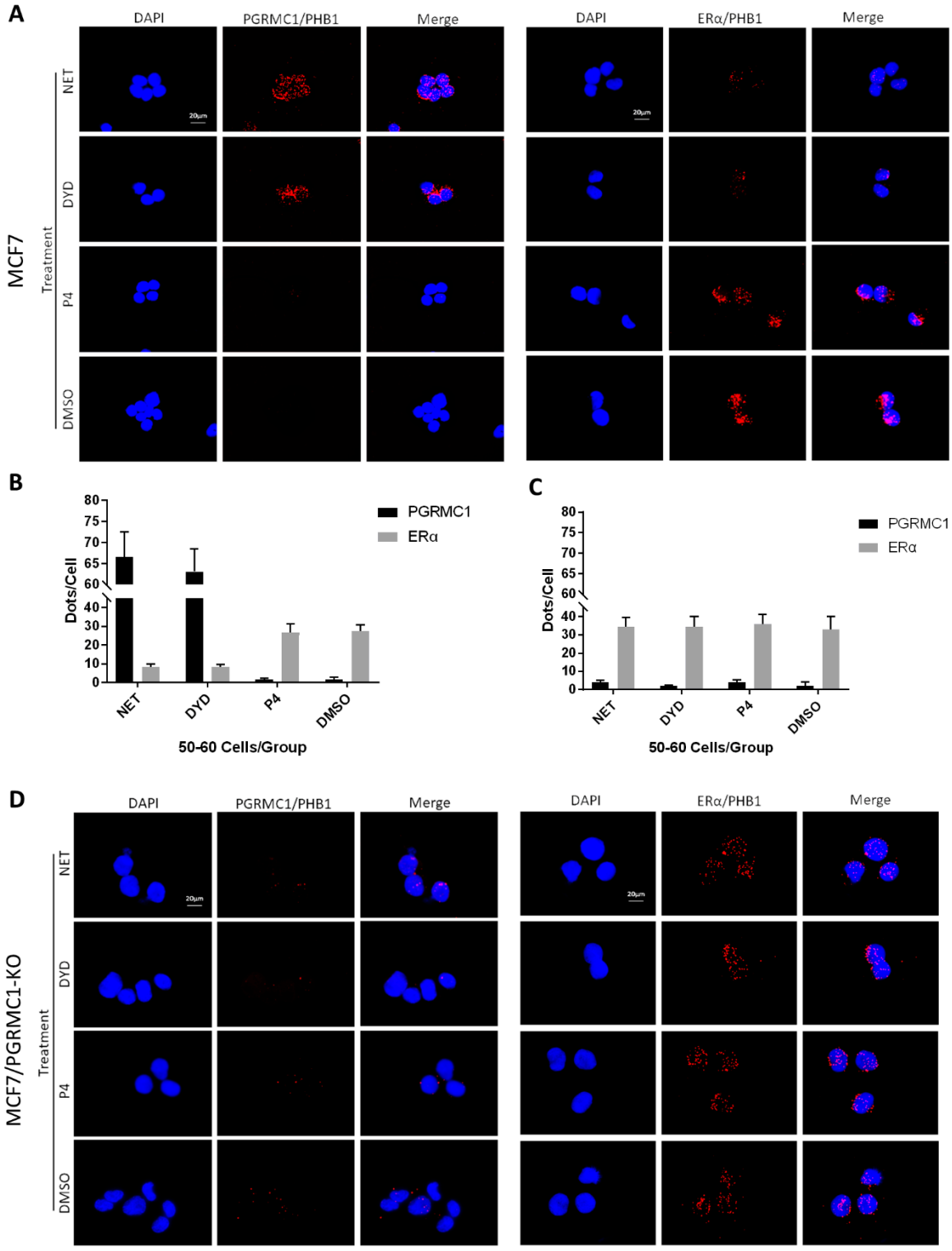

Figure 4. PGRMC1-PHBs interaction disturbs PHBs' binding to ERα. (**A**) Proximity ligation assay (PLA) for PGRMC1- (or ERα-) interactions with PHB1 upon treatment with NET, DYD, P4 (10^{-6} M) and DMSO in MCF7 cells. Analysis of PLA for PGRMC1- (or ERα-) interactions with PHB1 in (**B**) MCF7 and (**C**) MCF7/PGRMC1-KO cells upon treatment with progestins and DMSO. Dots per cell were counted for 50-60 cells in each sample. Cell number and PLA signals were quantified using imageJ software. (**D**) PLA for PGRMC1- (or ERα-) interactions with PHB1 upon treatment with progestins and DMSO in MCF7/PGRMC1-KO cells. Each red spot represents a single interaction. Nuclear stain: DAPI. Magnification 40×.

To test whether the decrease of associations between PHBs and ERα after treatment with NET and DYD is conveyed by PGRMC1, we established PGRMC1 deficient MCF7 cells (MCF7/PGRMC1-KO) using the CRISPR/Cas9 approach. As control, we used cells that were treated with the respective control plasmid (expressing an unspecific gRNA) and analogously expanded from single cell clones (MCF7/PGRMC1-KO/Control). In MCF7/PGRMC1-KO cells that have been selected by PCR screening of single cell clones, PGRMC1 expression was below detection level as tested by Western blotting using two different antibodies (Figures S6, S24 and S25). The PLA in MCF7/PGRMC1-KO cells demonstrated that in the absence of PGRMC1, the interaction between ERα and PHBs did not change with progestin treatment (Figure 4C,D and Figure S5C,D), while MCF7/PGRMC1-KO/Control cells behaved similarly to parental MCF7 cells (Figure S8A–D), implying a dependence upon PGRMC1 in the progestin-dependent release of ERα from PHBs. For isotype controls of the PLA reaction, see Figure S9A,B.

3.5. ERα Is Activated upon Progestin-Treatment in a PGRMC1-Dependent Manner

After demonstrating that ERα is released from PHBs upon binding of PGRMC1 to the latter after stimulation with PPPs, we speculated that progestin-dependent PGRMC1 interaction with PHB1 and PHB2 might result in elevated ERα activation and subsequent increase in ERα target gene expression. To examine this hypothesis, we analyzed the mRNA expression level of trefoil factor 1 (*TFF1*) as a reporter gene for ERα activation upon treatment with both PPPs and N-PPPs in MCF7/PGRMC1 as well as in T47D/PGRMC1 cells and their respective EVC cells. Additionally, we stimulated MCF7/PGRMC1-S181A cells, as the S181-phosphorylation site is critical for the interactions between PGRMC1 and PHBs. We observed increased expression of *TFF1* upon treatment with PPPs in both MCF7/PGRMC1 (Figure 5A) and T47D/PGRMC1 (Figure S11) cells compared to DMSO control, whereas treatment with N-PPPs did not result in any significant differences. Additionally, expression of *TFF1* in MCF7/PGRMC1-S181 cells did not vary upon treatment with any progestin relative to MCF7/EVC control cells (Figure 5A), emphasizing the importance of PGRMC1-S181 phosphorylation in progestin-dependent ERα activation.

Further, in order to verify that the proliferative effect observed after treatment with PPPs correlated with *TFF1* expression and ERα activation, we pre-treated the same cell lines with the selective ERα-degrader fulvestrant [35] before the stimulation with NET or DYD. As expected, degradation of ERα before progestin treatment (for confirmation of ERα-degradation, see Figures S12, S26 and S27) resulted in diminished *TFF1* expression (Figure 5C,D). In addition, the proliferative effect of NET was completely abolished after pre-treatment with fulvestrant, validating that the progestin-dependent increased breast cancer cell viability is conveyed through the ERα signaling pathway (Figure 5B). To further elucidate the role of PGRMC1 in progestin-dependent ERα activation, we pre-treated MCF7/PGRMC1 and MCF7/EVC cells with the putative PGRMC1 inhibitor AG-205 [45,46]. AG-205 antagonizes some PGRMC1 functions but also has PGRMC1-independent effects [47]. Treatment with AG-205 before the stimulation with NET or DYD representatively for PPPs completely abolished the increase of *TFF1* expression in both cell lines for DYD and significantly diminished the same for NET, indicating an essential role of PGRMC1 in progestin-dependent ERα activation (Figure 5E,F).

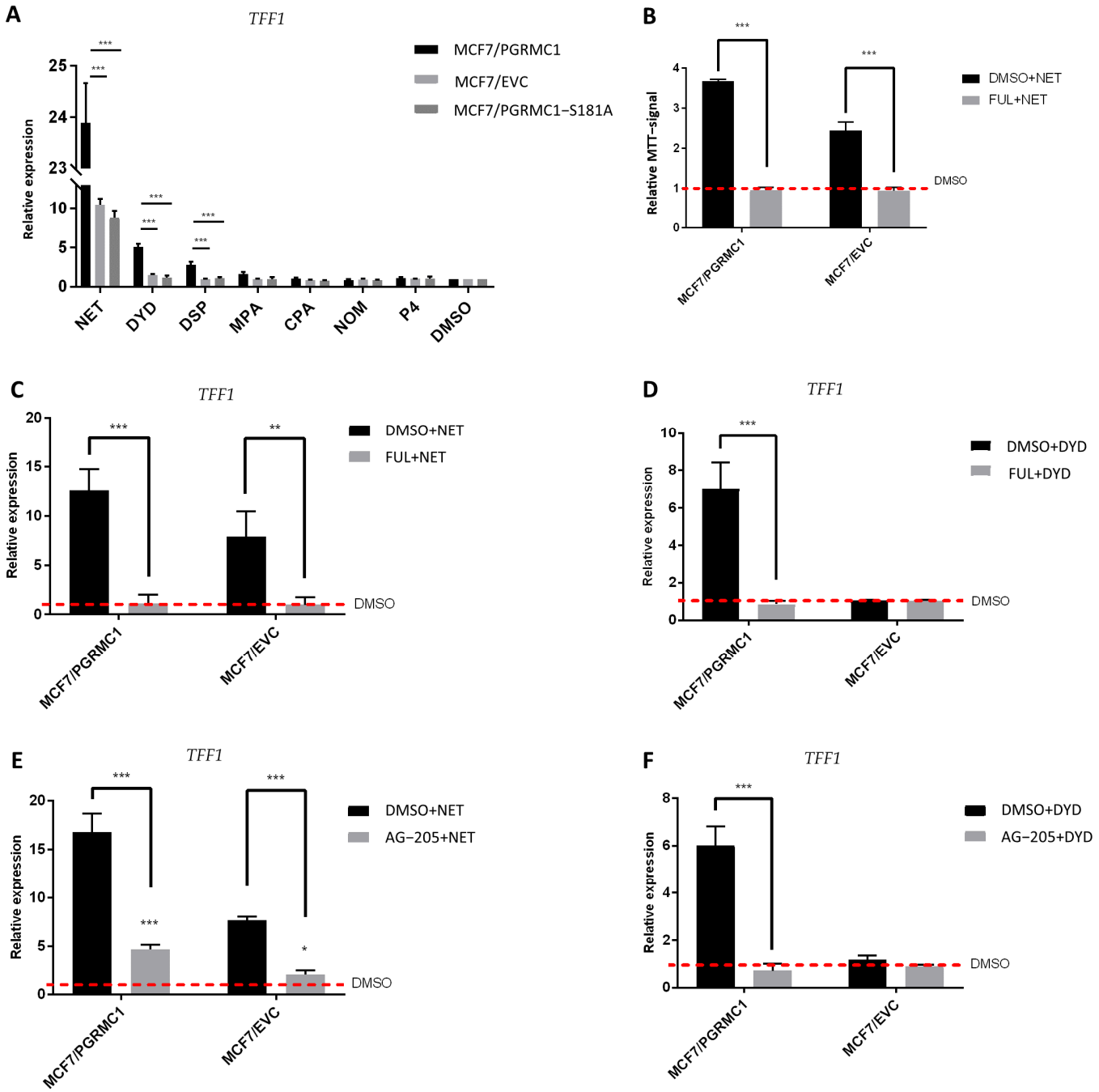

Figure 5. ERα is activated upon progestin-treatment in a PGRMC1-dependent manner. (**A**) qRT-PCR analysis of *TFF1* mRNA expression in MCF7/PGRMC1, MCF7/EVC and MCF7/PGRMC1-S181A cells upon treatment with progestins (10^{-6} M) or DMSO (0.01%) for 24 h. (**B**) Relative MTT signal as surrogate for cell number of MCF7/PGRMC1 and MCF7/EVC cells treated with fulvestrant (10^{-7} M) and NET (10^{-6} M) or DMSO (0.01%). Values were normalized to DMSO treated cells. qRT-PCR analysis of *TFF1* mRNA expression in MCF7/PGRMC1 and MCF7/EVC cells upon treatment with (**C**) fulvestrant (10^{-7} M) and NET (10^{-6} M), (**D**) fulvestrant and DYD (10^{-6} M), (**E**) AG-205 (25×10^{-6} M) and NET, (**F**) AG-205 and DYD, or DMSO, respectively. Signal intensity was normalized to respective DMSO control. Statistical analysis was performed by two-way ANOVA and Bonferroni post-hoc test. *: $p < 0.05$, **: $p < 0.01$, ***: $p < 0.001$.

4. Discussion

Various studies have demonstrated that elevated PGRMC1 expression promotes a more aggressive phenotype of breast cancer and participates in its carcinogenesis [48,49]. High expression of PGRMC1 correlates with poor outcome, which has been reported for breast-, lung-, ovarian- and kidney cancer [48,50–52]. In previous studies, we demonstrated that PGRMC1 is partially required for progestin signaling in MCF7 cells and therefore suggested a potential role of PGRMC1 in the increased breast cancer risk upon progestin-based HT [27–29].

Our present study focuses on a progestin-dependent crosstalk between PGRMC1 and ERα signaling in ERα/PR positive breast cancer cells. Our findings suggest the function of PGRMC1 as an important amplifier of ERα-dependent transcription upon treatment with the PPPs NET, DYD, DSP, and MPA, resulting in oncogenic signaling and tumor progression in ERα positive breast cancer cells. These results are in accordance with a study by Ruan et al., who also detected proliferation-enhancing effects of NET, DYD, DSP, and MPA, whereas no effect could be observed for NOM or P4 [31]. They are further supported by a recently published xenograft study by Zhao et al., who found higher tumor volumes of PGRMC1 overexpressing MCF7 and T47D cells in NET treated mice compared to tumor volumes of the respective EVC cells [30].

To identify responsible factors that are involved in oncogenic signaling of HR positive breast cancer cells, we performed Co-IP with HA-PGRMC1 followed by mass spectrometry and identified PHB1 and PHB2 as possible PGRMC1 interaction partners upon treatment with NET. We do not demonstrate direct physical interactions, however at the very least PGRMC1 and PHBs are present in the same Co-IP pellets and are sufficiently proximal to permit a positive PLA signal. As reviewed by Cahill et al., PGRMC1 phosphorylation could play a crucial role not only in terms of its function but also for its protein-protein interactions and subcellular localization [44]. In a previous study, we investigated PGRMC1 phosphorylation in MCF7 breast cancer cells after treatment with NET and identified S181 to be phosphorylated [27].

In the current investigation, we further demonstrate that PGRMC1-S181-phosphorylation is promoted by PPPs and correlates with increased proliferation of treated cells. We observed increased phosphorylation at S181 for both exogenously and endogenously expressed PGRMC1 after treatment with PPPs. Hence, ablation of the S181 phosphorylation site by single amino acid substitution to alanine or in combination with S57A significantly diminished proliferation of MCF7/PGRMC1-S181A and MCF7/PGRMC1-S57A/S181A cells. In addition, we demonstrated that PGRMC1-S181 phosphorylation is essential for association of PGRMC1 with PHBs after treatment with all PPPs and that the PGRMC1-PHB association is abolished in PGRMC1-S181 phosphorylation-deficient cells. According to these findings, we assume that phosphorylation of PGRMC1 at S181 is crucial for its downstream signaling and the resulting increase in cell proliferation upon progestin treatment. Future studies should address the role, if any, of the adjacent Y180 residue in PHB interactions. Mutation of Y180 in MIA PaCa-2 pancreatic cancer cells reduced signaling by the PI3K/Akt pathway, accompanied by large metabolic and epigenetic changes [43,53].

Both PHBs are reported to exert various functions depending on their localization in the cell and can act independently as well as in a heterodimeric complex [32]. In addition to being a scaffold for mitochondrial proteins in the inner mitochondrial membrane [32], both PHBs have been described as transcription factor modulators which interact with various transcription factors in the nucleus, particularly with ERα [32,39,40]. For luminal breast cancer, PHB2 has been discussed as a potential tumor suppressor since its overexpression significantly diminished ERα signaling, whereas its downregulation elevated the latter [40].

In the present study, we demonstrated that PGRMC1 may represent a regulating factor in the PHBs-ERα-interplay. Stimulation with PPPs increased the association between PGRMC1 and PHBs, which reduced the interactions between PHBs and ERα. A potential mechanism may be that this results in a reduced capability of PHBs inhibit ERα transcriptional activity in the promoter regions of ER-target genes (Figure 6). Indeed, the PLA

between the different proteins using NET and DYD representatively for the group of PPPs and P4 and DMSO as controls revealed significantly reduced interactions between ERα and PHBs and significantly elevated ERα activation (measured as *TFF1* transcription level) upon treatment with NET and DYD. This finding points towards an indirect stimulatory effect on ERα by PGRMC1 via neutralization of the inhibitory effect of PHBs. A similar role has been reported for the brefeldin A-inhibited guanine nucleotide-exchange protein 3 (BIG3) which binds PHB2 to prevent its translocation into the nucleus, and thereby acts as an ERα coactivator [54–56].

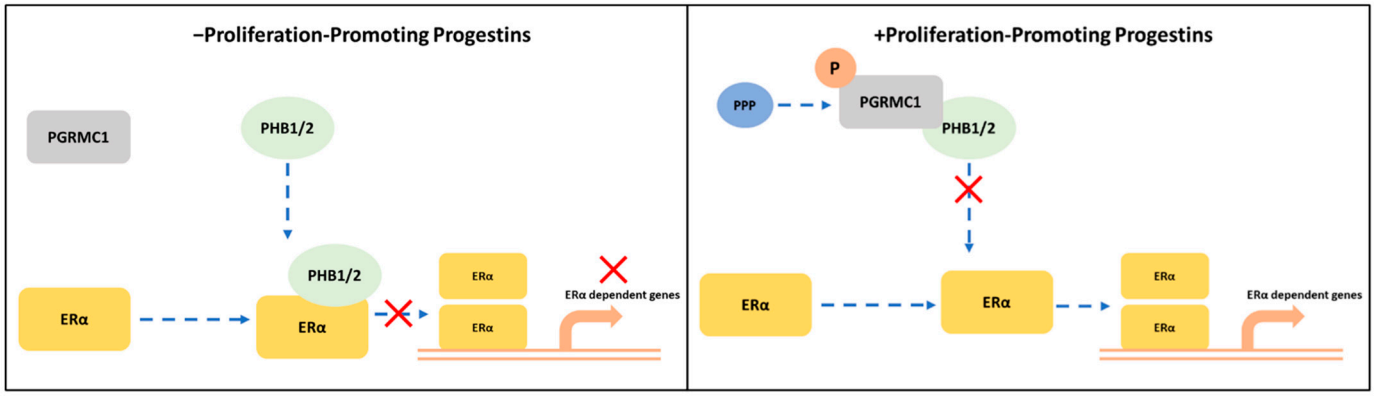

Figure 6. Potential crosstalk between PGRMC1 and PHB1/2 in ERα-signaling cascades. S181-phosphorylation on PGRMC1 mediates interaction with PHB1/2 upon treatment with proliferation-promoting progestins (PPPs). In absence of PPPs: PHB1/2 act as ERα co-regulators to inhibit the transcription of ERα-dependent genes. In presence of PPPs: S181-phosphorylated PGRMC1 interacts with PHB1/2, possibly inhibiting their function as transcription factor regulators and enabling the transcription of ERα-dependent genes.

Consistently with this model, pharmacological inhibition of each of PGRMC1 by AG-205 or ERα by fulvestrant annulled the stimulatory effect of DYD and significantly diminished the same for NET, substantiating the assumption that both PGRMC1 and ERα essentially contribute to the propagation of progestin signals in breast cancer. Interestingly, in a recent publication, Teakel and coauthors identified PHBs as PGRMC1 interaction partners in the pancreatic cancer cell line MIA PaCa-2 independently of progestin treatment [33], pointing towards an implication of PGRMC1 in PHB1/PHB2- function that is not limited to breast cancer or progestin stimulation, which deserves further investigation. This is especially interesting considering that PHBs regulate additional transcription factors to ERα, e.g., E2F1, p53 [57,58], and implicates new ways that PGRMC1 might modulate the context of oncogenic signaling and apoptosis in other tumor settings.

Concerning the inhibitory function of AG-205 on PGRMC1, it is important to mention that not all the effects observed upon AG-205 treatment in the literature appear to be PGRMC1-specific. AG-205 has been repeatedly used by several research groups as mutual PGRMC1 inhibitor to confirm the role of PGRMC1 in membrane trafficking and epithelial growth factor receptor (EGFR) activation, activation of glucagon-like peptide 1 receptor and fatty acid 2-hydrolase [50,59–61]. However, as recently demonstrated by Wang-Eckhardt et al., formation of large vesicular structures in response to AG-205 treatment occurred independently of PGRMC1 expression [47]. Furthermore, in endometrial cells, AG-205 treatment led to increased expression of genes involved in cholesterogenesis and steroidogenesis, both independently of PGRMC1 expression [62]. These two findings emphasize that caution is advised when using AG-205 as a mutual PGRMC1 inhibitor. Although the binding of AG-205 to PGRMC1 has been demonstrated [50], its exact mechanism of action and possible activity on other targets remains uncharacterized.

In our experiments, the strongest proliferative effect and the highest increase of *TFF1* expression was measured after NET stimulation, with DYD being the second most potent progestin. However, as to PGRMC1-S181 phosphorylation and the interaction between

PGRMC1 and PHBs, we found the highest level of PGRMC1-phosphorylation and the strongest increase of PHB-interactions for DYD.

Concerning this issue, it is important to mention that in T47D cells, NET was previously shown to be bioconverted into the ERα-agonists 3α,5α-norethisterone and 5α-norethisterone [63]. Hence, besides activation of PGRMC1 and associated downstream targets, metabolites of NET might also directly bind to ERα, facilitating ligand-dependent ERα signaling. This is consistent with the observation that inhibition of PGRMC1 using AG-205 resulted in a completely abolished increase of *TFF1* expression when treated with DYD, whereas treatment with NET was accompanied by a significantly decreased but still measurable ERα activation, perhaps through direct ERα binding by NET metabolites.

In an earlier publication dealing with increased breast cancer risk for women receiving combined hormone therapy, we used MPA in combination with E2 and reported that MPA sensitized PGRMC1-overexpressing MCF7 cells to E2 at low concentration [64]. Further, in in vivo studies a sequential combined treatment of E2 and NET significantly increased tumor growth of MCF7/PGRMC1 cells, compared to E2-only treatment [29]. In the present study, we treated the cells with the progestins alone in hormone free medium. Nevertheless, as previously described, we measured increased production of estradiol in MCF7/PGRMC1 cells [24], indicating that these cells might endogenously activate ERα even in the absence of exogenous E2. Therefore, the exact mechanism of ERα activation and recruitment to the *TFF1* promotor needs further investigation.

Our data rather describes the impact of PGRMC1 on PHBs' function as transcription factor modulators and contributes to revealing the PGRMC1 regulatory network with special focus on processes driving breast cancer progression. It is of notable interest that nuclear steroid receptor transcription factors, of which ERα was the first in chordates, evolved in bilaterian animals [65]. Bilaterians concomitantly gained the cognate of the T178/Y180/S181 module in the eumetazoan PGRMC C-terminus [66], suggesting that the processes we describe here may reflect ancient bilaterian biology that is perturbed in cancer. Future studies should further elucidate the mechanism of elevated ERα activation mediated by PGRMC1 to shed light on the regulation of this oncogenic signaling pathway. The interaction partners detected in the present study will be an important starting point to further investigate the PGRMC1 signaling cascade in HR positive breast cancer.

Since activated PGRMC1 may potentiate the oncogenic signaling of ERα and thereby promote breast cancer progression, it may serve as a therapeutic target. In this context, Kabe et al. recently identified glycyrrhizin, a major component in licorice extract with anti-inflammatory and anti-viral effects [67], as a substance that directly binds PGRMC1 and inhibits some of its functions [68]. In a human colon cancer cell line, glycyrrhizin inhibited the interaction of PGRMC1 with EGFR, suppressing EGFR signaling and increasing chemosensitivity towards erlotinib and cisplatin [68]. Future studies should investigate the effect of glycyrrhizin on PGRMC1 in the context of breast cancer. Given the potential mechanism presented in the current study, the possible pharmacologic inhibition of PGRMC1 in combination with antihormonal treatment could be of high interest.

5. Conclusions

In the present study, we identified PGRMC1 as a factor that inhibits PHBs' action as ERα co-regulators in the presence of certain progestins in our luminal breast cancer cell model. PGRMC1 is thereby involved in a key oncogenic signaling pathway in breast cancer. Our data underline the contribution of PGRMC1 to especially hormone receptor positive breast cancer pathogenesis and demonstrate the urgent need for further studies.

Supplementary Materials: The following are available online at https://www.mdpi.com/article/10.3390/cancers13225635/s1, Figure S1: Cell viability of breast cancer cells upon progestin treatment, Figure S2: Relative amount of precipitated PGRMC1, Figure S3: PGRMC1 is phosphorylated at S181 upon treatment with proliferation-promoting progestins, Figure S4: PHB1 and PHB2 are precipitated by PGRMC1 after treatment with PPPs, Figure S5: PLA for PGRMC1 and PHB2 or ERα and PHB2 in MCF7 cells, Figure S6: PGRMC1 protein level in parental MCF7 and PGRMC1-knockout cells,

Figure S7: PLA for PGRMC1 and PHB1/PHB2 or ERα and PHB1/PHB2 in T47D cells, Figure S8: PLA for PGRMC1 and PHB1/PHB2 or ERα and PHB1/PHB2 in MCF7/PGRMC1-KO/Control cells, Figure S9: Negative control PLA using isotype antibodies, Figure S10: Immunofluorescence staining of MCF7 cells for PGRMC1, PHB1, ERα and PHB2, Figure S11: qRT-PCR analysis of *TFF1* mRNA expression in T47D/PGRMC1 and T47D cells, Figure S13. Left panel: analysis of immunopurified (HA-based) precipitate from PGRMC1 overexpressing cell lines MCF7/PGRMC1 and MCF7/PGRMC1-GFP cells; detection of PHB1 and PGRMC1. Right panel: Protein level in whole cell, Figure S14. Left panel: analysis of immunopurified (HA-based) precipitate from PGRMC1 overexpressing cell lines MCF7/PGRMC1 and MCF7/PGRMC1-GFP cells; detection of PHB2 and PGRMC1. Right panel: Protein level in whole cell, Figure S15. Analysis of PGRMC1-S181-phosphorylation after progestin treatment in whole cell lysates of MCF7/PGRMC1 cells. Upper panel: detection of S181-phosphorylated PGRMC1; Lower panel: detection of PGRMC1 protein level, Figure S16. Analysis of immunopurified (HA-based) precipitate from MCF7/PGRMC1 cells after progestin treatment (upper panel) and protein level in whole cell lysates of the same samples (lower panel). Detection of PHB1, Figure S17. Analysis of immunopurified (HA-based) precipitate from MCF7 cells overexpressing PGRMC1 or phosphorylation-deficient PGRMC1 variants after treatment with DYD. Detection of PHB1, Figure S18. Analysis of PGRMC1-S181-phosphorylation after progestin treatment in whole cell lysates of MCF7/EVC cells. Upper panel: detection of S181-phosphorylated PGRMC1; Lower pan-el: detection of PGRMC1 protein level, Figure S19. Analysis of PGRMC1-S181-phosphorylation after progestin treatment in whole cell lysates of MCF7/PGRMC1-S181A cells. Upper panel: detection of S181-phosphorylated PGRMC1; Lower panel: detection of PGRMC1 protein level, Figure S20. Analysis of immunopurified (HA-based) precipitate from MCF7/PGRMC1 cells after progestin treatment (upper panel) and protein level in whole cell lysates of the same samples (lower panel). Detection of PHB2, Figure S21. Analysis of immunopurified (HA-based) precipitate from T47D/PGRMC1 cells after progestin treatment (upper panel) and protein level in whole cell lysates of the same samples (lower panel). Detection of PHB1, Figure S22. Analysis of immunopurified (HA-based) precipitate from T47D/PGRMC1 cells after progestin treatment (upper panel) and protein level in whole cell lysates of the same samples (lower panel). Detection of PHB2, Figure S23. Analysis of immunopurified (HA-based) precipitate from MCF7 cells overexpressing PGRMC1 or phosphorylation-deficient PGRMC1 variants after treatment with DYD. Detection of PHB2, Figure S24. Analysis of PGRMC1-expression in whole cell lysates from MCF7, MCF7/PGRMC1-KO/Control and MCF7/PGRMC1-KO cells. Detection of PGRMC1 with the N-terminal antibody (Cell Signaling), Figure S25. Analysis of PGRMC1-expression in whole cell lysates from MCF7, MCF7/PGRMC1-KO/Control and MCF7/PGRMC1-KO cells. Detection of PGRMC1 with the C-terminal antibody (Abcam), Figure S26. Analysis of ERα- and PGRMC1-protein level in MCF7/PGRMC1 and MCF7/EVC cells after treatment with fulvestrant and NET, Figure S27. Analysis of ERα- and PGRMC1-protein level in MCF7/PGRMC1 and MCF7/EVC cells after treatment with fulvestrant and DYD, Table S1: List of proteins identified in the precipitate by mass spectrometry after HA-based enrichment of PGRMC1 from whole cell lysates of MCF7/PGRMC1 and MCF7/PGRMC1-GFP cells treated with NET (10^{-6} M) or DMSO.

Author Contributions: Conceptualization, Y.B., M.L., N.S. and H.N.; methodology, G.P., M.L. and N.S.; formal analysis, Y.B., G.P., M.W. and N.S.; investigation, Y.B., M.L., G.P., M.W., J.O. and N.S.; validation, Y.B. and N.S.; data curation, Y.B., G.P. and N.S.; visualization, Y.B., G.P. and N.S.; writing—original draft preparation, Y.B., M.L. and N.S.; writing—review and editing, G.P., K.S., A.F., M.R., A.A., F.R., E.R., D.N., T.F., M.A.C., N.S. and H.N.; resources, K.S., D.N. and H.N., supervision, N.S. and H.N.; project administration, T.F., N.S. and H.N.; funding acquisition, M.L. and H.N. All authors have read and agreed to the published version of the manuscript.

Funding: This research was funded by "The German Research Foundation (Deutsche Forschungsgemeinschaft, DFG, NE 805/6-1)", and "The Brigitte and Dr. Konstanze Wegener Foundation (#51, Duesseldorf, Germany)", and "The Medical Faculty of the Heinrich-Heine University Duesseldorf (#48/2018)".

Institutional Review Board Statement: Not applicable.

Informed Consent Statement: Not applicable.

Data Availability Statement: Relevant data supporting the findings of this study are available within the article and Supplementary Materials and are available from the authors upon reasonable request.

The mass spectrometry proteomics data have been deposited to the ProteomeXchange Consortium via the PRIDE [37] partner repository with the dataset identifier PXD028537.

Acknowledgments: This study is based on and contains results of the dissertation 'Role of PGRMC1 in breast cancer progression and increased breast cancer risk upon progestin-based hormone therapy' submitted to the Faculty of Mathematics and Natural Sciences at the Heinrich-Heine-University Duesseldorf on 30 September 2017 by Marina Ludescher (née Willibald) [28]. The authors further thank Simon Eickhoff (Institute of Neuroscience and Medicine, Research Center, Juelich; Institute of Systems Neuroscience, Heinrich-Heine University, Duesseldorf) for his consultation on the statistical analysis, Daniel Nettersheim (Department of Urology, Urological Research Laboratory, Translational UroOncology, Heinrich-Heine University Duesseldorf) for his kind advice concerning CRISPR/Cas9 application and Dorothee Koehler (Department of Obstetrics and Gynecology, University Hospital and Medical Faculty of the Heinrich-Heine University Duesseldorf) for her assistance in generating cellular models.

Conflicts of Interest: The authors declare no conflict of interest.

Appendix A

Table S1: List of proteins identified in the precipitate by mass spectrometry after HA-based enrichment of PGRMC1 from whole cell lysates of MCF7/PGRMC1 and MCF7/PGRMC1-GFP cells treated with NET (10^{-6} M) or DMSO. In addition to the data on the statistical analysis, the tables contain mean values of LFQ-intensity values for the different groups and ratios of selected mean values as indicated. Additionally relevant protein identification and quantification data from MaxQuant is shown. For details please refer to Tyanova et al., 2016 [69]. List of 701 co-precipitated proteins (Table S1 701 Proteins) identified by mass spectrometry from HA-immunopurified proteins of MCF7/PGRMC1 and MCF7/PGRMC1-GFP cells treated with NET (10^{-6} M) or DMSO. GFP DMSO: immunopurified samples of DMSO treated MCF7/PGRMC1-GFP cells. GFP NET: immunopurified samples of NET treated MCF7/PGRMC1-GFP cells. HA DMSO: immunopurified samples of DMSO treated MCF7/PGRMC1 cells. HA NET: immunopurified samples of DMSO treated MCF7/PGRMC1 cells. Potential PGRMC1 interacting proteins were selected by a ratio HA/GFP > 2 and additionally a corrected p-value < 0.01 for the variable "TAG" in the 2 way-ANOVA. For the 253 remaining proteins (Table S1 253 Proteins) additionally Welch-tests were performed (significance analysis of microarrays, S0 = 0.1, 1% false discovery rate, Tusher et al., 2001) [70] comparison of NET and DMSO treated HA-PGRMC1 samples.

References

1. Sung, H.; Ferlay, J.; Siegel, R.L.; Laversanne, M.; Soerjomataram, I.; Jemal, A.; Bray, F. Global Cancer Statistics 2020: GLOBOCAN Estimates of Incidence and Mortality Worldwide for 36 Cancers in 185 Countries. *CA A Cancer J. Clin.* **2021**, *71*, 209–249. [CrossRef]
2. Howlader, N.; Altekruse, S.F.; Li, C.I.; Chen, V.W.; Clarke, C.A.; Ries, L.A.; Cronin, K.A. US incidence of breast cancer subtypes defined by joint hormone receptor and HER2 status. *J. Natl. Cancer Inst.* **2014**, *106*, dju055. [CrossRef] [PubMed]
3. McPherson, K.; Steel, C.M.; Dixon, J.M. ABC of breast diseases. Breast cancer-epidemiology, risk factors, and genetics. *BMJ (Clin. Res. Ed.)* **2000**, *321*, 624–628. [CrossRef]
4. L'Hermite, M. Bioidentical menopausal hormone therapy: Registered hormones (non-oral estradiol ± progesterone) are optimal. *Climact. J. Int. Menopause Soc.* **2017**, *20*, 331–338. [CrossRef]
5. Schonfeld, S.J.; Pfeiffer, R.M.; Lacey, J.V., Jr.; Berrington de González, A.; Doody, M.M.; Greenlee, R.T.; Park, Y.; Schairer, C.; Schatzkin, A.; Sigurdson, A.J.; et al. Hormone-related risk factors and postmenopausal breast cancer among nulliparous versus parous women: An aggregated study. *Am. J. Epidemiol.* **2011**, *173*, 509–517. [CrossRef] [PubMed]
6. Fournier, A.; Berrino, F.; Clavel-Chapelon, F. Unequal risks for breast cancer associated with different hormone replacement therapies: Results from the E3N cohort study. *Breast Cancer Res. Treat.* **2008**, *107*, 103–111. [CrossRef] [PubMed]
7. Chlebowski, R.T.; Anderson, G.L.; Prentice, R.L.; Rossouw, J.E.; Aragaki, A.K.; Manson, J.E. Reliable evidence from placebo-controlled, randomized, clinical trials for menopausal hormone therapy's influence on incidence and deaths from breast cancer. *Climact. J. Int. Menopause Soc.* **2015**, *18*, 336–338. [CrossRef] [PubMed]
8. Pickar, J.H.; Archer, D.F.; Kagan, R.; Pinkerton, J.V.; Taylor, H.S. Safety and benefit considerations for menopausal hormone therapy. *Expert Opin. Drug Saf.* **2017**, *16*, 941–954. [CrossRef] [PubMed]
9. Porch, J.V.; Lee, I.M.; Cook, N.R.; Rexrode, K.M.; Burin, J.E. Estrogen-progestin replacement therapy and breast cancer risk: The Women's Health Study (United States). *Cancer Causes Control CCC* **2002**, *13*, 847–854. [CrossRef]

10. Chlebowski, R.T.; Hendrix, S.L.; Langer, R.D.; Stefanick, M.L.; Gass, M.; Lane, D.; Rodabough, R.J.; Gilligan, M.A.; Cyr, M.G.; Thomson, C.A.; et al. Influence of estrogen plus progestin on breast cancer and mammography in healthy postmenopausal women: The Women's Health Initiative Randomized Trial. *JAMA* **2003**, *289*, 3243–3253. [CrossRef] [PubMed]
11. Trabert, B.; Sherman, M.E.; Kannan, N.; Stanczyk, F.Z. Progesterone and breast cancer. *Endocr. Rev.* **2020**, *41*, 320–344. [CrossRef]
12. Africander, D.; Verhoog, N.; Hapgood, J.P. Molecular mechanisms of steroid receptor-mediated actions by synthetic progestins used in HRT and contraception. *Steroids* **2011**, *76*, 636–652. [CrossRef] [PubMed]
13. Courtin, A.; Communal, L.; Vilasco, M.; Cimino, D.; Mourra, N.; de Bortoli, M.; Taverna, D.; Faussat, A.M.; Chaouat, M.; Forgez, P.; et al. Glucocorticoid receptor activity discriminates between progesterone and medroxyprogesterone acetate effects in breast cells. *Breast Cancer Res. Treat.* **2012**, *131*, 49–63. [CrossRef] [PubMed]
14. Moore, N.L.; Hickey, T.E.; Butler, L.M.; Tilley, W.D. Multiple nuclear receptor signaling pathways mediate the actions of synthetic progestins in target cells. *Mol. Cell. Endocrinol.* **2012**, *357*, 60–70. [CrossRef] [PubMed]
15. Neubauer, H.; Chen, R.; Schneck, H.; Knorrp, T.; Templin, M.F.; Fehm, T.; Cahill, M.A.; Seeger, H.; Yu, Q.; Mueck, A.O. New insight on a possible mechanism of progestogens in terms of breast cancer risk. *Horm. Mol. Biol. Clin. Investig.* **2011**, *6*, 185–192. [CrossRef]
16. Neubauer, H.; Ma, Q.; Zhou, J.; Yu, Q.; Ruan, X.; Seeger, H.; Fehm, T.; Mueck, A.O. Possible role of PGRMC1 in breast cancer development. *Climact. J. Int. Menopause Soc.* **2013**, *16*, 509–513. [CrossRef]
17. Cahill, M.A. Progesterone receptor membrane component 1: An integrative review. *J. Steroid Biochem. Mol. Biol.* **2007**, *105*, 16–36. [CrossRef] [PubMed]
18. Cahill, M.A.; Jazayeri, J.A.; Catalano, S.M.; Toyokuni, S.; Kovacevic, Z.; Richardson, D.R. The emerging role of progesterone receptor membrane component 1 (PGRMC1) in cancer biology. *Biochim. Biophys. Acta* **2016**, *1866*, 339–349. [CrossRef] [PubMed]
19. Meyer, C.; Schmid, R.; Scriba, P.C.; Wehling, M. Purification and partial sequencing of high-affinity progesterone-binding site(s) from porcine liver membranes. *Eur. J. Biochem.* **1996**, *239*, 726–731. [CrossRef] [PubMed]
20. Bali, N.; Arimoto, J.M.; Morgan, T.E.; Finch, C.E. Progesterone antagonism of neurite outgrowth depends on microglial activation via Pgrmc1/S2R. *Endocrinology* **2013**, *154*, 2468–2480. [CrossRef]
21. Cahill, M.A.; Medlock, A.E. Thoughts on interactions between PGRMC1 and diverse attested and potential hydrophobic ligands. *J. Steroid Biochem. Mol. Biol.* **2017**, *171*, 11–33. [CrossRef]
22. Friel, A.M.; Zhang, L.; Pru, C.A.; Clark, N.C.; McCallum, M.L.; Blok, L.J.; Shioda, T.; Peluso, J.J.; Rueda, B.R.; Pru, J.K. Progesterone receptor membrane component 1 deficiency attenuates growth while promoting chemosensitivity of human endometrial xenograft tumors. *Cancer Lett.* **2015**, *356*, 434–442. [CrossRef] [PubMed]
23. Peluso, J.J.; Yuan, A.; Liu, X.; Lodde, V. Plasminogen activator inhibitor 1 RNA-binding protein interacts with progesterone receptor membrane component 1 to regulate progesterone's ability to maintain the viability of spontaneously immortalized granulosa cells and rat granulosa cells. *Biol. Reprod.* **2013**, *88*, 20. [CrossRef]
24. Asperger, H.; Stamm, N.; Gierke, B.; Pawlak, M.; Hofmann, U.; Zanger, U.M.; Marton, A.; Katona, R.L.; Buhala, A.; Vizler, C.; et al. Progesterone receptor membrane component 1 regulates lipid homeostasis and drives oncogenic signaling resulting in breast cancer progression. *Breast Cancer Res. BCR* **2020**, *22*, 75. [CrossRef]
25. Hughes, A.L.; Powell, D.W.; Bard, M.; Eckstein, J.; Barbuch, R.; Link, A.J.; Espenshade, P.J. Dap1/PGRMC1 binds and regulates cytochrome P450 enzymes. *Cell Metab.* **2007**, *5*, 143–149. [CrossRef] [PubMed]
26. Kabe, Y.; Nakane, T.; Koike, I.; Yamamoto, T.; Sugiura, Y.; Harada, E.; Sugase, K.; Shimamura, T.; Ohmura, M.; Muraoka, K.; et al. Haem-dependent dimerization of PGRMC1/Sigma-2 receptor facilitates cancer proliferation and chemoresistance. *Nat. Commun.* **2016**, *7*, 11030. [CrossRef] [PubMed]
27. Willibald, M.; Bayer, G.; Stahlhut, V.; Poschmann, G.; Stühler, K.; Gierke, B.; Pawlak, M.; Seeger, H.; Mueck, A.O.; Niederacher, D.; et al. Progesterone receptor membrane component 1 is phosphorylated upon progestin treatment in breast cancer cells. *Oncotarget* **2017**, *8*, 72480–72493.[CrossRef]
28. Willibald, M. Role of PGRMC1 in Breast Cancer Progression and Increased Breast Cancer Risk upon Progestin-Based Hormone Therapy. Inaugural Dissertation, Heinrich-Heine-Universität Düsseldorf, Düsseldorf, Germany, 26 September 2017.
29. Neubauer, H.; Ruan, X.; Schneck, H.; Seeger, H.; Cahill, M.A.; Liang, Y.; Mafuvadze, B.; Hyder, S.M.; Fehm, T.; Mueck, A.O. Overexpression of progesterone receptor membrane component 1: Possible mechanism for increased breast cancer risk with norethisterone in hormone therapy. *Menopause* **2013**, *20*, 504–510. [CrossRef] [PubMed]
30. Zhao, Y.; Ruan, X.; Wang, H.; Li, X.; Gu, M.; Wang, L.; Li, Y.; Seeger, H.; Mueck, A.O. The presence of a membrane-bound progesterone receptor induces growth of breast cancer with norethisterone but not with progesterone: A xenograft model. *Maturitas* **2017**, *102*, 26–33. [CrossRef]
31. Ruan, X.; Neubauer, H.; Yang, Y.; Schneck, H.; Schultz, S.; Fehm, T.; Cahill, M.A.; Seeger, H.; Mueck, A.O. Progestogens and membrane-initiated effects on the proliferation of human breast cancer cells. *Climact. J. Int. Menopause Soc.* **2012**, *15*, 467–472. [CrossRef] [PubMed]
32. Mishra, S.; Murphy, L.C.; Murphy, L.J. The Prohibitins: Emerging roles in diverse functions. *J. Cell. Mol. Med.* **2006**, *10*, 353–363. [CrossRef] [PubMed]
33. Teakel, S.L.; Ludescher, M.; Thejer, B.M.; Poschmann, G.; Forwood, J.K.; Neubauer, H.; Cahill, M.A. Protein complexes including PGRMC1 and actin-associated proteins are disrupted by AG-205. *Biochem. Biophys. Res. Commun.* **2020**, *524*, 64–69. [CrossRef] [PubMed]

34. Neubauer, H.; Clare, S.E.; Wozny, W.; Schwall, G.P.; Poznanovic, S.; Stegmann, W.; Vogel, U.; Sotlar, K.; Wallwiener, D.; Kurek, R.; et al. Breast cancer proteomics reveals correlation between estrogen receptor status and differential phosphorylation of PGRMC1. *Breast Cancer Res. BCR* **2008**, *10*, R85. [CrossRef]
35. Krell, J.; Januszewski, A.; Yan, K.; Palmieri, C. Role of fulvestrant in the management of postmenopausal breast cancer. *Expert Rev. Anticancer Ther.* **2011**, *11*, 1641–1652. [CrossRef]
36. Willibald, M.; Wurster, I.; Meisner, C.; Vogel, U.; Seeger, H.; Mueck, A.O.; Fehm, T.; Neubauer, H. High Level of Progesteron Receptor Membrane Component 1 (PGRMC 1) in Tissue of Breast Cancer Patients is Associated with Worse Response to Anthracycline-Based Neoadjuvant Therapy. *Horm. Metab. Res. Horm. Stoffwechs. Horm. Metab.* **2017**, *49*, 595–603. [CrossRef] [PubMed]
37. Perez-Riverol, Y.; Csordas, A.; Bai, J.; Bernal-Llinares, M.; Hewapathirana, S.; Kundu, D.J.; Inuganti, A.; Griss, J.; Mayer, G.; Eisenacher, M.; et al. The PRIDE database and related tools and resources in 2019: Improving support for quantification data. *Nucleic Acids Res.* **2019**, *47*, D442–D450. [CrossRef]
38. Schneider, C.A.; Rasband, W.S.; Eliceiri, K.W. NIH Image to ImageJ: 25 years of image analysis. *Nat. Methods* **2012**, *9*, 671–675. [CrossRef] [PubMed]
39. Delage-Mourroux, R.; Martini, P.G.; Choi, I.; Kraichely, D.M.; Hoeksema, J.; Katzenellenbogen, B.S. Analysis of estrogen receptor interaction with a repressor of estrogen receptor activity (REA) and the regulation of estrogen receptor transcriptional activity by REA. *J. Biol. Chem.* **2000**, *275*, 35848–35856. [CrossRef]
40. He, B.; Feng, Q.; Mukherjee, A.; Lonard, D.M.; DeMayo, F.J.; Katzenellenbogen, B.S.; Lydon, J.P.; O'Malley, B.W. A repressive role for prohibitin in estrogen signaling. *Mol. Endocrinol.* **2008**, *22*, 344–360. [CrossRef] [PubMed]
41. Bavelloni, A.; Piazzi, M.; Raffini, M.; Faenza, I.; Blalock, W.L. Prohibitin 2: At a communications crossroads. *IUBMB Life* **2015**, *67*, 239–254. [CrossRef]
42. Montano, M.M.; Ekena, K.; Delage-Mourroux, R.; Chang, W.; Martini, P.; Katzenellenbogen, B.S. An estrogen receptor-selective coregulator that potentiates the effectiveness of antiestrogens and represses the activity of estrogens. *Proc. Natl. Acad. Sci. USA* **1999**, *96*, 6947–6952. [CrossRef]
43. Thejer, B.M.; Adhikary, P.P.; Kaur, A.; Teakel, S.L.; Van Oosterum, A.; Seth, I.; Pajic, M.; Hannan, K.M.; Pavy, M.; Poh, P.; et al. PGRMC1 phosphorylation affects cell shape, motility, glycolysis, mitochondrial form and function, and tumor growth. *BMC Mol. Cell Biol.* **2020**, *21*, 24. [CrossRef]
44. Cahill, M.A.; Jazayeri, J.A.; Kovacevic, Z.; Richardson, D.R. PGRMC1 regulation by phosphorylation: Potential new insights in controlling biological activity. *Oncotarget* **2016**, *7*, 50822–50827. [CrossRef]
45. Ahmed, I.S.; Rohe, H.J.; Twist, K.E.; Mattingly, M.N.; Craven, R.J. Progesterone receptor membrane component 1 (Pgrmc1): A heme-1 domain protein that promotes tumorigenesis and is inhibited by a small molecule. *J. Pharmacol. Exp. Ther.* **2010**, *333*, 564–573. [CrossRef] [PubMed]
46. Will, E.A.; Liu, X.; Peluso, J.J. AG 205, a progesterone receptor membrane component 1 antagonist, ablates progesterone's ability to block oxidative stress-induced apoptosis of human granulosa/luteal cells. *Biol. Reprod.* **2017**, *96*, 843–854. [CrossRef] [PubMed]
47. Wang-Eckhardt, L.; Eckhardt, M. A progesterone receptor membrane component 1 antagonist induces large vesicles independent of progesterone receptor membrane component 1 expression. *Biol. Chem.* **2020**, *401*, 1093–1099. [CrossRef]
48. Ruan, X.; Zhang, Y.; Mueck, A.O.; Willibald, M.; Seeger, H.; Fehm, T.; Brucker, S.; Neubauer, H. Increased expression of progesterone receptor membrane component 1 is associated with aggressive phenotype and poor prognosis in ER-positive and negative breast cancer. *Menopause* **2017**, *24*, 203–209. [CrossRef]
49. Zhang, Y.; Ruan, X.; Willibald, M.; Seeger, H.; Fehm, T.; Neubauer, H.; Mueck, A.O. May progesterone receptor membrane component 1 (PGRMC1) predict the risk of breast cancer? *Gynecol. Endocrinol. Off. J. Int. Soc. Gynecol. Endocrinol.* **2016**, *32*, 58–60. [CrossRef] [PubMed]
50. Ahmed, I.S.; Rohe, H.J.; Twist, K.E.; Craven, R.J. Pgrmc1 (progesterone receptor membrane component 1) associates with epidermal growth factor receptor and regulates erlotinib sensitivity. *J. Biol. Chem.* **2010**, *285*, 24775–24782. [CrossRef] [PubMed]
51. Hampton, K.K.; Stewart, R.; Napier, D.; Claudio, P.P.; Craven, R.J. PGRMC1 Elevation in Multiple Cancers and Essential Role in Stem Cell Survival. *Adv. Lung Cancer* **2015**, *4*, 37–51. [CrossRef]
52. Zhang, D.; Xia, X.; Wang, X.; Zhang, P.; Lu, W.; Yu, Y.; Deng, S.; Yang, H.; Zhu, H.; Xu, N.; et al. PGRMC1 Is a Novel Potential Tumor Biomarker of Human Renal Cell Carcinoma Based on Quantitative Proteomic and Integrative Biological Assessments. *PLoS ONE* **2017**, *12*, e0170453. [CrossRef] [PubMed]
53. Thejer, B.M.; Adhikary, P.P.; Teakel, S.L.; Fang, J.; Weston, P.A.; Gurusinghe, S.; Anwer, A.G.; Gosnell, M.; Jazayeri, J.A.; Ludescher, M.; et al. PGRMC1 effects on metabolism, genomic mutation and CpG methylation imply crucial roles in animal biology and disease. *BMC Mol. Cell Biol.* **2020**, *21*, 26. [CrossRef] [PubMed]
54. Kim, J.W.; Akiyama, M.; Park, J.H.; Lin, M.L.; Shimo, A.; Ueki, T.; Daigo, Y.; Tsunoda, T.; Nishidate, T.; Nakamura, Y.; et al. Activation of an estrogen/estrogen receptor signaling by BIG3 through its inhibitory effect on nuclear transport of PHB2/REA in breast cancer. *Cancer Sci.* **2009**, *100*, 1468–1478. [CrossRef] [PubMed]
55. Kim, N.H.; Yoshimaru, T.; Chen, Y.A.; Matsuo, T.; Komatsu, M.; Miyoshi, Y.; Tanaka, E.; Sasa, M.; Mizuguchi, K.; Katagiri, T. BIG3 Inhibits the Estrogen-Dependent Nuclear Translocation of PHB2 via Multiple Karyopherin-Alpha Proteins in Breast Cancer Cells. *PLoS ONE* **2015**, *10*, e0127707. [CrossRef]

56. Yoshimaru, T.; Komatsu, M.; Matsuo, T.; Chen, Y.A.; Murakami, Y.; Mizuguchi, K.; Mizohata, E.; Inoue, T.; Akiyama, M.; Yamaguchi, R.; et al. Targeting BIG3-PHB2 interaction to overcome tamoxifen resistance in breast cancer cells. *Nat. Commun.* **2013**, *4*, 2443. [CrossRef]
57. Fusaro, G.; Dasgupta, P.; Rastogi, S.; Joshi, B.; Chellappan, S. Prohibitin induces the transcriptional activity of p53 and is exported from the nucleus upon apoptotic signaling. *J. Biol. Chem.* **2003**, *278*, 47853–47861. [CrossRef] [PubMed]
58. Fusaro, G.; Wang, S.; Chellappan, S. Differential regulation of Rb family proteins and prohibitin during camptothecin-induced apoptosis. *Oncogene* **2002**, *21*, 4539–4548. [CrossRef]
59. Zhang, M.; Robitaille, M.; Showalter, A.D.; Huang, X.; Liu, Y.; Bhattacharjee, A.; Willard, F.S.; Han, J.; Froese, S.; Wei, L.; et al. Progesterone receptor membrane component 1 is a functional part of the glucagon-like peptide-1 (GLP-1) receptor complex in pancreatic β cells. *Mol. Cell. Proteom. MCP* **2014**, *13*, 3049–3062. [CrossRef] [PubMed]
60. Pedroza, D.A.; Rajamanickam, V.; Subramani, R.; Bencomo, A.; Galvez, A.; Lakshmanaswamy, R. Progesterone receptor membrane component 1 promotes the growth of breast cancers by altering the phosphoproteome and augmenting EGFR/PI3K/AKT signalling. *Nature* **2020**, *123*, 1326–1335. [CrossRef] [PubMed]
61. Hardt, R.; Winter, D.; Gieselmann, V.; Eckhardt, M. Identification of progesterone receptor membrane component-1 as an interaction partner and possible regulator of fatty acid 2-hydroxylase. *Biochem. J.* **2018**, *475*, 853–871. [CrossRef] [PubMed]
62. Thieffry, C.; Van Wynendaele, M.; Aynaci, A.; Maja, M.; Dupuis, C.; Loriot, A.; Marbaix, E.; Henriet, P. AG-205 Upregulates Enzymes Involved in Cholesterol Biosynthesis and Steroidogenesis in Human Endometrial Cells Independently of PGRMC1 and Related MAPR Proteins. *Biomolecules* **2021**, *11*, 1472. [CrossRef]
63. Pasapera, A.M.; Gutiérrez-Sagal, R.; Herrera, J.; Galicia-Canales, N.; García de la Mora, G.; Ulloa-Aguirre, A. Norethisterone is bioconverted to oestrogenic compounds that activate both the oestrogen receptor alpha and oestrogen receptor beta in vitro. *Eur. J. Pharmacol.* **2002**, *452*, 347–355. [CrossRef]
64. Neubauer, H.; Yang, Y.; Seeger, H.; Fehm, T.; Cahill, M.A.; Tong, X.; Ruan, X.; Mueck, A.O. The presence of a membrane-bound progesterone receptor sensitizes the estradiol-induced effect on the proliferation of human breast cancer cells. *Menopause* **2011**, *18*, 845–850. [CrossRef] [PubMed]
65. Cahill, M.A. The evolutionary appearance of signaling motifs in PGRMC1. *Biosci. Trends* **2017**, *11*, 179–192. [CrossRef] [PubMed]
66. Hehenberger, E.; Eitel, M.; Fortunato, S.A.V.; Miller, D.J.; Keeling, P.J.; Cahill, M.A. Early eukaryotic origins and metazoan elaboration of MAPR family proteins. *Mol. Phylogenetics Evol.* **2020**, *148*, 106814. [CrossRef]
67. Yang, R.; Yuan, B.C.; Ma, Y.S.; Zhou, S.; Liu, Y. The anti-inflammatory activity of licorice, a widely used Chinese herb. *Pharm. Biol.* **2017**, *55*, 5–18. [CrossRef] [PubMed]
68. Kabe, Y.; Koike, I.; Yamamoto, T.; Hirai, M.; Kanai, A.; Furuhata, R.; Tsugawa, H.; Harada, E.; Sugase, K.; Hanadate, K.; et al. Glycyrrhizin Derivatives Suppress Cancer Chemoresistance by Inhibiting Progesterone Receptor Membrane Component 1. *Cancers* **2021**, *13*, 3265. [CrossRef] [PubMed]
69. Tyanova, S.; Temu, T.; Cox, J. The MaxQuant computational platform for mass spectrometry-based shotgun proteomics. *Nat. Protoc.* **2016**, *11*, 2301–2319. [CrossRef] [PubMed]
70. Tusher, V.G.; Tibshirani, R.; Chu, G. Significance analysis of microarrays applied to the ionizing radiation response. *Proc. Natl. Acad. Sci. USA* **2001**, *98*, 5116–5121. [CrossRef] [PubMed]

8. PGRMC1-PHB Interactions in Endometrium

8.1. Impact of PGRMC1 on Female Fertility

PGRMC1 is involved in steroid metabolism, as demonstrated by several groups and by us in the first manuscript. PGRMC1 overexpression is associated with increased activity of CYP51A1 and with increased production of cholesterol and estradiol in hormone receptor positive MCF7 cells [99]. Taken together, it may be hypothesized that PGRMC1 impacts steroid metabolism and signaling in additional settings besides breast cancer.

Indeed, PGRMC1 has been widely associated with female fertility, a factor strongly regulated by steroid hormones. Male and female reproductive tracts are one of the main sites of PGRMC1 expression [28]. In the human endometrium, PGRMC1 is differentially expressed during menstrual cycle [125], while de-regulated PGRMC1 expression is associated with several infertility-related diseases [126], [127].

McCallum *et al.* generated PGRMC1-KO mice using the Cre-Lox system, lacking PGRMC1 selectively in the uterus or in the ovaries. Both PGRMC1-KO-mice demonstrated impaired fertility, producing fewer pups per litter or fewer litters, respectively, and an aberrant endometrial histopathology [15]. Similarly, in zebrafish, PGRMC1-KO resulted in reduced fertility manifested in a lower number of offspring, and a reduced steroidogenesis [128]. The effect on fertility was connected to impaired hormone signaling, strengthened by *in vitro* experiments on zebrafish oocytes [128].

8.2. Decidualization and Fertility

During female menstruation cycle, the human endometrium undergoes substantial structural changes, mainly regulated by the female ovarian hormones estradiol and progesterone. The endometrial cycle comprises of two major phases: endometrium is built up in the proliferative phase after menstruation in control of the hormone E2, followed by differentiation and morphological change of the newly built endometrial stomal cells in the secretory phase, mediated by increased levels of P4, preparing the endometrium for embryo implantation. The process of dramatic morphological and functional changes of the endometrial stromal cells during the secretory phase is termed decidualization (Figure 11). This process is a key prerequisite of a receptive endometrium and is therefore tightly connected with fertility. Deregulation of decidualization leads to implantation failure, even after in-vitro fertilization [129].

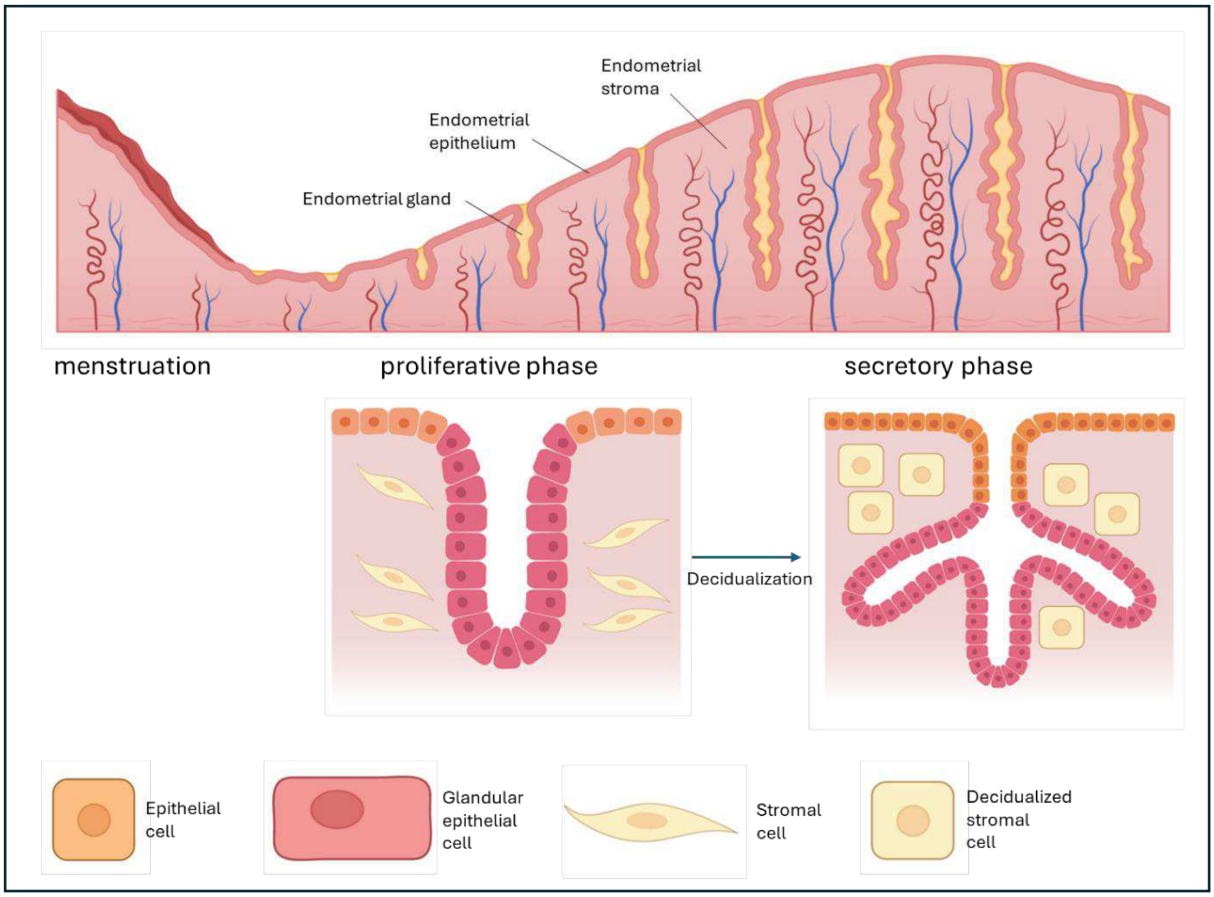

Figure 11: Schematic representation of the human endometrium during different menstrual phases. Endometrial tissue is built up during the proliferative phase, followed by decidualization of endometrial stromal cells in the secretory phase. The stromal cells (yellow, left) undergo morphological and functional changes during decidualization and differentiate into decidualized cells (right). Based on [129]. Created with BioRender.

The onset of stromal cell decidualization is marked by an increase of progesterone production and intracellular cAMP. Decidualization of stromal cells can be stimulated *in vitro*, by addition of cAMP and P4 or a progestin to cultured human endometrial stromal cells (ESC). The essential receptor for progesterone during decidualization is the nuclear PR, and ablation of PR in mice results in abrogated decidualization. However, PGRMC1 has been additionally investigated in this context. Salsano *et al.* performed co-immunoprecipitation of PGRMC1 in decidualized and non-decidualized ESC and suggested involvement of PGRMC1 in morphologic remodeling of ESC [130]. Later, the same group used AG-205 as a PGRMC1 inhibitor on ESC during decidualization and observed changes in transcriptome compared to control cells [131]. The authors assumed that PGRMC1 impacts metabolism and vesicular transport during morphological changes in ESC. However, the molecular mechanism by which PGRMC1 is involved in decidualization remains unsolved.

Since decidualization is a major factor in female fertility, a possible impact of PGRMC1 on this process is intriguing. Maximal knowledge should be collected about biological mechanisms of

endometrial restructure to develop future treatment options for infertility-related diseases. In the following manuscript, we used an *in vitro* ESC decidualization model and studied the impact of PGRMC1 expression level on morphological and biochemical changes during the process. Further, we detected interactions between PGRMC1 and PHBs, that we previously observed in breast cancer cells, additionally in ESC cells, demonstrating the broad context of these interactions.

8.3. Manuscript III (Aim 4)

"Progesterone-induced progesterone receptor membrane component 1 rise-to-decline changes are essential for decidualization"

Hailun Liu, André Franken, Alexandra P. Bielfeld, Tanja Fehm, Dieter Niederacher, Zhongping Cheng, Hans Neubauer[*+] and **Nadia Stamm**[*+]

[*]: These authors contributed equally to this manuscript.

[+]: Corresponding authors.

Original research article in *Reproductive Biology and Endocrinology*

Impact factor: 4.2 (2023)

Authorship: Shared senior author, corresponding author

Status: published in February 2024

DOI: 10.1186/s12958-024-01188-9

Full citation: Liu, H., Franken, A., Bielfeld, A.P. *et al.* Progesterone-induced progesterone receptor membrane component 1 rise-to-decline changes are essential for decidualization. *Reprod Biol Endocrinol* **22**, 20 (2024). https://doi.org/10.1186/s12958-024-01188-9

Author contribution:

I planned experiments and discussed and analyzed data, did literature research and conceptual design of the manuscript together with Hailun Liu. I revised the original draft and adapted the reviewed manuscript, uploaded and managed publication and communication with the editors/reviewers.

8.4. Summary

This study by Liu *et al.* explores the role of PGRMC1 in the process of decidualization, which is essential for embryo implantation and placenta formation. Decidualization is driven by rising levels of progesterone following ovulation and is necessary for the transformation of endometrial stromal cells and preparation of a receptive endometrium.

To investigate the role of PGRMC1, RNA-sequencing datasets were analyzed to track PGRMC1 expression throughout the menstrual cycle. Further, an *in vitro* decidualization model was utilized to study PGRMC1's impact on the process. We detected a rise-to-decline PGRMC1 expression pattern during decidualization, which was crucial for the process, since knocking down PGRMC1 before induction resulted in decidualization failure. However, when PGRMC1 was knocked down after the induction phase, decidualization proceeded unaffected, indicating that the initial increase in PGRMC1 is essential for initiating decidualization but not for maintaining it.

Importantly, PGRMC1 interacted with PHB1 and PHB2 during decidualization. These interactions appear to play a role in regulating the process, as knocking down either of the PHBs resulted in delayed decidualization. This suggests that PGRMC1 works in concert with PHBs to ensure proper endometrial transformation.

These findings highlight the importance of the dynamic regulation of PGRMC1 during decidualization. Disruptions in the rise-to-decline pattern of PGRMC1 expression could impair decidualization and potentially contribute to infertility. By shedding light on the mechanisms governing decidualization, this study provides new perspectives on fertility and potential targets for treating infertility-related conditions.

Liu *et al.*
Reproductive Biology and Endocrinology (2024) 22:20
https://doi.org/10.1186/s12958-024-01188-9

Reproductive Biology and Endocrinology

RESEARCH Open Access

Progesterone-induced progesterone receptor membrane component 1 rise-to-decline changes are essential for decidualization

Hailun Liu[1], André Franken[1], Alexandra P. Bielfeld[2], Tanja Fehm[1], Dieter Niederacher[1], Zhongping Cheng[3,4], Hans Neubauer[1*†] and Nadia Stamm[1*†]

Abstract

Background Decidualization of endometrial cells is the prerequisite for embryo implantation and subsequent placenta formation and is induced by rising progesterone levels following ovulation. One of the hormone receptors contributing to endometrial homeostasis is Progesterone Receptor Membrane Component 1 (PGRMC1), a non-classical membrane-bound progesterone receptor with yet unclear function. In this study, we aimed to investigate how PGRMC1 contributes to human decidualization.

Methods We first analyzed PGRMC1 expression profile during a regular menstrual cycle in RNA-sequencing datasets. To further explore the function of PGRMC1 in human decidualization, we implemented an inducible decidualization system, which is achieved by culturing two human endometrial stromal cell lines in decidualization-inducing medium containing medroxyprogesterone acetate and 8-Br-cAMP. In our system, we measured PGRMC1 expression during hormone induction as well as decidualization status upon PGRMC1 knockdown at different time points. We further conferred proximity ligation assay to identify PGRMC1 interaction partners.

Results In a regular menstrual cycle, PGRMC1 mRNA expression is gradually decreased from the proliferative phase to the secretory phase. In in vitro experiments, we observed that PGRMC1 expression follows a rise-to-decline pattern, in which its expression level initially increased during the first 6 days after induction (PGRMC1 increasing phase) and decreased in the following days (PGRMC1 decreasing phase). Knockdown of PGRMC1 expression before the induction led to a failed decidualization, while its knockdown after induction did not inhibit decidualization, suggesting that the progestin-induced 'PGRMC1 increasing phase' is essential for normal decidualization. Furthermore, we found that the interactions of prohibitin 1 and prohibitin 2 with PGRMC1 were induced upon progestin treatment. Knocking down each of the prohibitins slowed down the decidualization process compared to the control, suggesting that PGRMC1 cooperates with prohibitins to regulate decidualization.

Conclusions According to our findings, PGRMC1 expression followed a progestin-induced rise-to-decline expression pattern during human endometrial decidualization process; and the correct execution of this expression program

†Hans Neubauer and Nadia Stamm contributed equally to this work.

*Correspondence:
Hans Neubauer
Hans.Neubauer@med.uni-duesseldorf.de
Nadia Stamm
Nadia.Stamm@med.uni-duesseldorf.de
Full list of author information is available at the end of the article

was crucial for successful decidualization. Thereby, the results of our in vitro model explained how PGRMC1 dysregulation during decidualization may present a new perspective on infertility-related diseases.

Keywords Decidualization, Progesterone receptor membrane component 1 (PGRMC1), Endometrium, Telomerase-immortalized human endometrial stromal cells (T-HESCs), Infertility, Prohibitin-1 (PHB1), Prohibitin-2 (PHB2), AG205, Rise-to-decline pattern

Background

Human endometrium tissue is highly dynamic going through proliferative, secretory, and menses phases during a regular menstrual cycle [1–3]. Correspondingly, its functional layer exhibits steroid hormone-dependent proliferation, progesterone-stimulated differentiation, and shedding in the absence of the trophoblast [3]. After the postovulatory phase, the rising circulating levels of progesterone drive human endometrial stromal cells (HESCs) to differentiate into decidual cells, which is referred to as the decidualization process [2–5]. Decidualization is the morphological transformation of HESCs from a proliferating fibroblastic phenotype to an enlarged and rounded epithelial shape, accompanied by secretion of prolactin (PRL) and insulin-like growth factor binding protein-1 (IGFBP-1), which is required for female fertility [2, 3, 5]. In the presence of a trophoblast, the decidualized endometrium will be maintained through the increased level of progesterone. Otherwise, it will be shed away with a rapid drop of the progesterone level [3]. A successful decidualization process is an essential prerequisite for embryo implantation and subsequent placenta formation.

During decidualization, progesterone (P4) classically affects the endometrium through activation of two major well-characterized progesterone receptor PR-A and PR-B [5]. Progesterone receptor membrane component 1 (PGRMC1), one of the non-classical progesterone receptors, also rapidly respond to progesterone during decidualization; however, its function in this process is still being elucidated. In the human endometrium, PGRMC1 is abundantly expressed during the proliferative phase of the menstrual cycle in both endometrial and stromal cells. Whereas, in the secretory phase its expression levels dramatically decreased [6]. Overexpression of PGRMC1 in primary HESCs abrogated decidualization [7] and reduced PGRMC1 expression observed in multiple gynecological and obstetrics diseases [8–10]. Therefore, PGRMC1 was proposed as a fertility stabilizer to decidualization, whose expression must be finely tuned during the entire decidualization to support female fertility [11]. How this is achieved remains an enigma.

The prohibitin proteins (PHBs), prohibitin-1 (PHB1) and prohibitin-2 (PHB2), are ubiquitously expressed and highly conserved in eukaryotic cells [12]. PHBs has been reported to act as transcriptional corepressors for ERα in vitro and in vivo [13–15]. Loss of PHBs led to dysfunctional mitochondria, further resulting in male infertility and ovarian aging in females [16, 17]. Besides, PHB1 is downregulated in the eutopic and ectopic endometrium of patients with endometriosis compared to women without endometriosis [18]. An uterus-selective, conditional PHB2 knockout mouse model showed a subfertility phenotype with litters reduced both in number and size [19]. This implies that appropriate protein levels of PHB1/2 as well as of PGRMC1 are required for optimal uterine function and fertility. In breast cancer cells, progestin-activated PGRMC1 associated with PHBs to stimulate cellular proliferation [20]. Binding of activated PGRMC1 to PHBs was accompanied by decreased PHBs-ERα-interaction, resulting in elevated expression of ER-dependent genes. Whether the progestin-depended interaction between PHBs and PGRMC1 also occurs during decidualization has never been characterized before. Therefore, the role of their interaction with regards to female fertility remains to be elucidated.

In this study, we aimed to explore the functional role of PGRMC1 and PHBs, and their interplay for successful decidualization.

Materials and Methods

Data sources

We collected the associated gene expression profiles in publicly available Gene Expression Omnibus (GEO) database (https://www.ncbi.nlm.nih.gov/geo/). Samples from different menstruation phases (proliferative/PE, early secretory/ESE, mid-secretory/MSE, late secretory/LES) were chosen from GSE4888 and GSE56364 to detect expression of PGRMC1 [21, 22]. All raw data were background-subtracted and normalized.

Cell culture

The hTERT-immortalized human endometrial stromal cells (T-HESCs) were purchased from abm (T0533). Both the cell lines T-HESCs and St-T1 were maintained in phenol-red free Dulbecco's Modified Eagle Medium// Ham's F12 (DMEM/F12; Gibco, Thermo Fisher Scientific, 11039021) medium supplemented with 10% (*v/v*) charcoal-stripped fetal bovine serum (Thermo Fisher Scientific, 12676029), 100 units/mL penicillin–streptomycin

(Thermo Fisher Scientific, 2321118), 50 µg/ml gentamycin sulfate (Biowest, L0012), 200 µM sodium pyruvate (Biowest, L0624) and 1.5 g/L sodium bicarbonate (Biowest, L0680) (hereafter referred to as complete medium) in a humidified incubator at 37 °C in the presence of 5% CO_2. Cells (passage number < 10) were regularly tested negative for mycoplasma.

Chemical compounds

AG205 (Sigma-Aldrich) was diluted in 2% charcoal-stripped FBS complete medium to 15 mM. Medroxyprogesterone acetate (MPA) and 8-Br-cAMP MPA (cAMP) were prepared from a 10 mM and 5 mM stock solution, respectively.

MTT Assay

We measured activated cellular metabolism as a surrogate for proliferation by performing the MTT assay. Briefly, T-HESCs cells (5 X 10^3 cells per well) were seeded in triplicates in 96-well plate in complete medium and grown for 24 h. After the attachment, cells were either treated with or without induction cocktail in decidualization medium. On the day of assay, cells were incubated with 0.25 mg/ml MTT (Sigma-Aldrich) in decidualization medium for 3 h at 37 oC. Following 1 h of incubation with DMSO at 37 oC and 300 rpm in a microplate shaker, absorption was measured at 540 nm using TECAN Spark® spectrophotometer.

Immunofluorescence staining

Cells were seeded and cultured in chamber slides (Nunc Lab-Tek, Thermo Fisher Scientific C7182-1PAK) fixed with 4% formaldehyde (Sigma-Aldrich, 20649296018) for 10 min at room temperature (RT), washed with washing buffer (Dako, Glostrup, Denmark, S3006) (3×5 min each). Then, cells were permeabilized with 0.1% Triton X-100 (Sigma-Aldrich, T8787) in PBS for 10 min at RT and washed with washing buffer again (3×5 min each). DAKO protein block buffer (Dako, X0909) was added and incubated for 1 h at RT before incubating with primary antibodies specific for PGRMC1 (Abcam, ab48012), PHB1 (Abcam, ab75766), PHB2 (Cell signaling, 14084S) and Vimentin (Abcam, ab02547) overnight at 4 °C. The next day, cells were washed with washing buffer (3×5 min each) and incubated with secondary antibodies (Donkey-anti-goat, Alexa 488: Invitrogen, A11055; Donkey-anti-rabbit, Alexa 488: Invitrogen, A31573) for 1 h at RT in a humidified chamber in the dark. Nucleic acid was stained with DAPI (Thermo Fisher Scientific, 15733122) simultaneously with co-incubated secondary antibodies. After the final wash, the cells were mounted with Fluorescent Mounting Medium (Dako, S3023). Negative controls were prepared for each sample following the same staining procedure with isotype controls instead of primary antibodies. Fluorescence signals were detected with an Axioplan 2 Imaging fluorescence microscope (Carl Zeiss Microscopy GmbH, Jena, Germany).

Proximity ligation assay

The *in-situ* proximity ligation assay (PLA) procedure was performed with the Duolink® PLA Kit (Sigma-Aldrich, DUO92008) and following the manufacturers protocol. The cells were incubated with the primary antibodies i.e., anti-PGRMC1 (Abcam, ab48012) with PHB1 (Abcam, ab75766) and PHB2 (Cell signaling, 14085S) overnight at 4 °C. The slides were washed twice for 5 min with buffer A, followed by incubation with the PLA probes (anti-goat PLUS and anti-rabbit MINUS) in antibody diluent for 60 min at 37 °C. After washing twice for 5 min with buffer A, ligation was performed using ligase diluted in ligation buffer for 30 min at 37 °C. Then the cells were washed with buffer A before incubation for 100 min with amplification stock solution at 37 °C. After washing twice for 10 min with buffer B, nuclear DNA was labeled with DAPI for 10 min and slides were mounted with mounting medium. Negative PLA control was performed using respective isotype control antibodies (isotype goat, Abcam, ab37373; isotype rabbit, Abcam, ab37415). Red fluorescence dots inside the cellular areas representing a single protein–protein interaction were quantified using image J software.

Western blotting

Cell suspensions were washed twice with ice cold PBS (Thermo Fisher Scientific, 2176323) and lysed in RIPA lysis buffer (50 mM TRIS (Sigma-Aldrich, 74,385), 150 mM NaCl (VWR corporation, 16C030032), 1% NP-40 (Sigma-Aldrich, 74,385), 0.5% Sodium deoxycholate (Sigma-Aldrich, D6750), 0.1% SDS (Sigma-Aldrich, S34121136), containing protease inhibitor (Roche, 49,422,800) and phosphatase inhibitor (Roche, 49121300). Protein concentration was determined using Pierce™ BCA Protein Assay Kit (Thermo Fisher Scientific, 23225). An amount of 20 µg of total protein was supplemented with 4×Laemmli buffer (Bio-Rad, Feldkirchen, Germany, 1610747) containing 2-Mercaptoethanol (Sigma-Aldrich, M6250) and loaded onto Mini-PROTEAN® Precast Gels (Bio-Rad, 4568123) and separated via SDS-PAGE in SDS buffer (25 mM TRIS, 192 mM glycine (Sigma-Aldrich, 50046), 0.1% SDS, pH 8.3) at 100-150 V. Protein was transferred to Immun-Blot® PVDF Membranes (Bio-Rad,1620177) overnight at 4 °C and 10 mA in blotting buffer (20 mM TRIS, 200 mM glycine, 20% (v/v) methanol). Unspecific binding was blocked by incubation of the PVDF membrane with 5% skim milk powder (Sigma-Aldrich, 70166) in TRIS-buffer

(20 mM TRIS, 150 mM NaCl, pH 7.6) containing 0.1% Tween 20 (TBS-T) for 1 h at RT. Primary antibodies including PGRMC1 (Cell signaling, Danvers, MA, USA, D6M5M), PHB1 (Cell signaling, 2426S), PHB2 (Cell signaling, 14085S) and ß-actin (Santa Cruz Biotechnology, sc-4778) were added in 5% skim milk—TBS-T and incubated overnight at 4 oC. Secondary antibodies were applied in 5% skim milk—TBS-T at RT for 1 h. Proteins were detected using Amersham™ ECL™ Western Blotting Detection Reagent (Cytiva, 17190731).

Subcellular protein fractionation

A subcellular protein fractionation kit (Thermo Fisher Scientific) was used to fractionate proteins into cytoplasmic, membrane, and nuclear fractions. Cells were harvested as pellets. The pellet was lysed with cytoplasmic extraction buffer, membrane extraction buffer, and nuclear extraction buffer. Primary antibodies specific for β-actin (Santa Cruz Biotechnology), Calreticulin (Santa Cruz Biotechnology), and Histon H3 (Cell signaling) were used to indicate the purity of the cytoplasmic, membrane, and nuclear fractions, respectively.

Co-immunoprecipitation

Co-immunoprecipitation was performed using the Pierce Co-IP kit (Thermo Fisher Scientific). Briefly, the anti-PGRMC1 antibody (Cell signaling) was first immobilized for 2 h using AminoLink Plus coupling resin. In parallel, cell pellets were resuspended in ice-cold IP Lysis buffer. An amount of 500 µg protein was incubated with resin at 4 °C overnight. After incubation, the resin was washed, and protein complexes bound to the antibody were eluted using elution buffer. Subsequent western blot analyses were performed as described before.

Gene silencing (siRNA Transfection)

To knock down PGRMC1 expression in T-HESCs, FlexiTube GeneSolution (Qiagen) was used, containing four siRNA(s) that specifically target human PGRMC1 mRNAs. Cells were transfected with the final concentration of 10 nM *PGRMC1* siRNA(s) or negative control siRNA (siCTL) (Thermo Fisher Scientific) using Lipofectamine RNAiMAX Transfection Reagent (Thermo Fisher Scientific) according to recommended procedures. Afterwards, cells were treated with decidualization medium containing either induction cocktail or DMSO, and harvested at different time points for downstream experiments. For PHB1 and PHB2 mRNA expression inhibition (siPHB1, siPHB2: Qiagen), the same siRNAs concentration was used.

Quantitative reverse-transcription PCR (qRT-PCR)

RNA was isolated using the RNeasy Mini Kit (Qiagen) according to the manufacturer's specifications. Reverse transcription of RNA into cDNA was performed with the Omniscript RT kit (Qiagen) according to the manufacturer's instructions. Quantitative PCR was performed using QuantiFast SYBR Green PCR Kit (Qiagen) and LightCycler ®480 System (Roche). Primers for *PGRMC1* (Qiagen), *PRL* (Qiagen) and *HPRT1* (Qrigene, Rockville, MD, USA). The delta-delta cycle threshold method was used to normalized expression to the reference gene HPRT1 [23, 24].

Statistical analysis

A two-tailed paired Student's *t*-test was used to analyze experiments comparing two experimental groups or two-way ANOVA for multiple comparisons of more than two groups. A value of $p < 0.05$ was considered significant. All statistical analyses were performed with GraphPad Prism 9.0. Results were reported as means with standard deviation.

Results

PGRMC1 expression profile during regular menstrual cycle

To understand the dynamics of PGRMC1's expression changes during normal decidualization, we initially investigated its expressional profile by mining publicly available RNA-sequencing data sets from endometrial biopsies (GEO accession numbers: GSE6364 and GSE4888). In a regular menstrual period, PGRMC1 mRNA level gradually decreased from the proliferative phase to the secretory (including early-, mid-, and late-) phase, manifesting the highest level in the proliferation phase and the lowest level in the late-secretory phase (Fig. 1A-B), consistent with previously reported data [9, 25]. This indicates that PGRMC1 may have an important role in regulating cellular proliferation and may not be required for decidualization in the secretory phase as it is consecutively decreased at mRNA level after progesterone stimulation. We hypothesized that the dynamic changes of PGRMC1 have an important role during the menstrual cycle that must be finely tuned.

Rise-to-decline trend of PGRMC1 expression during in vitro decidualization

To investigate our hypothesis, we established a hormone-inducible in vitro decidualization model in T-HESCs based on visualizing its morphological changes and by measuring the expression level of the decidual marker prolactin (PRL) (Fig. 2A). After being exposed to the decidualization induction cocktail consisting of the P4 analog MPA plus cAMP for 10 days, morphological

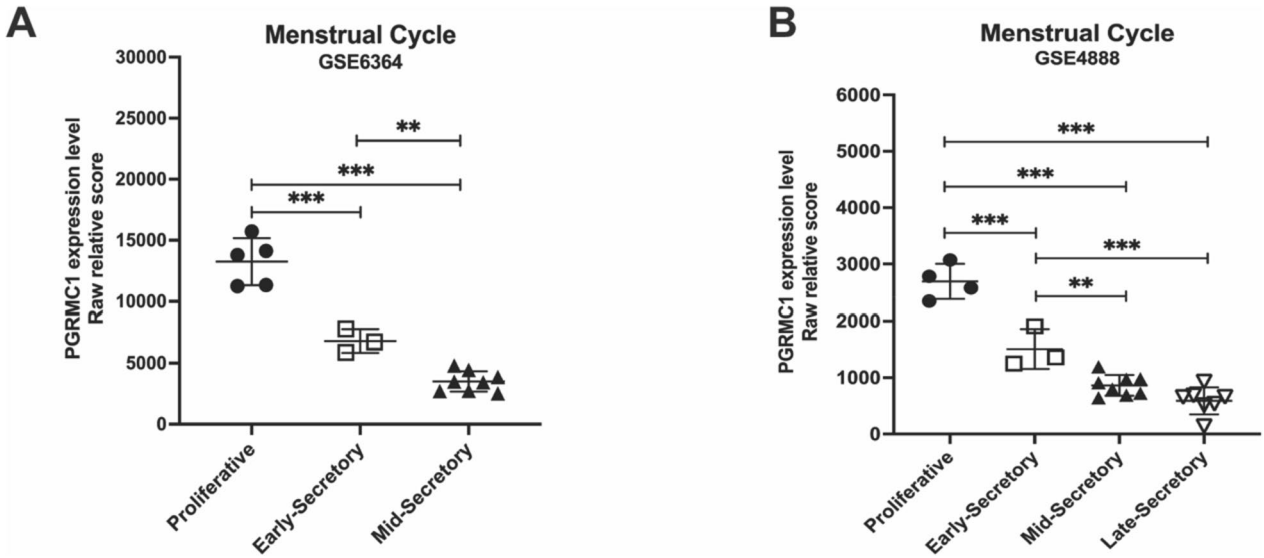

Fig. 1 PGRMC1 expression profile during menstrual cycle. Relative transcript scores of PGRMC1 expression in different stages of a regular menstrual cycle (GSE6364) **(A)** and (GSE4888) **(B)**. Relative transcript scores of PGRMC1 expression level are shown as mean ± SEM. Statistical analysis was performed by two-way ANOVA. *$p < 0.05$, **$p < 0.01$, ***$p < 0.001$, ****$p < 0.0001$

changes of T-HESCs were inspected by microscopy in bright-field and by immunofluorescent analysis of the cytoskeletal marker vimentin. With this protocol, T-HESCs underwent a transformation from a fibroblast-like shape to a polygonal epithelial-like shape (Fig. 2B-C) accompanied with a significant increase of PRL mRNA expression compared to non-induced controls (Fig. 2D). Both the morphological changes and enhanced expression of PRL indicate a successfully established the hormone-induced decidualization model, allowing to investigate the role of PGRMC1 in decidualization.

We aimed to determine and modulate the expression level of PGRMC1 in our system to study its impact on the decidualization process. First, we determined the protein expression profile of PGRMC1 during the in vitro decidualization program. Intriguingly, we found that PGRMC1 expression gradually increased from the day the induction cocktail had been added (D0), peaking at day 6 (D6) post-induction, followed by a constant decrease until day 14 (D14) (Fig. 2E-F). This protein expression change could also be observed in the St-T1 cell line (Supplementary Fig. 1A). In contrast with the observation of gradually decreased mRNA levels of PGRMC1 during the secretory phase of the normal menstrual cycle (Fig. 1A-B), our in vitro decidualization model revealed that the promotion of cells into decidualized state comprises a PGRMC1 increasing phase and a PGRMC1 decreasing phase, both on protein and mRNA level (Fig. 2E-G). This data suggests that PGRMC1 was regulated at transcriptional level during decidualization. We termed this PGRMC1 protein dynamic changes as PGRMC1 'rise-to-decline' changes in decidualization.

It is well known that increasing P4 levels initiate decidualization, although the activity of PGRMC1 in decidualization seems to be independent of P4 [3, 5]. Consistently, the T-HESC cells can go through the decidualization process treated with either P4, MPA, or cAMP (Supplementary Fig. 1B-C). Intriguingly, the PGRMC1 expression changes can be observed at each condition, which led us to the conclusion that the PGRMC1 rise-to-decline changes are a universal mechanism within the decidualization program.

The rise-to-decline changes of PGRMC1 are required for decidualization

To explore the potential role of the PGRMC1 rise-to-decline changes during the decidualization, we firstly downregulated its expression before hormone induction with an optimized concentration of an siRNA-mix specific for PGRMC1 mRNA (Fig. 3A). Importantly, PGRMC1 mRNA levels were remained suppressed throughout 10 days post-siRNA-transfection (Fig. 3B). Likewise, expression of PGRMC1 protein was completely abrogated from day 2 (D2) to day 10 (D10) after siRNA transfection (Supplementary Fig. 2A-B).

T-HESCs with suppressed PGRMC1 expression were further treated with the decidualization induction cocktail. As indicated by the lack of morphological transformation and PRL production over 10 days of hormone treatment period (Fig. 3C, Supplementary Fig. 3), these

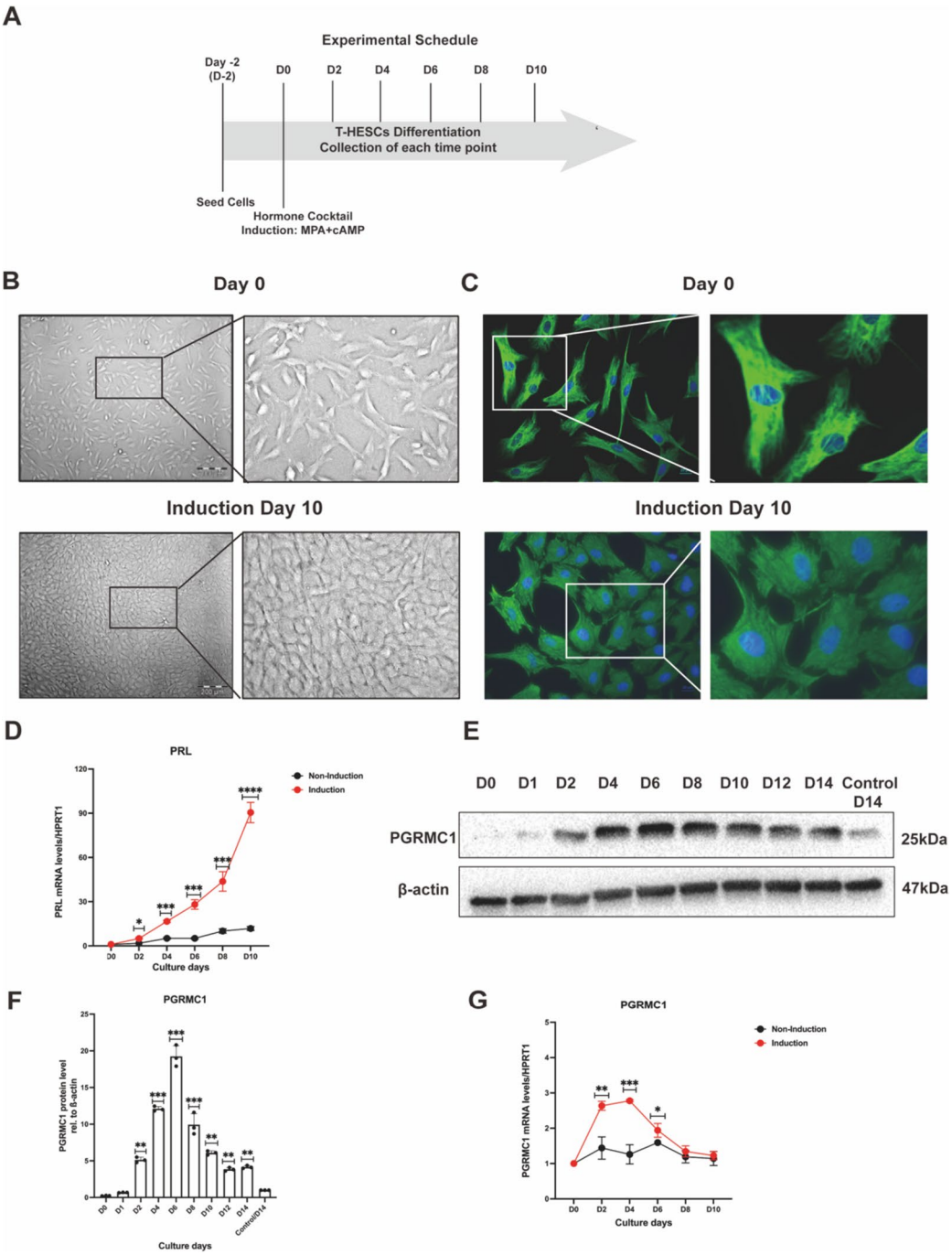

Fig. 2 A rise-to-decline expression pattern of PGRMC1 was revealed by in vitro decidualization. **A** Schematic representation of in vitro decidualization system. The cellular morphology changes of T-HESCs on day 0 and day 10 were imaged with microscopy in bright filed **(B)** or immunofluorescence staining **(C).** PGRMC1 was stained by Alexa Fluor-488 (green), and the nucleus was stained by DAPI in blue. Scale bar: 200 μm. The mRNA expression levels of *PRL* in T-HESCs were analyzed with qRT-PCR when cells were cultured with MPA/cAMP (red line) for decidualization or DMSO (black line) as control **(D)**. The dynamic changes of PGRMC1 protein expression from 1 to 14 days induction and non-induction control (on Day 14) were measured by western blot **(E)** and the bar plot with the relative densitometric analysis of the corresponding PGRMC1 protein level (*p* value calculation based on 'D0') **(F)**. β-actin was used as a loading control. The mRNA expression levels of *PGRMC1* in T-HESCs during decidualization **(G)**. Results are shown as the mean ± SEM from three biological replicates. Statistical analysis was performed by two-way ANOVA. *$p < 0.05$, **$p < 0.01$, ***$p < 0.001$, ****$p < 0.0001$

cells did not undergo decidualization. Thus, in the absence of the progestin-induced PGRMC1 increasing phase decidualization failed.

These results prompted us to investigate if expression of PGRMC1 is needed for decidualization at the time point of induction – as a kind of a program switch – or later. To this aim, we postponed the transfection of PGRMC1 suppressing siRNAs to after the induction of decidualization. First, we treated T-HESC cells for 2 days with the combination of MPA and cAMP to induce decidualization followed siRNA transfection (Fig. 3D) and investigated the cells up to day 10 (D10) after induction. As expected, PGRMC1 mRNA levels started to decrease (Fig. 3E, blue line) after 2 days of transfection of PGRMC1-specific siRNAs and the PGRMC1 mRNA levels stayed below mRNA levels reached during normal induction of decidualization (Fig. 3E, red line). Interestingly, in addition to morphological changes (Supplementary Fig. 4), PRL mRNA expression level first dropped, but between D6 and D8 not only recovered to a comparative level to that of normal induction, was even four days earlier compared to the normal induction, indicating a promoted decidualization (Fig. 3F). We further measured the effects of knocking down PGRMC1 after 4 days of induction with MPA/cAMP on the decidualization program. The results are very similar to the outcome achieved when suppressing PGRMC1 after 2 days of induction (Fig. 3G-H). The results could be additionally reproduced in the St-T1 cell line (Supplementary Fig. 5A-D). Taken together, the PGRMC1 rise-to decline changes are required for a proper decidualization.

PGRMC1-signal increases in the peri-nuclear region during decidualization

It has been reported that PGRMC1 translocates from cytoplasmic membranes to the nucleus during decidualization [7]. Recently, PGRMC1-mediated proteomic changes have been well characterized after decidualization, suggesting that PGRMC1 binds to proteins involved in translation, ATP generation, protein maturation, glucose transport, and lipid metabolism [26]. Almost all these proteins locate in the cytoplasm or on membranes, but not in the nucleus. This raises the question of why proteins interacting with PGRMC1 are barely found to be in the nucleus.

To better understand the question, we initially assessed PGRMC1 protein subcellular localization by immunofluorescence. Without induction of decidualization PGRMC1 was essentially located in the cytoplasm, but more intense signals were observed around the nucleus after 10 days induction (Fig. 4A). To further verify these observations, we fractionated the cells into soluble parts containing cytoplasm, membrane, and nucleus and detected the PGRMC1 protein by western blot. In line with the immunofluorescence results, PGRMC1 was only observed in the membrane fraction but not in the nucleus (Fig. 4B). This indicates an accumulation of PGRMC1 in the peri-nuclear region during hormone-induced decidualization.

Interactions of PHB1/PHB2 to PGRMC1 mediate decidualization

We have recently demonstrated in breast cancer cells, that progestin-activated PGRMC1 interacts with PHB1/PHB2 resulting in enhanced ERα-dependent transcription and cell proliferation [27]. In analogy, here we found that PGRMC1 colocalized with PHB1 and PHB2 in the cytoplasm and at the nucleus periphery after induction, whereas barely colocalization signals could be observed without induction revealed by immunofluorescence (Supplementary Fig. 6A-B). This suggests a potential interaction between PHBs and PGRMC1 introduced by progestin treatment. Then, PLA was performed to further explore the associations between PGRMC1 and PHB1/2. Upon induction, a significantly higher PLA signal suggesting the interaction of PGRMC1 to PHB1/2 could be observed compared to the control (Fig. 5A-B, Supplementary Fig. 7A-B).

To explore the function of PGRMC1-PHBs interaction during decidualization, we downregulated PHBs via siRNA transfection, reaching expression levels decreased by 60–80% compared to the control for individual PHBs

(See figure on next page.)

Fig. 3 The rise-to-decline changes of PGRMC1 are required for decidualization. (**A**): Schematic representation of in vitro decidualization system after PGRMC1 downregulation by siRNA. qRT-PCR analysis of *PGRMC1* mRNA expression changes in T-HESCs transfected with either 10 nM of siRNA against PGRMC1 (siPGRMC1) or 10 nM control siRNA (siCTL) for up to 10 days **(B)**. The *PRL* mRNA expression level in T-HESCs after MPA/cAMP-induced decidualization upon transfection with 10 nM siPGRMC1 or siCTL, analyzed with qRT-PCR **(C)**. The workflow for PGRMC1 downregulation after decidualization induction **(D)**. mRNA expression levels of *PGRMC1* **(E, G)** and *PRL* **(F, H)** in T-HESCs treated with MPA/cAMP for decidualization induction (red line) and non-induction (black line). Blue lines indicate the mRNA levels of *PGRMC1* and *PRL* when transfected with 10 nM siPGRMC1 on the second (**E, F**) and fourth (**G, H**) day after decidualization induction, respectively. The statistical analysis of mRNA levels of *PGRMC1* (and *PRL*) between cells with non-induction and induction indicated by red stars, or cells with PGRMC1 knockdown after induction indicated by blue stars. Results are shown as the mean ± SEM from three independent biological replicates. Statistical analysis was performed by two-way ANOVA. *$p < 0.05$, **$p < 0.01$, ***$p < 0.001$, ****$p < 0.0001$

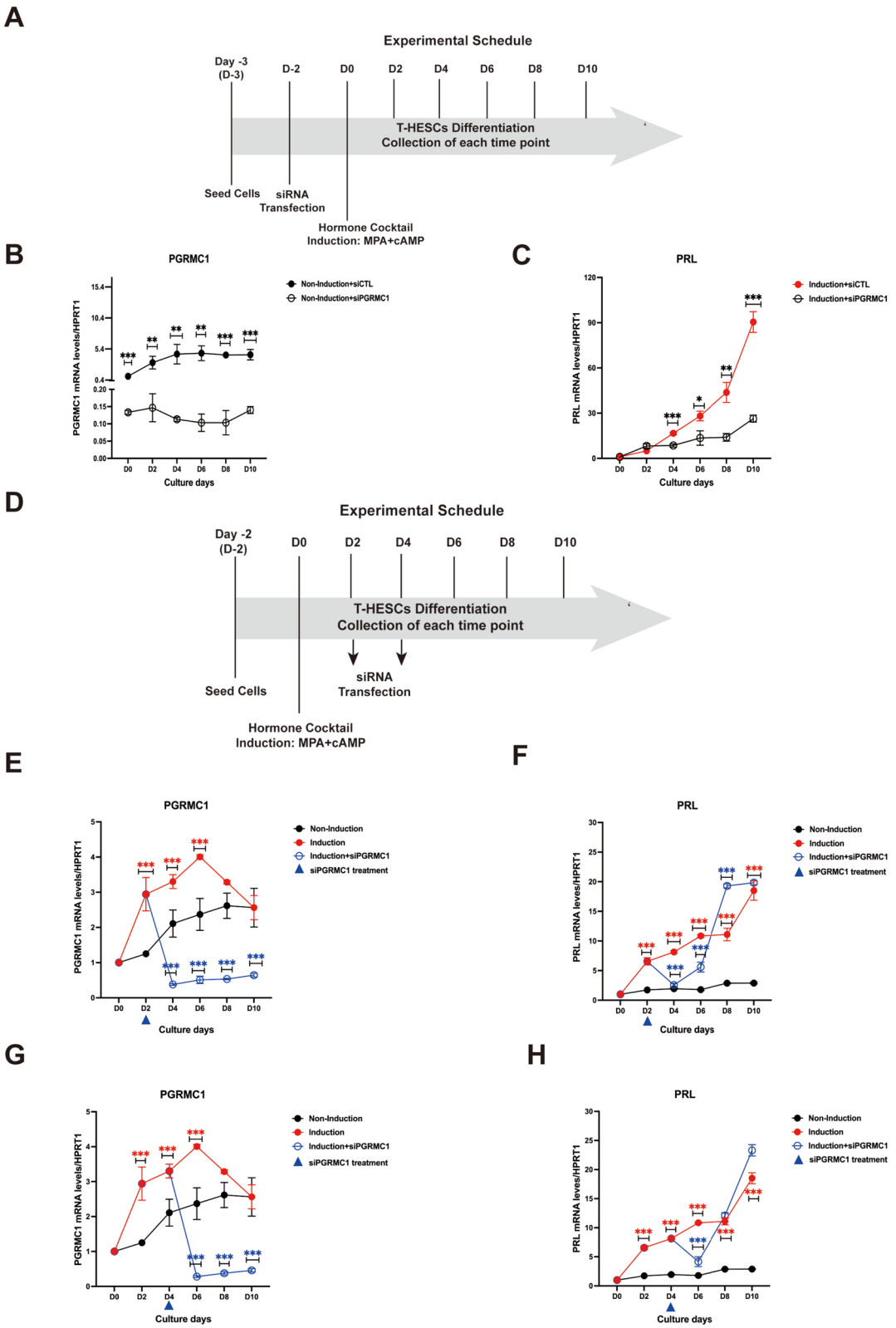

Fig. 3 (See legend on previous page.)

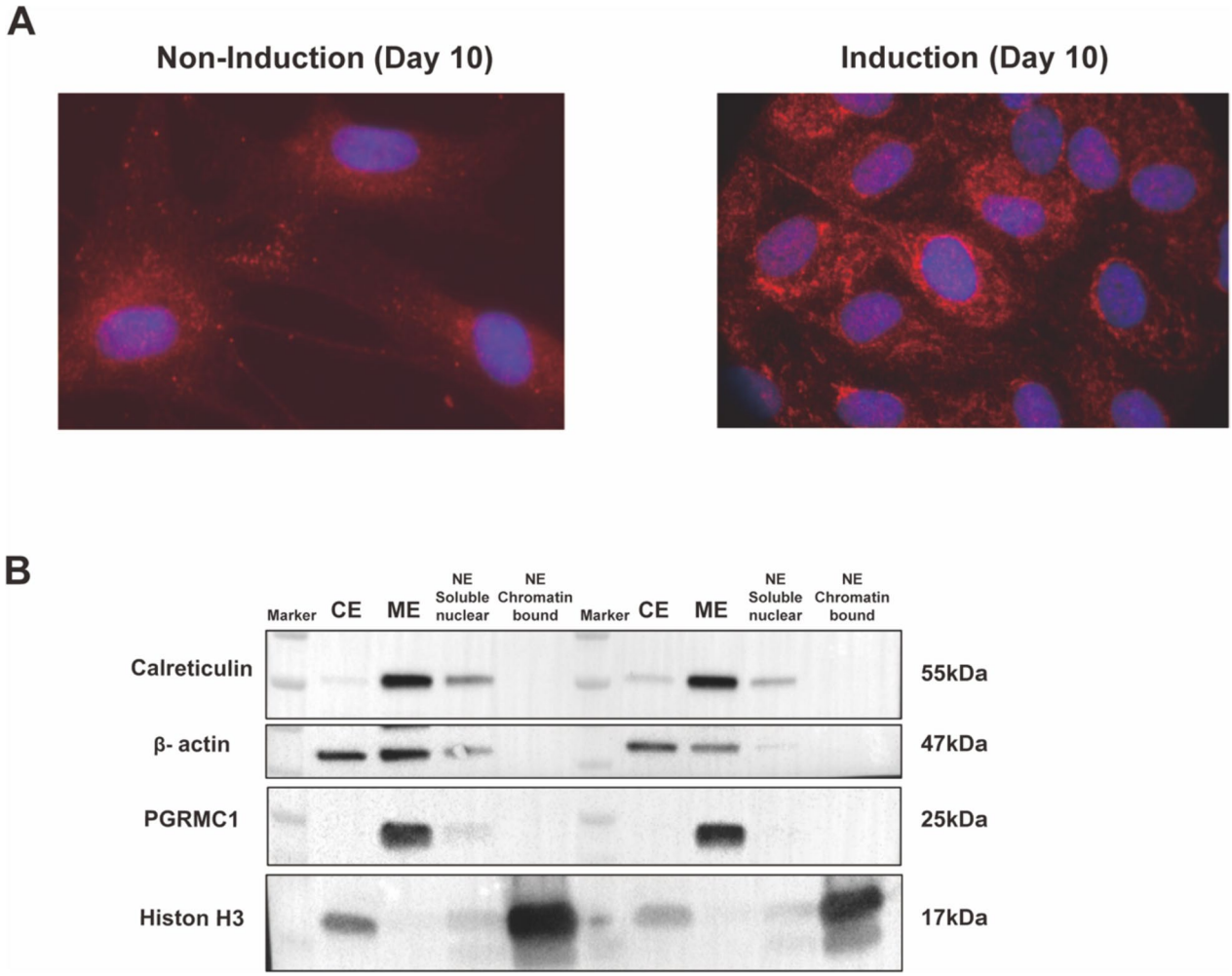

Fig. 4 Prei-nuclear PGRMC1-signal increased during decidualization. (**A**): Immunofluorescence staining of PGRMC1 in T-HESCs treated with DMSO (left) as control or MPA/cAMP (right) for 10 days decidualization induction. PGRMC1 shows in red and the nucleus was stained with DAPI in blue. Scale bar: 200 μm. (**B**) Analysis of PGRMC1 localization by subcellular fractionation in T-HESCs treated with DMSO (left) or MPA/cAMP (right), measured by western blot. PGRMC1 was immunoblotted in equal amounts of cytoplasmic (CE), membrane (ME), and nuclear (NE) biomaterial. Compartment-specific markers: Calreticulin (55 kDa), β-actin (47 kDa), and Histon H3 (17 kDa) were used as loading controls for the membrane, cytoplasmic, and nuclear fractions, respectively

(Fig. 6A-B). Knocking down each of the PHBs before hormone induction partly impaired the decidualization process (Fig. 6C-E), but the cells still could achieve morphological transformation (Supplementary Fig. 9). These effects on decidualization are comparable to the results achieved with suppressed PGRMC1.

AG205 does not affect PGRMC1 rise-to-decline changes and decidualization

AG205 was reported to be a specific inhibitor of PGRMC1 and was broadly used to explore PGRMC1's role in decidualization [28, 29]. Recent data, however, question the specificity of AG205 for PGRMC1 [29–31].

Taking advantage of the critical role of PGRMC1 rise-to-decline changes for decidualization, we tested the effect of AG205 on PGRMC1 and the decidualization process. Since AG205 concentrations used in previous reports were high enough to impair cellular viability [30, 32, 33], we initially determined the appropriate concentration of AG205 that did not affect cell viability. In the MTT assay (Fig. 7A), a concentration below 15 μM had no (or a moderate) effect, whereas a concentration higher than 15 μM had a detrimental effect on cellular viability, which is consistent with previously reported [29]. In addition, decidualization was successfully achieved with T-HESCs treated AG205 with concentrations below 15 μM, as indicated by the increasing

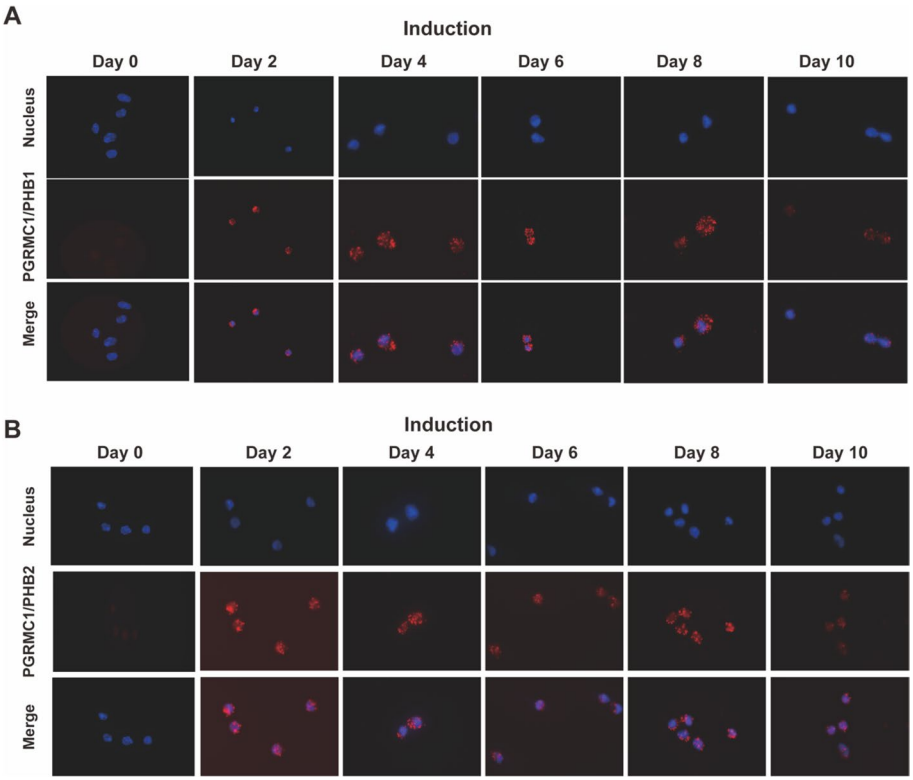

Fig. 5 PGRMC1 interacts with PHBs during decidualization. The interactions between PGRMC1 and PHB1 (**A**) or PHB2 (**B**) in T-HESCs were analyzed with proximity ligation assay upon decidualization induction from day 2 to day 10. 'Day 0' indicates the induction day. Each red spot represents a single interaction. Nuclear stain: DAPI. Magnification 40×

expression of PRL and the change in cell morphology (Fig. 7B-C). Furthermore, AG205 treatment did neither affect PCRMC1 protein level during decidualization, nor its rise-to-decline expression profile (Fig. 7D). Moreover, the interaction of PGRMC1 to PHBs was not disturbed as confirmed by PLA (Fig. 7E-F), which is in line with a previous report [32]. Based on these results, we propose that AG205 (< 15 μM) has no effect on the observed PGRMC1 functions during decidualization.

Discussion

PGRMC1 has been demonstrated to play a role in various reproductive tissues, particularly endometrial stromal cells [27, 34–36]. It influences the decidualization process and female fertility [37]. We revealed that PGRMC1 protein exhibits a rise-to-decline pattern after progestin stimulation, essential for normal decidualization (Supplementary Fig. 10). Additionally, during decidualization, PGRMC1 interacted with PHB1 and PHB2, suggesting their joint contribution to the decidualization program. Despite the unclear mechanisms behind PGRMC1-dependent decidualization failure, PGRMC1 expression profile may serve as a useful fertility indicator.

Previous reports focused on PGRMC1 mRNA profile changes during decidualization, with few investigations into protein level dynamics. We measured both mRNA and protein levels of PGRMC1 after inducing decidualization and observed a rise-to-decline pattern. The observed increase and decrease of PGRMC1 protein expression fits into cyclic changes observed in vivo [25]. The overall dynamic changes of the PGRMC1 protein level during a normal menstrual cycle are composed of two peaks: one occurs in the secretory phase, as revealed in this study and the other one occurs in the proliferative phase as previously reported [9, 25]. It resembles estrogen dynamics during the menstrual cycle, suggesting PGRMC1 expression may be regulated by estrogen concentration or a similar mechanism [1–3]. As PGRMC1 overexpression in breast cancer cells leads to higher E2 secretion, T-HESCs E2 production might depend on PGRMC1 activation. Further research is needed to understand the relationship between estrogen and PGRMC1 expression, including the possibility of estrogen receptor-mediated transcription regulation.

Knocking down PGRMC1 before hormone treatment inhibited decidualization, highlighting its crucial role as a 'switch' at this stage. Appropriate PGRMC1 protein

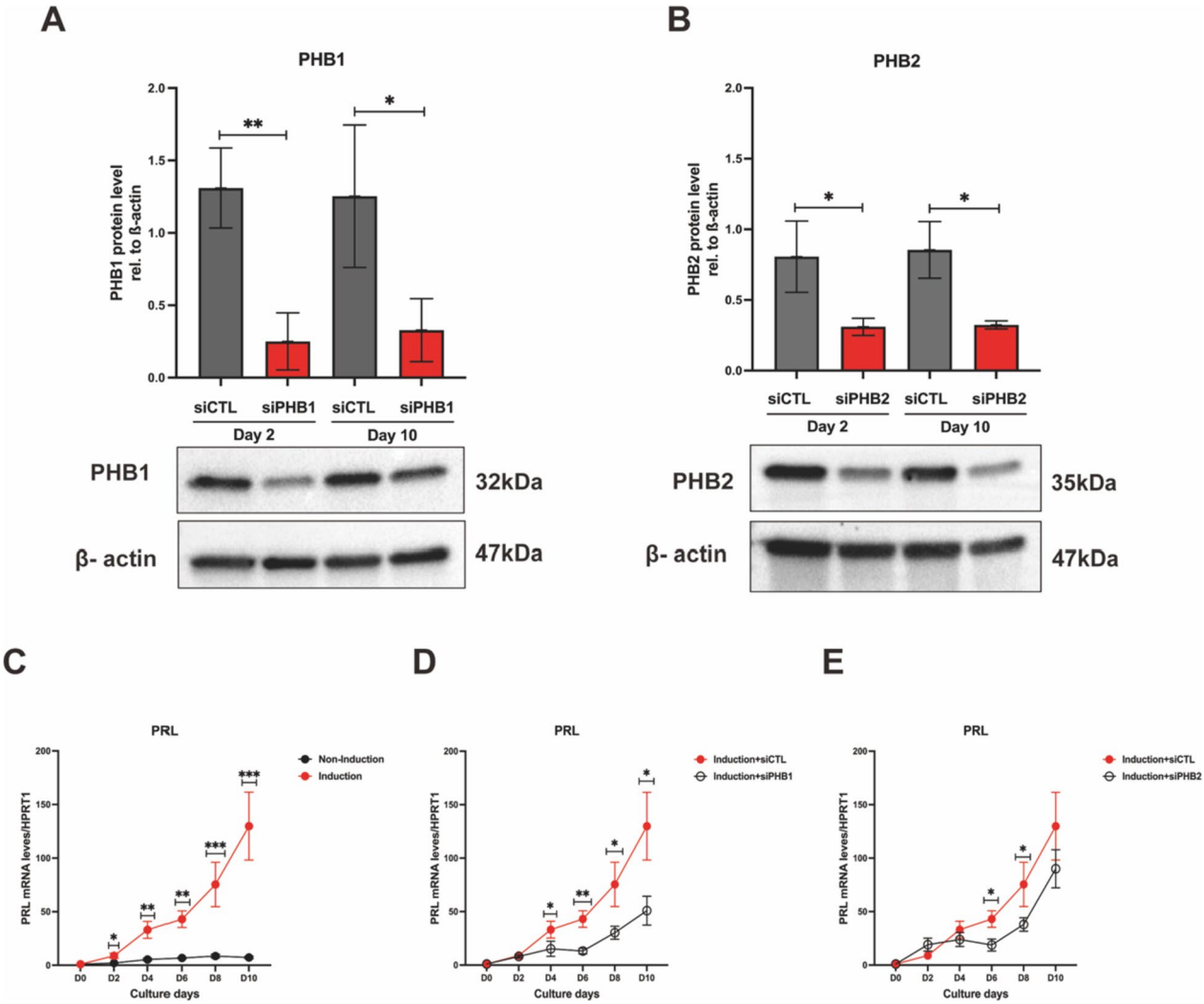

Fig. 6 Downregulation of PHBs partly impairs decidualization. The PHBs protein expression level on day 2 or day 10 after transfection of T-HESCs with 10 nM siPHB1 (**A**), 10 nM siPHB2 (**B**), respectively, was analyzed by western blot. Densitometric analysis was performed with imagej and values were normalized to β-actin. The *PRL* mRNA expression changes in T-HESCs with (red line) and without (black line) induction was determined by qPCR and normalized to *HPRT1* as a reference gene (**C**). The *PRL* mRNA expression changes in T-HESCs transfected with 10 nM siPHB1 (**D**), 10 nM siPHB2 (**E**) upon decidualization induction were determined by qPCR. Results are shown as the mean ± SEM from three biological replicates. Statistical analysis was performed by two-way ANOVA. *$p < 0.05$, **$p < 0.01$, ***$p < 0.001$, ****$p < 0.0001$

(See figure on next page.)

Fig. 7 AG205 does not affect decidualization. The influence of AG205 on T-HESCs viability was performed after the cells were incubated with indicated concentrations of AG025 for 10 days and analyzed with colorimetric assay **(A)**. The absorbance values for cultures with AG205 were compared to the DMSO control (0 μM). The *PRL* mRNA expression levels were analyzed after cells were cultured with (black line) or without (red line) 15 μM AG205 **(B)**. Results are shown as the mean ± SEM from three independent biological replicates. Statistical analysis was performed by two-way ANOVA. *$p < 0.05$, **$p < 0.01$, ***$p < 0.001$, ****$p < 0.0001$. The cellular morphology changes of T-HESCs were imaged with microscopy in the bright field when cells were cultured without (upper panel) or with (down panel) MPA/cAMP upon 15 μM AG205 treatment **(C)**. Scale bar: 200 μm. The PGRMC1 protein expression changes in T-HESCs were analyzed by western blot when cells were treated with DMSO (left panel) or 15 μM AG205 (right panel) upon decidualization induction **(D)**. β-actin was used as a loading control. The interactions between PGRMC1 and PHB1 **(E)** or PHB2 **(F)** in T-HESCs were analyzed by proximity ligation assay when cells were cultured with 15 μM AG205 upon decidualization induction. Each red spot represents a single interaction. Nuclear stain: DAPI. Magnification 40×

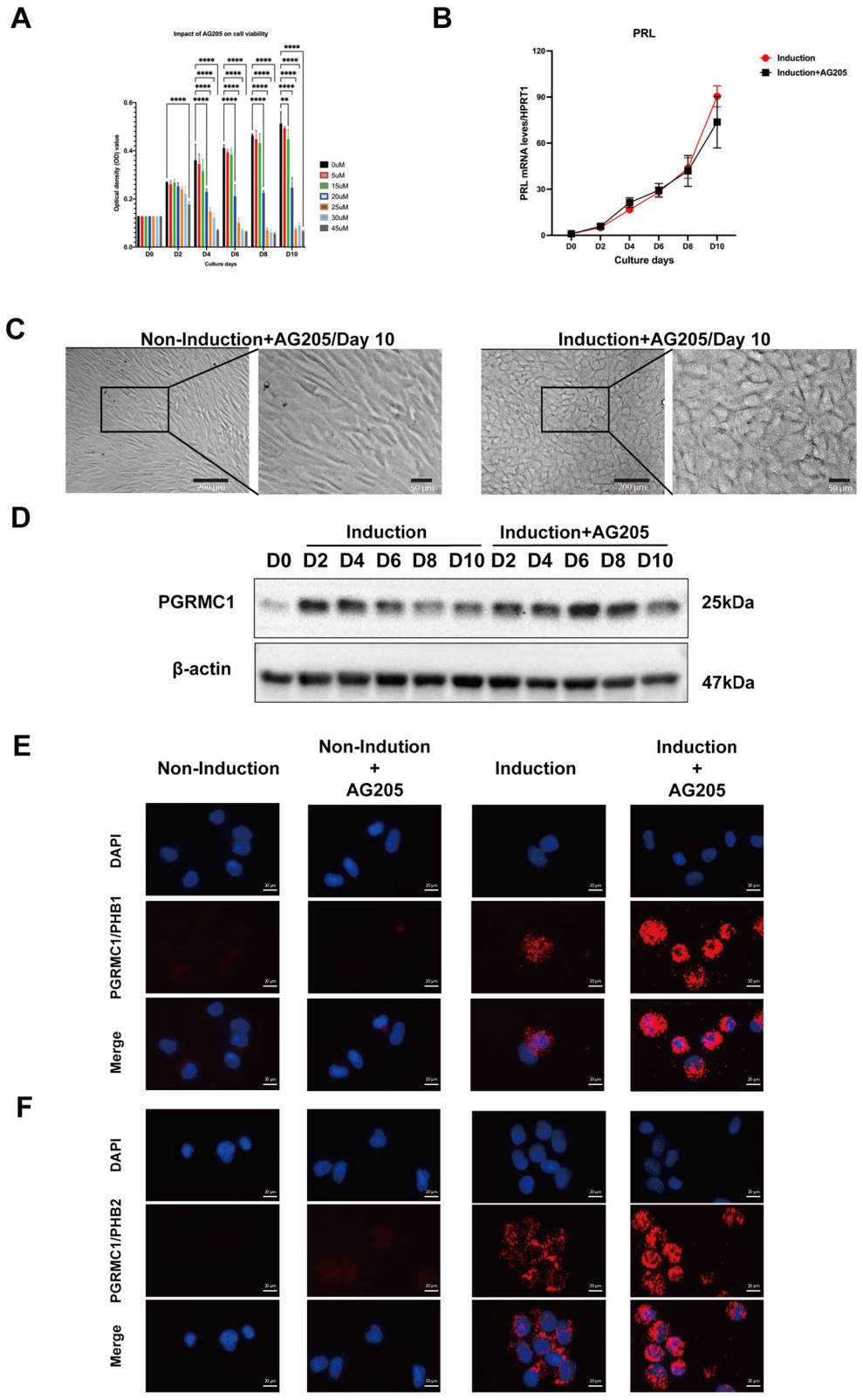

Fig. 7 (See legend on previous page.)

levels are needed to initiate decidualization upon P4/cAMP stimulation. The PGRMC1 rise-to-decline pattern can be induced by various treatments (Supplementary Fig. 1), suggesting a common signaling pathway that correlates with decidualization, which requires further investigation. PGRMC1 seems less necessary after decidualization initiation, as knocking it down either does not affect or even facilitates the process. It is unclear why PRL expression initially drops and then increases when PGRMC1 is knocked down after decidualization induction. Downregulating PGRMC1 after progestin treatment doesn't hamper decidualization, indicating its critical role during the increasing phase and induction. This aligns with observations that PGRMC1 downregulation in the secretory phase promotes decidualization [28]. Overall, PGRMC1 activation by P4 may facilitate the switch from cellular proliferation to decidualization initiation through various biological processes, while the mechanism of how downregulated PGRMC1 promotes decidualization warrants further investigation.

PGRMC1 has been known to occupy multiple subcellular locations, from endoplasmic reticulum, cytoplasm, plasma membrane, nucleus, and mitochondria, and its localization is regulated by including phosphorylation, ubiquitination, and sumoylation [34, 36]. In our study, we noticed an induction-associated peri-nuclear phenomenon, presenting as more intense signals in the peri-nuclear region at 10 day's induction (Fig. 4A). PGRMC1's peri-nuclear expression has been observed in various cells, suggesting its involvement in processes near or within the nucleus [7, 38, 39]. In our current study, we did not detect any nuclear PGRMC1 under the explored conditions, as demonstrated by subcellular fractionation analysis (Fig. 4B).

PGRMC1 associates with proteins involved in protein biosynthesis, intracellular transport, and mitochondrial activity to promote decidualization [26, 35]. However, little is known about how PGRMC1 interacts with these proteins to regulate decidualization. We found that PGRMC1 binds to PHBs at the nucleus periphery after P4 treatment, suggesting it may function as a scaffold protein for decidualization in endometriosis stromal cells. PGRMC1 could be anchored on the membrane of various organelles, co-transporting with them during decidualization-related morphological changes [40]. PHBs form a super complex in mitochondria, playing roles in lipid biogenesis, ATP generation, and more [12, 41]. Knocking down PHBs partially impaired decidualization, similar to PGRMC1 knockdown, suggesting PGRMC1-PHBs interactions may influence decidualization as a complex, requiring further investigation. We speculate that PGRMC1 binding to PHBs may inhibit cellular proliferation and facilitate differentiation, acting as a proliferation-differentiation switch.

We found that the small molecule AG205 neither affect PGRMC1-PHBs interaction, nor decidualization in our study (Fig. 7). Although AG205 has been shown to interact with PGRMC1 in vitro, its in vivo interaction remains unknown. Our data align with a recent study demonstrating that AG205 concentrations over 15 μM reduce cell proliferation, and concentrations above 30 μM result in cell death in HEC-1A and T-HESC cells [29]. Furthermore, our findings are consistent with a previous report indicating that a high concentration (50 μM) of AG205 did not affect decidualization [30].

This study on PGRMC1-PHB association, while informative, presents several limitations. Firstly, while PLA data suggests a close proximity and potential functional interaction between PGRMC1 and PHB, confirming a physical interaction necessitates additional in vivo interaction detection methods. Co-immunoprecipitation (Co-IP) has significant limitations, as it disrupts cellular integrity and loses crucial information about protein localization and physiologically relevant interactions due to cell lysis and potential interference from the buffer system, particularly for detecting weak, transient interactions or those confined to specific cellular compartments. Thus, in vivo crosslinking, which enables interaction detection in their native environment, should be considered. Secondly, the efficiency of PHB1 and PHB2 silencing via siRNA is lower compared to the almost complete knockdown of PGRMC1, suggesting the need for PHB knockout or stable knockdown models for clearer background results. Finally, a general limitation needs to be taken into account. The in vitro experiments performed in cell lines assured reproducibility within the established system, while primary patient endometrium tissues are highly heterogeneous and, in general, require analysis of a large cohort in order to obtain a statistically significant result. Consequently, this study primarily analyzed publicly available datasets and two cell lines. However, to validate the switch-like rise-to-decline expression pattern of PGRMC1 in vivo, future studies could utilize a mouse model with inducible PGRMC1-downregulation.

Conclusion

Based on the results of our study, we postulate that P4/progestin-induced PGRMC1 rise-to-decline expression is essential to start the decidualization program, but, once decidualization started, PGRMC1 is not needed to drive it. Our PGRMC1-knockdown experiments demonstrated that PGRMC1 expression is specifically important at decidualization induction, leading to decidualization failure upon disruption. Taken together, we explained how dysregulated PGRMC1 expression could impact endometrial stromal cell decidualization, which may provide a new perspective on infertility-related diseases.

Supplementary Information

The online version contains supplementary material available at https://doi.org/10.1186/s12958-024-01188-9.

Additional file 1: Supplementary Fig. 1. Rise-to-decline expression pattern of PGRMC1 is linked to the decidualization program. **(A)** PGRMC1 protein expression changes during 9 days of decidualization were measured by western blot in the St-T1 cell line. **(B)** PGRMC1 protein expression changes during 10 days of stimulation with MPA, cAMP, and DMSO, respectively, were measured by western blot in T-HESCs. **(C)** PGRMC1 protein expression levels on day 6 and day 10 when cultured with DMSO, nomegestrel (NOM), P4, cAMP, MPA/cAMP (M + A), and MPA, respectively, measured by western blot in T-HESCs. **Supplementary Fig. 2.** PGRMC1 is effectively downregulated by siRNA on protein level. **(A)** The PGRMC1 protein expression on day 2 and day 10 after transfection of T-HESCs with either 10 nM anti-PGRMC1 siRNA (siPGRMC1) or unspecific scrambled-control siRNA (siCTL). **(B)** A comparison of the PGRMC1 protein expression changes within 10 days after transfection of T-HESCs with either 10 nM siPGRMC1 or 10 nM siCTL. **Supplementary Fig. 3**. PGRMC1-downregulation before decidualization induction impairs morphological remodeling of T-HESCs. The cellular morphology changes of the T-HESCs induced with either DMSO (upper panel) or MPA/cAMP (down panel) after 10 days of siRNA treatment (siCTL, left panel; siPGRMC1, right panel). Scale bar: 200 µm. **Supplementary Fig. 4.** PGRMC1-downregulation after decidualization induction does not impair morphological remodeling of T-HESCs. The cellular morphology changes of the T-HESCs induced with either DMSO (non-induction, column 1) or MPA/cAMP (Induction, columns 2–4). I (column 3) and II (column 4) indicate that siRNA treatment on T-HESCs was conducted on day 2 or day 4 of decidualization induction, respectively. Scale bar: 200 µm. **Supplementary Fig. 5.** PGRMC1-downregulation after progestin induction does not impair decidualization in the St-T1 cell line. The mRNA expression levels of *PGRMC1* **(A, C)** and *PRL* **(B, D)** in St-T1 treated with MPA/cAMP for decidualization induction (red line), and non-induction (black line). The mRNA expression levels of *PGRMC1* and *PRL* in St-T1 cells transfected with 10 nM siPGRMC1 (blue line) on the second (**A, B**) and fourth day (**C, D**) after decidualization induction, respectively. Results are shown as the mean ± SEM from three independent biological replicates. Statistical analysis was performed by a two-way ANOVA test. *$p < 0.05$, **$p < 0.01$, ***$p < 0.001$, ****$p < 0.0001$. The red * indicates the comparison between the red and black lines. The blue * indicates the comparison between the red and blue lines. **Supplementary Fig. 6.** PGRMC1 and PHB1/PHB2 co-localize in T-HESCs. Double Immunofluorescence staining for PGRMC1 (red) and PHB1 (green) or PHB2 (green) in T-HESCs treated with DMSO **(A)** as control or MPA/cAMP **(B)** for decidualization induction. Magnification: 40x. Scale bar: 20 µm. **Supplementary Fig. 7.** PGRMC1 does not interact with PHBs without induction. The interactions between PGRMC1 and PHB1 **(A)** and PHB2 **(B)** in T-HESCs without induction were analyzed with proximity ligation assay from day 2 to day 10. Each red spot represents a single interaction. Nuclear stain: DAPI. Magnification 40X. **Supplementary Fig. 8.** PGRMC1 co-precipitate with PHB1/PHB2 upon decidualization induction. PGRMC1 was immunopurified from native whole cell lysates of T-HESCs using anti-PGRMC1 antibody. Western blot analyses of co-immunoprecipitated PHB1 (upper) and PHB2 (bottom) in T-HESCs with and without decidualization induction. **Supplementary Fig. 9.** Morphological changes during decidualization upon PHBs downregulation. The cellular morphology changes of the T-HESCs induced with either DMSO (non-Induction) or MPA/cAMP (Induction) upon either PHBs knockdown alone or both. Scale bar: 200 µm. **Supplementary Fig. 10.** Overview over the role of PGRMC1 in human endometrial decidualization. Upon stimulation with progesterone or MPA, the PGRMC1 rise-to-decline changes are essential for successful decidualization of the human endometrial cells (upper panel). With downregulated PGRMC1 expression before induction, the decidualization program cannot be carried out, leading to decidualization failure (bottom panel).

Acknowledgements
We are grateful to our colleagues in the Department of Gynecology and Obstetrics, Heinrich-Heine University Duesseldorf for their helpful comments.

Authors' contributions
Conceptualization, H.L., H.N.; Investigation, H.L., N.S.; Methodology, H.L., A.P.B. and N.S.; Supervision, T.F., D.N., Z.C., N.S., H.N.; Project administration, T.F., H.N.; Writing-original draft, H.L.; Writing-review and editing, A P.B., A.F., N.S. and H.N. All authors have read and agreed to the published version of the manuscript.

Funding
Open Access funding enabled and organized by Projekt DEAL. This project was funded by the "German Research Foundation (Deutsche Forschungsgemeinschaft, DFG, NE 805/6–1)", and "The Brigitte and Dr. Konstanze Wegener Foundation (#51, Duesseldorf, Germany)", and "The Medical Faculty of the Heinrich-Heine University Duesseldorf (#48/2018)", and "The Shanghai Shenkang Hospital Development Center (SHDC12021113)".

Availability of data and materials
The datasets analyzed in this study are available at Gene Expression Omnibus (GEO) database: https://www.ncbi.nlm.nih.gov/geo/ with the GEO accessions GSE6364 and GSE4888.

Declarations

Ethics approval and consent to participate
Not applicable.

Consent for publication
Not applicable.

Competing interests
The authors declare no competing interests.

Author details
[1]Department of Obstetrics and Gynecology, Life Science Center, University Hospital and Medical Faculty of the Heinrich-Heine University Duesseldorf, Duesseldorf, Germany. [2]Department of OB/GYN & REI, UniKiD, University Hospital and Faculty of Medicine, Heinrich Heine University, Duesseldorf, Germany. [3]Department of Obstetrics and Gynecology, Shanghai Tenth People's Hospital, Tongji University School of Medicine, Shanghai 200072, China. [4]Institute of Gynecological Minimally Invasive Medicine, Tongji University School of Medicine, Shanghai 200072, China.

Received: 6 June 2023 Accepted: 20 January 2024
Published online: 03 February 2024

References

1. Reed BG, Carr BR. The Normal Menstrual Cycle and the Control of Ovulation. [Updated 2018 Aug 5]. In: Feingold KR, Anawalt B, Blackman MR, Boyce A, Chrousos G, Corpas E, de Herder WW, Dhatariya K, Dungan K, Hofland J, Kalra S, Kaltsas G, Kapoor N, Koch C, Kopp P, Korbonits M, Kovacs CS, Kuohung W, Laferrère B, Levy M, McGee EA, McLachlan R, New M, Purnell J, Sahay R, Shah AS, Singer F, Sperling MA, Stratakis CA, Trence DL, Wilson DP, editors. Endotext [Internet]. South Dartmouth (MA): MDText.com, Inc.; 2000.
2. Jabbour HN, et al. Endocrine regulation of menstruation. Endocr Rev. 2006;27(1):17–46.
3. Mihm M, Gangooly S, Muttukrishna S. The normal menstrual cycle in women. Anim Reprod Sci. 2011;124(3–4):229–36.
4. Gellersen B, Brosens JJ. Cyclic decidualization of the human endometrium in reproductive health and failure. Endocr Rev. 2014;35(6):851–905.
5. Ng SW, et al. Endometrial Decidualization: The Primary Driver of Pregnancy Health. Int J Mol Sci. 2020;21(11):4092.
6. Chen JI, et al. Proteomic characterization of midproliferative and midsecretory human endometrium. J Proteome Res. 2009;8(4):2032–44.
7. Salsano S, et al. Dynamic expression of PGRMC1 and SERBP1 in human endometrium: an implication in the human decidualization process. Fertil Steril. 2017;108(5):832-842 e1.
8. Abdalla M, et al. miRNAs as a novel clinical biomarker and therapeutic targets in polycystic ovary syndrome (PCOS): A review. Life Sci. 2020;259:118174.

9. Bunch K, et al. Expression patterns of progesterone receptor membrane components 1 and 2 in endometria from women with and without endometriosis. Reprod Sci. 2014;21(2):190–7.
10. Feng L, et al. Progesterone receptor membrane component 1 (PGRMC1) expression in fetal membranes among women with preterm premature rupture of the membranes (PPROM). Placenta. 2014;35(5):331–3.
11. Gerhardt K. PGRMC1: A Fertility Stabilizer. Biol Reprod. 2016;95(3):49.
12. Mishra S, Murphy LC, Murphy LJ. The Prohibitins: emerging roles in diverse functions. J Cell Mol Med. 2006;10(2):353–63.
13. Signorile A, et al. Prohibitins: A Critical Role in Mitochondrial Functions and Implication in Diseases. Cells. 2019;8(1):71.
14. Hernando-Rodriguez B, Artal-Sanz M. Mitochondrial Quality Control Mechanisms and the PHB (Prohibitin) Complex. Cells. 2018;7(12):238.
15. He B, et al. A repressive role for prohibitin in estrogen signaling. Mol Endocrinol. 2008;22(2):344–60.
16. Zhang LF, et al. PHB regulates meiotic recombination via JAK2-mediated histone modifications in spermatogenesis. Nucleic Acids Res. 2020;48(9):4780–96.
17. Wang T, Zhang M, Jiang Z, Seli E. Mitochondrial dysfunction and ovarian aging. Am J Reprod Immunol. 2017;77(5). https://doi.org/10.1111/aji.12651. Epub 2017 Feb 13. PMID: 28194828.
18. Qi X, et al. Knockdown of prohibitin expression promotes glucose metabolism in eutopic endometrial stromal cells from women with endometriosis. Reprod Biomed Online. 2014;29(6):761–70.
19. He B, et al. Estrogen-regulated prohibitin is required for mouse uterine development and adult function. Endocrinology. 2011;152(3):1047–56.
20. Bai Y, et al. PGRMC1 Promotes Progestin-Dependent Proliferation of Breast Cancer Cells by Binding Prohibitins Resulting in Activation of ERalpha Signaling. Cancers (Basel). 2021;13(22):5635.
21. Talbi S, et al. Molecular phenotyping of human endometrium distinguishes menstrual cycle phases and underlying biological processes in normo-ovulatory women. Endocrinology. 2006;147(3):1097–121.
22. Burney RO, et al. Gene expression analysis of endometrium reveals progesterone resistance and candidate susceptibility genes in women with endometriosis. Endocrinology. 2007;148(8):3814–26.
23. Vestergaard AL, et al. Transcriptional expression of type-I interferon response genes and stability of housekeeping genes in the human endometrium and endometriosis. Mol Hum Reprod. 2011;17(4):243–54.
24. Nayyar A, et al. Menstrual Effluent Provides a Novel Diagnostic Window on the Pathogenesis of Endometriosis. Front Reprod Health. 2020;2:3.
25. Thieffry C, et al. Spatiotemporal expression pattern of Progesterone Receptor Component (PGRMC) 1 in endometrium from patients with or without endometriosis or adenomyosis. J Steroid Biochem Mol Biol. 2022;223:106153.
26. Salsano S, et al. Novel nonclassic progesterone receptor PGRMC1 pulldown-precipitated proteins reveal a key role during human decidualization. Fertil Steril. 2020;113(5):1050-1066 e7.
27. Peluso JJ, Pru JK. Progesterone Receptor Membrane Component (PGRMC)1 and PGRMC2 and Their Roles in Ovarian and Endometrial Cancer. Cancers (Basel). 2021;13(23):5953.
28. Tsuru A, et al. PGRMC1 Regulates Cellular Senescence via Modulating FOXO1 Expression in Decidualizing Endometrial Stromal Cells. Biomolecules. 2022;12(8):1046.
29. Thieffry C, et al. AG-205 Upregulates Enzymes Involved in Cholesterol Biosynthesis and Steroidogenesis in Human Endometrial Cells Independently of PGRMC1 and Related MAPR Proteins. Biomolecules. 2021;11(10):1472.
30. Salsano S, et al. Deciphering the Role of PGRMC1 During Human Decidualization Using an In Vitro Approach. J Clin Endocrinol Metab. 2021;106(8):2313–27.
31. Wang-Eckhardt L, Eckhardt M. A progesterone receptor membrane component 1 antagonist induces large vesicles independent of progesterone receptor membrane component 1 expression. Biol Chem. 2020;401(9):1093–9.
32. Teakel SL, et al. Protein complexes including PGRMC1 and actin-associated proteins are disrupted by AG-205. Biochem Biophys Res Commun. 2020;524(1):64–9.
33. Ahmed IS, et al. Progesterone receptor membrane component 1 (Pgrmc1): a heme-1 domain protein that promotes tumorigenesis and is inhibited by a small molecule. J Pharmacol Exp Ther. 2010;333(2):564–73.
34. Cahill MA. Progesterone receptor membrane component 1: an integrative review. J Steroid Biochem Mol Biol. 2007;105(1–5):16–36.
35. Velazquez Hernandez DM, Vazquez-Martinez ER, Camacho-Arroyo I. The role of progesterone receptor membrane component (PGRMC) in the endometrium. Steroids. 2022;184:109040.
36. Cahill MA, et al. The emerging role of progesterone receptor membrane component 1 (PGRMC1) in cancer biology. Biochim Biophys Acta. 2016;1866(2):339–49.
37. McCallum ML, et al. Conditional Ablation of Progesterone Receptor Membrane Component 1 Results in Subfertility in the Female and Development of Endometrial Cysts. Endocrinology. 2016;157(9):3309–19.
38. Ahmed IS, et al. Pgrmc1 (progesterone receptor membrane component 1) associates with epidermal growth factor receptor and regulates erlotinib sensitivity. J Biol Chem. 2010;285(32):24775–82.
39. Wang R, Sheehan PM, Brennecke SP. Changes in myometrial expression of progesterone receptor membrane components 1 and 2 are associated with human parturition at term. Reprod Fertil Dev. 2016;28(5):618–27.
40. Chen YJ, et al. PGRMC1 acts as a size-selective cargo receptor to drive ER-phagic clearance of mutant prohormones. Nat Commun. 2021;12(1):5991.
41. Merkwirth C, Langer T. Prohibitin function within mitochondria: essential roles for cell proliferation and cristae morphogenesis. Biochim Biophys Acta. 2009;1793(1):27–32.

Publisher's Note

9. Discussion and Outlook

Breast cancer accounts for 25% of all new cancer cases in women, making it the most common female cancer. Although various therapeutic options are available for all breast cancer-subtypes, relapse and metastasis occur in nearly 30 % of patients, which calls for identification of novel cancer dependencies and vulnerabilities to improve treatment options [132].

One of the factors contributing to breast cancer progression is the multifunctional and highly conserved putative progesterone receptor PGRMC1 [133]. In the context of breast cancer, PGRMC1 overexpression in tissue biopsies was associated with worse overall survival [134].

9.1. PGRMC1 Associates with Enzymes of the Mevalonate Pathway and Impacts Sterol Metabolism

In the first manuscript presented in this thesis, we described the influence of PGRMC1 on sterol metabolism and oncogenic signaling. Overexpression of PGRMC1 in hormone receptor positive breast cancer cells resulted in increased proliferation in cell culture and in mice xenografts. In the same cells, PGRMC1 interacted with enzymes of the mevalonate pathway CYP51A1 and FDFT1, and of the lipid synthesis pathway SCD1. Further, PGRMC1-overexpressing MCF7 cells contained more neutral lipids, more cholesterol, more lipid rafts compared to controls, and the amount of estradiol released to culture medium was likewise increased. Importantly, MCF7/PGRMC1 cells also presented a higher expression and activation level of ERα, and an increased activation of EGFR and MAPK signaling, while PGRMC1 downregulation by siRNA resulted in the opposite effect. Finally, treatment of simvastatin in PGRMC1-overexpressing cells significantly reduced proliferation compared with respective control cells, emphasizing the importance of the mevalonate pathway for these cells. Taken together, data of this manuscript provided evidence towards the involvement of PGRMC1 in sterol homeostasis and thereby in oncogenic signaling.

Although several observations of PGRMC1 involvement in sterol metabolism were presented in 4.3.3, additional aspects shall be discussed in the following paragraph. PGRMC1 reportedly interacted with two key regulators of cholesterol (and its precursor mevalonate)- and lipid-synthesis pathways Insig-1 and SCAP [13], as well as with several CYP450 enzymes [135]. CYP450-enzymes are involved in synthesis and metabolism of sterols, steroid hormones, and hydrophobic substances. Consequently, increased activation of CYP3A4 by PGRMC1 led to detoxification from doxorubicin and increased chemoresistance in human colon cancer cells

in a heme dependent manner [22] and PGRMC1 overexpression was associated with decreased response to anthracyclin therapy in breast cancer [134]. Further, interaction with CYP51A1, an enzyme catalyzing the second last step of cholesterol *de-novo* synthesis, was detected in different systems [14], [22], [99]. The implication of PGRMC1 in lipid metabolism in the context of cancer is relevant, since energy production within cancer cells differs from that of non-malignant cells: cancer cells take advantage of alterations in lipid metabolism involving changes in lipid synthesis, lipid catabolism, and fatty acid oxidation in order to meet the demands for energy, membrane biogenesis and signaling molecule generation [78], [75]. Several studies have confirmed that inhibition of different enzymes within the fatty acid biosynthesis pathway can block cancer cell growth, whereas genes involved in lipid synthesis and oxidation appear to be highly upregulated during rapid growth of breast cancer [137], [138], [139]. Interestingly, activation of lipid metabolism and uptake take place in the healthy breast tissue before cancer diagnosis, potentially predisposing or favoring cancer initiation, emphasizing lipid metabolic reprogramming as an important hallmark for breast cancer progression [140].

Additionally, PGRMC1 expression was found to be associated with oncogenic signaling of EGFR and ERα. Concerning the ERα signaling pathway, the observed elevation of endogenous estradiol production by the cells themselves could activate ERα intrinsically and boost proliferation of hormone receptor positive breast cancer cells. Further, ERα could be activated by other cholesterol derivates that bind ERα as selective estrogen receptor modulators (SERMs). This effect has been demonstrated for 27-hydroxycholesterol and is speculated to apply also to other metabolites [74] [141]. To dissect the role of different cholesterol metabolites in the observed read-outs, lipidome analysis on cells with different PGRMC1 expression levels could be performed. In general, PGRMC1 association with ERα has been observed by several groups [142] [143]. Nevertheless, PGRMC1 is overexpressed also in a fraction of hormone receptor negative breast cancers [144] and may be involved in distinct functions there.

Concerning PGRMC1's connection with EGFR-signaling, several observations were obtained by different groups. Kabe *et al.* described interaction between dimerized PGRMC1 and EGFR [22]. Further, Pedroza *et al.* observed decreased EGFR and PI3K signaling when PGRMC1 was downregulated, while the same pathways were activated when PGRMC1 was overexpressed in benign breast MCF10a cells [59]. A possible explanation for these effects could be increased

abundance of lipid rafts in the plasma membrane, where EGFR and other surface receptors are harbored.

Further, an interesting observation was the inhibition of MCF7/PGRMC1 cells' proliferation upon treatment with simvastatin. Importantly, statins have been used in several clinical trials to reduce breast cancer risk or to prevent recurrence if combined with endocrine therapy, and most studies indicated a protective function of statin use on breast cancer incidence/recurrence [145]. An additional retrospective analysis of PGRMC1 expression in these cohorts would be beneficial to evaluate whether PGRMC1 expression could be a prognostic factor for efficacy of combined statin therapy.

PGRMC1 itself could also be possibly targeted in future. A lot of research has been performed with a putatively PGRMC1-specific inhibitor, the small-molecule AG-205. AG-205 has been identified as a ligand for an *Arabidopsis thaliana* MAPR protein [146] and first used as a PGRMC1-ligand in 2010 by Ahmed *et al.* [147]. Since then, it has been associated with PGRMC1 in several readouts [17], [59], [148]. However, emerging evidence pointed towards PGRMC1-independent AG-205 effects [100], [149], [150]. Recently, Kabe *et al.* revealed a binding and inhibition of PGRMC1 by glycyrrhizin (a natural compound of licorice) and screened glycyrrhizin derivatives for PGRMC1 affinity [151]. Of note, particularly one derivative bound PGRMC1 with increased affinity *in vitro* and treatment with that derivative in combination with cisplatin had a synergistic effect in mouse xenograft tumors *in vivo.* Interestingly, AG-205 *in vitro* binding to PGRMC1 could not be detected in the same study by Kabe *et al.* [151] Whether the synergistic effect is indeed based on PGRMC1 inhibition, remains to be evaluated in future studies. Glycyrrhizin has been reported to bind at least one other protein (high-mobility group box 1 (HMGB1)) and is surely not PGRMC1-specific [152]. However, another step towards a PGRMC1 inhibitor is made, opening up perspectives for inhibitor design in the future.

9.2. Possible Implication in Ferroptosis: Oxidative Damage-Triggered Cell Death and PGRMC1

Within the lipid metabolic pathway, PGRMC1 interacted with SCD1, a key enzyme in fatty acid metabolism, and PGRMC1 overexpression upregulated SCD1 mRNA. SCD1 is an iron-containing enzyme that catalyzes a rate-limiting step in the synthesis of mono-unsaturated fatty acids. The expression of the protein is associated with increased tumor growth, since its

activity feeds dividing tumor cells with fatty acids and protects cancer cells from ferroptotic cell death – a form of cell death from oxidation of cellular membranes by reactive oxygen species resulting from excessive cellular metabolism [153]. Although SCD1 is not an oncogene, beneficial gain-of-function mutations of SCD1 have been observed in some tumors, driving metabolic reprogramming of rapidly diving cells [137]. Although we did not characterize the nature of PGRMC1-SCD1-interactions (activating/stabilizing or inhibitory), the measured increased level of neutral lipids in PGRMC1-overexpressing cells may indicate an activating interaction, which would boost SCD1 enzymatic activity and stimulate cancer growth. However, the amount of mono-unsaturated fatty acids in the cells could be measured by gas chromatography to confirm this hypothesis.

Interestingly, PGRMC1 possesses several features/functions that indicate its involvement in the above mentioned ferroptotic cell death. PGRMC1 chelates heme and thereby iron [22], it is involved in lipid production and interacts with SCD1 [99] and FECH [29], both crucial enzymes in the context of ferroptosis. PGRMC1's contribution to the process has been addressed with yet controversial results. You *et al.* observed an increased sensitivity towards ferroptosis inducers upon overexpression of PGRMC1 in head and neck cancer cells [154], while Zhao *et al.* described a protective effect of PGRMC1 on ferroptosis in MDA-MB-231 breast cancer cells [155]. Since ferroptosis is recently being discussed as an important damage regulation mechanism that needs to be overcome by cancer cells and could be chemically induced to improve cancer treatment, the involvement of PGRMC1 in ferroptosis seems intriguing and deserves further investigation.

9.3. PGRMC1-Knockout Cells Do Not Present Any Deficiency Phenotype

To further characterize PGRMC1 implications in breast cancer progression, CRISPR/Cas9 technology was used to generate PGRMC1-knockout cells in three breast cancer cell lines. Using plasmids for three different gRNAs simultaneously transfected into cells in a transient manner, and subsequent limiting dilution, clones with absent PGRMC1 protein could be successfully generated for MCF7, T47D and MDA-MB-231 cell lines. These clones were further characterized by sequencing of PCR fragments in the mutated PGRMC1-locus, as well as sequencing the mutated mRNA, if present. Functional analysis was performed for MCF7 cells with different PGRMC1 protein expression levels. Long-term PGRMC1-KO cells did not present any deficiency phenotype in contrast to transient downregulation of PGRMC1 by siRNA as performed for manuscript 1. Proliferation of MCF7/PGRMC1-KO43 and MCF7/PGRMC1-KO64

and production of neutral lipids was not significantly different from parental PGRMC1-WT cells. Interestingly, one clone (MCF7/PGRMC1-KO5) had elevated expression of EGFR and increased activation of EGFR and MAPK signaling. The same clone demonstrated highest response to EGF treatment. However, the second tested clone had a different expression pattern, so that no PGRMC1-KO associated tendency could be detected.

The CRISPR/Cas9 approach selected for this thesis did not include any selection for successfully manipulated clones. The straightforward technique allowed transcription of gRNAs and Cas9 from plasmids transfected into the cells. Once transcribed, the CRISPR/Cas9 reaction could take place, before the cells were detached and subcloned via limiting dilution. The efficiency of this workflow could have been improved if a plasmid with a resistance cassette flanked by homology arms targeting the PGRMC1 locus had been transfected together with the CRISPR/Cas9 plasmids [156]. This way, in case of repair by HDR, the resistance cassette would have been inserted into the PGRMC1 locus and destroyed the gene, providing an opportunity to select for successfully manipulated clones. Another mean to improve efficiency would have been lentiviral transduction of cells with the respective CRISPR/Cas9 plasmids [157]. However, in both ways the genome is disturbed by stable insertion of either a resistance gene or the CRISPR/Cas9 genes under regulation of constitutively active promoters, which could potentially interfere with cellular functions. Therefore, an approach which would leave back as little modifications of the genome as possible was selected, taking the costs of more intensive and thorough screening.

The resulting clones were demonstrating different DNA aberration patterns, resulting mostly from CRISPR/Cas9 reaction at gRNA 2 and gRNA 3 binding sites (exon 2 and exon 3, respectively). In clone MCF7/PGRMC1-KO64, two mutations were detected on DNA (insertion of guanine in exon 2 and deletion of 24 nucleotides in exon 3 and on mRNA. The G-insertion alone results in a frameshift and a truncated protein. Both mutations are located on the same chromosome, since both were detected on mRNA. For clone MCF7/PGRMC1-KO43, two transcripts were sequenced, with a deletion of 7 base pairs or 10 base pairs at the same location, respectively, while on DNA only the 7 base pair mutation was detected. The reason for this is likely alternative splicing, since the mutation is close to the splicing site. However, some clones did not produce any detectable band neither in PCR on DNA, nor on mRNA that could be sequenced (clones MCF7/PGRMC1-KO5, MDA-MB-231/PGRMC1-KO34, -KO18; T47D/PGRMC1-KO146). These clones are potentially the ones with largest aberrations on both

alleles and best suitable for future experiments. The locus could be sequenced using next generation sequencing methods to confirm potential loss of the PGRMC1 locus.

In other clones, only one mutation was detected, pointing towards a non-mutated second chromosome. However, even in those cases PGRMC1 protein expression was completely absent. Important for the understanding of this phenomenon is the location of PGRMC1 on the X-chromosome. One of the X-chromosomes is subject to X-chromosomal inactivation to balance out gene doses effects. Not the entire X-chromosome is inactivated and condensed by this process, but some genes escape inactivation and remain transcriptively active [158]. Importantly, the PGRMC1 locus is located in the inactivated region, resulting in only one actively transcribed PGRMC1 allele [159], [160]. If this allele is subject to CRISPR/Cas9 reaction, the consequence is a phenotypic knockout, even in presence of an intact but silenced allele. This circumstance may explain why some knockout clones with only a single identified mutation on one allele are totally absent of PGRMC1 protein. Importantly, mutations in other chromosomes and genes generated by off-target binding of gRNAs and additional changes in not sequenced PGRMC1 regions cannot be excluded. Therefore, if this information is required in the future, long-read sequencing for the PGRMC1 locus or whole exome sequencing for off-target effects may be performed.

Regarding the functional assays, the common information from all read-outs was the lack of a definite PGRMC1-knockout phenotype – based on the read-out systems applied by us. A possible explanation for this discrepancy to previously observed PGRMC1 knock-down phenotypes may be genetic compensation, which occurs when homologues or genes with related function are upregulated in response to a loss-of-function mutation. Genetic compensation has been observed in different biologic systems, where knockdown results could not be reproduced in genetic knockouts. In zebrafish, knockdown of the gene *egfl7* results in vascular defects, while *egfl7* deleterious mutants did not exhibit any phenotype [161]. The authors performed proteome and transcriptome analysis and identified several differentially expressed genes, which were confirmed to rescue the loss-of-function phenotype. Genetic compensation was further reported in mice and in human cells, as reviewed by Brolosy and Stainier [162]. The authors provide an overview of published studies with phenotypic discrepancy between transient knockdown and permanent gene loss, and outline that genetic compensation is a common phenomenon. The mechanism by which compensating genes are upregulated upon a mutation may be related to the mutant mRNA.

A recent publication demonstrated that nonsense-mediated mRNA decay – a process to degrade error-bearing mRNA – triggers upregulated expression of genes that exhibit sequence similarity with the degraded mRNA, suggesting compensation for a gene's loss by upregulation of homologues [163]. To test this hypothesis in cells generated in this thesis, proteome and/or transcriptome analyses could be performed. A candidate for compensatory effects could be PGRMC2, but since compensation does not only apply to homologous genes, an -omics technique could provide insights into compensating pathways and into essential PGRMC1 functions.

9.4. PGRMC1 Interacts with PHBs and Influences ERα-Signaling in Breast Cancer Cells

PGRMC1's ability to bind progesterone is not proven yet. However, previous finding indicated an involvement of PGRMC1 in signaling of progesterone and its synthetic analogues progestins, since PGRMC1 overexpressing breast cancer cells exhibited increased proliferation upon stimulation with progestins, and PGRMC1 was shown to be phosphorylated at S181 upon treatment with the progestin NET [124].

NET is used in hormone replacement therapy together with estradiol to counteract menopausal symptoms. Several studies have revealed an increased risk for breast cancer for women with HRT, especially if the progestin compound was NET, MPA and cyproterone acetate [123]. Since PGRMC1 is phosphorylated upon progestin treatment and confers a proliferative effect on breast cancer cells, it seems reasonable that the increased incidence for breast cancer under specific HRT may be at least partially associated with PGRMC1 activation.

To address this hypothesis in manuscript 2, PGRMC1's interaction partners upon stimulation with NET were analyzed by mass spectrometry, and PHBs were identified to be significantly enriched after PGRMC1 co-immunoprecipitation. Interaction between PHBs and PGRMC1 was further demonstrated by PLA selectively after treatment with progestins that increase proliferation (proliferation-promoting progestins, PPPs), and was absent after treatment with progestins that do not increase proliferation (non-proliferation-promoting progestins; NPPPs). Importantly, PHB2 has been reported to negatively regulate stimulative function of ERα, putatively by binding ERα in the nucleus and preventing transcription of its' target genes [164], [165]. By PLA, binding of PHBs to ERα and to PGRMC1 was then analyzed. Both PHBs were

found to associate either with PGRMC1, or ERα, but not with both simultaneously. After stimulation with NET or other PPPs, PGRMC1 was phosphorylated at S181 and associated with PHBs, while PHBs-ERα interaction was significantly reduced. When stimulated with NPPPs, this effect could not be observed. Importantly, in this context, PLA in MCF7/PGRMC1-KO64 did not provide any significant signal for PGRMC1-PHBs interaction after treatment with PPPs (since PGRMC1 was absent), and PHBs were associated with ERα when treated with both PPPs and NPPPs. Therefore, we hypothesize that PGRMC1, when phosphorylated at S181, associates with PHBs, thereby preventing their binding to ERα and negative regulation of ERα-signaling. ERα could thereafter establish an increased activity and increased proliferative signaling.

Negative regulation of PHB2 has been demonstrated for another protein, brefeldin A-inhibited guanine nucleotide-exchange protein 3 (BIG3). Kim and colleagues found out that BIG3 associates with PHB2, putatively via binding a specific region that is necessary for nuclear import and thereby prevents PHB2's translocation into the nucleus [166]. Later, the same group targeted the BIG3-PHB2 complex by a cell-permeable peptide inhibitor to decrease ERα-dependent growth of breast cancer cells *in vivo* and *in vitro* and to reduce resistance to tamoxifen [167]. For PGRMC1, a similar function could be hypothesized. PGRMC1 could associate with PHBs directly or through adapter proteins/in a protein complex and thereby regulate their function.

PHB1 and PHB2 are evolutionary conserved ubiquitous proteins, reported to be localized in the nucleus, the mitochondria and the cytosol [168]. Depending on the localization, they exhibit distinct functions. For instance, in mitochondrial membranes, PHB1 and PHB2 form hetero-multimeric complexes with yet speculative stoichiometry and putatively serve as scaffolds for respiratory chain complexes. Deregulation of PHBs results in increased degradation and lower expression of some respiratory chain complexes and is associated with defects in proliferation and increased apoptosis [169]. Further, PHBs are reported to interact with transcription factors other than ERα in the nucleus, and to differentially regulate gene expression. In the breast cancer cell line T47D also used in this study, PHB1 was demonstrated to suppress activity of E2F transcription factors, which in their majority convey proliferative and anti-apoptotic signals. Additionally, PHB1 also bound retinoblastoma (Rb), a tumor suppressor, without inhibiting the protein [170]. In MCF7 breast cancer and B-cell lymphoma cells, PHB1 overexpression mediated transcription of the tumor-suppressor p53 dependent genes and suppressed activity of E2F transcription factors [171].

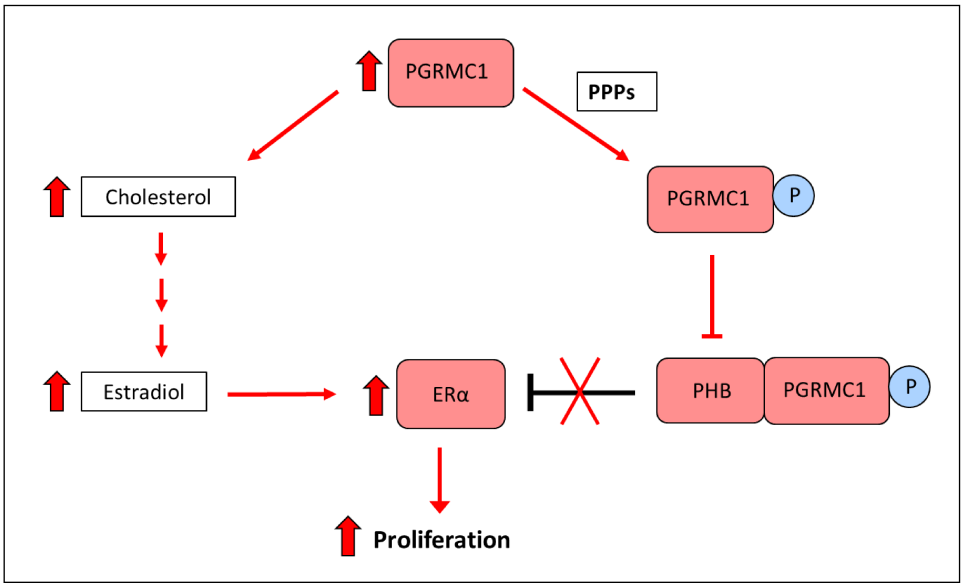

Figure 12: Schematic representation of the hypothetic interplay between ERα and PGRMC1 through stimulation of cholesterol and estradiol production on one hand, and through binding of ERα negative regulators PHB1 and PHB2 on the other hand. PGRMC1 was associated with increased cholesterol and estradiol levels in manuscript 1 [99], and was demonstrated to interact with PHBs upon stimulation with proliferation-promoting progestins (PPPs), possibly inhibiting the ERα-PHBs interaction, in manuscript 2 [108]. Both described pathways potentially increase ERα oncogenic signaling.

Taking this background into account, assuming a possible involvement of PGRMC1 in regulation of PHBs is intriguing. By interaction with PHBs, PGRMC1 could indirectly enhance oncogenic signaling of several transcription factors and possibly decrease activity of others (like the tumor suppressor p53) and thereby promote breast cancer progression. Since PGRMC1 is not only upregulated in breast cancer, but also in other tumor entities like lung, cervical, head and neck cancer and others [62], [61], the interplay between PGRMC1 and PHBs could be further evaluated there.

Interestingly, PGRMC1 was associated with ERα signaling in manuscript 1 and 2 in two different mechanistical ways. As described in Asperger *et al.*, increased production of cholesterol and estradiol by PGRMC1 overexpression could trigger a vicious circle of hormone dependent breast cancer, having cancer cells providing their own proliferation-stimulating factor. Second, as addressed in Bai *et al.*, PGRMC1 could inhibit negative ERα-regulation by blocking PHBs, allowing ERα to fully exert its proliferative potential. Both mechanistic pathways indicate a deep implication of PGRMC1 in ERα-signaling, which should be further evaluated in breast cancer tissues. Getting insights into the impact of these mechanisms *in vivo* would provide a better understanding of breast cancer dependencies and vulnerabilities and potentially offer a new avenue for cancer treatment.

9.5. PGRMC1 Interacts with PHBs and Influences Decidualization in Endometrial Stromal Cells

Besides cancer, female fertility is a prominent field in PGRMC1 research. Its implication has been demonstrated in mice and zebrafish, and women with infertility related diseases often have a dysregulated PGRMC1 expression in the endometrium [12].

Since PHB2 was reported to be downregulated during decidualization and to control the process, and PGRMC1 was hypothesized to be a potential co-regulator of PHB2 activity, we decided to address the role of PGRMC1 in decidualization and its interplay with PHBs.

Therefore, a decidualization workflow using human endometrial stromal cell lines HESC and St-T1 was established, using 8-Br-cAMP and MPA as decidualization inducers in cell culture and by performing a qPCR for the prolactin (PRL) gene mRNA, which secretion marks successful decidualization. Subsequently, PGRMC1 expression was analyzed throughout the decidualization process and a PGRMC1 rise-to-decline expression pattern was revealed.

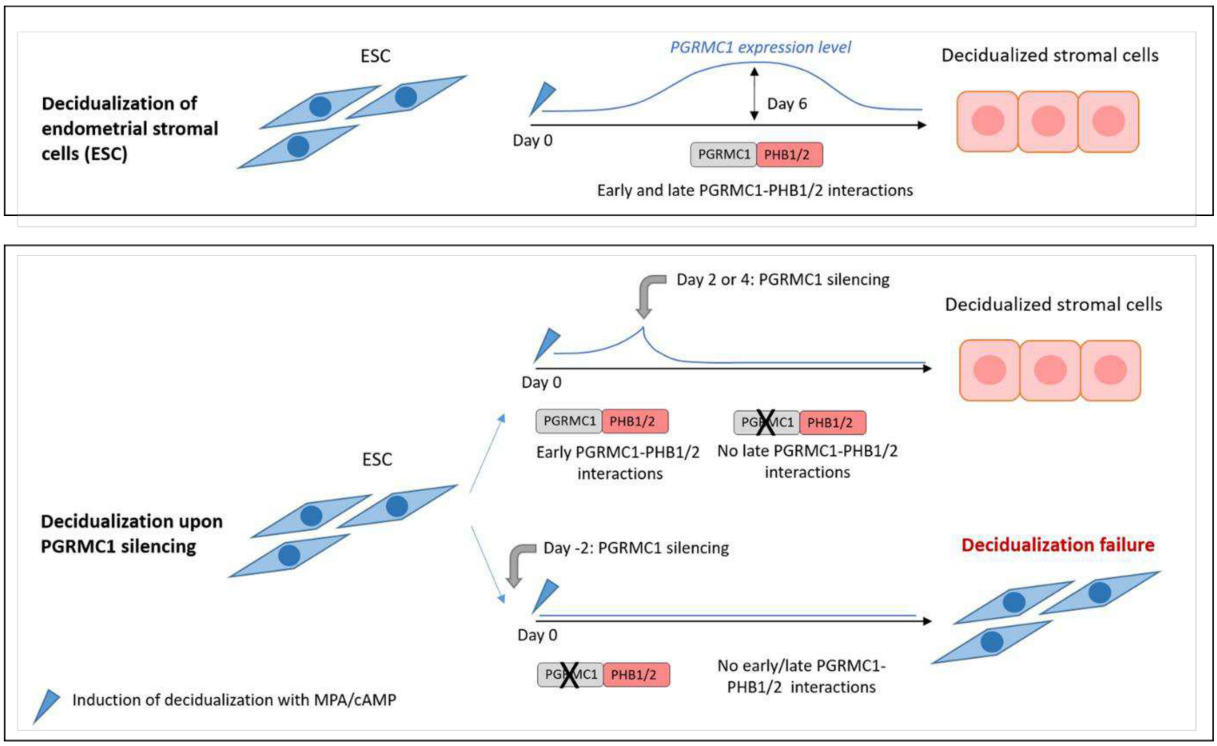

Figure 13: Graphical overview over the findings presented in manuscript 3. Endometrial stromal cells (ESC) are treated with MPA/cAMP (blue triangle) to trigger decidualization. PGRMC1-expression follows a rise-to-decline expression pattern, represented in the upper panel. If *PGRMC1*-expression was silenced on day 2 or 4 after decidualization induction (panel 2, upper path), cells were still able to decidualize. If *PGRMC1*-expression was silenced before decidualization induction (panel 2, lower path), ESCs were unable to decidualize. This graph was created by me and published as Supplementary Figure 10 in Liu *et al.* [172]. Reproduced with the journal's permission.

Further, PGRMC1 was downregulated before decidualization induction leading to decidualization failure, pointing toward an essential role of PGRMC1 expression induction during decidualization start. When PGRMC1 was downregulated at day 3 after decidualization induction, no difference in or rather an increased decidualization could be detected. Importantly, throughout its rise-to-decline expression change, PGRMC1 interacted with PHB1 and PHB2 [172].

The PGRMC1 expression peak during decidualization was essential for the successfully completed process and raises the hypothesis of a possibly impaired decidualization in infertility-related diseases with PGRMC1-deficiency. PHB2 was discovered to be downregulated towards the end of decidualization, suggesting that its function requires reduction during HESC differentiation. A possible role of PGRMC1 as an additional PHB2 inhibitor during decidualization similar to its role in breast cancer may be suggested. The findings of this study emphasize the possible general function of PGRMC1-PHBs interactions which is probably not limited to the analyzed breast cancer and endometrial stromal cells but may occur in several tissues and organs.

9.6. Outlook

The findings presented in this thesis provide novel insights into the role of PGRMC1 in breast cancer progression, sterol metabolism, oncogenic signaling, and female reproductive biology. PGRMC1 has been demonstrated to interact with enzymes of the mevalonate pathway and to enhance cholesterol, estradiol and lipid production, potentially influencing ERα and EGFR signaling. Further, PGRMC1 interacted with PHBs upon stimulation with progestins that stimulated proliferation, presumably preventing PHBs-ERα interaction and thereby indirectly promoting ERα-signaling. Interestingly, this mechanism could be strengthened by observations in newly generated PGRMC1-KO cells. The same interaction has been observed in endometrial stromal cells during decidualization, emphasizing the broad context and overarching relevance of these interactions. During decidualization, PGRMC1 expression followed a rise-to-decline pattern, and the presence of PGRMC1 at the start of the process was essential for successful decidualization.

Although this work emphasizes the potential involvement of PGRMC1 in central cellular networks, several questions remain to be addressed in the future. One major aspect to explore is the precise molecular mechanism through which PGRMC1 modulates sterol metabolism and

oncogenic signaling. Lipidomic and transcriptomic analyses in PGRMC1-overexpressing and knockout models could help dissecting how PGRMC1 influences cholesterol metabolism, lipid raft composition, and estradiol biosynthesis in breast cancer cells. Since sterol metabolism is a key determinant of cancer cell survival and therapy resistance, targeting PGRMC1's involvement in these pathways could offer new therapeutic opportunities, particularly in hormone receptor-positive breast cancer.

Another critical area for future research is the apparent discrepancy between transient knockdown and long-term knockout of PGRMC1. The lack of a distinct knockout phenotype suggests potential genetic compensation, which could be investigated through genome-wide transcriptomic and proteomic analyses. Identifying compensatory pathways may reveal PGRMC1-dependent vulnerabilities and thereby provide new ideas on the exact PGRMC1-function.

The interaction between PGRMC1 and PHBs, particularly in the context of ERα signaling and breast cancer proliferation, opens up another avenue for research. Given that PHBs are involved in transcriptional regulation of other transcription factors besides ERα, PGRMC1-PHB-interaction my present a mechanism of general indirect transcriptional regulation. The potential parallels between PGRMC1's modulation of PHBs and other known PHB regulatory proteins, such as BIG3, also deserve further exploration.

Beyond breast cancer, the role of PGRMC1 in female reproductive health, particularly in decidualization and fertility, presents another intriguing research direction. The dynamic regulation of PGRMC1 during decidualization, its interaction with PHBs, and its impact on endometrial function highlight its relevance in reproductive biology. Investigating PGRMC1 in the context of infertility-related disorders, such as endometriosis or recurrent pregnancy loss, could provide valuable translational insights.

In summary, projects associated with this thesis have uncovered novel functions of PGRMC1 in cancer metabolism, signaling, and reproductive biology, while also raising important questions about its precise molecular mechanisms. Future studies integrating functional genomics, metabolomics, and *in vivo* models will be essential to fully understand the implications of PGRMC1 and to translate these findings into clinical applications.

10. References

[1] I. Kimura *et al.*, “Functions of MAPR (membrane-associated progesterone receptor) family members as heme/steroid-binding proteins.,” *Curr Protein Pept Sci*, 2012, doi: 10.2174/138920312804142110.

[2] M. A. Cahill, J. A. Jazayeri, S. M. Catalano, S. Toyokuni, Z. Kovacevic, and D. R. Richardson, “The emerging role of progesterone receptor membrane component 1 (PGRMC1) in cancer biology,” *Biochim Biophys Acta Rev Cancer*, vol. 1866, no. 2, pp. 339–349, 2016, doi: 10.1016/j.bbcan.2016.07.004.

[3] C. Meyer, R. Schmid, P. C. Scriba, and M. Wehling, “Purification and partial sequencing of high-affinity progesterone-binding site(s) from porcine liver membranes,” *Eur J Biochem*, 1996, doi: 10.1111/j.1432-1033.1996.0726u.x.

[4] O. Selmin *et al.*, “Isolation and characterization of a novel gene induced by 2, 3, 7, 8-tetrachlorodibenzo-p-dioxin in rat liver,” *Carcinogenesis*, vol. 17, no. 12, pp. 2609–2615, Dec. 1996, doi: 10.1093/CARCIN/17.12.2609.

[5] D. Gerdes, M. Wehling, B. Leube, and E. Falkenstein, “Cloning and tissue expression of two putative steroid membrane receptors.,” *Biol Chem*, 1998.

[6] M. M. Ho, S. Barker, and G. P. Vinson, “Distribution of the adrenocortical inner zone antigen,” *J Endocrinol*, vol. 141, no. 3, pp. 459–466, 1994, doi: 10.1677/JOE.0.1410459.

[7] I. S. Ahmed, C. Chamberlain, and R. J. Craven, “S2R(Pgrmc1): the cytochrome-related sigma-2 receptor that regulates lipid and drug metabolism and hormone signaling.,” *Expert Opin Drug Metab Toxicol*, 2012, doi: 10.1517/17425255.2012.658367.

[8] S. U. R. Mir *et al.*, “Progesterone receptor membrane component 1/ Sigma-2 receptor associates with MAP1LC3B and promotes autophagy,” *Autophagy*, vol. 9, no. 10, pp. 1566–1578, 2013, doi: 10.4161/auto.25889.

[9] A. Riad *et al.*, “Sigma-2 Receptor/TMEM97 and PGRMC-1 Increase the Rate of Internalization of LDL by LDL Receptor through the Formation of a Ternary Complex,” *Sci Rep*, vol. 8, no. 1, Dec. 2018, doi: 10.1038/S41598-018-35430-3.

[10] Y. T. Tang *et al.*, “PAQR proteins: A novel membrane receptor family defined by an ancient 7-transmembrane pass motif,” *J Mol Evol*, 2005, doi: 10.1007/s00239-004-0375-2.

[11] M. A. Cahill, “The evolutionary appearance of signaling motifs in PGRMC1,” *Biosci Trends*, vol. 11, no. 2, pp. 179–192, 2017, doi: 10.5582/bst.2017.01009.

[12] M. A. Cahill, “Unde venisti PGRMC? Grand-Scale Biology from Early Eukaryotes and Eumetazoan Animal Origins,” *Frontiers in Bioscience - Landmark*, vol. 27, no. 11, 2022, doi: 10.31083/j.fbl2711317.

[13] M. Suchanek, A. Radzikowska, and C. Thiele, “Photo-leucine and photo-methionine allow identification of protein-protein interactions in living cells,” *Nat Methods*, 2005, doi: 10.1038/nmeth752.

[14] A. L. Hughes *et al.*, “Dap1/PGRMC1 Binds and Regulates Cytochrome P450 Enzymes,” *Cell Metab*, 2007, doi: 10.1016/j.cmet.2006.12.009.

[15] M. L. Mccallum *et al.*, “Conditional Ablation of Progesterone Receptor Membrane Component 1 Results in Subfertility in the Female and Development of Endometrial Cysts,” *Endocrinology*, vol. 157, no. 9, pp. 3309–3319, Sep. 2016, doi: 10.1210/EN.2016-1081.

[16] N. J. Izzo *et al.*, “Alzheimer’s therapeutics targeting amyloid beta 1-42 oligomers II: Sigma-2/PGRMC1 receptors mediate Abeta 42 oligomer binding and synaptotoxicity,” *PLoS One*, 2014, doi: 10.1371/journal.pone.0111899.

[17] K. K. Hampton, K. Anderson, H. Frazier, O. Thibault, and R. J. Craven, “Insulin Receptor Plasma Membrane Levels Increased by the Progesterone Receptor Membrane Component 1,” *Mol Pharmacol*, vol. 94, no. 1, pp. 665–673, 2018, doi: 10.1124/mol.117.110510.

[18] I. S. Ahmed, H. J. Rohe, K. E. Twist, and R. J. Craven, “Pgrmc1 (progesterone receptor membrane component 1) associates with epidermal growth factor receptor and regulates erlotinib sensitivity,” *Journal of Biological Chemistry*, 2010, doi: 10.1074/jbc.M110.134585.

[19] J. J. Peluso, D. Griffin, X. Liu, and M. Horne, “Progesterone Receptor Membrane Component-1 (PGRMC1) and PGRMC-2 Interact to Suppress Entry into the Cell Cycle in Spontaneously Immortalized Rat Granulosa Cells1,” *Biol Reprod*, 2014, doi: 10.1095/biolreprod.114.122986.

[20] M. Willibald *et al.*, “High level of Progesteron Receptor Membrane Component 1 in tissue of breast cancer patients is associated with worse response to neoadjuvant therapy,” *Hormone and Metabolic Research*, vol. 1, 2017, doi: 10.1055/s-0043-113635.

[21] H. Neubauer *et al.*, “Overexpression of progesterone receptor membrane component 1: Possible mechanism for increased breast cancer risk with norethisterone in hormone therapy,” *Menopause*, vol. 20, no. 5, pp. 504–510, May 2013, doi: 10.1097/GME.0B013E3182755C97.

[22] Y. Kabe *et al.*, “Haem-dependent dimerization of PGRMC1/Sigma-2 receptor facilitates cancer proliferation and chemoresistance,” *Nat Commun*, 2016, doi: 10.1038/ncomms11030.

[23] M. R. McGuire *et al.*, “Progesterone receptor membrane component 1 (PGRMC1) binds and stabilizes cytochromes P450 through a heme-independent mechanism,” *J Biol Chem*, vol. 297, no. 5, p. 101316, Nov. 2021, doi: 10.1016/J.JBC.2021.101316.

[24] M. R. McGuire and P. J. Espenshade, “PGRMC1: An enigmatic heme-binding protein,” *Pharmacol Ther*, 2023, doi: 10.1016/j.pharmthera.2022.108326.

[25] M. A. Cahill, J. A. Jazayeri, Z. Kovacevic, and D. R. Richardson, “PGRMC1 regulation by phosphorylation: potential new insights in controlling biological activity!,” *Oncotarget*, vol. 67, no. 12, pp. 1079–82, 2016, doi: 10.18632/oncotarget.10691.

[26] L. Schrödinger, “The PyMOL Molecular Graphics System,” 3.0. Accessed: Dec. 05, 2024. [Online]. Available: http://www.pymol.org/pymol

[27] J. Jumper *et al.*, “Highly accurate protein structure prediction with AlphaFold,” *Nature 2021 596:7873*, vol. 596, no. 7873, pp. 583–589, Jul. 2021, doi: 10.1038/s41586-021-03819-2.

[28] M. Uhlén *et al.*, “Proteomics. Tissue-based map of the human proteome,” *Science*, vol. 347, no. 6220, Jan. 2015, doi: 10.1126/SCIENCE.1260419.

[29] R. B. Piel *et al.*, “A Novel Role for Progesterone Receptor Membrane Component 1 (PGRMC1): A Partner and Regulator of Ferrochelatase,” *Biochemistry*, vol. 55, no. 37, pp. 5204–5217, Sep. 2016, doi: 10.1021/ACS.BIOCHEM.6B00756.

[30] K. Ghosh *et al.*, “Spectroscopic and biochemical characterization of heme binding to yeast Dap1p and mouse PGRMC1p,” *Biochemistry*, vol. 44, no. 50, pp. 16729–16736, Dec. 2005, doi: 10.1021/BI0511585.

[31] L. Min *et al.*, “Molecular identification of adrenal inner zone antigen as a heme-binding protein,” *FEBS J*, vol. 272, no. 22, pp. 5832–5843, Nov. 2005, doi: 10.1111/J.1742-4658.2005.04977.X.

[32] A. M. Thompson *et al.*, “Measurement of the heme affinity for yeast dap1p, and its importance in cellular function,” *Biochemistry*, vol. 46, no. 50, pp. 14629–14637, Dec. 2007, doi: 10.1021/BI7013739.

[33] I. Hamza and H. A. Dailey, “One ring to rule them all: Trafficking of heme and heme synthesis intermediates in the metazoans,” *Biochimica et Biophysica Acta (BBA) - Molecular Cell Research*, vol. 1823, no. 9, pp. 1617–1632, Sep. 2012, doi: 10.1016/J.BBAMCR.2012.04.009.

[34] R. B. Piel, H. A. Dailey, and A. E. Medlock, “The Mitochondrial Heme Metabolon: Insights into the Complex(ity) of Heme Synthesis and Distribution,” *Mol Genet Metab*, vol. 128, no. 3, p. 198, Nov. 2019, doi: 10.1016/J.YMGME.2019.01.006.

[35] A. Galmozzi *et al.*, “PGRMC2 is an intracellular haem chaperone critical for adipocyte function,” *Nature 2019 576:7785*, vol. 576, no. 7785, pp. 138–142, Nov. 2019, doi: 10.1038/s41586-019-1774-2.

[36] X. Yuan *et al.*, “Regulation of intracellular heme trafficking revealed by subcellular reporters,” *Proc Natl Acad Sci U S A*, vol. 113, no. 35, pp. E5144–E5152, Aug. 2016, doi: 10.1073/PNAS.1609865113.

[37] D. W. Nebert, K. Wikvall, and W. L. Miller, “Human cytochromes P450 in health and disease,” *Philosophical Transactions of the Royal Society B: Biological Sciences*, vol. 368, no. 1612, p. 20120431, Feb. 2013, doi: 10.1098/RSTB.2012.0431.

[38] J. Liu, Y. F. Lu, J. C. Corton, and C. D. Klaassen, “Expression of cytochrome P450 isozyme transcripts and activities in human livers,” *Xenobiotica*, vol. 51, no. 3, p. 279, 2020, doi: 10.1080/00498254.2020.1867929.

[39] B. T. Zhu, “On the General Mechanism of Selective Induction of Cytochrome P450 Enzymes by Chemicals: Some Theoretical Considerations,” *Expert Opin Drug Metab Toxicol*, vol. 6, no. 4, p. 483, Apr. 2010, doi: 10.1517/17425250903578642.

[40] L. W. Weber, M. Boll, and A. Stampfl, “Maintaining cholesterol homeostasis: Sterol regulatory element-binding proteins,” *World J Gastroenterol*, 2004, doi: 10.3748/wjg.v10.i21.3081.

[41] Y. Sakakura *et al.*, “Sterol regulatory element-binding proteins induce an entire pathway of cholesterol synthesis,” *Biochem Biophys Res Commun*, 2001, doi: 10.1006/bbrc.2001.5375.

[42] A. Jeong, K. F. Suazo, W. G. Wood, M. D. Distefano, and L. Li, “Isoprenoids and Protein Prenylation: Implications in the Pathogenesis and Therapeutic Intervention of Alzheimer’s Disease,” *Crit Rev Biochem Mol Biol*, vol. 53, no. 3, p. 279, May 2018, doi: 10.1080/10409238.2018.1458070.

[43] F. Bray Bsc *et al.*, “Global cancer statistics 2022: GLOBOCAN estimates of incidence and mortality worldwide for 36 cancers in 185 countries,” *CA Cancer J Clin*, vol. 74, no. 3, pp. 229–263, May 2024, doi: 10.3322/CAAC.21834.

[44] K. McPherson, C. M. Steel, and J. M. Dixon, “Breast cancer—epidemiology, risk factors, and genetics,” *Bmj*, vol. 321, no. 7261, p. 624, 2000, doi: 10.1136/bmj.321.7261.624.

[45] D. Hanahan and R. A. Weinberg, “The hallmarks of cancer,” *Cell*, vol. 100, no. 1, pp. 57–70, Jan. 2000, doi: 10.1016/S0092-8674(00)81683-9.

[46] D. Hanahan, “Hallmarks of Cancer: New Dimensions,” *Cancer Discov*, vol. 12, no. 1, pp. 31–46, Jan. 2022, doi: 10.1158/2159-8290.CD-21-1059.

[47] R. K. Thomas *et al.*, “High-throughput oncogene mutation profiling in human cancer,” *Nat Genet*, vol. 39, no. 3, pp. 347–351, Mar. 2007, doi: 10.1038/NG1975.

[48] X. Zhu *et al.*, “Metastatic non-small-cell lung cancer without driver mutations: projections by therapy line in Western Europe, 2021–2026,” *Future Oncology*, vol. 19, no. 33, pp. 2237–2250, Oct. 2023, doi: 10.2217/FON-2023-0063.

[49] L. Chen, S. Liu, and Y. Tao, “Regulating tumor suppressor genes: post-translational modifications,” *Signal Transduction and Targeted Therapy 2020 5:1*, vol. 5, no. 1, pp. 1–25, Jun. 2020, doi: 10.1038/s41392-020-0196-9.

[50] S. Sioshansi, K. E. Huber, and D. E. Wazer, “The Implications of Breast Cancer Molecular Phenotype for Radiation Oncology,” *Front Oncol*, vol. 1, no. June, pp. 1–9, 2011, doi: 10.3389/fonc.2011.00012.

[51] K. J. Thompson *et al.*, “Luminal androgen receptor breast cancer subtype and investigation of the microenvironment and neoadjuvant chemotherapy response,” *NAR Cancer*, vol. 4, no. 2, Apr. 2022, doi: 10.1093/NARCAN/ZCAC018.

[52] C. Fougner, H. Bergholtz, J. H. Norum, and T. Sørlie, “Re-definition of claudin-low as a breast cancer phenotype,” *Nature Communications 2020 11:1*, vol. 11, no. 1, pp. 1–11, Apr. 2020, doi: 10.1038/s41467-020-15574-5.

[53] R. M. Pommier *et al.*, “Comprehensive characterization of claudin-low breast tumors reflects the impact of the cell-of-origin on cancer evolution,” *Nature Communications 2020 11:1*, vol. 11, no. 1, pp. 1–12, Jul. 2020, doi: 10.1038/s41467-020-17249-7.

[54] T. Sorlie *et al.*, “Gene expression patterns of breast carcinomas distinguish tumor subclasses with clinical implications,” *Proc Natl Acad Sci U S A*, vol. 98, no. 19, pp. 10869–10874, 2001, doi: 10.1073/pnas.191367098.

[55] A. Zarros, A. J. Fornace, T. Simoncini, and V. M. Quirke, “Tamoxifen from Failed Contraceptive Pill to Best-Selling Breast Cancer Medicine: A Case-Study in Pharmaceutical Innovation,” *Front Pharmacol*, vol. 8, no. SEP, p. 620, Sep. 2017, doi: 10.3389/FPHAR.2017.00620.

[56] “Kommission Mamma | Leitlinien & Empfehlungen | Leitlinien & Stellungnahmen | AGO - Die Arbeitsgemeinschaft Gynäkologische Onkologie.” Accessed: Feb. 16, 2025. [Online]. Available: https://www.ago-online.de/leitlinien-empfehlungen/leitlinien-empfehlungen/kommission-mamma

[57] R. L. N. Godone, G. M. Leitão, N. B. Araújo, C. H. M. Castelletti, J. L. Lima-Filho, and D. B. G. Martins, “Clinical and molecular aspects of breast cancer: Targets and therapies,” *Biomedicine and Pharmacotherapy*, vol. 106, no. January, pp. 14–34, 2018, doi: 10.1016/j.biopha.2018.06.066.

[58] Y. Zhao and X. Ruan, “Identification of PGRMC1 as a Candidate Oncogene for Head and Neck Cancers and Its Involvement in Metabolic Activities,” *Front Bioeng Biotechnol*, vol. 7, p. 502795, Jan. 2020, doi: 10.3389/FBIOE.2019.00438/BIBTEX.

[59] D. A. Pedroza, V. Rajamanickam, R. Subramani, A. Bencomo, A. Galvez, and R. Lakshmanaswamy, “Progesterone receptor membrane component 1 promotes the growth of breast cancers by altering the phosphoproteome and augmenting EGFR/PI3K/AKT signalling,” *Br J Cancer*, vol. 123, no. 8, pp. 1326–1335, Oct. 2020, doi: 10.1038/S41416-020-0992-6.

[60] X. Ruan *et al.*, “Increased expression of progesterone receptor membrane component 1 is associated with aggressive phenotype and poor prognosis in ER-positive and negative breast cancer,” *Menopause*, vol. 24, no. 2, pp. 203–209, 2017, doi: 10.1097/GME.0000000000000739.

[61] C. C. Shih *et al.*, “Role of PGRMC1 in cell physiology of cervical cancer,” *Life Sci*, vol. 231, Aug. 2019, doi: 10.1016/J.LFS.2019.06.016.

[62] K. K. Hampton, R. Stewart, D. Napier, P. P. Claudio, and R. J. Craven, “PGRMC1 Elevation in Multiple Cancers and Essential Role in Stem Cell Survival,” *Adv Lung Cancer (Irvine)*, vol. 4, no. 3, pp. 37–51, 2015, doi: 10.4236/ALC.2015.43006.

[63] D. Zhang *et al.*, “PGRMC1 is a novel potential tumor biomarker of human renal cell carcinoma based on quantitative proteomic and integrative biological assessments,” *PLoS One*, 2017, doi: 10.1371/journal.pone.0170453.

[64] C. R. Cardwell, B. M. Hicks, C. Hughes, and L. J. Murray, “Statin Use After Colorectal Cancer Diagnosis and Survival: A Population-Based Cohort Study.,” *J Clin Oncol*, 2014, doi: 10.1200/JCO.2013.54.4569.

[65] E. H. Allott *et al.*, “Serum lipid profile and risk of prostate cancer recurrence: Results from the SEARCH database.,” *Cancer Epidemiol Biomarkers Prev*, 2014, doi: 10.1158/1055-9965.EPI-14-0458.

[66] E. J. Jacobs, C. C. Newton, M. J. Thun, and S. M. Gapstur, “Long-term use of cholesterol-lowering drugs and cancer incidence in a large United States cohort,” *Cancer Res*, 2011, doi: 10.1158/0008-5472.CAN-10-2953.

[67] K. Shafique, P. McLoone, K. Qureshi, H. Leung, C. Hart, and D. S. Morrison, “Cholesterol and the risk of grade-specific prostate cancer incidence: evidence from two large prospective cohort studies with up to 37 years’ follow up,” *BMC Cancer*, 2012, doi: 10.1186/1471-2407-12-25.

[68] L. Cedó, S. T. Reddy, E. Mato, F. Blanco-Vaca, and J. C. Escolà-Gil, “HDL and LDL: Potential New Players in Breast Cancer Development,” *J Clin Med*, vol. 8, no. 6, p. 853, Jun. 2019, doi: 10.3390/JCM8060853.

[69] C. Rodrigues Dos Santos *et al.*, “LDL-cholesterol signaling induces breast cancer proliferation and invasion,” *Lipids Health Dis*, vol. 13, no. 1, pp. 1–9, 2014, doi: 10.1186/1476-511X-13-16.

[70] G. Llaverias *et al.*, “Role of cholesterol in the development and progression of breast cancer,” *Am J Pathol*, vol. 178, no. 1, pp. 402–412, 2011, doi: 10.1016/J.AJPATH.2010.11.005.

[71] K. Pelton *et al.*, “Hypercholesterolemia induces angiogenesis and accelerates growth of breast tumors in vivo,” *Am J Pathol*, vol. 184, no. 7, pp. 2099–2110, 2014, doi: 10.1016/J.AJPATH.2014.03.006.

[72] C. J. Antalis, A. Uchida, K. K. Buhman, and R. A. Siddiqui, “Migration of MDA-MB-231 breast cancer cells depends on the availability of exogenous lipids and cholesterol esterification,” *Clin Exp Metastasis*, 2011, doi: 10.1007/s10585-011-9405-9.

[73] J. A. Menendez and R. Lupu, “Fatty acid synthase and the lipogenic phenotype in cancer pathogenesis,” *Nat Rev Cancer*, vol. 7, no. 10, pp. 763–777, 2007, doi: 10.1038/nrc2222.

[74] G. Marwarha, S. Raza, K. Hammer, and O. Ghribi, “27-hydroxycholesterol: A novel player in molecular carcinogenesis of breast and prostate cancer,” *Chem Phys Lipids*, vol. 207, pp. 108–126, 2017, doi: 10.1016/j.chemphyslip.2017.05.012.

[75] E. R. Nelson, C. yi Chang, and D. P. McDonnell, “Cholesterol and breast cancer pathophysiology,” *Trends in Endocrinology and Metabolism*, vol. 25, no. 12, pp. 649–655, 2014, doi: 10.1016/j.tem.2014.10.001.

[76] A. S. Greenberg *et al.*, “The role of lipid droplets in metabolic disease in rodents and humans,” *J Clin Invest*, vol. 121, no. 6, p. 2102, Jun. 2011, doi: 10.1172/JCI46069.

[77] F. Mollinedo and C. Gajate, “Lipid rafts as major platforms for signaling regulation in cancer,” *Adv Biol Regul*, 2015, doi: 10.1016/j.jbior.2014.10.003.

[78] Y. C. Li, M. J. Park, S. K. Ye, C. W. Kim, and Y. N. Kim, “Elevated levels of cholesterol-rich lipid rafts in cancer cells are correlated with apoptosis sensitivity induced by cholesterol-depleting agents,” *American Journal of Pathology*, vol. 168, no. 4, pp. 1107–1118, 2006, doi: 10.2353/ajpath.2006.050959.

[79] G. Orr, D. Hu, S. Özçelik, L. K. Opresko, H. S. Wiley, and S. D. Colson, “Cholesterol dictates the freedom of EGF receptors and HER2 in the plane of the membrane,” *Biophys J*, 2005, doi: 10.1529/biophysj.104.056192.

[80] S. Morandell, T. Stasyk, S. Skvortsov, S. Ascher, and L. A. Huber, “Quantitative proteomics and phosphoproteomics reveal novel insights into complexity and dynamics of the EGFR signaling network,” *Proteomics*, 2008, doi: 10.1002/pmic.200800204.

[81] E. M. Fox, J. Andrade, and M. A. Shupnik, “Novel actions of estrogen to promote proliferation: Integration of cytoplasmic and nuclear pathways,” *Steroids*, 2009, doi: 10.1016/j.steroids.2008.10.014.

[82] C. D. DuSell, M. Umetani, P. W. Shaul, D. J. Mangelsdorf, and D. P. McDonnell, “27-Hydroxycholesterol Is an Endogenous Selective Estrogen Receptor Modulator,” *Molecular Endocrinology*, vol. 22, no. 1, pp. 65–77, 2008, doi: 10.1210/me.2007-0383.

[83] D. J. Slamon, G. M. Clark, S. G. Wong, W. J. Levin, A. Ullrich, and W. L. McGuire, “Human breast cancer: correlation of relapse and survival with amplification of the HER-2/neu

oncogene," *Science*, vol. 235, no. 4785, pp. 182–191, 1987, doi: 10.1126/SCIENCE.3798106.

[84] S. Arnesen *et al.*, "Estrogen Receptor Alpha Mutations in Breast Cancer Cells Cause Gene Expression Changes through Constant Activity and Secondary Effects," *Cancer Res*, vol. 81, no. 3, pp. 539–551, Feb. 2021, doi: 10.1158/0008-5472.CAN-20-1171.

[85] J. A. Wickenden and C. J. Watson, "Key signalling nodes in mammary gland development and cancer. Signalling downstream of PI3 kinase in mammary epithelium: a play in 3 Akts," *Breast Cancer Res*, vol. 12, no. 2, p. 202, Apr. 2010, doi: 10.1186/BCR2558.

[86] J. J. K. Lee *et al.*, "ERα-associated translocations underlie oncogene amplifications in breast cancer," *Nature 2023 618:7967*, vol. 618, no. 7967, pp. 1024–1032, May 2023, doi: 10.1038/s41586-023-06057-w.

[87] X. Liu *et al.*, "The importance of EGFR as a biomarker in molecular apocrine breast cancer," *Hum Pathol*, vol. 77, pp. 1–10, Jul. 2018, doi: 10.1016/J.HUMPATH.2018.01.016.

[88] C. Gillett *et al.*, "Cyclin D1 and Prognosis In Human Breast Cancer," *Int. J. Cancer (Pred. Oncol.)*, vol. 0, pp. 92–99, 1996, doi: 10.1002/(SICI)1097-0215(19960422)69:2.

[89] S. Lehn *et al.*, "Down-Regulation of the Oncogene Cyclin D1 Increases Migratory Capacity in Breast Cancer and Is Linked to Unfavorable Prognostic Features," *Am J Pathol*, vol. 177, no. 6, pp. 2886–2897, Dec. 2010, doi: 10.2353/AJPATH.2010.100303.

[90] S. Banerji *et al.*, "Sequence analysis of mutations and translocations across breast cancer subtypes," *Nature 2012 486:7403*, vol. 486, no. 7403, pp. 405–409, Jun. 2012, doi: 10.1038/nature11154.

[91] J. A. Wickenden and C. J. Watson, "The components of the PI3K/Akt pathway," *Breast Cancer Research*, 2010, Accessed: Dec. 31, 2024. [Online]. Available: http://breast-cancer-research.com/content/12/2/202

[92] A. K. Witkiewicz and E. S. Knudsen, "Retinoblastoma tumor suppressor pathway in breast cancer: prognosis, precision medicine, and therapeutic interventions," *Breast Cancer Res*, vol. 16, no. 3, p. 207, May 2014, doi: 10.1186/BCR3652.

[93] K. B. Kuchenbaecker *et al.*, “Risks of breast, ovarian, and contralateral breast cancer for BRCA1 and BRCA2 mutation carriers,” *JAMA*, 2017, doi: 10.1001/jama.2017.7112.

[94] Y. Zhao *et al.*, “The presence of a membrane-bound progesterone receptor induces growth of breast cancer with norethisterone but not with progesterone: A xenograft model,” *Maturitas*, 2017, doi: 10.1016/j.maturitas.2017.05.007.

[95] H. Neubauer *et al.*, “Breast cancer proteomics reveals correlation between estrogen receptor status and differential phosphorylation of PGRMC1,” *Breast Cancer Research*, vol. 10, no. 5, pp. 1–16, 2008, doi: 10.1186/bcr2155.

[96] B. M. Thejer *et al.*, “PGRMC1 phosphorylation affects cell shape, motility, glycolysis, mitochondrial form and function, and tumor growth,” *BMC Mol Cell Biol*, vol. 21, no. 1, pp. 1–24, Apr. 2020, doi: 10.1186/S12860-020-00256-3/FIGURES/7.

[97] J. Y. Kim *et al.*, “Progesterone Receptor Membrane Component 1 suppresses the p53 and Wnt/β-catenin pathways to promote human pluripotent stem cell self-renewal,” *Sci Rep*, vol. 8, no. 1, pp. 1–16, 2018, doi: 10.1038/s41598-018-21322-z.

[98] M. Willibald, “Role of PGRMC1 in breast cancer progression and increased breast cancer risk upon progestin-based hormone therapy,” Dissertation, Heinrich-Heine University Duesseldorf, 2017.

[99] H. Asperger *et al.*, “Progesterone receptor membrane component 1 regulates lipid homeostasis and drives oncogenic signaling resulting in breast cancer progression,” *Breast Cancer Research*, 2020, doi: 10.1186/s13058-020-01312-8.

[100] L. Wang-Eckhardt and M. Eckhardt, “A progesterone receptor membrane component 1 antagonist induces large vesicles independent of progesterone receptor membrane component 1 expression,” *Biol Chem*, 2020, doi: 10.1515/hsz-2019-0417.

[101] R. Barrangou *et al.*, “CRISPR provides acquired resistance against viruses in prokaryotes,” *Science*, vol. 315, no. 5819, pp. 1709–1712, Mar. 2007, doi: 10.1126/SCIENCE.1138140.

[102] M. Jinek, K. Chylinski, I. Fonfara, M. Hauer, J. A. Doudna, and E. Charpentier, “A programmable dual-RNA-guided DNA endonuclease in adaptive bacterial immunity,”

Science (1979), vol. 337, no. 6096, pp. 816–821, Aug. 2012, doi: 10.1126/SCIENCE.1225829/SUPPL_FILE/JINEK.SM.PDF.

[103] Y. Ishino, H. Shinagawa, K. Makino, M. Amemura, and A. Nakatura, "Nucleotide sequence of the iap gene, responsible for alkaline phosphatase isozyme conversion in Escherichia coli, and identification of the gene product," *J Bacteriol*, vol. 169, no. 12, pp. 5429–5433, 1987, doi: 10.1128/JB.169.12.5429-5433.1987.

[104] R. Barrangou, "CRISPR-Cas systems and RNA-guided interference," *Wiley Interdiscip Rev RNA*, vol. 4, no. 3, pp. 267–278, May 2013, doi: 10.1002/WRNA.1159.

[105] M. Pacesa, O. Pelea, and M. Jinek, "Past, present, and future of CRISPR genome editing technologies," *Cell*, vol. 187, no. 5, pp. 1076–1100, Feb. 2024, doi: 10.1016/J.CELL.2024.01.042.

[106] C. Xue and E. C. Greene, "DNA repair pathway choices in CRISPR-Cas9 mediated genome editing," *Trends Genet*, vol. 37, no. 7, p. 639, Jul. 2021, doi: 10.1016/J.TIG.2021.02.008.

[107] H. D. Soule, J. Vazquez, A. Long, S. Albert, and M. Brennan, "A Human Cell Line From a Pleural Effusion Derived From a Breast Carcinoma 2," *JNCI: Journal of the National Cancer Institute*, vol. 51, no. 5, pp. 1409–1416, 1973, doi: 10.1093/jnci/51.5.1409.

[108] Y. Bai *et al.*, "Pgrmc1 promotes progestin-dependent proliferation of breast cancer cells by binding prohibitins resulting in activation of erα signaling," *Cancers (Basel)*, vol. 13, no. 22, p. 5635, Nov. 2021, doi: 10.3390/CANCERS13225635/S1.

[109] R. Cailleau, R. Young, M. Olivé, and W. J. Reeves, "Breast tumor cell lines from pleural effusions," *J Natl Cancer Inst*, 1974, doi: 10.1093/jnci/53.3.661.

[110] A. Untergasser *et al.*, "Primer3--new capabilities and interfaces," *Nucleic Acids Res*, vol. 40, no. 15, Aug. 2012, doi: 10.1093/NAR/GKS596.

[111] F. Corpet, "Multiple sequence alignment with hierarchical clustering," *Nucleic Acids Res*, vol. 16, no. 22, pp. 10881–10890, Nov. 1988, doi: 10.1093/NAR/16.22.10881.

[112] E. Gasteiger, A. Gattiker, C. Hoogland, I. Ivanyi, R. D. Appel, and A. Bairoch, "ExPASy: The proteomics server for in-depth protein knowledge and analysis," *Nucleic Acids Res*, vol. 31, no. 13, pp. 3784–3788, Jul. 2003, doi: 10.1093/NAR/GKG563.

[113] K. Labun, T. G. Montague, M. Krause, Y. N. Torres Cleuren, H. Tjeldnes, and E. Valen, “CHOPCHOP v3: expanding the CRISPR web toolbox beyond genome editing,” *Nucleic Acids Res*, vol. 47, no. W1, pp. W171–W174, Jul. 2019, doi: 10.1093/NAR/GKZ365.

[114] S. Bae, J. Park, and J. S. Kim, “Cas-OFFinder: a fast and versatile algorithm that searches for potential off-target sites of Cas9 RNA-guided endonucleases,” *Bioinformatics*, vol. 30, no. 10, pp. 1473–1475, May 2014, doi: 10.1093/BIOINFORMATICS/BTU048.

[115] Julia Oles, “Characterization of PGRMC1-deficient breast cancer cell lines,” M. Sc.Thesis, Heinrich-Heine University Hospital Duesseldorf, Duesseldorf, 2023.

[116] J. J. Peluso, J. Romak, and X. Liu, “Progesterone Receptor Membrane Component-1 (PGRMC1) Is the Mediator of Progesterone’s Antiapoptotic Action in Spontaneously Immortalized Granulosa Cells As Revealed by PGRMC1 Small Interfering Ribonucleic Acid Treatment and Functional Analysis of PGRMC1 Mutations,” *Endocrinology*, vol. 149, no. 2, p. 534, Feb. 2007, doi: 10.1210/EN.2007-1050.

[117] D. Kaluka, D. Batabyal, B. Y. Chiang, T. L. Poulos, and S. R. Yeh, “Spectroscopic and Mutagenesis Studies of Human PGRMC1,” *Biochemistry*, vol. 54, no. 8, p. 1638, Mar. 2015, doi: 10.1021/BI501177E.

[118] P. Thomas, Y. Pang, and J. Dong, “Enhancement of Cell Surface Expression and Receptor Functions of Membrane Progestin Receptor α (mPRα) by Progesterone Receptor Membrane Component 1 (PGRMC1): Evidence for a Role of PGRMC1 as an Adaptor Protein for Steroid Receptors,” *Endocrinology*, vol. 155, no. 3, p. 1107, Mar. 2014, doi: 10.1210/EN.2013-1991.

[119] D. Fitzpatrick, K. Pirie, G. Reeves, J. Green, and V. Beral, “Combined and progestagen-only hormonal contraceptives and breast cancer risk: A UK nested case–control study and meta-analysis,” *PLoS Med*, vol. 20, no. 3, p. e1004188, Mar. 2023, doi: 10.1371/JOURNAL.PMED.1004188.

[120] J. Niemeyer Hultstrand, K. Gemzell-Danielsson, H. K. Kallner, H. Lindman, P. Wikman, and I. Sundström-Poromaa, “Hormonal contraception and risk of breast cancer and breast cancer in situ among Swedish women 15–34 years of age: A nationwide register-based study,” *The Lancet Regional Health - Europe*, vol. 21, p. 100470, Oct. 2022, doi: 10.1016/J.LANEPE.2022.100470.

[121] R. A. Lobo, J. H. Pickar, J. C. Stevenson, W. J. Mack, and H. N. Hodis, “Back to the future: Hormone replacement therapy as part of a prevention strategy for women at the onset of menopause,” *Atherosclerosis*, vol. 254, pp. 282–290, Nov. 2016, doi: 10.1016/J.ATHEROSCLEROSIS.2016.10.005.

[122] E. Banks *et al.*, “Breast cancer and hormone-replacement therapy in the Million Women Study,” *Lancet*, vol. 362, no. 9382, pp. 419–427, Aug. 2003, doi: 10.1016/S0140-6736(03)14065-2.

[123] A. Fournier, F. Berrino, and F. Clavel-Chapelon, “Unequal risks for breast cancer associated with different hormone replacement therapies: Results from the E3N cohort study,” *Breast Cancer Res Treat*, 2008, doi: 10.1007/s10549-007-9523-x.

[124] M. Willibald *et al.*, “Progesterone receptor membrane component 1 is phosphorylated upon progestin treatment in breast cancer cells.,” *Oncotarget*, 2017, doi: 10.18632/oncotarget.19819.

[125] J. I. C. Chen *et al.*, “Proteomic characterization of midproliferative and midsecretory human endometrium,” *J Proteome Res*, vol. 8, no. 4, pp. 2032–2044, Apr. 2009, doi: 10.1021/PR801024G.

[126] L. Feng *et al.*, “Progesterone receptor membrane component 1 (PGRMC1) expression in fetal membranes among women with preterm premature rupture of the membranes (PPROM),” *Placenta*, vol. 35, no. 5, pp. 331–333, 2014, doi: 10.1016/J.PLACENTA.2014.03.008.

[127] M. Abdalla, H. Deshmukh, S. L. Atkin, and T. Sathyapalan, “miRNAs as a novel clinical biomarker and therapeutic targets in polycystic ovary syndrome (PCOS): A review,” *Life Sci*, vol. 259, Oct. 2020, doi: 10.1016/J.LFS.2020.118174.

[128] X. J. Wu, P. Thomas, and Y. Zhu, “Pgrmc1 knockout impairs oocyte maturation in zebrafish,” *Front Endocrinol (Lausanne)*, vol. 9, no. SEP, p. 400527, Sep. 2018, doi: 10.3389/FENDO.2018.00560.

[129] H. Okada, T. Tsuzuki, and H. Murata, “Decidualization of the human endometrium,” *Reprod Med Biol*, Dec. 2018, doi: 10.1002/rmb2.12088.

[130] S. Salsano *et al.*, “Novel nonclassic progesterone receptor PGRMC1 pulldown-precipitated proteins reveal a key role during human decidualization,” *Fertil Steril*, vol. 113, no. 5, pp. 1050-1066.e7, May 2020, doi: 10.1016/J.FERTNSTERT.2020.01.008.

[131] S. Salsano, R. González-Martín, A. Quiñonero, S. Pérez-Debén, and F. Domínguez, “Deciphering the Role of PGRMC1 During Human Decidualization Using an In Vitro Approach,” *J Clin Endocrinol Metab*, vol. 106, no. 8, pp. 2313–2327, Jul. 2021, doi: 10.1210/CLINEM/DGAB303.

[132] H. Sung *et al.*, “Global Cancer Statistics 2020: GLOBOCAN Estimates of Incidence and Mortality Worldwide for 36 Cancers in 185 Countries,” *CA Cancer J Clin*, 2021, doi: 10.3322/caac.21660.

[133] M. A. Cahill, “Progesterone receptor membrane component 1: An integrative review,” *Journal of Steroid Biochemistry and Molecular Biology*, Jan. 2007, doi: 10.1016/j.jsbmb.2007.02.002.

[134] M. Willibald, I. Wurster, C. Meisner, U. Vogel, H. Seeger, and H. Neubauer, “High level of Progesteron Receptor Membrane Component 1 in tissue of breast cancer patients is associated with worse response to neoadjuvant therapy,” vol. 1, no. Pgrmc 1, 2017.

[135] C. S. Ryu, K. Klein, and U. M. Zanger, “Membrane associated progesterone receptors: Promiscuous proteins with pleiotropic functions - Focus on interactions with cytochromes P450,” *Front Pharmacol*, vol. 8, no. MAR, pp. 1–8, 2017, doi: 10.3389/fphar.2017.00159.

[136] U. Sen, C. Coleman, and T. Sen, “Stearoyl coenzyme A desaturase-1: multitasker in cancer, metabolism, and ferroptosis,” *Trends Cancer*, vol. 9, no. 6, pp. 480–489, Jun. 2023, doi: 10.1016/J.TRECAN.2023.03.003.

[137] E. Currie, A. Schulze, R. Zechner, T. C. Walther, and R. V. Farese, “Cellular fatty acid metabolism and cancer,” *Cell Metab*, 2013, doi: 10.1016/j.cmet.2013.05.017.

[138] M. E. Monaco, “Fatty acid metabolism in breast cancer subtypes,” *Oncotarget*, 2017, doi: 10.18632/oncotarget.15494.

[139] N. Marino *et al.*, “Upregulation of lipid metabolism genes in the breast prior to cancer diagnosis,” *npj Breast Cancer 2020 6:1*, vol. 6, no. 1, pp. 1–13, Oct. 2020, doi: 10.1038/s41523-020-00191-8.

[140] R. Lappano *et al.*, “The Cholesterol Metabolite 25-Hydroxycholesterol Activates Estrogen Receptor α-Mediated Signaling in Cancer Cells and in Cardiomyocytes,” *PLoS One*, vol. 6, no. 1, p. e16631, 2011, doi: 10.1371/JOURNAL.PONE.0016631.

[141] R. J. Craven, “PGRMC1: A new biomarker for the estrogen receptor in breast cancer,” *Breast Cancer Research*, vol. 10, no. 6, pp. 6–7, 2008, doi: 10.1186/bcr2191.

[142] D. A. Pedroza *et al.*, “Crosstalk between progesterone receptor membrane component 1 and estrogen receptor α promotes breast cancer cell proliferation,” *Lab Invest*, vol. 101, no. 6, pp. 733–744, Jun. 2021, doi: 10.1038/S41374-021-00594-6.

[143] X. Xu *et al.*, “Comprehensive Analysis of the Implication of PGRMC1 in Triple-Negative Breast Cancer,” *Front Bioeng Biotechnol*, vol. 9, p. 714030, Oct. 2021, doi: 10.3389/FBIOE.2021.714030.

[144] S. Borgquist, O. Bjarnadottir, S. Kimbung, and T. P. Ahern, “Statins: a role in breast cancer therapy?,” *J Intern Med*, vol. 284, no. 4, p. 346, Oct. 2018, doi: 10.1111/JOIM.12806.

[145] N. Yoshitani *et al.*, “A structure-based strategy for discovery of small ligands binding to functionally unknown proteins: Combination of in silico screening and surface plasmon resonance measurements,” *Proteomics*, vol. 5, no. 6, pp. 1472–1480, Apr. 2005, doi: 10.1002/PMIC.200401032.

[146] I. S. Ahmed, H. J. Rohe, K. E. Twist, M. N. Mattingly, and R. J. Craven, “Progesterone receptor membrane component 1 (Pgrmc1): A heme-1 domain protein that promotes tumorigenesis and is inhibited by a small molecule,” *Journal of Pharmacology and Experimental Therapeutics*, 2010, doi: 10.1124/jpet.109.164210.

[147] M. Zhang *et al.*, “Progesterone receptor membrane component 1 is a functional part of the glucagon-like peptide-1 (GLP-1) receptor complex in pancreatic β cells,” *Molecular and Cellular Proteomics*, 2014, doi: 10.1074/mcp.M114.040196.

[148] C. Thieffry *et al.*, "AG-205 Upregulates Enzymes Involved in Cholesterol Biosynthesis and Steroidogenesis in Human Endometrial Cells Independently of PGRMC1 and Related MAPR Proteins," *Biomolecules 2021, Vol. 11, Page 1472*, vol. 11, no. 10, p. 1472, Oct. 2021, doi: 10.3390/BIOM11101472.

[149] L. Wang-Eckhardt, I. Becker, and M. Eckhardt, "The PGRMC1 Antagonist AG-205 Inhibits Synthesis of Galactosylceramide and Sulfatide," *Cells*, vol. 10, no. 12, Dec. 2021, doi: 10.3390/CELLS10123520.

[150] Y. Kabe *et al.*, "Glycyrrhizin derivatives suppress cancer chemoresistance by inhibiting progesterone receptor membrane component 1," *Cancers (Basel)*, vol. 13, no. 13, p. 3265, Jul. 2021, doi: 10.3390/CANCERS13133265/S1.

[151] H. Oh, A. Choi, N. Seo, J. S. Lim, J. S. You, and Y. E. Chung, "Protective effect of glycyrrhizin, a direct HMGB1 inhibitor, on post-contrast acute kidney injury," *Scientific Reports 2021 11:1*, vol. 11, no. 1, pp. 1–12, Aug. 2021, doi: 10.1038/s41598-021-94928-5.

[152] C. Wang *et al.*, "Stearoyl-CoA desaturase 1 (SCD1) facilitates the growth and anti-ferroptosis of gastric cancer cells and predicts poor prognosis of gastric cancer," *Aging*, vol. 12, no. 15, pp. 15374–15391, Aug. 2020, doi: 10.18632/AGING.103598.

[153] J. H. You, J. Lee, and J. L. Roh, "PGRMC1-dependent lipophagy promotes ferroptosis in paclitaxel-tolerant persister cancer cells," *Journal of Experimental and Clinical Cancer Research*, vol. 40, no. 1, pp. 1–18, 2021, doi: 10.1186/s13046-021-02168-2.

[154] Y. Zhao, X. Ruan, J. Cheng, X. Xu, M. Gu, and A. O. Mueck, "PGRMC1 promotes triple-negative breast cancer cell growth via suppressing ferroptosis," *Climacteric*, vol. 26, no. 2, pp. 135–142, 2023, doi: 10.1080/13697137.2023.2170225.

[155] A. Ishibashi, K. Saga, Y. Hisatomi, Y. Li, Y. Kaneda, and K. Nimura, "A simple method using CRISPR-Cas9 to knock-out genes in murine cancerous cell lines," *Scientific Reports 2020 10:1*, vol. 10, no. 1, pp. 1–10, Dec. 2020, doi: 10.1038/s41598-020-79303-0.

[156] C. J. Giuliano, A. Lin, V. Girish, and J. M. Sheltzer, "Generating Single Cell–Derived Knockout Clones in Mammalian Cells with CRISPR/Cas9," *Curr Protoc Mol Biol*, vol. 128, no. 1, p. e100, Sep. 2019, doi: 10.1002/CPMB.100.

[157] T. Yang, J. Ou, and E. Yildirim, “Xist exerts gene-specific silencing during XCI maintenance and impacts lineage-specific cell differentiation and proliferation during hematopoiesis,” *Nature Communications 2022 13:1*, vol. 13, no. 1, pp. 1–19, Aug. 2022, doi: 10.1038/s41467-022-32273-5.

[158] T. Tukiainen *et al.*, “Landscape of X chromosome inactivation across human tissues,” *Nature 2017 550:7675*, vol. 550, no. 7675, pp. 244–248, Oct. 2017, doi: 10.1038/nature24265.

[159] L. Carrel and H. F. Willard, “X-inactivation profile reveals extensive variability in X-linked gene expression in females,” *Nature 2005 434:7031*, vol. 434, no. 7031, pp. 400–404, Mar. 2005, doi: 10.1038/nature03479.

[160] A. Rossi *et al.*, “Genetic compensation induced by deleterious mutations but not gene knockdowns,” *Nature 2015 524:7564*, vol. 524, no. 7564, pp. 230–233, Jul. 2015, doi: 10.1038/nature14580.

[161] M. A. El-Brolosy and D. Y. R. Stainier, “Genetic compensation: A phenomenon in search of mechanisms,” *PLoS Genet*, vol. 13, no. 7, p. e1006780, Jul. 2017, doi: 10.1371/JOURNAL.PGEN.1006780.

[162] M. A. El-Brolosy *et al.*, “Genetic compensation triggered by mutant mRNA degradation,” *Nature 2019 568:7751*, vol. 568, no. 7751, pp. 193–197, Apr. 2019, doi: 10.1038/s41586-019-1064-z.

[163] R. Delage-Mourroux, P. G. V. Martini, I. Choi, D. M. Kraichely, J. Hoeksema, and B. S. Katzenellenbogen, “Analysis of estrogen receptor interaction with a repressor of estrogen receptor activity (REA) and the regulation of estrogen receptor transcriptional activity by REA,” *Journal of Biological Chemistry*, vol. 275, no. 46, pp. 35848–35856, Nov. 2000, doi: 10.1074/JBC.M001327200.

[164] B. He *et al.*, “A repressive role for prohibitin in estrogen signaling,” *Molecular Endocrinology*, 2008, doi: 10.1210/me.2007-0400.

[165] J. W. Kim *et al.*, “Activation of an estrogen/estrogen receptor signaling by BIG3 through its inhibitory effect on nuclear transport of PHB2/REA in breast cancer,” *Cancer Sci*, 2009, doi: 10.1111/j.1349-7006.2009.01209.x.

[166] T. Yoshimaru *et al.*, “Targeting BIG3-PHB2 interaction to overcome tamoxifen resistance in breast cancer cells,” *Nat Commun*, 2013, doi: 10.1038/ncomms3443.

[167] S. Mishra, L. C. Murphy, and L. J. Murphy, “The prohibitins: Emerging roles in diverse functions,” *J Cell Mol Med*, 2006, doi: 10.1111/j.1582-4934.2006.tb00404.x.

[168] A. Signorile, G. Sgaramella, F. Bellomo, and D. De Rasmo, “Prohibitins: A Critical Role in Mitochondrial Functions and Implication in Diseases,” *Cells*, vol. 8, no. 1, p. 71, Jan. 2019, doi: 10.3390/CELLS8010071.

[169] S. Wang, N. Nath, M. Adlam, and S. Chellappan, “Prohibitin, a potential tumor suppressor, interacts with RB and regulates E2F function,” *Oncogene 1999 18:23*, vol. 18, no. 23, pp. 3501–3510, Jun. 1999, doi: 10.1038/sj.onc.1202684.

[170] G. Fusaro, P. Dasgupta, S. Rastogi, B. Joshi, and S. Chellappan, “Prohibitin Induces the Transcriptional Activity of p53 and Is Exported from the Nucleus upon Apoptotic Signaling,” *Journal of Biological Chemistry*, 2003, doi: 10.1074/jbc.M305171200.

[171] H. Liu *et al.*, “Progesterone-induced progesterone receptor membrane component 1 rise-to-decline changes are essential for decidualization,” *Reproductive Biology and Endocrinology*, vol. 22, no. 1, pp. 1–15, Dec. 2024, doi: 10.1186/S12958-024-01188-9.

11. Supplementary Material

11.1. Supplementary Figures

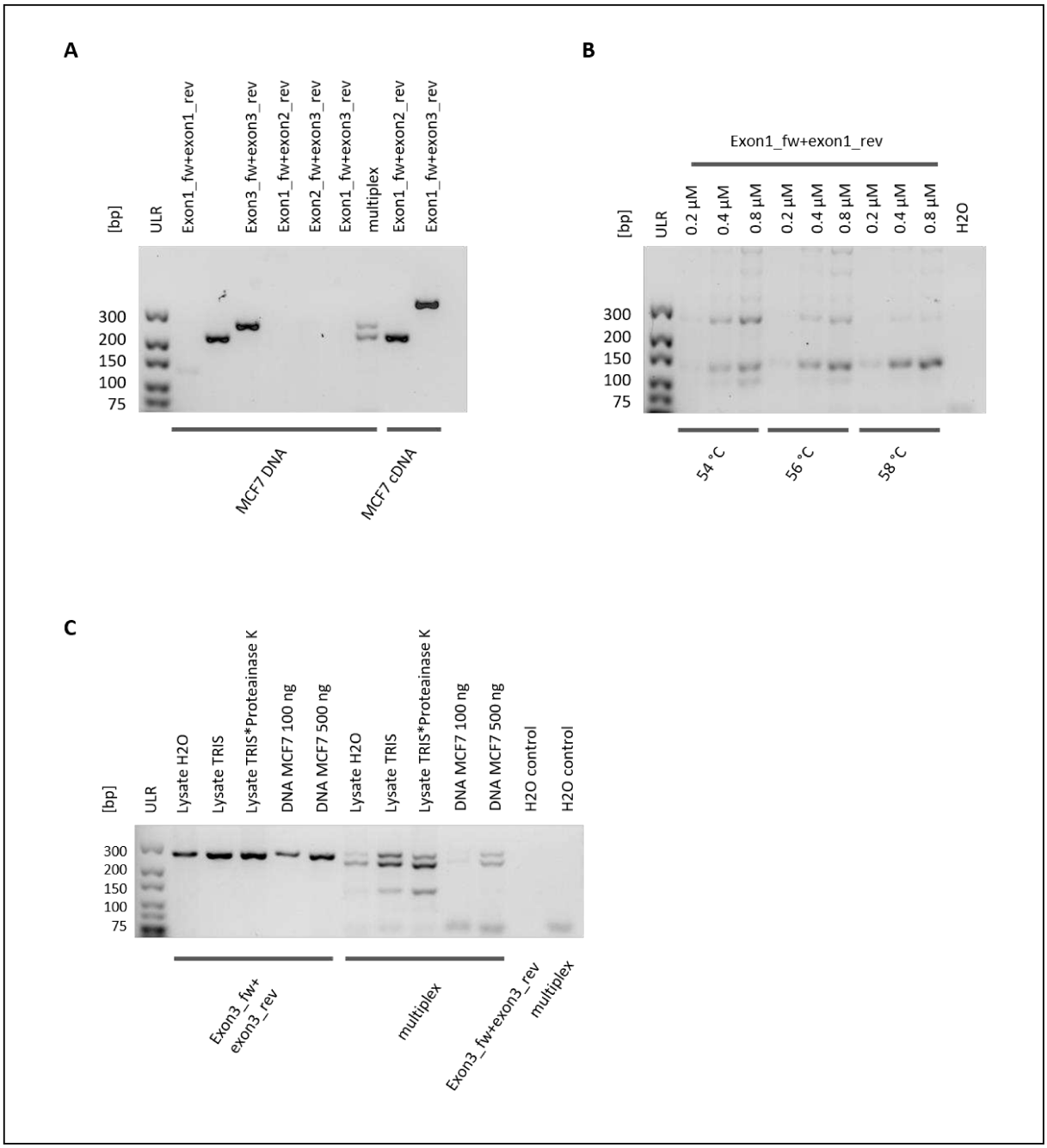

Supplementary Figure 1: Establishment of direct screening PCR using primers flanking each gRNA binding site. A: PCR on isolated MCF7 DNA (500 ng) and cDNA (1 µg) using each of the primer pair separately in 0.2 µM and in combination (multiplex). Detected bands correspond to predicted 125 bp (exon 1), 213 bp (exon 2), 250 bp (exon 3) and 203 bp for exon1_fw+exon2_rev on cDNA and 335 bp for exon1_fw+exon3_rev on cDNA. B: Temperature and concentration gradient for primer pair exon1_fw+exon1_rev on isolated MCF7 DNA (500 ng), predicted band size: 125 bp. C: Comparison of PCR on lysates in different solvents and conditions (ultrapure water = lysate H2O; TRIS lysate buffer = Lysate TRIS; TRIS lysate buffer + proteinase K digestion = Lysate TRIS+Proteinase K), purified MCF7 DNA (100 ng or 500 ng) for primer pair exon3_fw+exon3_rev or multiplex PCR. Predicted band sizes: 250 bp for exon3_fw+exon3_rev; 250 bp, 213 bp and 125 bp for multiplex.

Supplementary Table 1: Statistics of the CRISPR/Cas9 knockouts in MCF7, T47D and MDA-MB-231. MCF7 cells were subcloned by two approaches: FACS and limiting dilution. Up to 131 cell clones were screened by PCR to detect PGRMC1-KO cells. KO-rates between 0.3 and 2.6 % were achieved.

	MCF7	MCF7	T47D	MDA-MB-231
Subcloning	FACS	Lim. dilution	Lim. dilution	Lim. Dilution
Number of clones screened (% of seeded)	14 (7%)	61 (10%)	131 (22%)	105 (18%)
Number of (potential)PGRMC1-KOs (% of screened)	5 (36%)	2 (3%)	3 (2%)	5 (5%)
Rate of PGRMC1-KOs (% of seeded)	2.6%	0.3%	0.5%	0.8%

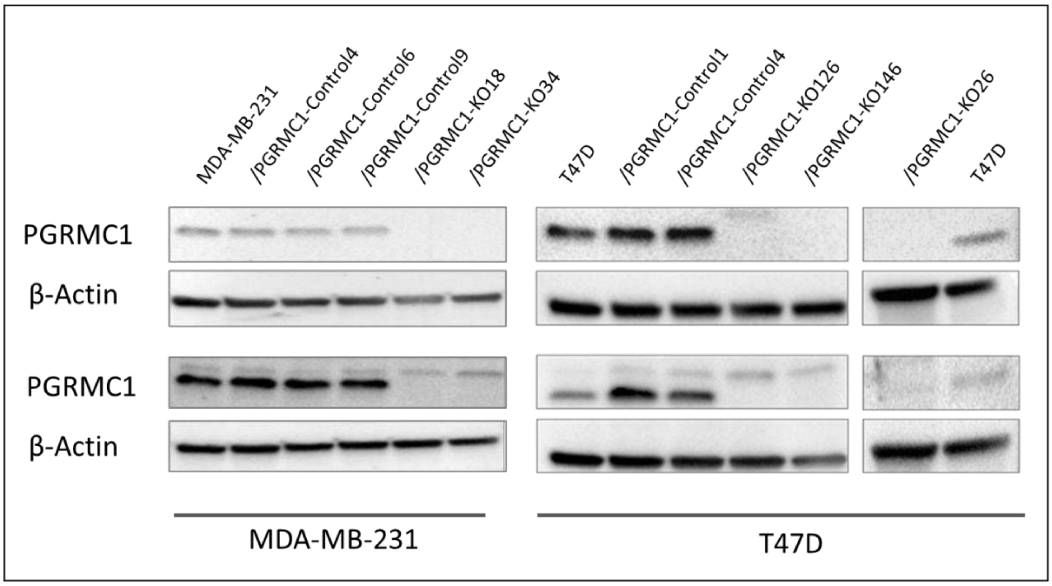

Supplementary Figure 2: Western blot of CRISR/Cas9-modified MDA-MB-231 and T47D cells. Whole cell lysates were blotted and analyzed with two different α-PGRMC1 antibodies. A+C: N-terminus detecting antibody (Cell signaling); B+D: Antibody binding the C-terminus of PGRMC1 (Abcam). As loading control, β-Actin was detected. Adapted according to Oles, 2013.

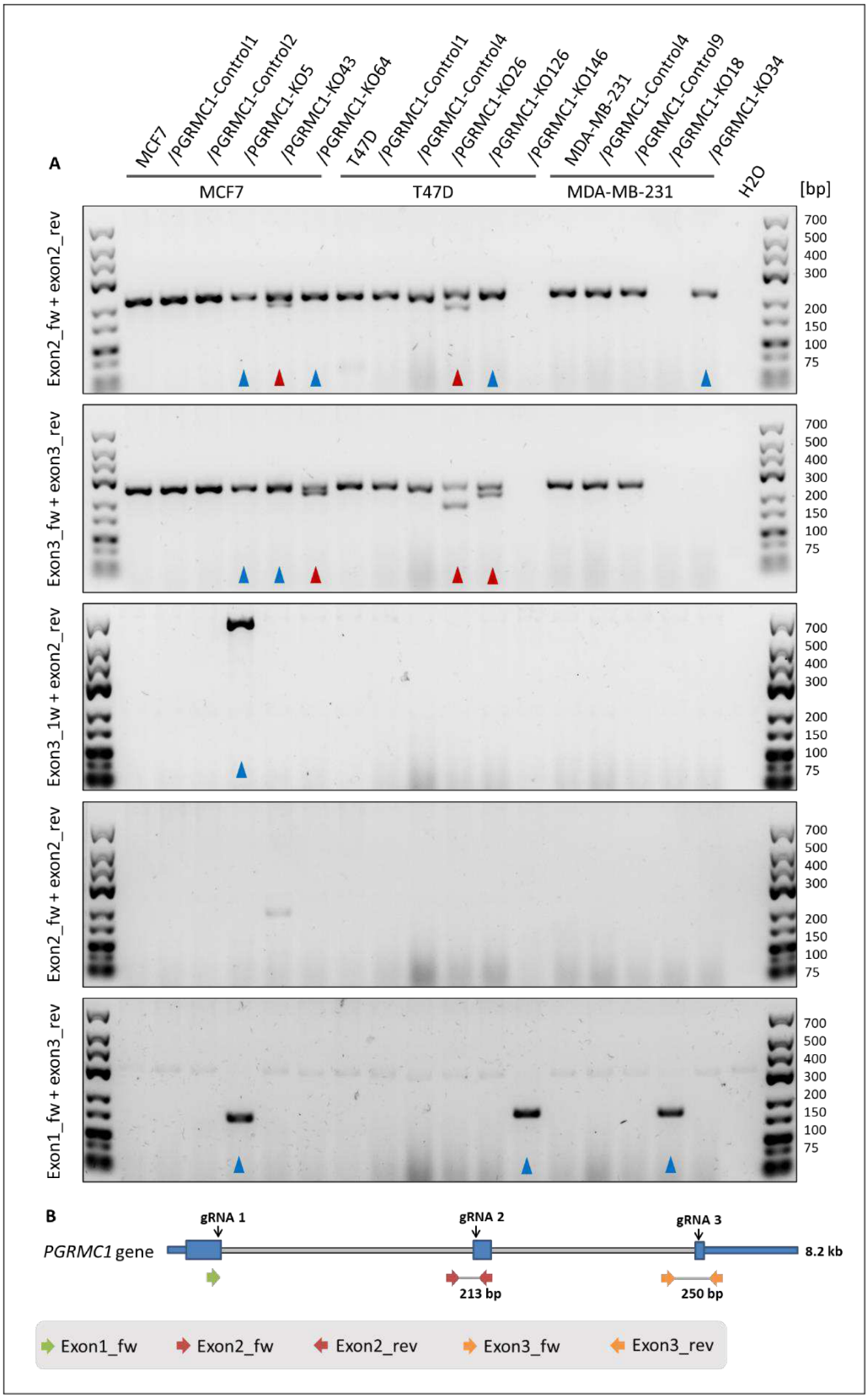

Supplementary Figure 3: A: Analysis of PCR products resulting from different primer combinations on all selected CRSIPR/Cas9- modified clones for the cell lines MCF7, T47D and MDA-MB-231 and the respective control cells. Combinations of primers from top to bottom: Exon2_fw+Exon2_rev; Exon3_fw+Exon3_rev; Exon1_fw+Exon2_rev; Exon2_fw+Exon3_rev; Exon1_fw+Exon2_rev. Bands sequenced from PCR are marked with a blue triangle; bands sequenced after TA-cloning and purification in *E. coli* are marked with a red triangle. B: graphical presentation of the primer binding sites in the *PGRMC1* locus. bp: base pairs; kb: kilo base pairs. Reference band sizes: 213 pb for parental cells in panel 1; 250 bp for parental cells in panel 2.

Supplementary Table 2: Overview of the detected aberrations in CRISPR/Cas9 generated PGRMC1-deficient cells.

Cell line	DNA	cDNA
MCF7/PGRMC1-		
KO5	• Deletion 1: 6491 bp from exon 1 to exon 3 • Deletion 2: 3651 bp from exon 1 to exon 2 with insertion of 482 bp originating from exon 3	• Not amplified
KO43	• Deletion 1: 7bp exon 3 • Deletion 2: 22 bp exon 2	• Deletion 1: 7 bp exon 3 • Deletion 2: 10 bp exon 3
KO64	• Deletion: 24 bp exon	• Deletion: 24 bp exon 3
T47D/PGRMC1-		
KO26	• Deletion: 38 bp exon 2	• Deletion: 38 bp exon 2
KO126	• Deletion: 36 bp exon 3	• Deletion: 36 bp exon 3
KO146	• Deletion: 6474 bp from exon 1 to exon 3	• Not amplified
MDA-MB-231/PGRMC1-		
KO18	• Deletion: 6474 bp from exon 1 to exon 3	• Not amplified
KO34	• No mutation in the amplified fragment from exon 2 • Missing fragment from exon 3	• Not amplified

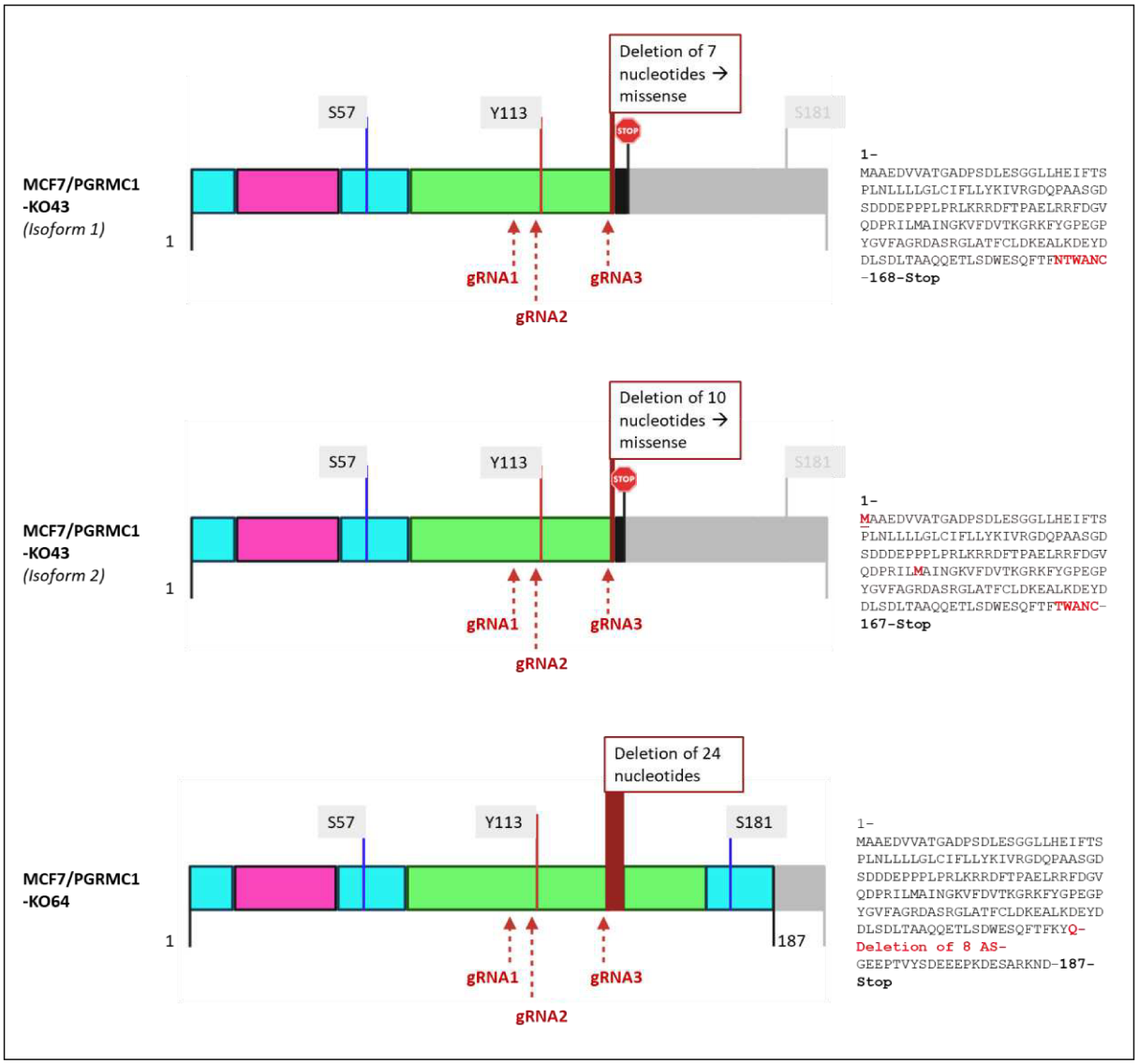

Supplementary Figure 4: Schematic representation of the primary PGRMC1-protein structure resulting from the mutated DNA/mRNA, with color code analogous to Figure 1 (magenta: TMH; green CytB5-domain, important phosphorylated amino acids tagged with a flag), and the position gRNAs on respective DNA indicated by the arrows. Structure is depicted for MCF7/PGRMC1-KO43 with only one mutation detected on DNA (deletion of 7 nucleotides in exon 2), but two mutations found on mRNA (*Isoform 1 and Isoform 2*). Both mutations would lead to an early stop codon and a truncated protein. For MCF7/PGRMC1-KO64, one 24 bp in-frame-deletion in exon 3 was detected. However, Only for MCF7/PGRMC1-KO43, a weak band of lower size was detected in western blot, while in -KO64 PGRMC1 protein was absent.

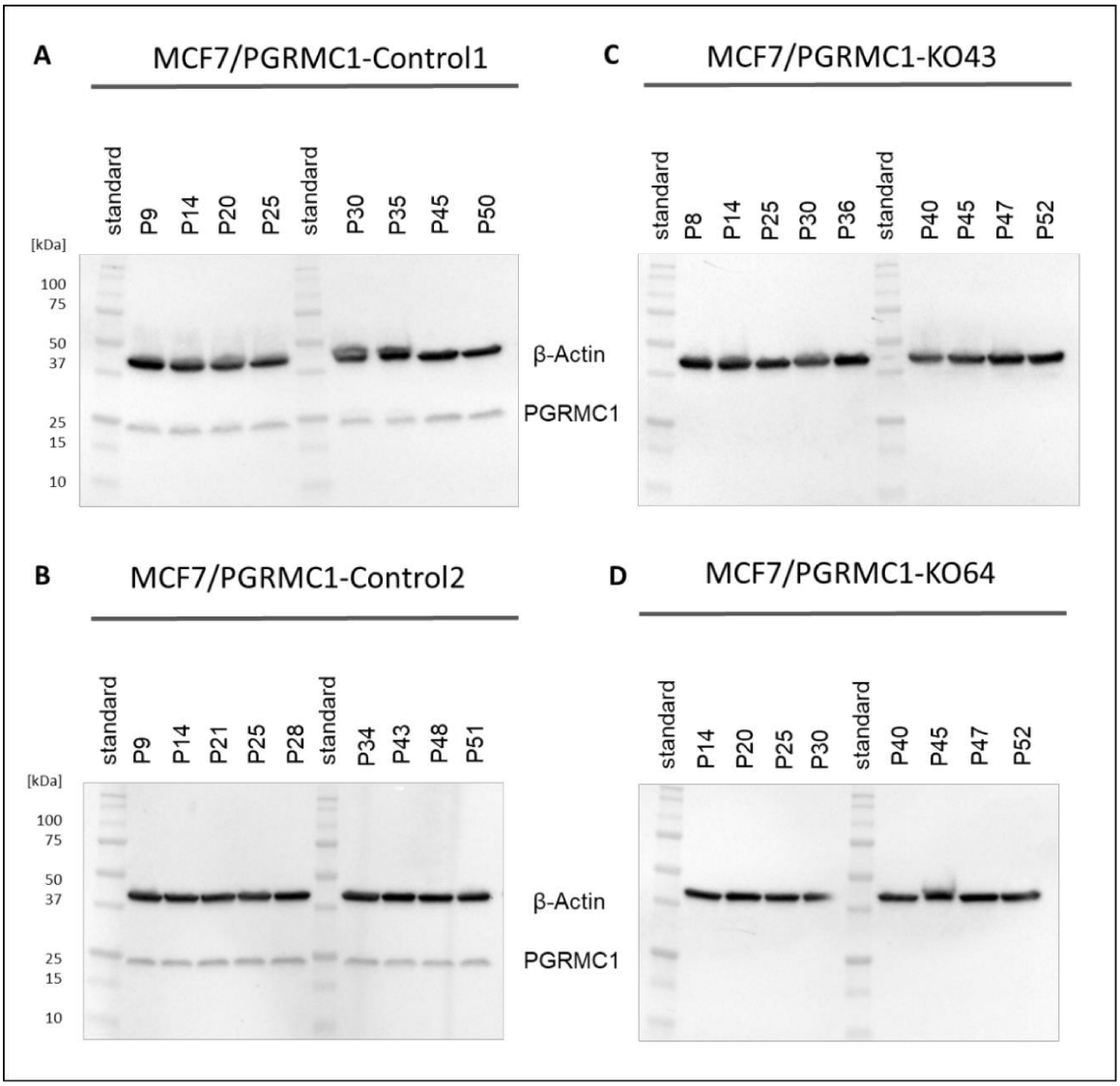

Supplementary Figure 5: Western blot analysis of long-term PGRMC1 expression in CRISPR/Cas9-generated MCF7/PGRMC1-Control and -KO clones. Cell were cultured for up to 52 passages and whole cell lysates were analyzed for A: MCF7/PGRMC1-Control1; B: MCF7/PGRMC1-Control2; C: MCF7/PGRMC1-KO43; D: MCF7/PGRMC1-KO64. For loading control, β-actin was detected.

11.2. Supplementary figures of uncropped western blots

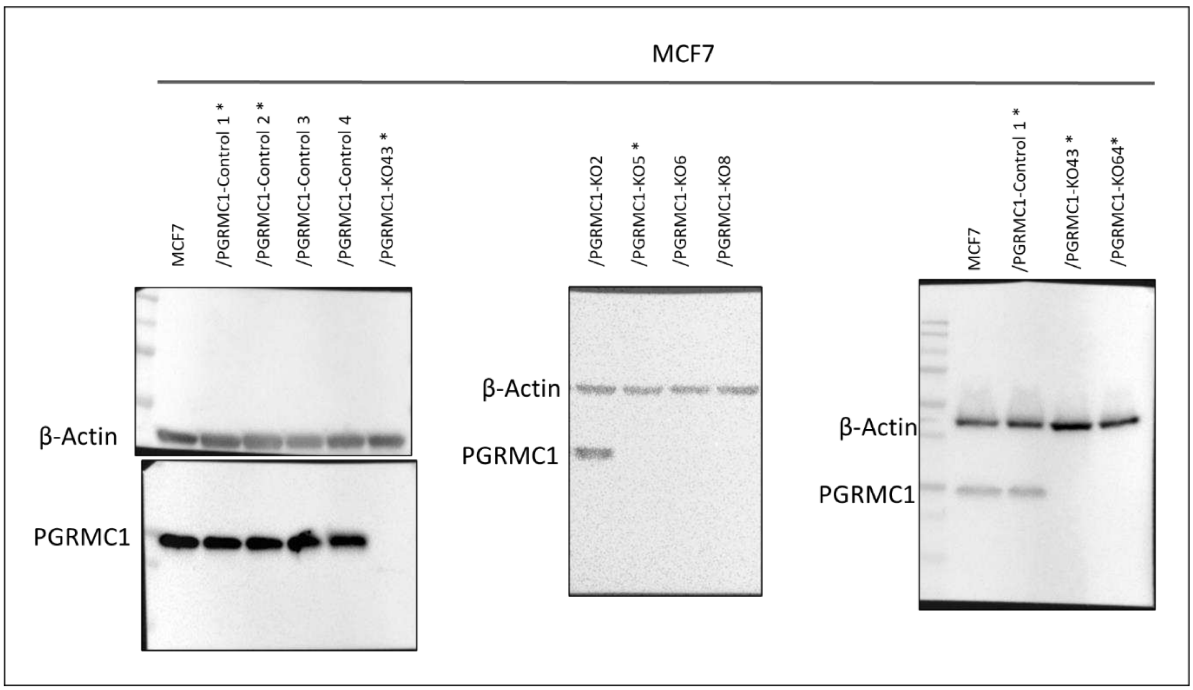

Supplementary Figure 6: Presentation of entire western blot membranes for Figure 6A. Western blot analysis of some PGRMC1-KO and -Control clones of MCF7. PGRMC1 was detected by the N-Terminus binding antibody (Cell Signaling). For loading control, β-Actin was detected. Clones selected for further analysis are marked with an asterisk (*).

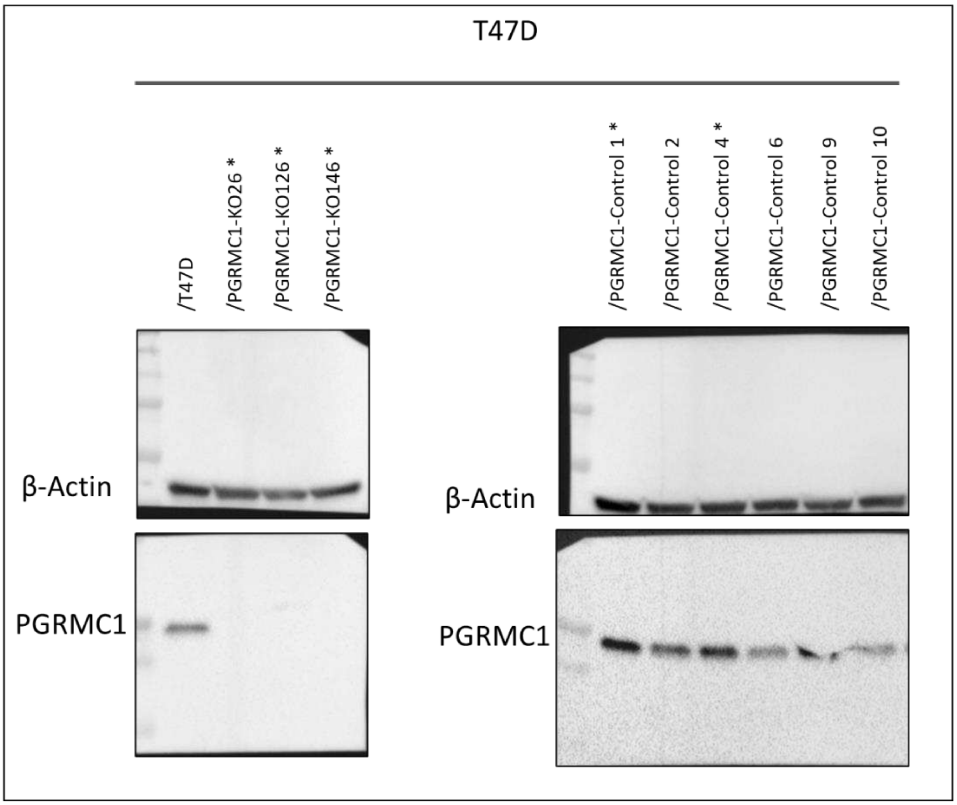

Supplementary Figure 7: Presentation of entire western blot membranes for Figure 6B. Western blot analysis of some PGRMC1-KO and -Control clones of T47D. PGRMC1 was detected by the N-Terminus binding antibody (Cell Signaling). For loading control, β-Actin was detected. Clones selected for further analysis are marked with an asterisk (*).

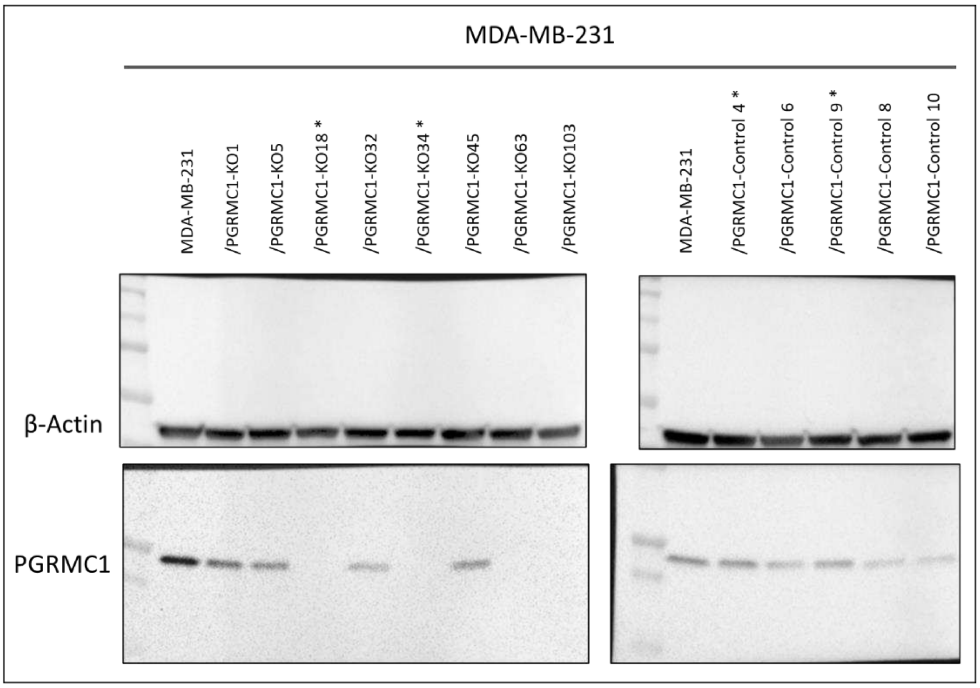

Supplementary Figure 8: Presentation of entire western blot membranes for Figure 6C. Western blot analysis of some PGRMC1-KO and -Control clones of MDA-MB-231. PGRMC1 was detected by the N-Terminus binding antibody (Cell Signaling). For loading control, β-Actin was detected. Clones selected for further analysis are marked with an asterisk (*).

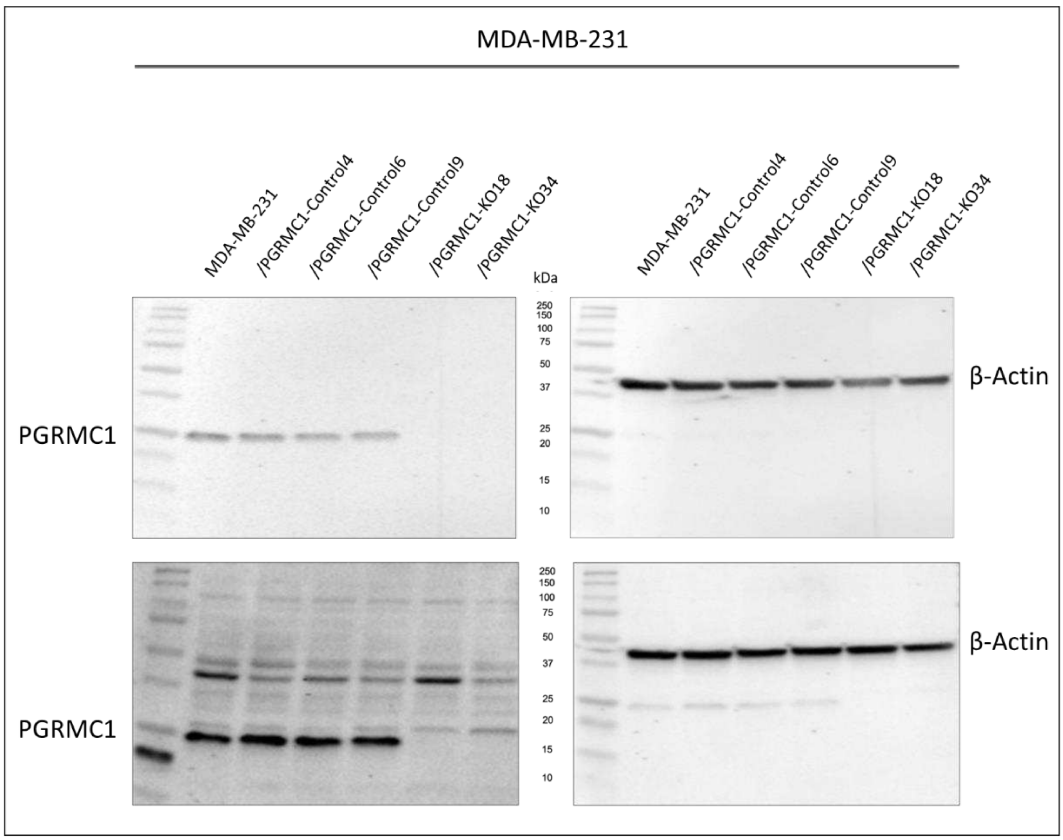

Supplementary Figure 9: Presentation of entire western blot membranes for Supplementary Figure 2 – MDA-MB-231. Western blot analysis of some PGRMC1-KO and -Control clones of MDA-MB-231. PGRMC1 was detected by the N-Terminus binding antibody (Cell Signaling). For loading control, β-Actin was detected. Clones selected for further analysis are marked with an asterisk (*).

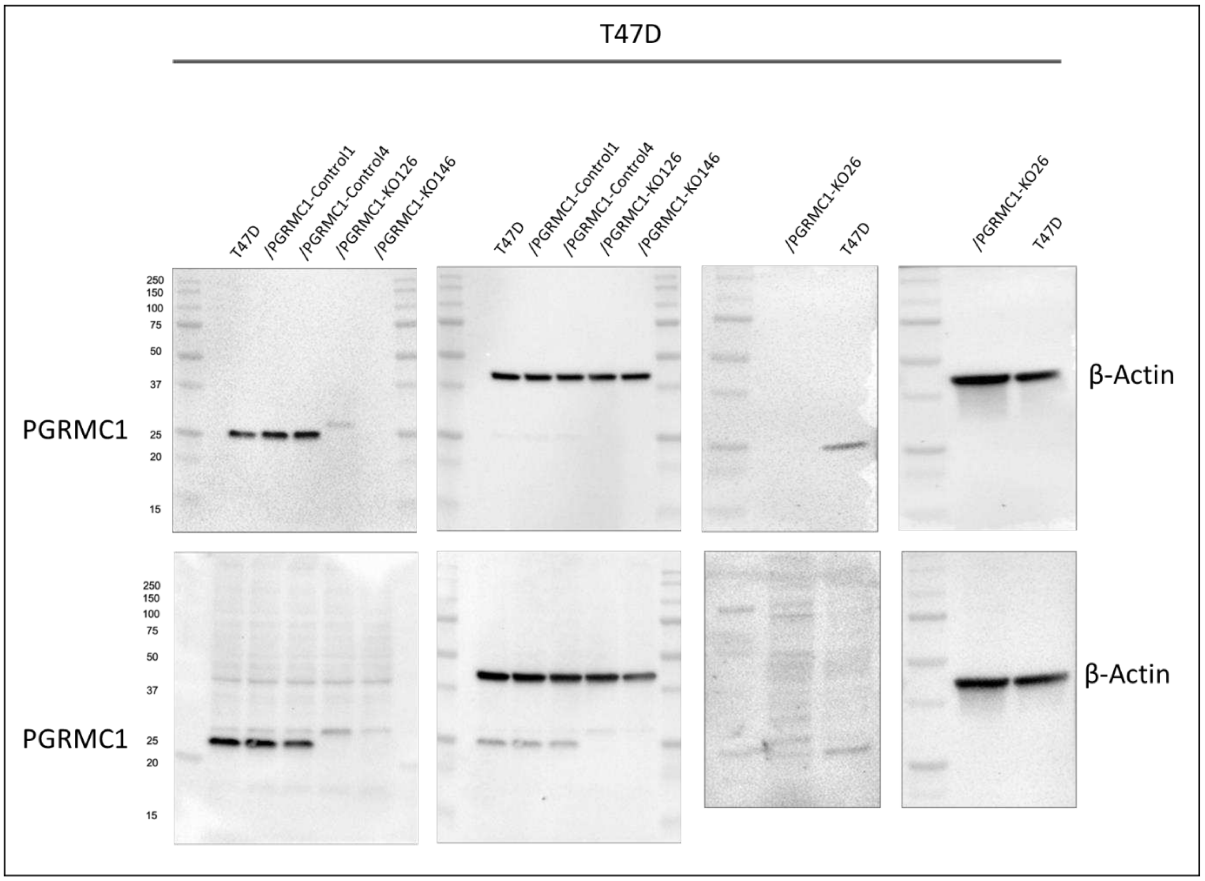

Supplementary Figure 10: Presentation of entire western blot membranes for Supplementary Figure 2 – T47D. Western blot analysis of some PGRMC1-KO and -Control clones of MDA-MB-231. PGRMC1 was detected by the N-Terminus binding antibody (Cell Signaling). For loading control, β-Actin was detected. Clones selected for further analysis are marked with an asterisk (*).

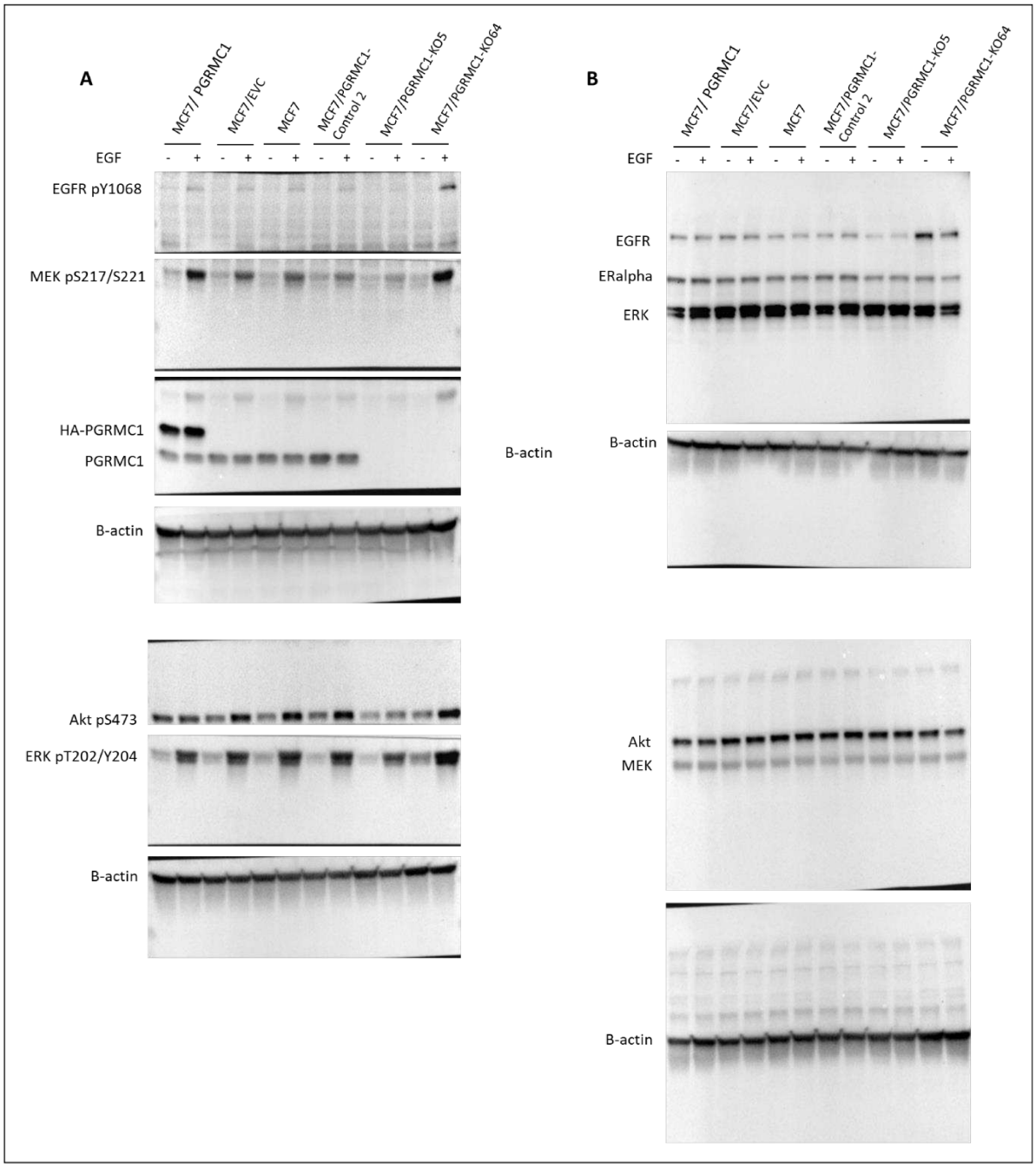

Supplementary Figure 11: Presentation of entire western blot membranes for Figure 10. Activation of oncogenic signaling upon stimulation with hormones in MCF7 cells with different PGRMC1-expression levels. A+B: Westen blot analysis of whole cell lysates of MCF7/PGRMC1 (HA-tagged), MCF7/EVC, parental MCF7, MCF7/PGRMC1-Control2, MCF7/PGRMC1-KO5 and -KO64 upon stimulation with 10 ng/ml EGF or control medium for 10 min. A: Detection of pEGFR, pMEK, pERK, pAKT, PGRMC1 and β-Actin on two separate blots (upper panel and lower panel). For blot 1, sequence of detection was as follows: 1. MEKpS217/S221, 2. PGRMC1, 3. B-Actin. For blot 2, sequence of detection was as follows: 1. ERK pT202/Y204, 2. B-Actin. B: Detection of total protein levels of EGFR, MEK, ERK, ERα and β-Actin on two different blots (upper panel and lower panel). For blot 1, sequence of detection was as follows: 1. EGFR, 2. ERK, 3. ERα, 4. β-Actin. For blot 2, sequence of detection was as follows: 1. MEK, 2. Akt, 3. B-Actin.

12. Publications and Conference Contributions

Publications

1. Liu, […], Neubauer and **Stamm**. Progesterone-induced Progesterone Receptor Membrane Component 1 Rise-to-Decline Changes are Essential for Decidualization. *Reproductive Biology and Endocrinology.* 2024.
2. Rivandi M, Franken A, Yang L, Abramova A, **Stamm N**, […], Neubauer H. ZeptoCTC-Sensitive protein analysis of true single cell lysates using reverse phase protein arrays (RPPA). Journal of Translational Medicine. 2024.
3. Abramova A, Rivandi M, Yang L, **Stamm N**, […], Franken A. A Workflow for the Enrichment, the Identification, and the Isolation of Non-Apoptotic Single Circulating Tumor Cells for RNA Sequencing Analysis. Cytometry. 2023.
4. Bai, […], **Stamm** and Neubauer. PGRMC1 Promotes Progestin-Dependent Proliferation of Breast Cancer Cells by Binding Prohibitins Resulting in Activation of ERα Signaling. *Cancers.* 2021.
5. Asperger, **Stamm**, […], Neubauer and Ludescher. Progesterone receptor membrane component 1 regulates lipid homeostasis and drives oncogenic signaling resulting in breast cancer progression. *Breast Cancer Research.* 2020.

Talks and Poster Presentations

1. **Stamm**, Wyrich, Hasenkox, Bai, Niederacher, Fehm, Neubauer. Norethisterone exhibits a dual effect on estrogen receptor alpha and promotes breast cancer progression. **Talk at the Congress of the German Senelogy Society 2023.**
2. Stamm, Bai, Ludescher, Niederacher, Fehm, Neubauer. PGRMC1 binds to prohibitins upon progestin treatment and promotes ERα activation in breast cancer cells. **Deutscher Krebskongress 2022.**

1. **Stamm**, Asperger, Ludescher, Fehm, Neubauer. PGRMC1 Alters *de novo* Lipid Biosynthesis Resulting in Enhanced Oncogenic Signaling. **Deutscher Krebskongress 2020**.
2. **Stamm**, Ludescher, Asperger, Fehm, Neubauer. PGRMC1 Interacts with Enzymes of the Cholesterol Biosynthesis Pathway Resulting in Altered Cholesterol Metabolism and Enhanced Oncogenic Signaling. **International AEK Cancer Congress 2019**.

3. Asperger, Ludescher, **Stamm**, Cieslik, Hofmann, Zanger, Kovacevic, Richardson, Ruckhäberle, Fehm, Niederacher, Neubauer. Progesterone receptor membrane component 1 - A novel key regulator in lipid homeostasis drives oncogenic signaling resulting in breast cancer progression. Proceedings of the **2019 San Antonio Breast Cancer Symposium**.

As well as numerous others.

13. Theses supervised as part of this dissertation

1. “Impact of Hypoxia on Progesterone Receptor Membrane Component 1 in Breast Cancer”, **Shanshan Deng**, in progress since 2023
2. Einfluss von PGRMC1 auf Ferroptose in Mammakarzinom-Zelllinien, **Yaren Daglayan**, in progress since 2023
3. Progesterone-induced Progesterone Receptor Membrane Component 1 Rise-to-Decline Changes are Essential for Decidualization”, **Hailun Liu**, 2025
4. “PGRMC1 promotes progestin-dependent proliferation of breast cancer cells by binding prohibitins and activating ERα signaling”, **Yingxue Bai**, 2024
5. „Die Untersuchung von Brustkrebszellinien mit unterschiedlichen PGRMC1-Expressionsniveaus“, **Azin Yousefiboroujeni**, 2024
6. „Systematische Untersuchung des Einflusses von PGRMC1 und PHB2 auf die Aktivierung und Lokalisation von ERa nach Stimulation mit dem Progestin NET in Brustkrebszelllinien“, **Josephine Hasenkox**, 2023
7. “Characterization of PGRMC1-deficient breast cancer cell lines”, **Julia Oles**, 2023
8. “Role of PGRMC1 in progestin-dependent breast cancer progression”, **Martine Wyrich**, 2021

14. Eidesstattliche Erklärung

Hiermit versichere ich, Nadia Stamm, an Eides statt, dass die vorliegende Abschlussarbeit mit dem Titel **"Progesterone Receptor Membrane Component 1: Cellular Mechanisms and Involvement in Breast Cancer Pathology and Endometrial Decidualization"** von mir selbstständig und ohne unzulässige fremde Hilfe verfasst wurde. Ich habe keine anderen als die von mir angegebenen Quellen benutzt. Die Stellen der Arbeit, die dem Wortlaut oder dem Sinne nach anderen Werken entnommen wurden, wurden in jedem Fall unter Angabe der Quelle kenntlich gemacht. Die eingebundenen Publikationen/Grafiken wurden mit Genehmigung der entsprechenden Journale übernommen.

Ort, Datum Unterschrift

15. Danksagung

Zuallererst möchte ich Herrn Prof. Neubauer und Frau Prof. Fehm für die Möglichkeit danken, diese Dissertation im Forschungslabor der Klinik für Frauenheilkunde und Geburtshilfe anfertigen zu dürfen. Ich danke beiden außerdem dafür, allen Lebensumständen zum Trotz hinter mir gestanden und mich geduldig unterstützt zu haben. Das war für mich von unschätzbarem Wert.

Prof. Neubauer und Prof. Heinzel möchte ich außerdem für die Übernahme der Betreuung und die zügige Erstellung der Gutachten danken. Prof. Nettersheim danke ich für die Beratung in CRISPR-Angelegenheiten.

Mein besonderer Dank gilt dem gesamten Laborteam und der freundlichen und produktiven Atmosphäre, die dank dieser Menschen im Forschungslabor herrscht. Danke, liebe Ulla, für deine Unterstützung durch dick und dünn, danke an Dieter, Helmut, Ellen, Nora, Dagmar, Doro K., Linda, Karin und Doro R. für den wertvollen technischen Rat, danke an Dilay, Mihaela, Shanshan, Menglin, Hailun, Yingxue, Gleice, Knud und Andrea für die vielen Gespräche, den wertvollen Austausch und auch die netten Kaffeezeiten zwischendurch. Danke auch an Marina und Johanna für die Starthilfe zu Beginn der Arbeit. Ein großer Dank gilt Anna und Mahdi, die in dieser Zeit tolle Freunde geworden ist. Besonders danken möchte ich André für einfach alles: den wissenschaftlichen Rat, die tatkräftige Unterstützung bei der Durchführung, den unermüdlichen Einsatz über vernünftige Arbeitsstunden hinweg, den Trost bei Rückschlägen.

Ein riesengroßer Dank gilt in dieser Zeit meinen Eltern für ihre bedingungslose Unterstützung und die liebevolle Betreuung meiner Kinder, und meinen Kindern für die Geduld, das Durchhaltevermögen und das schwesterliche Kümmern umeinander. Ich danke außerdem meinen Freunden für die moralische Unterstützung in dieser ganzen Zeit! Ihr alle zusammen seid die Allerbesten!